856

REPRODUCEABILITY PARAMETERS IN THICK FILM

by

L. DALTON MOLSON

PART A: INDUSTRIAL PROJECT*

A project report submitted in partial fulfillment
of the requirements for the degree of

Master of Engineering

Dept. of Engineering Physics

McMaster University

Hamilton, Ontario

1974

*One of two project reports. The other is designated
PART B: MCMASTER (ON-CAMPUS) PROJECT

TITLE (PART A) : Reproduceability Parameters in Thick Film

AUTHOR: L. Dalton Molson, B.Sc. (Waterloo)

SUPERVISOR : Dr. R.S. Sennett

Number of Pages: i, 104

MASTER OF ENGINEERING
(Engineering Physics)

McMaster University
Hamilton, Ontario

Reproduceability Parameters in Thick-Film Resistors

L. Dalton Molson

List of Illustrations

ABSTRACT

Thick-film resistors are being used in the hybrid microelectronics industry. One characteristic that has been considered for the thick film resistor is the reproduceability in resistor value associated with the production techniques employed in the reproduceability in resistor value associated with the production techniques employed in the resistor manufactured.

One parameter that has been associated with reproduceability is the yield figure; another parameter is the width of the resistance distribution for a given resistor production. These parameters can be used to identify the degree of reproduceability for the resistor production. A high yield figure or a small spread figure indicates a high degree of reproduceability.

The effect of aspect ratio and sheet resistivity on the reproduceability has been evaluated for paste system A. Aspect ratios of 10, 5, 2 and 0.7 for a range of sheet resistivities (100, 1K, 10K, 100K, and 1M ohms per square) were investigated. Results show that for a given aspect ratio the amount of variation in spread for the range of sheet resistivities is negligible within the limits of error in the experiment. For a given sheet resistivity, the variation in spread for the range of aspect ratios is considerable. The spread of an aspect ratio of 10 is 25 $\pm$ 4%. For an aspect ratio of 0.7 the spread is 59 $\pm$ 7%.

The effect of resistor location on spread for a 2" x 2" substrate has been studied. Results indicate that a higher degree of reproduceability can be associated with resistors located near the central (1" x 1") region of the substrate than the resistors located

near the perimeter.

The effect of increasing the resistor width on the reproduceability has been evaluated for resistors having aspect ratios near unity. Results show that as the resistor width is increased the spread in resistance decreases. For a width of 30 mil. the spread in resistance is 37%. When the width is increased to 100 mil., the spread decreases to 21%.

ACKNOWLEDGEMENTS

The author wishes to express his appreciation to the Thick Film group at Garrett Microelectronics (Toronto) for their co-operation and guidance throughout the project.

Special thanks goes to Dr. Roy Sennett (Garrett) and Dr. John Shewchun (McMaster University, Hamilton) for their supervision of the research.

The author wishes to acknowledge the receipt of a Province of Ontario Graduate Fellowship and McMaster University Fellowship.

1. INTRODUCTION

The use of thick film devices in the hybrid microelectronics industry has been expanding rapidly, and they are now being employed in spacecraft memory systems, automotive voltage regulators, television and radio circuits, desk calculators, and a wide variety of measuring and control systems.

One of the most common thick film elements in these system is the thick film resistor. Consider a basic description of this element.

1.1 Basic Description of Thick Film

A simple as-fired film resistor consists of thick film material on a substrate as illustrated in FIG. 1(a). The substrate is used as the foundation for the thick film. It is usually a ceramic material that can withstand temperatures in excess of 1000°C. Thick film conductor material is used to make contact with the thick film resistor material as well as provide electrical paths required for a complete circuit.

On a microscopic scale the thick film material, after processing, basically consists of metal particles in a glass matrix. These particles are usually covered with a layer of their particular oxide as indicated in FIG. 1. There is a random arrangement of the constituents of the material where metal particles may or may not be in contact. The conduction process occurs from metal particle to metal particle. Glass frit that might be positioned between metal particles would act as an electrical isolation and tend to inhibit the conduction process.

On a macroscopic scale the resistance of the device depends not only on the glass content of the thick film material but on the physical

geometry shape of the resistor as well.

The effect of these parameters on the resistance can best be illustrated by Ohms Law. Consider an ideal resistor for which Ohms Law can be written as:

$$R = \frac{\varrho \ell}{A} = r_s \frac{\ell}{W} = r_s \, a \qquad (1)$$

where - R is the resistance of the device

ϱ is the volume resistivity of the thick film material

ℓ is the length of the resistor

w is the width of the resistor

A is the cross sectional area of the resistor

and a is the aspect ratio of the resistor.

The resistance calculated from equation (1) however, is not an exact prediction for the resistance of a typical thick film resistor. The final value of the resistor is also dependent on the processing of the material. Consider the processing involved in the fabrication of typical thick film resistor material.

1.2 Process Flow for Thick Film Fabrication

The processing flow for a typical device is illustrated in FIG. 2. When the basic circuit design and layout have been completed, the screen patterns for the conductor and resistor materials are produced. The patterns shown in FIG. 2 are used in the manufacture of a substrate containing some twenty-five individual devices. Each device contains four thick film resistors and the associated conductor paths required for the circuit. The first stage in making the circuits is to print and fire the conductor on a clean substrate. The firing

process is usually done with a belt furnace to ensure a proper firing profile. The profile would have a firing temperature and firing time. The next step is to print the resistor pattern with the resistor material of the desired sheet resistivity and then fire the substrate to the required profile. An overglaze to cover any area of the circuit that has to be protected against environmental hazards is then screened on and fired. This completes the fabrication stage of the thick film resistor.

Should the resistor value be outside the tolerance limits set by the circuit requirement, an additional step involving a resistance trim is required to bring the resistor value into the desired range. However, with trimming techniques, only an increase in resistance is possible and any resistors that are out of tolerance above the required value cannot be recovered without more elaborate processing.

The ability to produce resistors within a specified tolerance of a required value without the use of trimming techniques would be a definite advantage. Apart from the obvious savings in production time and costs, performance characteristics such as noise and stability that can be degraded by the trimming process would not be affected.

In order to determine tolerance bands that might be feasible with thick film production, the inherent variation in resistance observed in the production of thick film resistors must be identified.

1.3 Experimental Parameters in Thick Film

The variation in resistance can be attributed to several factors. One factor is the thick film paste from which the resistor is made.

Since the paste consists of several powdered materials of different densities, it must be mixed thoroughly to ensure a uniform distribution of the paste constituents. Any variation in the uniformity during the production run, there is a change in the amount of paste that is transferred to the substrate with a corresponding change in resistance. The viscosity is very dependent on temperature and humidity so that a controlled environment is required to minimize this contribution to the resistance variations.

The printing equipment is another factor that contributes to the variation in resistance. Any thick film screen printer has a certain degree of reproduceability. The reproduceability depends on the repeatability of the squeegie movement across the screen pattern and the interaction of the squeegie with the screen. The variables associated with the squeegie movment are illustrated in Fig. 3 and include:

(1) Squeegie pressure

(2) Squeegie travel and speed

(3) Machine rigidity

(4) Screen tension control

The squeegie pressure affects the uniformity of the print. A variation in pressure will create a variation in the thickness of the print and result in a variation in resistor values during a production run. The squeegie speed and travel have a similar effect on the print in that any vibrations or bounce would produce a variation in the thickness of the print as well. A controlled speed must be used in order to obtain a consistent print thickness. Screen wear,

especially during a long production run will alter the tension and the breakaway distance and degrade the degree of reproduceability associated with the equipment. With poor tension the edge of the print loses its crispness and the thickness cannot be maintained.

The afore mentioned parameters represent variables that are inherent with a specific production facility and paste manufacturer. One thick film parameter that is a common feature to every production facility is the aspect ratio of the resistor. Consider the effect that this parameter has on the as-fired resistance spread for the thick film production facility at Garrett Microelectronics.

2. THE EXPERIMENT

Clearly, there are many parameters associated with thick film production that can contribute to the spread in resistance. An experiment has been designed to investigate the effect of aspect ratio and sheet resistivity on the spread of the as-fired thick film resistors.

2.1 Resistor Print and Fire Techniques

The printer parameters have been kept at as constant a setting as possible. Values for the measurable parameters are given in FIG. 4. The effect of paste viscosity and screen wear have been minimized by using only short production runs of twenty-five substrates for each investigation. The print and firing order was recorded for each run so that any correlation between the printing parameters and experimental results could be investigated. Each substrate was printed using standard thick film techniques and then passed through the dryer. Sample prints were used to set up the firing profile in the zone furnace to vary the resistor values to a preselected nominal value. The nominal value was chosen so that for a given sheet resistance and aspect ratio the fired resistor value would correspond to that given by equation (1). The firing order was the same as the printing order for the substrates in all cases.

2.2 Description of Test Pattern

The test pattern employed in the experiment is shown in FIG. 5. It has been designed to contain a wide range of aspect ratios and dimensions typical to a production environment. The pattern consists of some 576 resistors on a 2" x 2" substrate. Each quadrant of the

substrate has an identical resitor array for the aspect ratios and geometries to be investigated. The resistors have been identified using the formula.

i-Rj (2)

where "i" is the quadrant number and "Rj" is the resistor identification in each quadrant as showen in FIG. 5(b). Resistor dimensions are given in FIG. 6 for the aspect ratios to be investigated.

2.3 Scope of the Experiment

Aspect ratios for a range of values from 0.7 to 10 were investigated. For each aspect ratio a range of sheet resistivities from 100 ohms per square to one megohm per square were evaluated. A standard sample of twenty-five substrates was fabricated for each sheet resistivity investigated which generated a minimum resistor sample size of 200 resistors for any aspect ratio and sheet resistivity.

The various sheet resistivity pastes were members of a commercially available paste system that will be identified as "Material A". The thick film conductor paste is also commercially available and will be identified as "Material C1". The same conductor material was employed throughout the experiment.

2.4 Resistor Measurements

The equipment used to measure the as-fired resistance is shown in FIG. 6. The substrate under investigation is loaded onto the stage of an IPT model MP-4 prober. Probes make contact with the conductor pads of the resistors to be measured. Usually eight resistors with the same aspect ratio are probed at the same time. The

probes are connected to the resistance measuring device through a channel selector that permitted measurement of each resistor. The schematic diagram for the selector is shown in FIG. 7. A DANA (model 533) digital voltmeter is used to measure resistors below 10 megohms. For resistances above 10 megohms a bridge technique using a Leeds and Northrup Wheatstone Bridge (model 4735) has been used.

3. DATA ANALYSIS

The as-fired resistor values obtained during the experiment have been tabulated in Appendix One. Each table corresponds to a specific sheet resistivity and aspect ratio that has been investigated. A computer program has been used to assist in the analysis of the results and will be described in the next section.

3.1 The Computer Program

The computer program has been written to provide a graphical display of the resistance values and spreads as well as the statistical analysis for each experiment. A copy of the Fortran statements of the program is found in Appendix Two.

The program calculates the total mean of the resistors under investigation for all the substrates in the run as well as the standard deviation about the mean for the entire sample. The mean resistance and standard deviation for all the specified resistors on one substrate is calculated. The mean resistance and standard deviation of the same resistor for all the substrates is also determined. A sample output of these statistics is shown in FIG. 8.

The program then generates a histogram of the resistor values to provide a display of the entire sample. A sample histogram is shown in FIG. 9. It also plots the resistance values of each resistor investigated on each substrate in the order of substrate printing as shown in FIG. 10. The plot is centered about the total mean for the sample with the x-axis divided in units of percent of the total mean. Each number represents a particular resistor on the substrate. For example, in FIG. 10 the number "1" represents the resistor 1-R1

and the number "8" represents the resistor 2-R3 using the resistor identification given by equation (2).

The final stage in the program is to calculate the yield associated with a specified tolerance band for the entire group of resistors. Yields associated with bands of $\pm$ 1%, $\pm$ 2%, $\pm$ 5%, $\pm$ 10%, $\pm$ 15%, and $\pm$ 20% are calculated.

3.1.1. Program Segments

The program consists of one mainline and seven subroutines. Their purposes are listed below:-

TST	-	mainline to control the program
INRES	-	input for the resistor values
SDMEA	-	calculates the mean and standard deviation of the resistors selected by SUMSD and SUMSR
SUMSD	-	finds the mean and standard deviation for specified resistors on each substrate
SUMSR	-	finds the mean and standard deviation for same resistor on all the substrates
HISTO	-	plots the histogram
SPLOT	-	plots resistor value against substrate number
YIELD	-	calculates the yield to tolerance bands for the entire sample

The data for the program has the following format. The information on the first eight cards is used as a title and is copied directly from the input to the output. The next card contains two integers that indicate the number of resistors per substrate to be investigated and the number of substrates in the sample respectively. They must

be coded in "I10" format. The program also has the restriction that the maximum number of resistors per substrate is 8 and the maximum number of substrate is 250. The as-fired resistor values are inputted in the next section of cards. They are coded in "Free Format". The last data card contains four numbers that are used as scaling factors for the histogram and substrate plot and are summarized below:-

1 = The histogram full scale in percent of the total number (25%)

2 = The substrate plot full scale as a percent of the total mean $\pm$ 25%

3 = The histogram interval in units of resistance (1% of the mean)

4 = The histogram central value in resistance units (Total Mean)

When any of these numbers are unspecified or zero the program assigns the values in brackets to the scaling factors. The numbers are coded in 4F10.0 format.

3.2. Definition of Distribution Characteristics

It is important to standardize the technique for analyzing the histogram results. The envelope of the histogram is an experimental representation of the actual distribution function for the results. The analysis would be simplified if a single number could be used to characterize the distribution curve. One number that has been implemented to evaluate results is the yield figure. The yield to a given tolerance band can be quoted in an analysis; however, this number would not be enough to adequately describe the distribution curve associated with the histogram.

The first step is to identify a standard technique for obtaining the histogram curve. Consider the histogram results illustrated in

FIG. 9. This histogram is the distribution of as-fired resistor values for a typical thick film resistor. The cell width used in the histogram represents one percent of the statistical mean for the sample. The cell width determines the scale of the relative frequency axis of the histogram. When histograms with different cell widths are to be compared a "normalized" frequency can be used. The normalized frequency is defined as;-

$$\text{Normalized Frequency (\%)} = NF = \frac{N_i}{N_t \times W} \times 100 \quad (3)$$

where N_i is the number of resistors in the sample and W is the width of the statistical cell in percent.

Now that a standard approach for generating the histogram has been adopted the technique for obtaining the distribution curve can be defined.

The method that has been found to be most useful in evaluating a distribution is the symmetry approach. The method consists of identifying the mean value of the distribution and then fit the best symmetric curve about the mean on a visual basis. In most cases this technique works very well. However, in the case of skewed distributions, another technique can be used. This technique relies on only a best visual fit of the histogram results as illustrated in FIG. 11.

Both techniques offer advantages and disadvantages. By applying a best visual fit alone, any deviation from a typical distribution

can be easily identified. When the curve fit is applied using the symmetry approach these deviations would be masked to some extent but a more systematic approach to the analysis can be obtained. In cases where the histogram results indicate a deviation from normal, both techniques would be applied to ensure a proper evaluation.

When a distribution curve has been generated, a spread analysis can be performed. The term "total-spread" refers to the width of the base of the distribution curve as illustrated in FIG. 12 and is used as a characteristic for the distribution. Another characteristic that can be considered for the distribution is the "tangent-spread". This characteristic is defined as the spread of the distribution derived using tangents to the curve as illustrated in FIG. 12. This parameter represents a more realistic approach than a total-spread value for distributions with extended tails. Although the choice of tangent point is arbitrary, the tangent to the curve at the half-maximum normalized frequency has been used in evaluating the tangent-spread wherever possible.

4. RESULTS

4.1. Effect of Aspect Ratio on Spread

Now that the parameters associated with the as-fired resistance distributions have been defined, they can be applied to the experimental results. The as-fired resistance distributions for the 100 ohms per square resistor paste are given in FIG. 13 to FIG. 16 for the aspect ratios of 10, 5, 2 and 0.7 respectively.

The resistors associated with these aspect ratios that were investigated are listed in FIG. 17. In each case a total of 200 resistors on 25 substrates contributed to the distribution.

Results for the 1K ohms per square material are found in FIG. 18 to FIG. 21 for the range of aspect ratios of interest and the 10K ohms per square results are in FIG. 26 to FIG. 29 and the 1 megohm per square results are in FIG. 30 to FIG. 33 for the range of aspect ratios investigated. The resistors that were investigated for each aspect ratio correspond to those given in FIG. 17 for all the above cases except for the 100K ohm paste and the 1M ohm material with aspect ratio of 10. In the 1M ohm case the resistors: 3-R1, 3-R2, 4-R1, 4-R2, 3-R3, 3-R4, 4-R3 and 4-R4 were used for the investigation. For the 100K paste only the last four resistors in each group for each aspect ratio were investigated.

The total-spreads and tangent-spreads associated with these distributions have been tabulated in FIG. 34. A feature common to all the sheet resistivities is the increase in resistance spread with decreasing aspect ratio. A plot of the total-spread in resistance as a function of aspect ratio for the results is given in FIG. 35. The resistance spread increases dramatically for aspect ratios

below 2. The variation in spread with paste sheet resistivity for a constant aspect ratio is minimal as indicated in FIG. 35 by the close packing of the experimental results for the range of pastes investigated.

4.2. Effect of Resistor Location on Spread

The effect of the resistor location on the substrate relative to the as-fired resistance spread has been investigated. Resistors having an aspect ratio of 10 in the four quadrants of the test pattern were analyzed for the 100 ohm per square paste. The resistors contributing to the investigation are given by:-

$$i - R1, \quad i - R2$$

$$i - R3, \quad i - R4$$

where i = 1, 2, 3, 4. Each resistor represents a particular position on the substrate. The statistical variation in resistance for this study has been calculated using the formula:-

$$\text{Statistical Variation } (\%) = 3 \times \frac{\text{Standard Deviation}}{\text{Resistor Mean Value}} \times 100 \qquad (4)$$

where the mean and standard deviation have been calculated for the same resistor on 25 substrates. The results are shown in FIG. 36 with the spread values positioned schematically on a 2" x 2" substrate to illustrate the spread associated with substrate location.

The spread in resistance for the resistors on the perimeter of the substrate tends to be larger than for the resistors located near the central region of the substrate. This can be attributed to less control of squeegie - screen interaction at the outer edges of the substrate. With the squeegie motion as indicated in FIG. 36 the

left edge resistors are affected by the squeegie snap-down onto the screen. The position where the squeegie first touches the screen can vary and this will alter the paste transfer process creating a variation in resistance. A similar problem occurs at the end of the squeegie travel creating a variation in resistance at the right edge of the substrate. The variation at the top and bottom edges is attributed to the disign of the printer and the lack of control of squeegie pressure at the extremes of the squeegie blade.

4.3. Effect of Resistor Width on Spread

The effect of increasing the resistor width on the resistance spread has been investigated for resistors with similar aspect ratios. The smallest width resistors on the test pattern are the i-R43 and i-R44 geometries. They have an aspect ratio of 0.7 with a resistor width of 30 mil. The as-fired resistance distribution for these resistors for all four quadrants is given in FIG. 37.

Resistors with an intermediate width and aspect ratio near unity on the test pattern are associated with the i - R31 and i - R32 geometry. This geometry has a resistor width of 65 mil and an aspect ratio of 1. The distribution associated with these resistors are given in FIG. 38.

The largest width for a resistor available on the test pattern can be obtained by using the resistors i - R37, i - R38, i - R39, and i - R40 in series. The combined resistor has an aspect ratio of 0.8 and a width of 100 mil. The distribution for this configuration is given in FIG. 39.

The total-spread values for these distributions have been plotted in FIG. 40. Although it is difficult to estimate the true dependence of spread on resistor width from the limited experimental data but the results indicate that there is a decrease in total spread for an increase in resistor area within the range of widths investigated.

4.4. Yield Analysis

Results for a yield analysis of the as-fired resistors for the range of sheet resistivities and aspect ratios investigated are found in FIG. 41. Tolerance bands of $\pm$ 1%, $\pm$ 2%, $\pm$ 5%, $\pm$ 10%, $\pm$ 15% and $\pm$ 20% were chosen for an evaluation of the distributions. The effect of aspect ratio on yield is illustrated in FIG. 42 for the 100 ohms per square paste. There is some degradation in yield for the lower aspect ratios. This is consistent with the total-spread results that indicate an increased spread for the lower aspect ratios. A more dramatic comparison of the tolerances associated with aspect ratio can be seen in FIG. 43. This is a plot of resistor value relative to the mean of the sample for each substrate investigated. Each resistor is identified by a single digit. The results in FIG. 43 (a) are for the resistors with an aspect ratio of 10 and the FIG. 43 (b) results are for an aspect ratio of 0.7 .

The effect of sheet resistivity on yield is illustrated in FIG. 44 for resistors with an aspect ratio of 2. The curve for the 100 ohms per square material gives the highest yield figures and the 1M ohm per square material has the poorest yield figures.

The substrate plots for these sheet resistivities given in FIG. 45 confirm these findings. The plot for the 100 ohm material indicates a close-packing of the resistor values about the sample mean which results in a higher yield figure for each tolerance band. The 1M ohm material exhibits close packing to a less degree and as a consequence the yield figure is worse.

5. CONCLUSIONS

The effect of aspect ratio on the as-fired resistance spread has been investigated for the material "A" paste system. It has been found that the aspect ratio plays a major role in determining the resistance spread. For aspect ratios less than 2 the spread increases dramatically.

The effect of sheet resistivity on the as-fired spread has been evaluated for paste system "A". The variations in spread that have been observed for the range of sheet resistivities investigated approaches the error limits in the experiment and cannot be considered significant.

The investigation of resistor placement on a 2" x 2" substrate indicates that the spread in resistance for resistors in the central region of the substrate is less than the spread associated with resistors near the perimeter. For close tolerance resistors, only the central (1" x 1") region should be used.

Results for the effect of resistor width on the resistance spread indicate that the spread can be improved by employing a larger width in the resistor design.

6. REFERENCES

References

1. Theodore C. Reissing, "An Overview of Today's Thick-Film Technology," Proc. IEEE, Vol. 55, No. 10, October 1971, pp 1448 - 1454.

2. J.R. Rairden, "Thick and Thin Films for Electronic Applications - Materials and Processes Review," Solid State Technology, January 1970, pp 37 - 41.

3. Roland Ho, "Electrostatic Effects on Film Resistors," Insulation/Circuits, Vol. 34, April 1971, pp 33 - 36.

4. Dr. C.Y. Kuo, "The Contact Resistance in Thick Film Resistors," Proc. 1969, Hybrid Microelectronics Symposium, Dallas, Texas, pp 236 - 270.

5. W.G. Dryden, "Achieving Consistent Results with Thick Film," Solid State Technology, September 1971, pp 54 - 57.

6. A.B. Usowski, A.J. Van Zeeland, "Characterization of a Thick Film Resistor Conduction Mechanism," International Symposium on Hybrid Microelectronics, 1972, Washington, pp 2A21 - 2A25.

7. Jennifer B. McCloghrie, "Thick Film Resistor Production Monitoring by Means of a Graphical Computer Printout," 1972 International Microelectronics Symposium, pp 2B21 - 2B225.

8. Darwin Herbst, Martin Greenfield, "Theory of Conduction in Thick Film Conductors," 1971 International Microelectronics Symposium, pp 4-7-1 - 4-7-12.

9. C.W.H. Brestow, W.L. Clough, Dr. P.L. Kirby, "Current Noise and Non-Linearity of Thick Film Resistors," 1971 International Microelectronics Symposium, pp 7-6-1 - 7-6-13.

10. George D. Lane, "Designing with High Reliability Thick Film Resistors," Second Symposium on Hybrid Microelectronics, Boston, 1967, pp 57 - 60.

11. Ralph E. Trease, Raymond L. Dietz, "Rheology of Pastes in Thick-Film Printing," Solid State Technology, January 1972, pp 39 - 43.

12. Duane R. Kobs, Donald R. Voigt, "Parametric Dependencies in Thick Film Screening," Solid State Technology, February 1971, pp 34 - 41.

References (Continued)

13. Lynn J. Brady, "The Mechanism of Conduction in Thick-Film Cermet Resistors," 1967 Electronic Components Conference, pp 238 - 246.

14. Jon A. VanHise "Process Variables in Thick-Film Resistor Fabrication", Solid State Technology, July 1970 pp 58 - 64 .

FIGURES

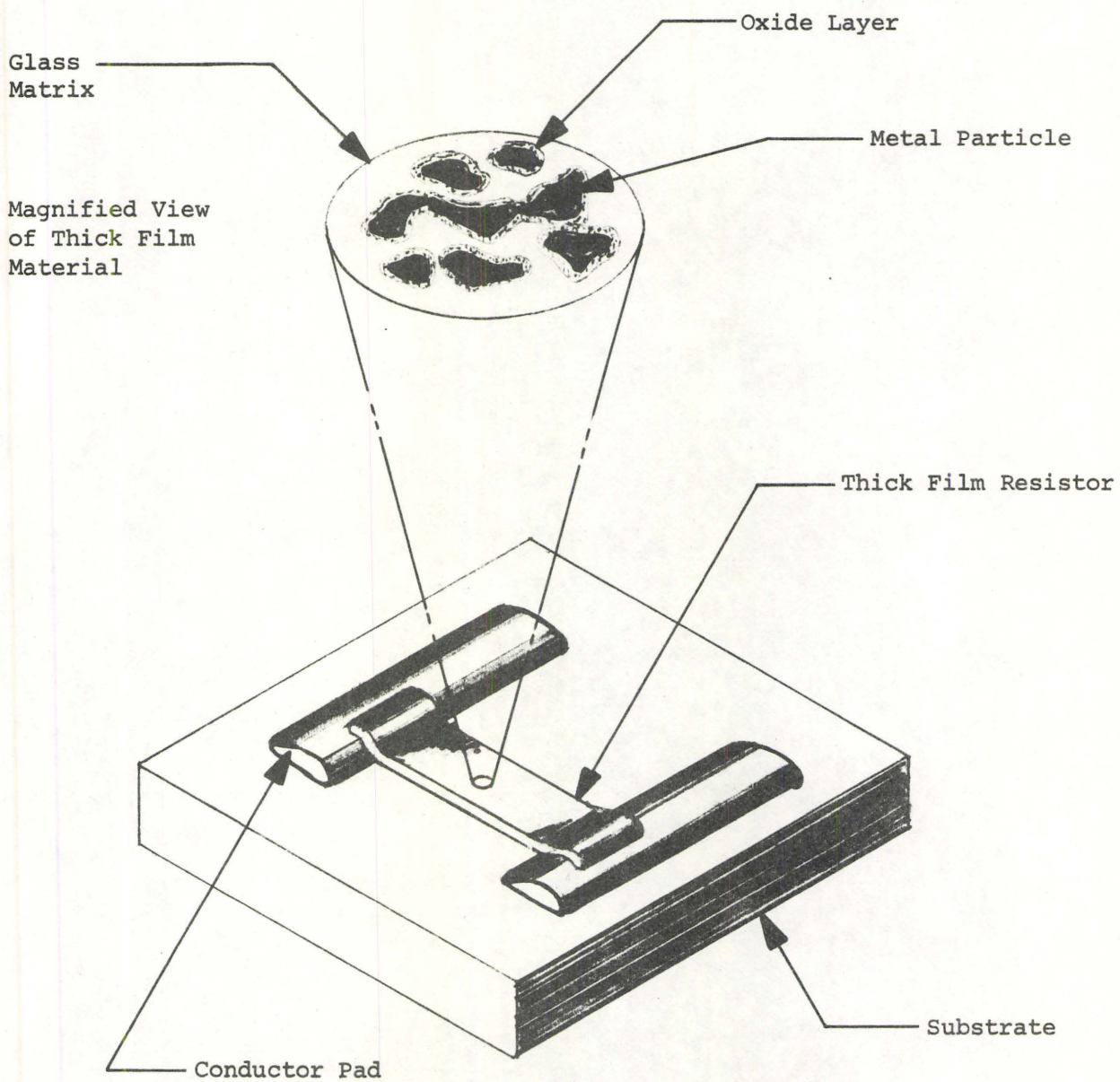

SCHEMATIC OF THE COMPOSITION IN A THICK FILM RESISTOR

FIGURE 1

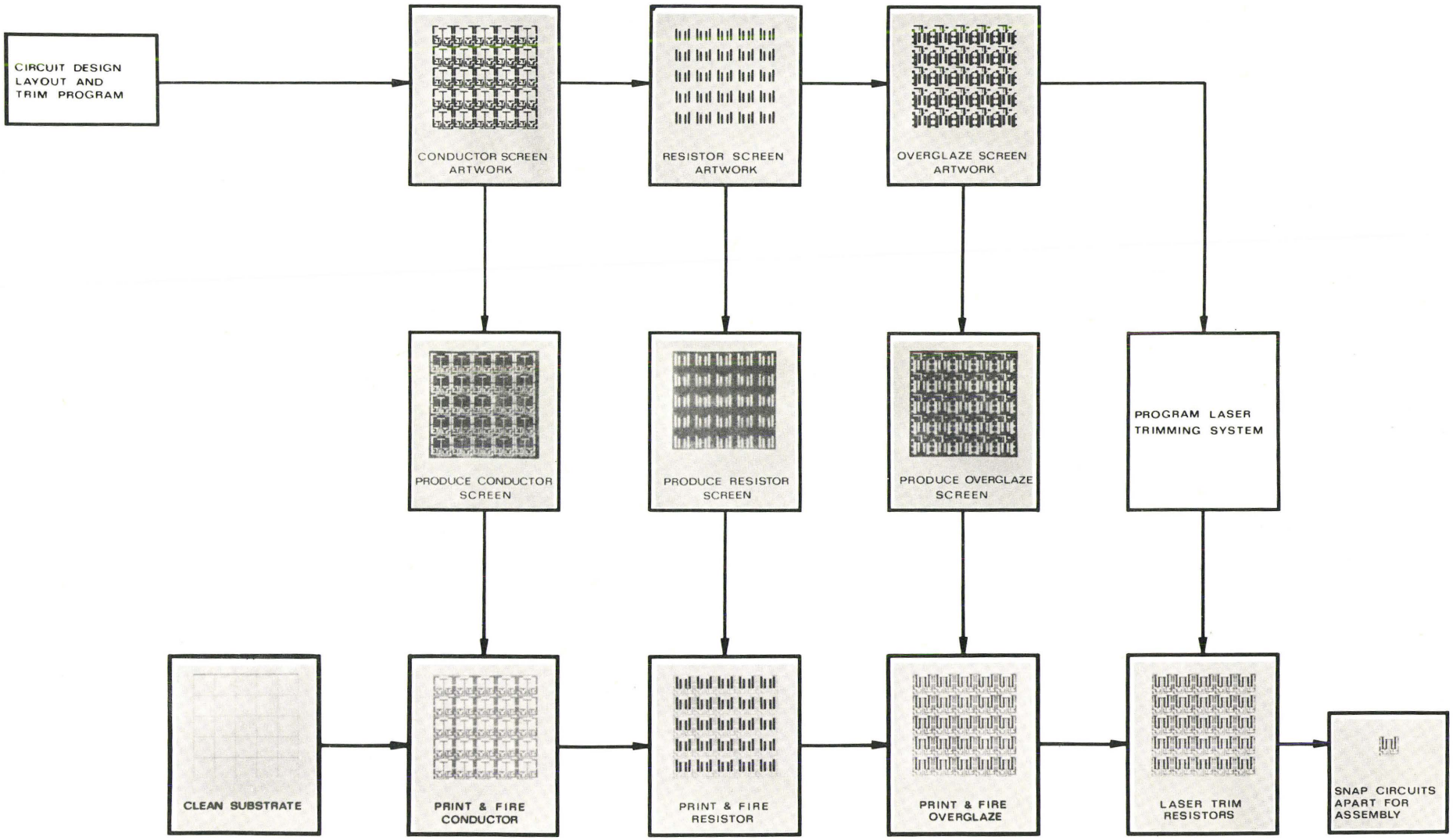

FIGURE 2

PROCESS FLOW CHART FOR THICK FILM RESISTOR DEVICES

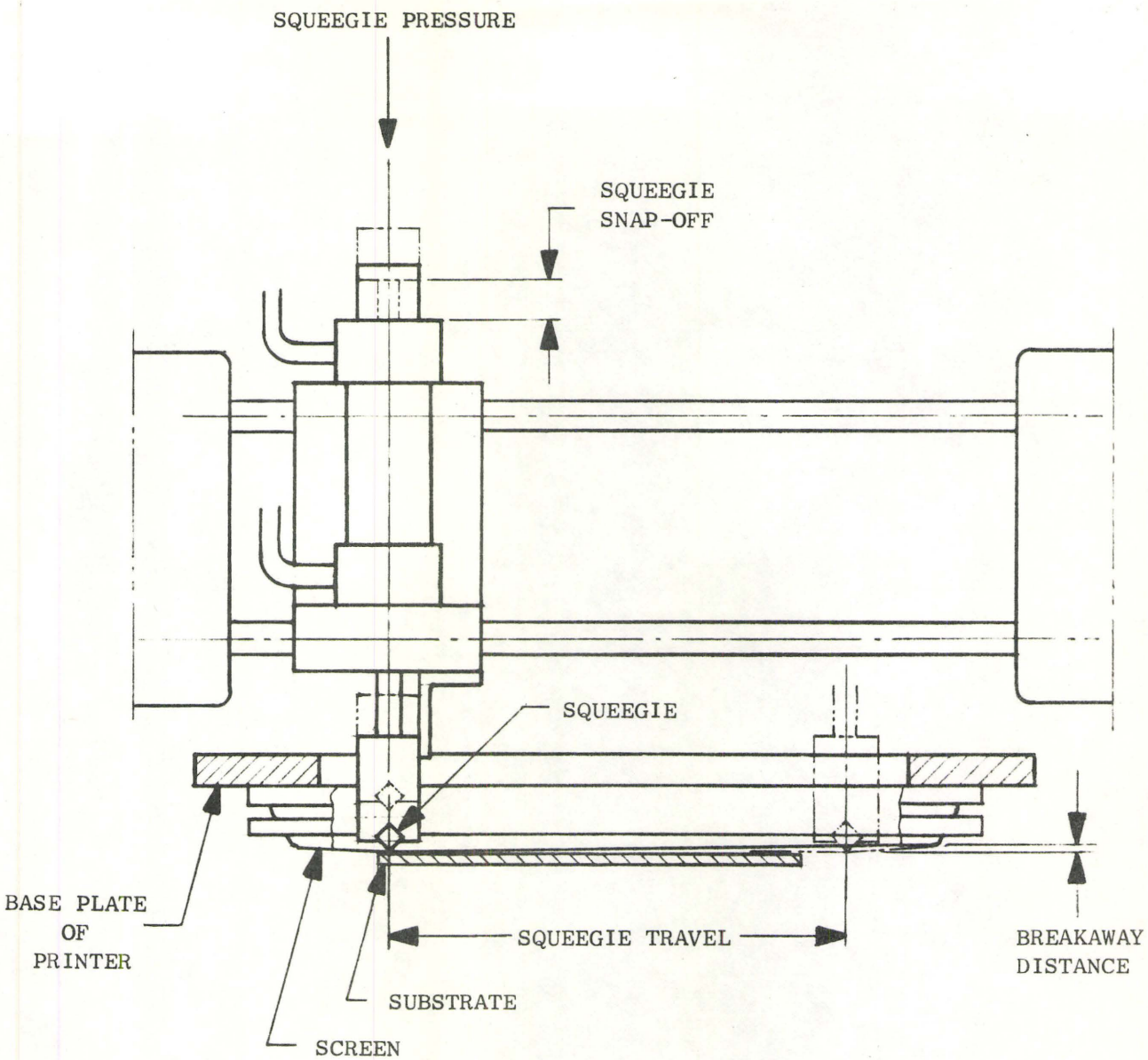

PARAMETERS FOR PRINTING EQUIPMENT

FIGURE 3

Paste (ohm/square)	Viscosity* (cps)	Mean Peak Firing Temperature** (^{o}C)
100	228,000	$T_1 + 15$
1K	285,000	$T_1 + 15$
10K	140,000	T_1
100K	160,000	$T_1 + 15$
1000K	125,000	$T_1 + 15$

* Measured with Brookfield RVT, Spindle #7, 10 RPM at 25 $\pm$ 1^{o}C

** Peak firing temperature has been coded for commercial secrecy.

Paste System	Material A
Screen Mesh Size	$\sim$ 200 squares per inch
Screen Emulsion Thickness	$\sim$ 0.001 inch
Squeegee Angle	$\sim$ 45 degrees

VALUES FOR THE PRINTER-FURNACE PARAMETERS

FIGURE 4

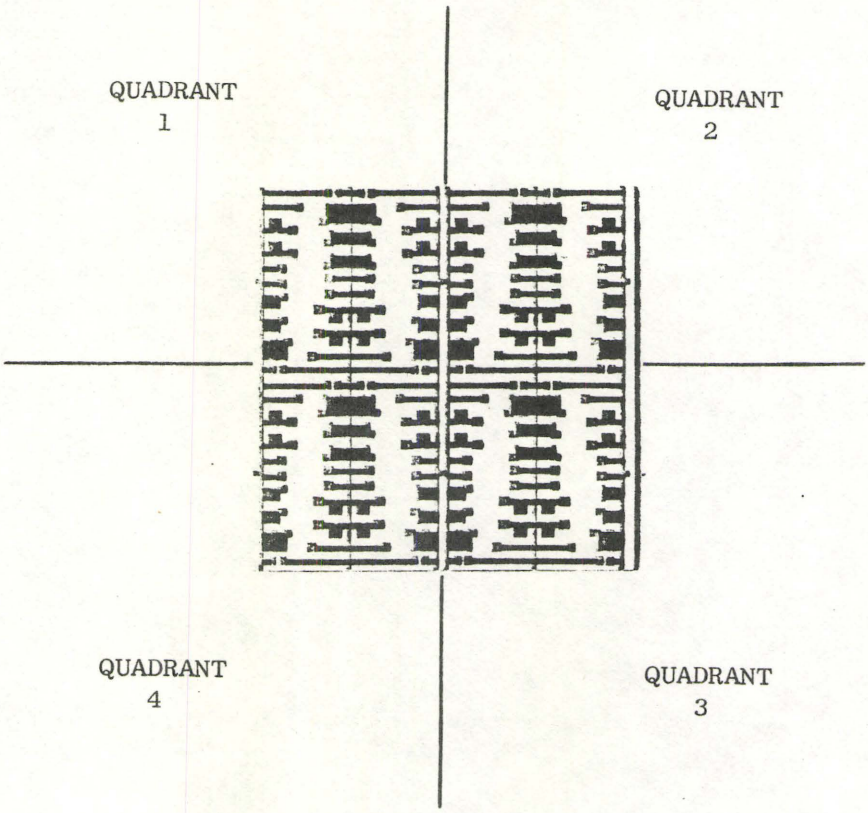

ILLUSTRATION OF TEST PATTERN RK1101

FIGURE 5(a)

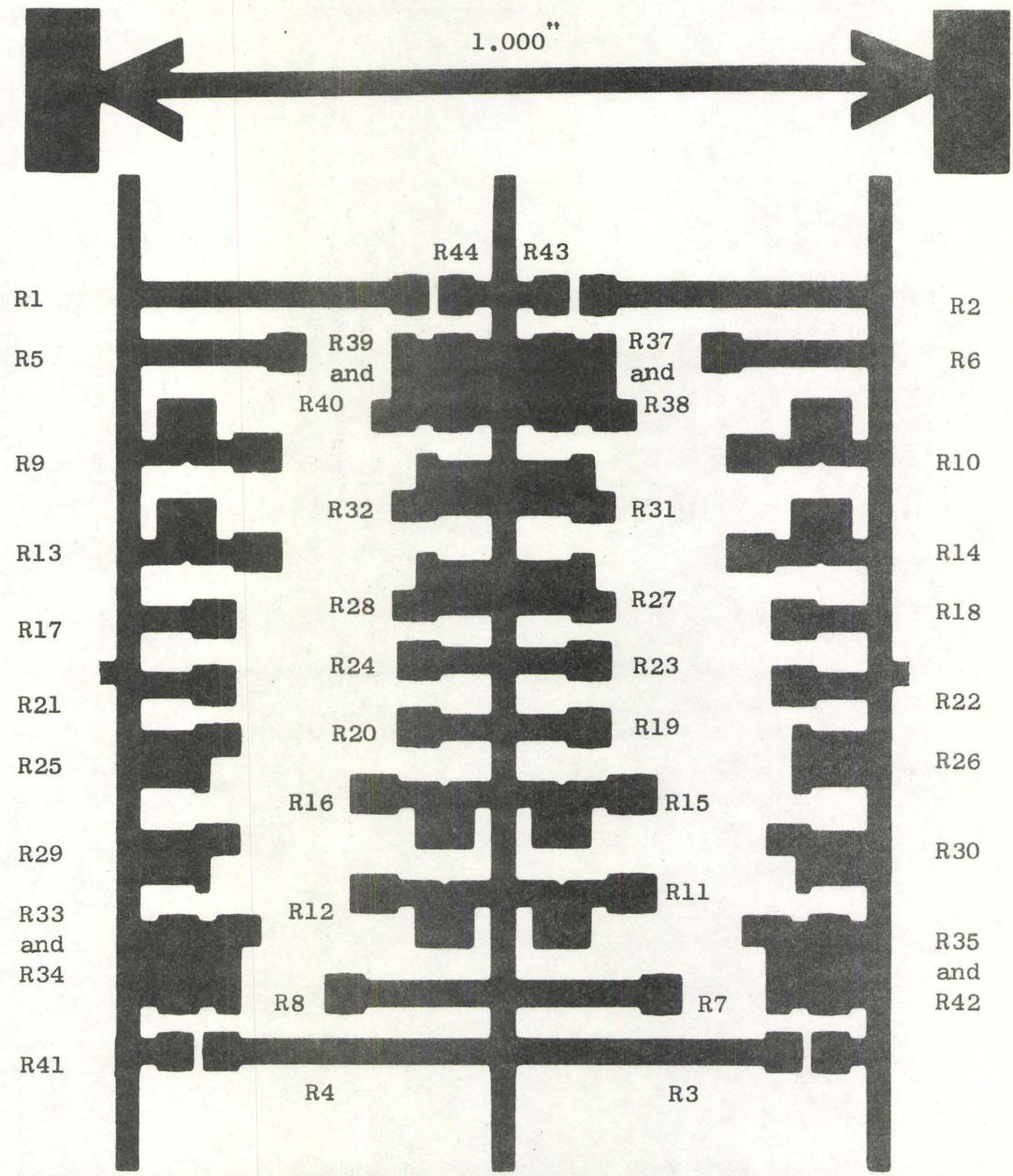

RESISTOR IDENTIFICATION IN A QUADRANT
OF TEST PATTERN RK1101

FIGURE 5(b)

(A) Equipment for Measuring Resistors Below 10 M Ohms

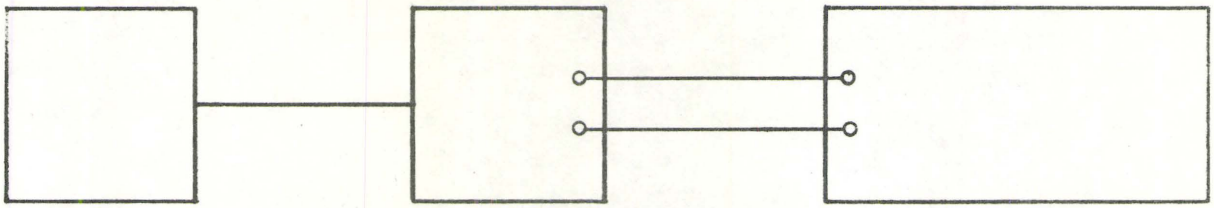

(B) Equipment for Measuring Resistors Above 10 M Ohms

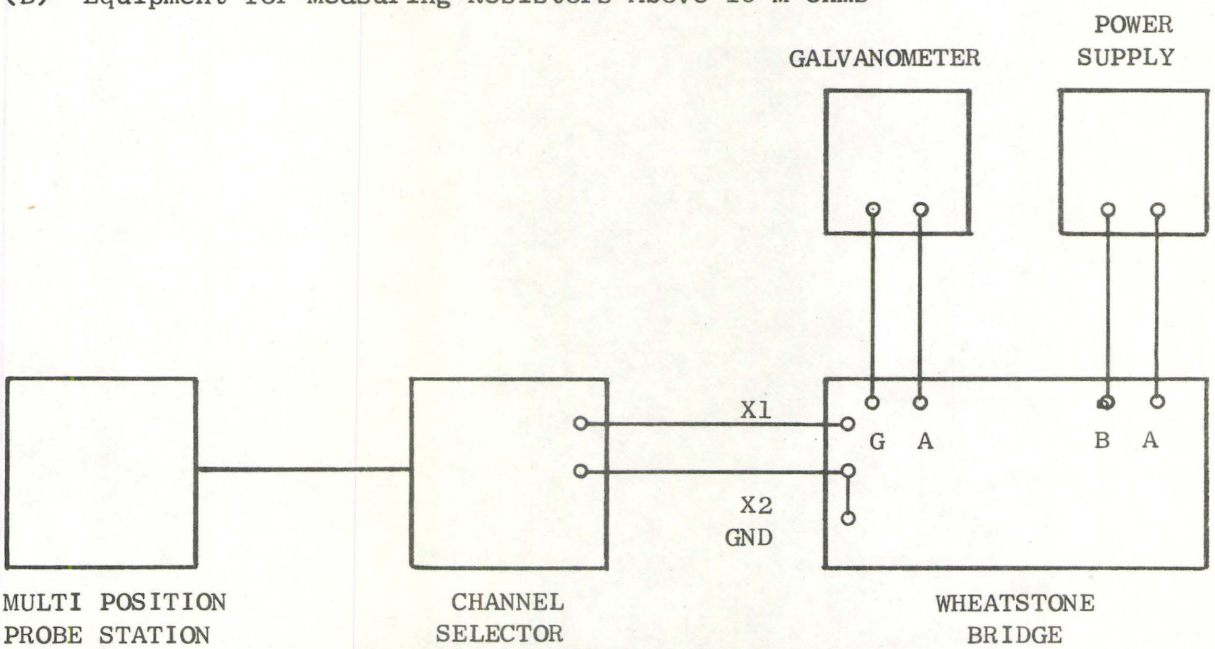

EQUIPMENT USED TO MEASURE RESISTANCE

FIGURE 6

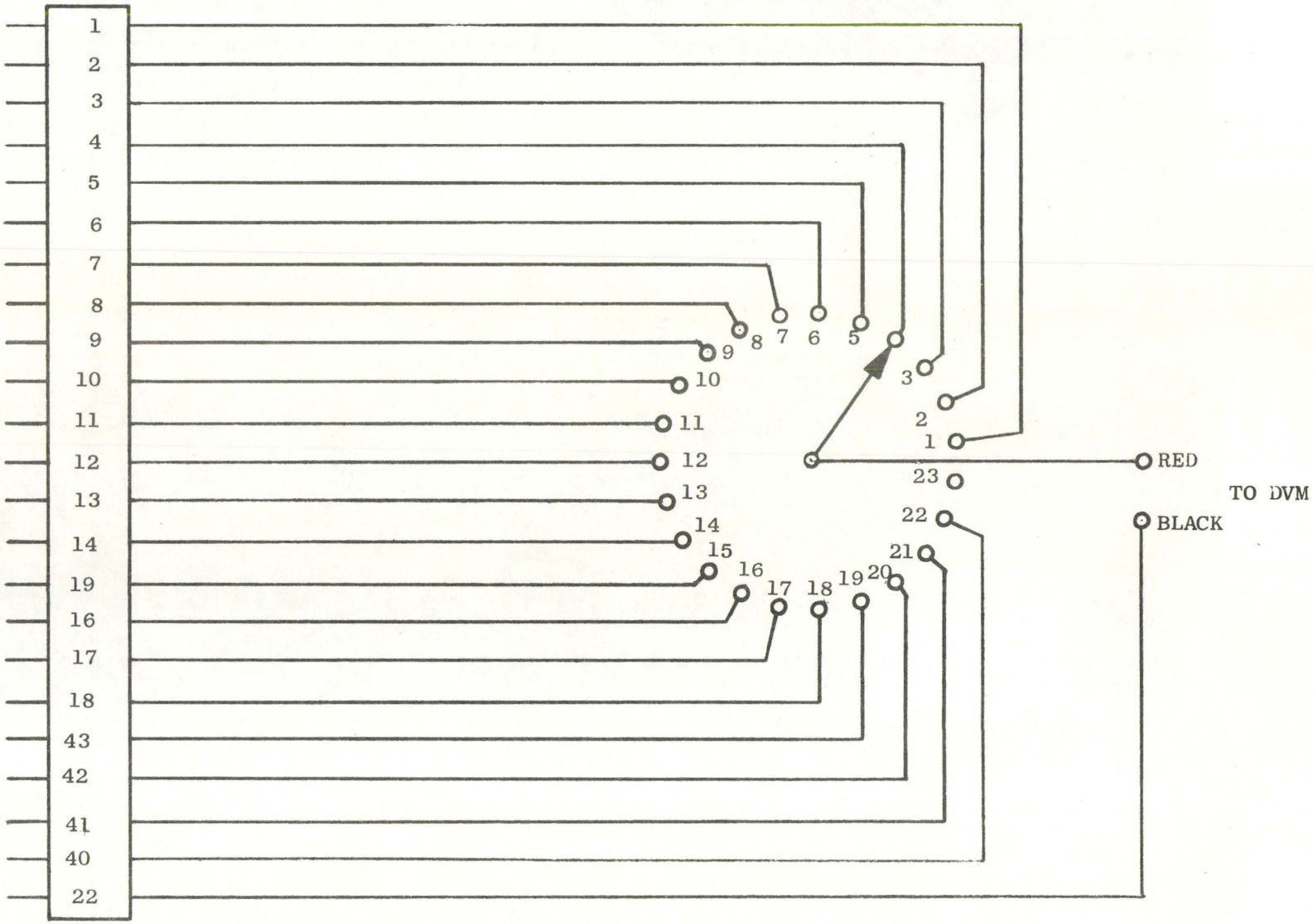

SCHEMATIC FOR CHANNEL SELECTOR

FIGURE 7

T A B L E O N E

TOLERANCE STUDY
TEST PATTERN RK 1101
ASPECT RATIO = 10
WIDTH = 30 MIL
RESISTORS 1-R1 TO 2-R2
RESISTOR PASTE = 100 OHMS PER SQUARE

TOTAL MEAN = 1052. TOTAL STAN.DEV.= 88.

SUBSTRATE NO.	MEAN	STAN. DEV.	
1	1132.	78.	
2	1057.	21.	
3	1069.	66.	
4	1016.	101.	
5	1034.	30.	
6	979.	92.	
7	1106.	70.	
8	1031.	64.	
9	1064.	65.	
10	1041.	44.	INVESTIGATION
11	1049.	95.	OF A GROUP OF
12	1006.	113.	EIGHT RESISTORS
13	974.	96.	ON TWENTY-FIVE
14	1098.	44.	SUBSTRATES
15	1063.	67.	
16	1081.	32.	
17	1054.	88.	
18	1024.	89.	
19	1006.	104.	
20	1045.	39.	
21	1096.	74.	
22	1057.	89.	
23	1065.	29.	
24	978.	98.	
25	1177.	66.	

RESISTOR NO.	MEAN	STAN. DEV.	
1	986.	140.	INVESTIGATION
2	1088.	94.	OF SIMILAR
3	1062.	66.	RESISTORS ON
4	1003.	119.	TWENTY-FIVE
5	1043.	35.	SUBSTRATES
6	1080.	33.	
7	1059.	24.	
8	1095.	38.	

SAMPLE OF THE STATISTICS FOR RESULTS
OF AN EXPERIMENT

FIGURE 8

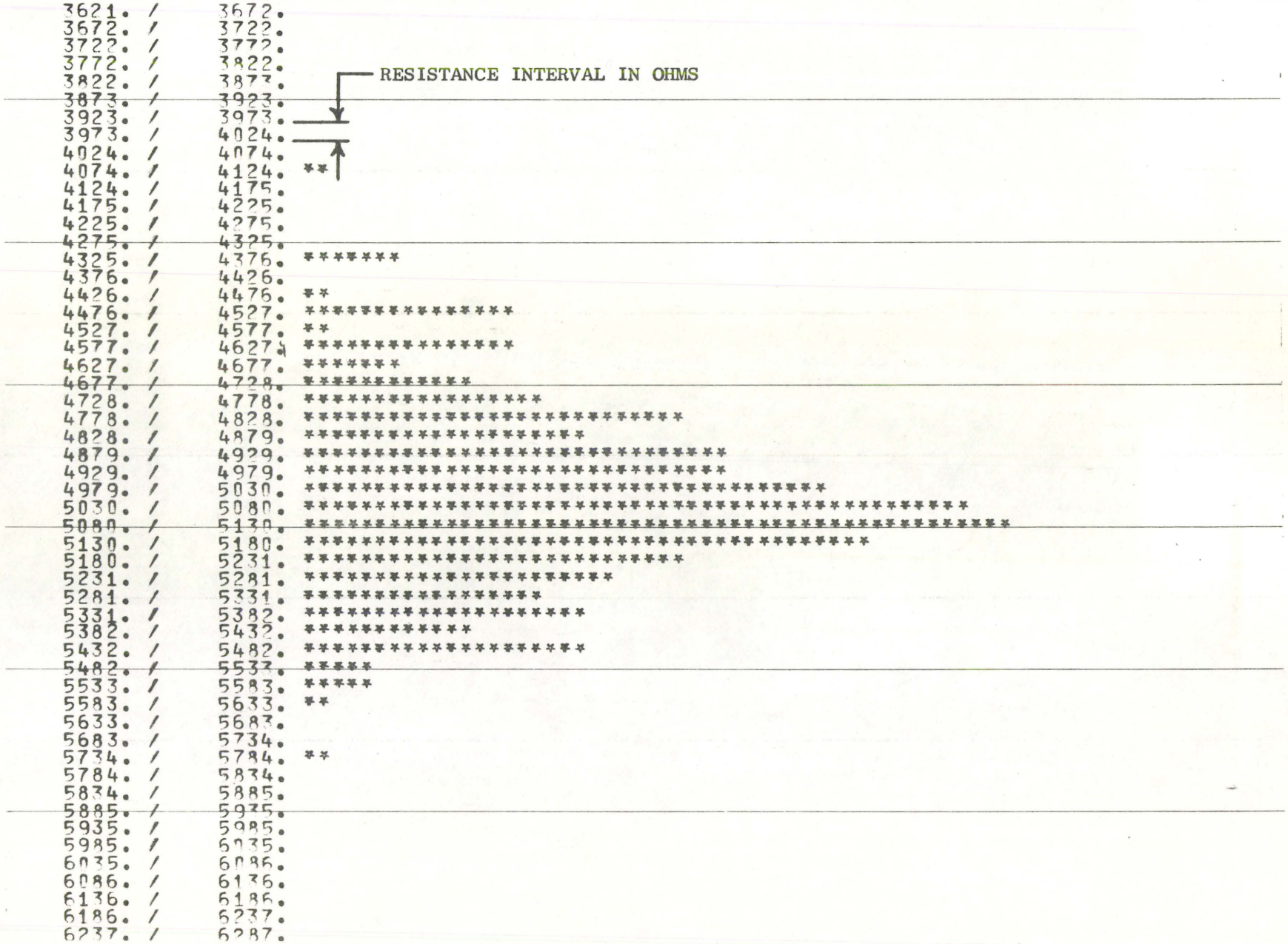

SAMPLE OUTPUT OF THE HISTOGRAM ROUTINE

FIGURE 9

DEVIATION FROM THE MEAN (%)

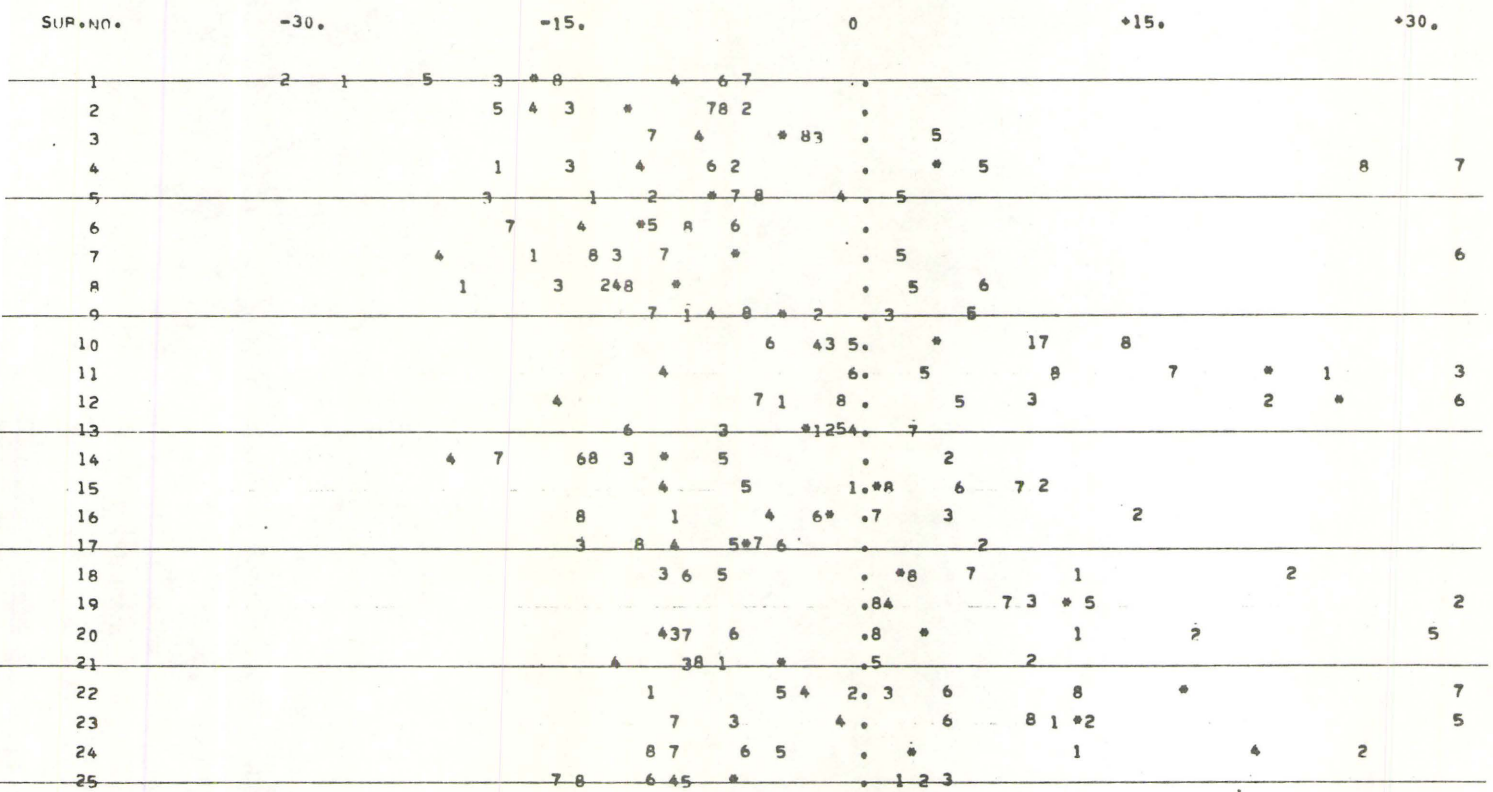

EACH RESISTOR
IS IDENTIFIED BY
A SINGLE DIGIT
(eg. 2 = 1-R2)

SAMPLE OUTPUT OF THE SUBSTRATE PLOT

FIGURE 10

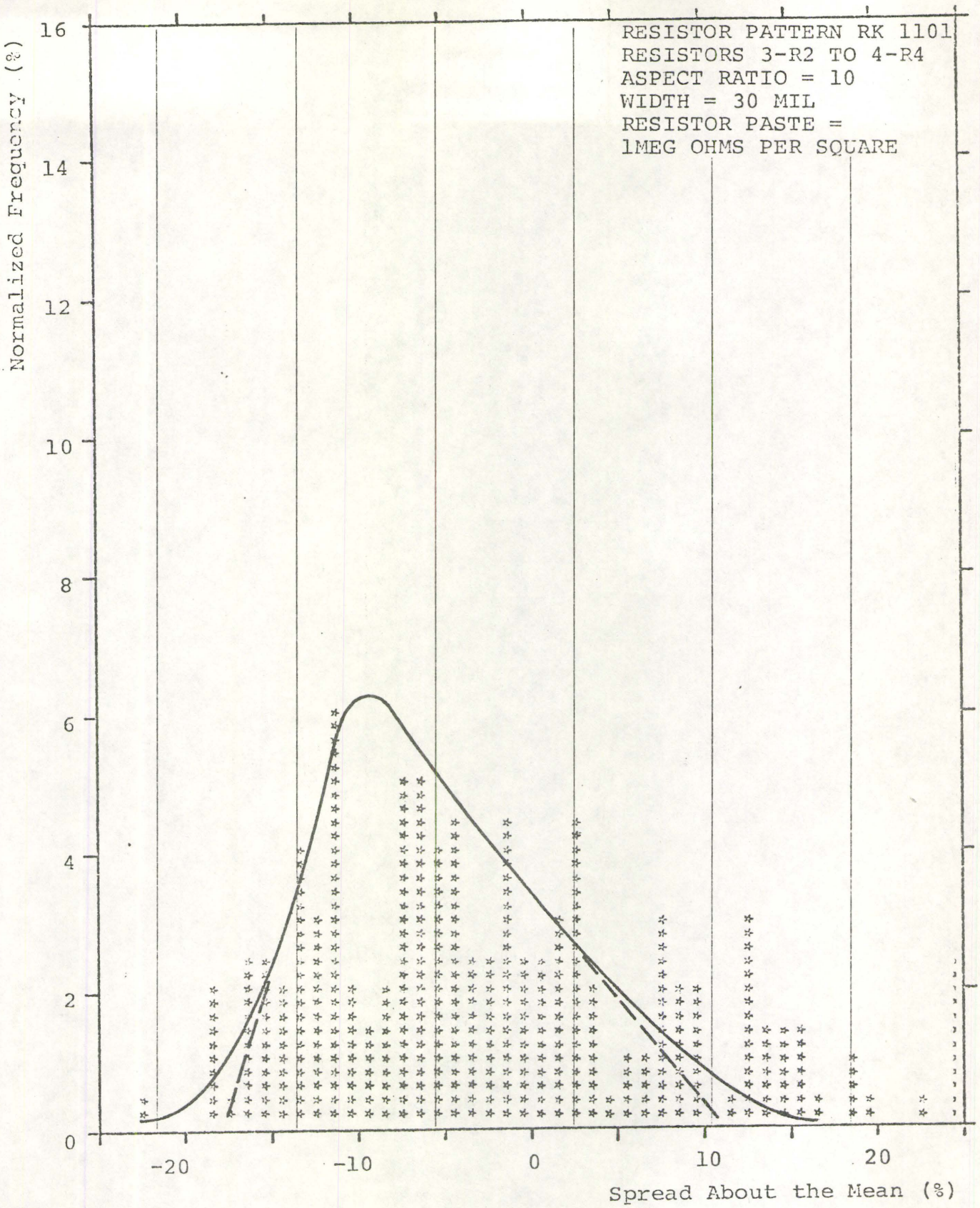

BEST VISUAL FIT OF HISTOGRAM RESULTS

FIGURE 11

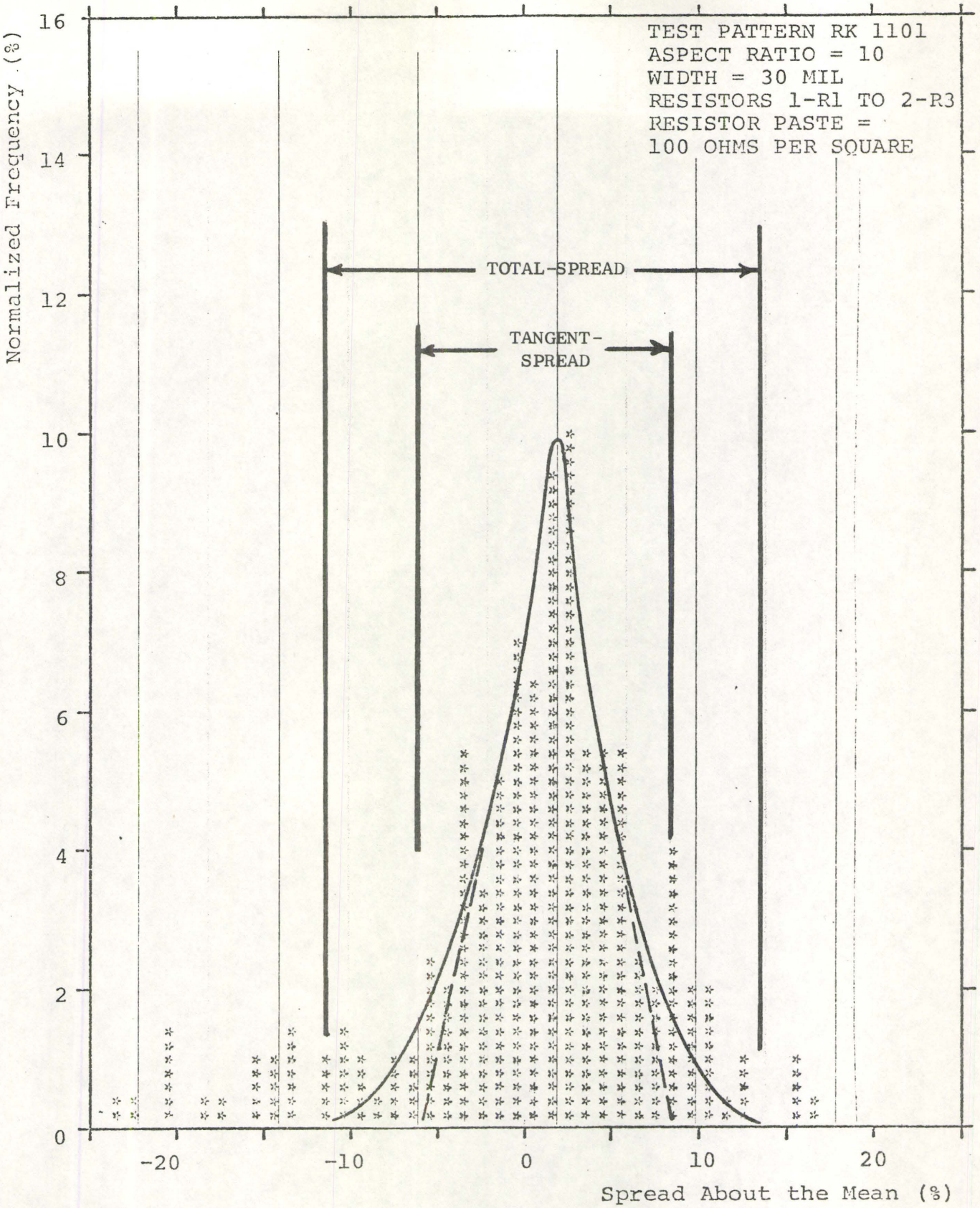

ILLUSTRATUON OF TOTAL-SPREAD AND TANGENT-SPREAD

FIGURE 12

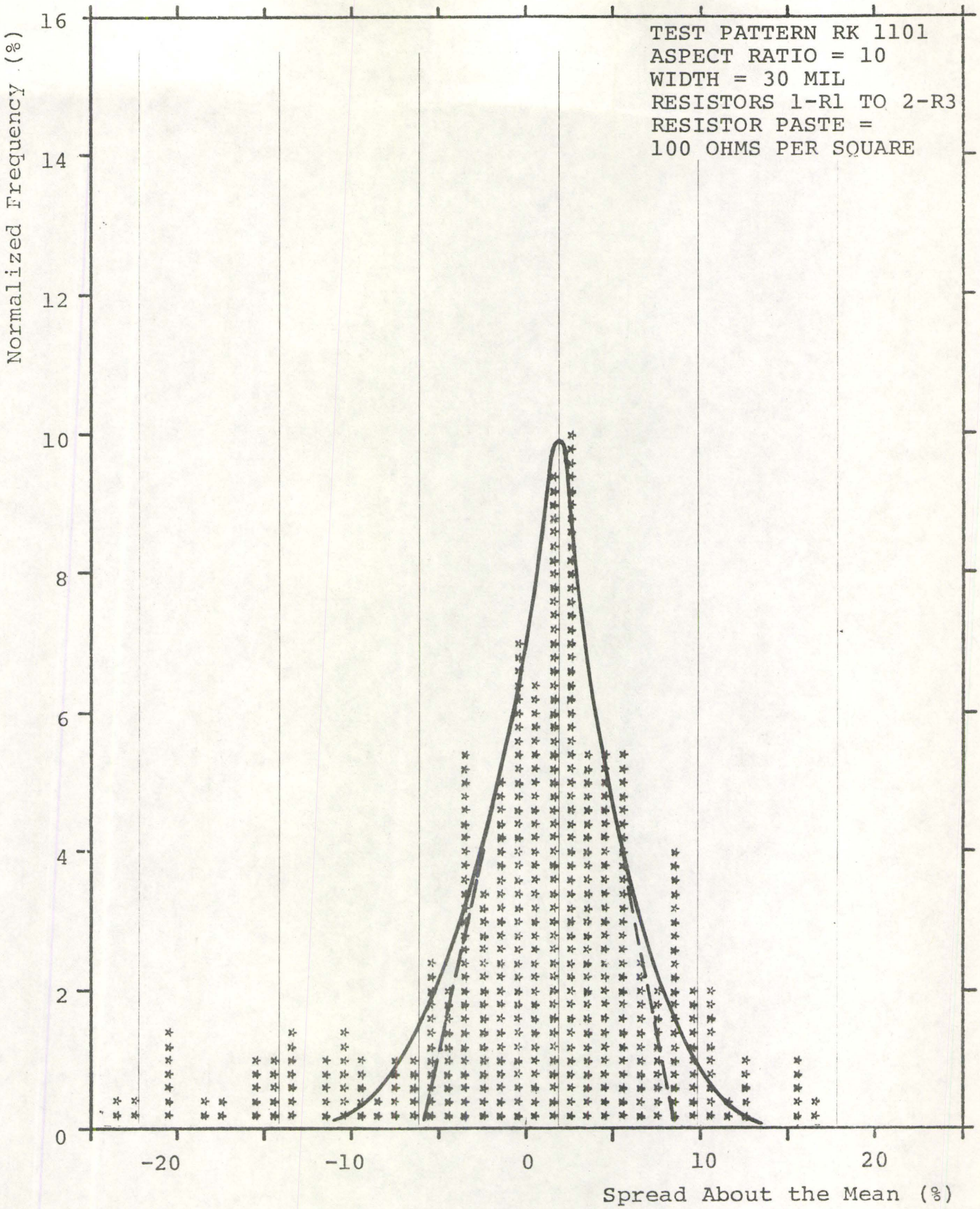

RESISTANCE DISTRIBUTION FOR ASPECT RATIO 10
AND 100 OHMS PER SQUARE MATERIAL

FIGURE 13

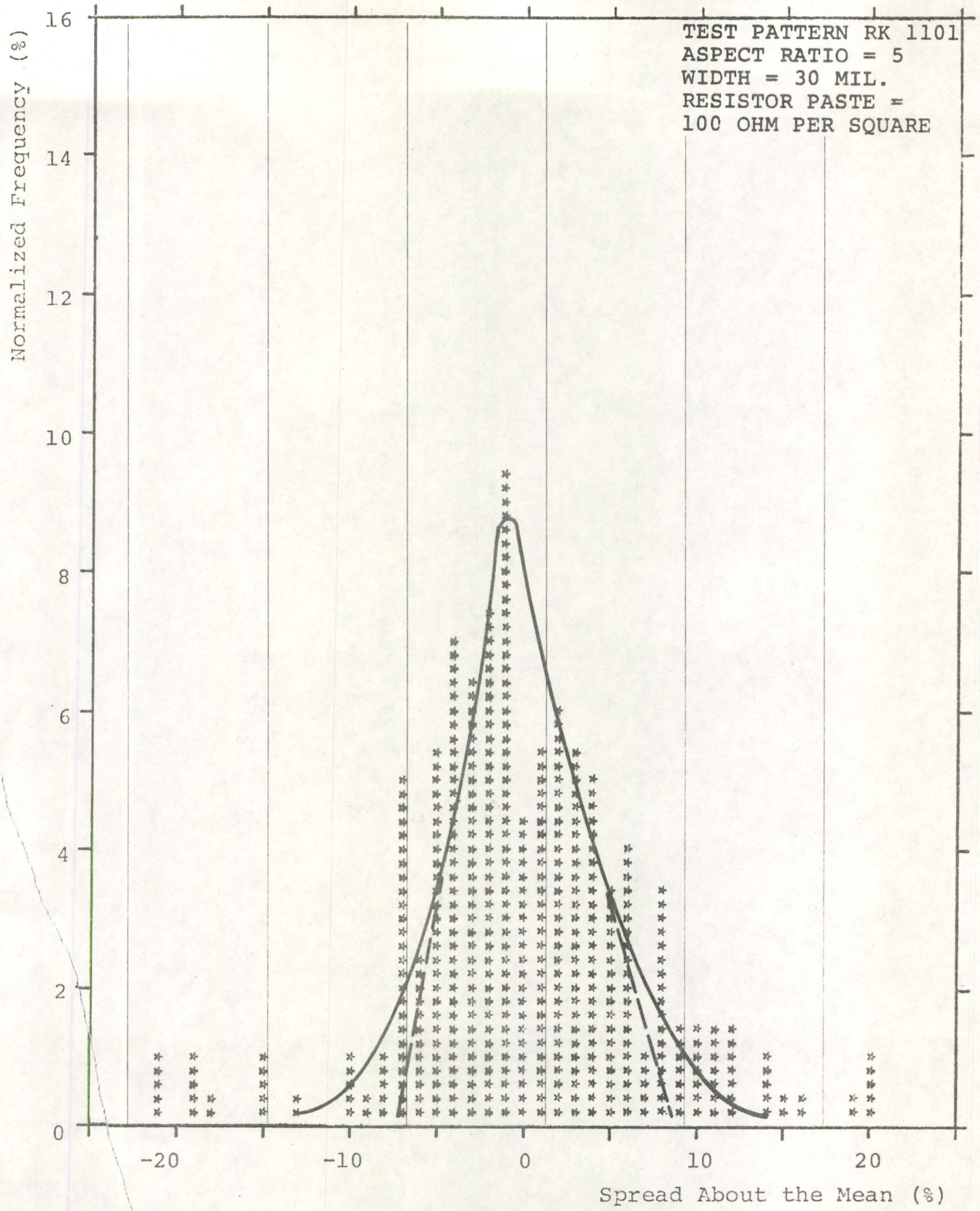

RESISTANCE DISTRIBUTION FOR ASPECT RATIO 5
AND 100 OHMS PER SQUARE MATERIAL

FIGURE 14

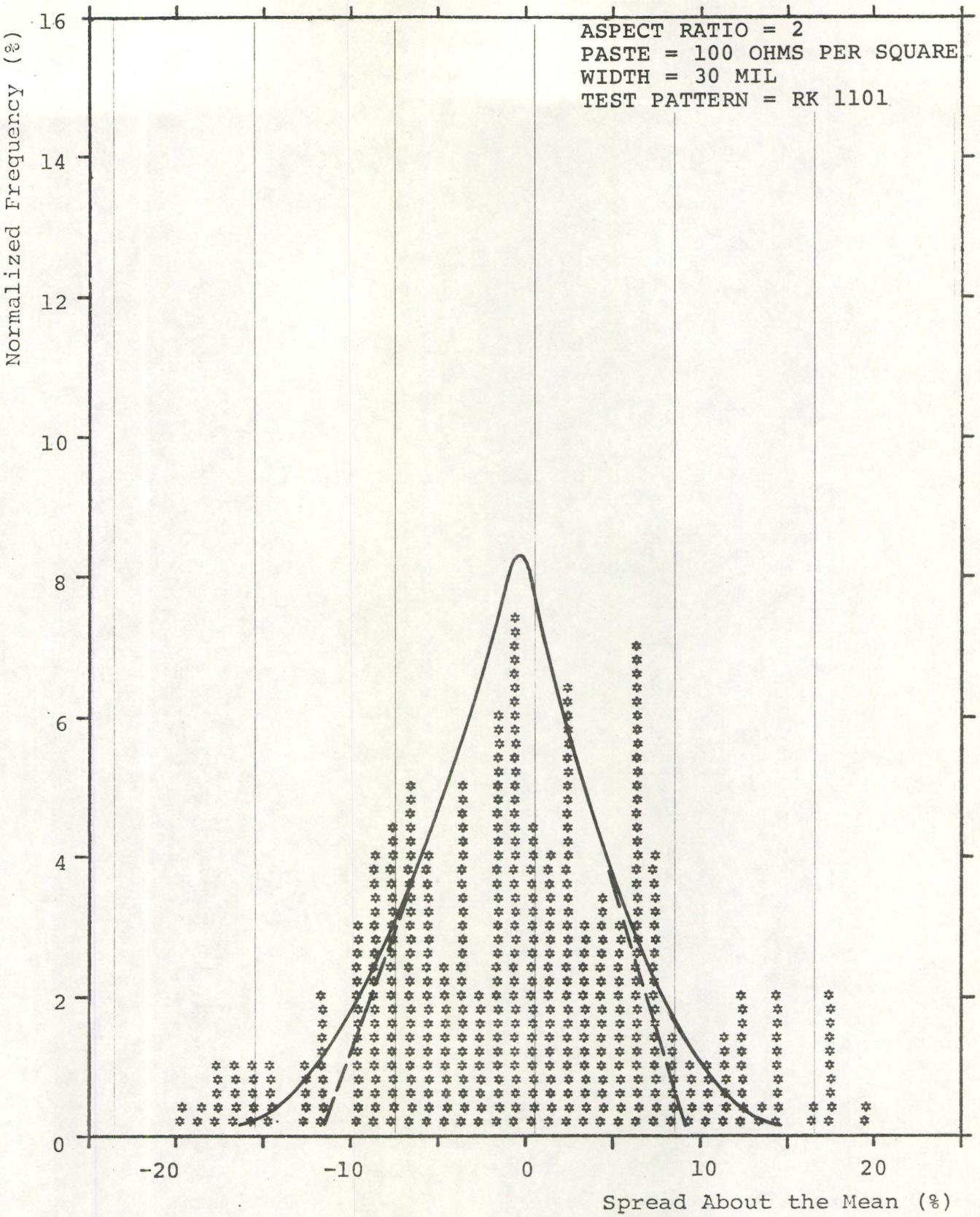

RESISTANCE DISTRIBUTION FOR ASPECT RATIO 0.7
AND 100 OHM PER SQUARE MATERIAL

FIGURE 15

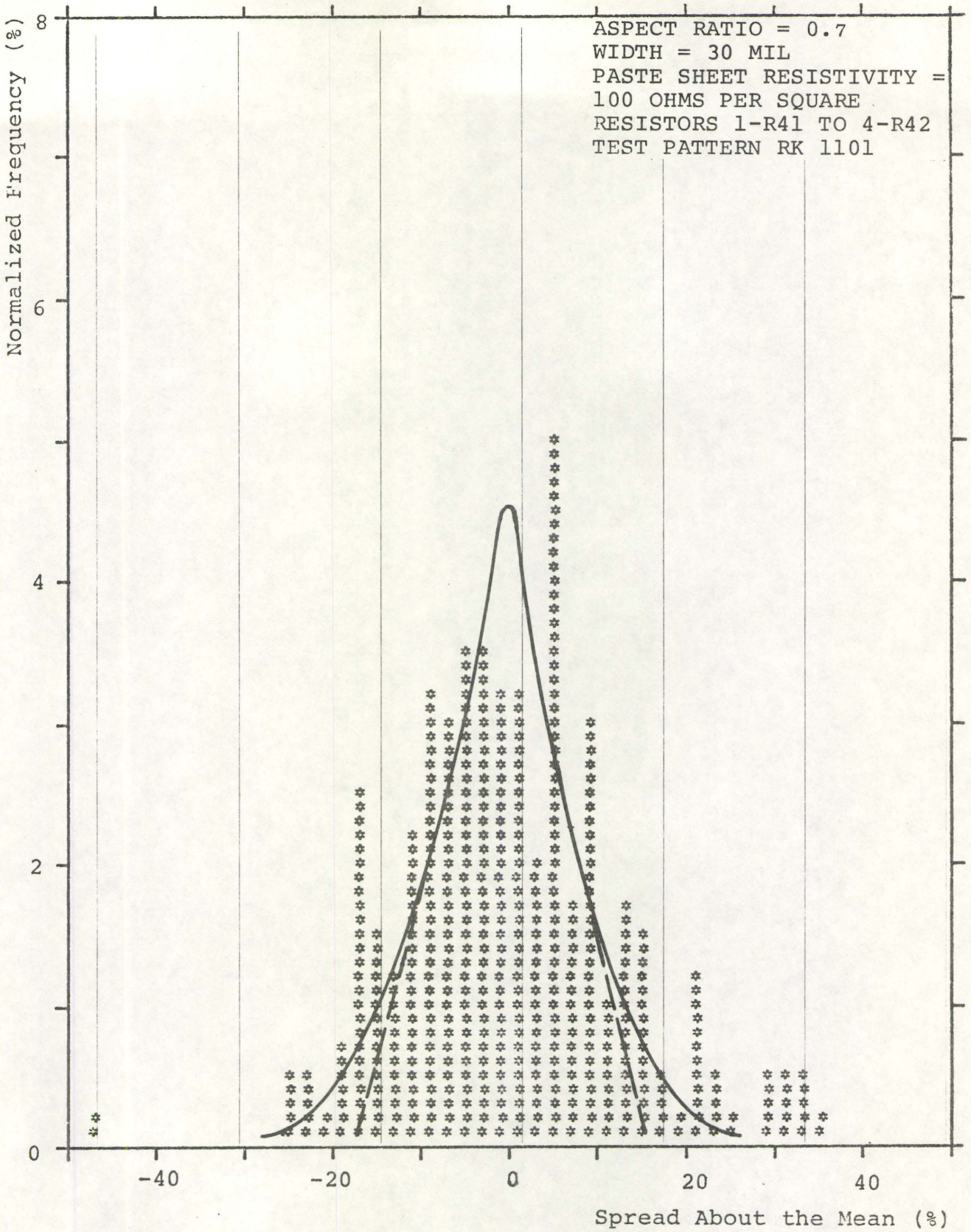

RESISTANCE DISTRIBUTION FOR ASPECT RATIO 0.7
AND 100 OHM PER SQUARE MATERIAL

FIGURE 16

Aspect Ratio	Resistors Investigated	
10	1-R1	1-R2
	2-R1	2-R2
	1-R4	1-R3
	2-R4	2-R3
5	1-R5	1-R6
	2-R5	2-R6
	1-R8	1-R7
	2-R8	2-R7
2	1-R17	1-R21
	1-R18	1-R22
	2-R17	2-R21
	2-R18	2-R22
0.7	1-R41	1-R42
	2-R41	2-R42
	4-R41	4-R42
	3-R41	3-R42

RESISTORS INVESTIGATED FOR EACH ASPECT RATIO
FOR THE 100 OHM PER SQUARE MATERIAL

FIGURE 17

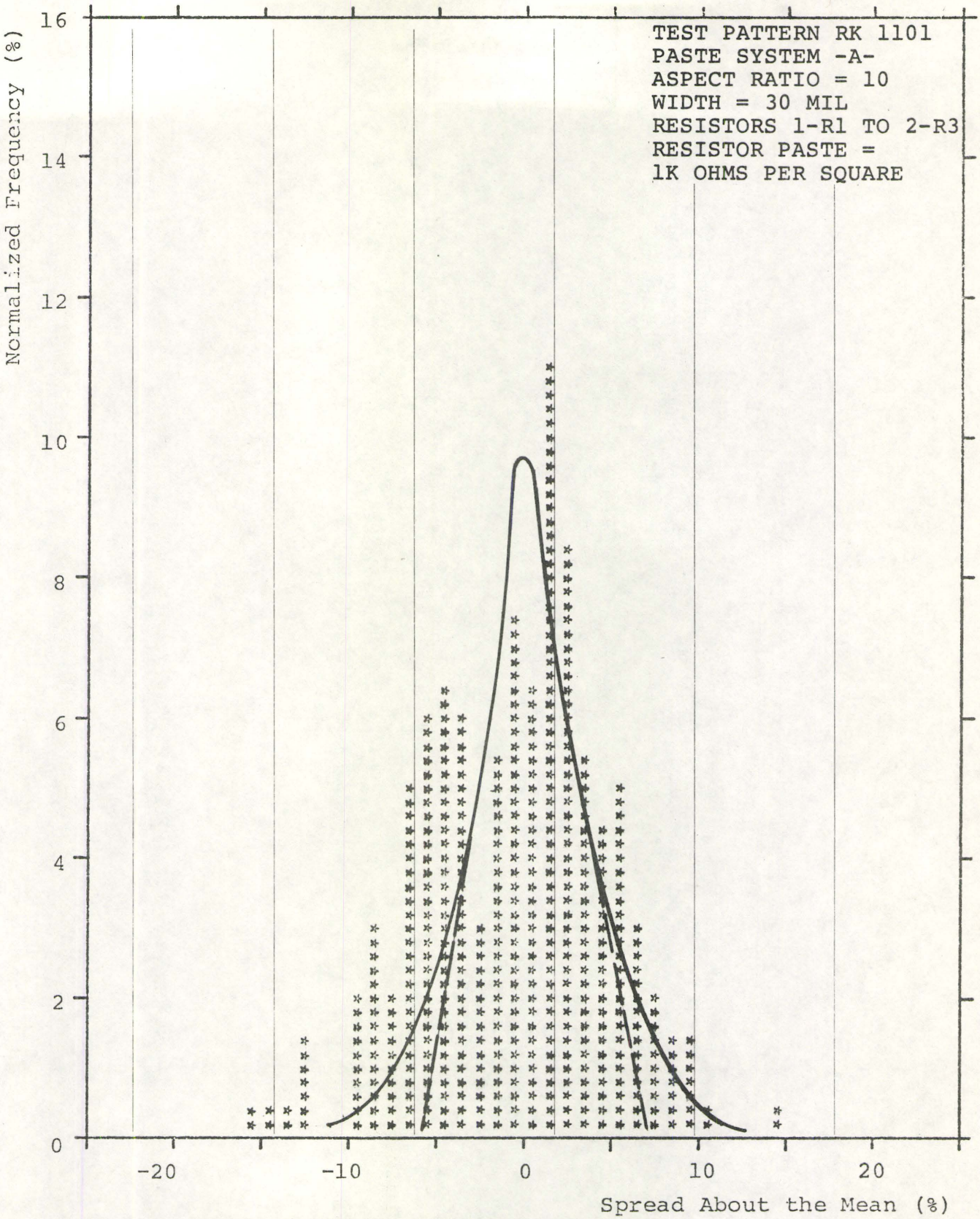

RESISTANCE DISTRIBUTION FOR ASPECT RATIO 10
AND 1K OHM PER SQUARE MATERIAL

FIGURE 18

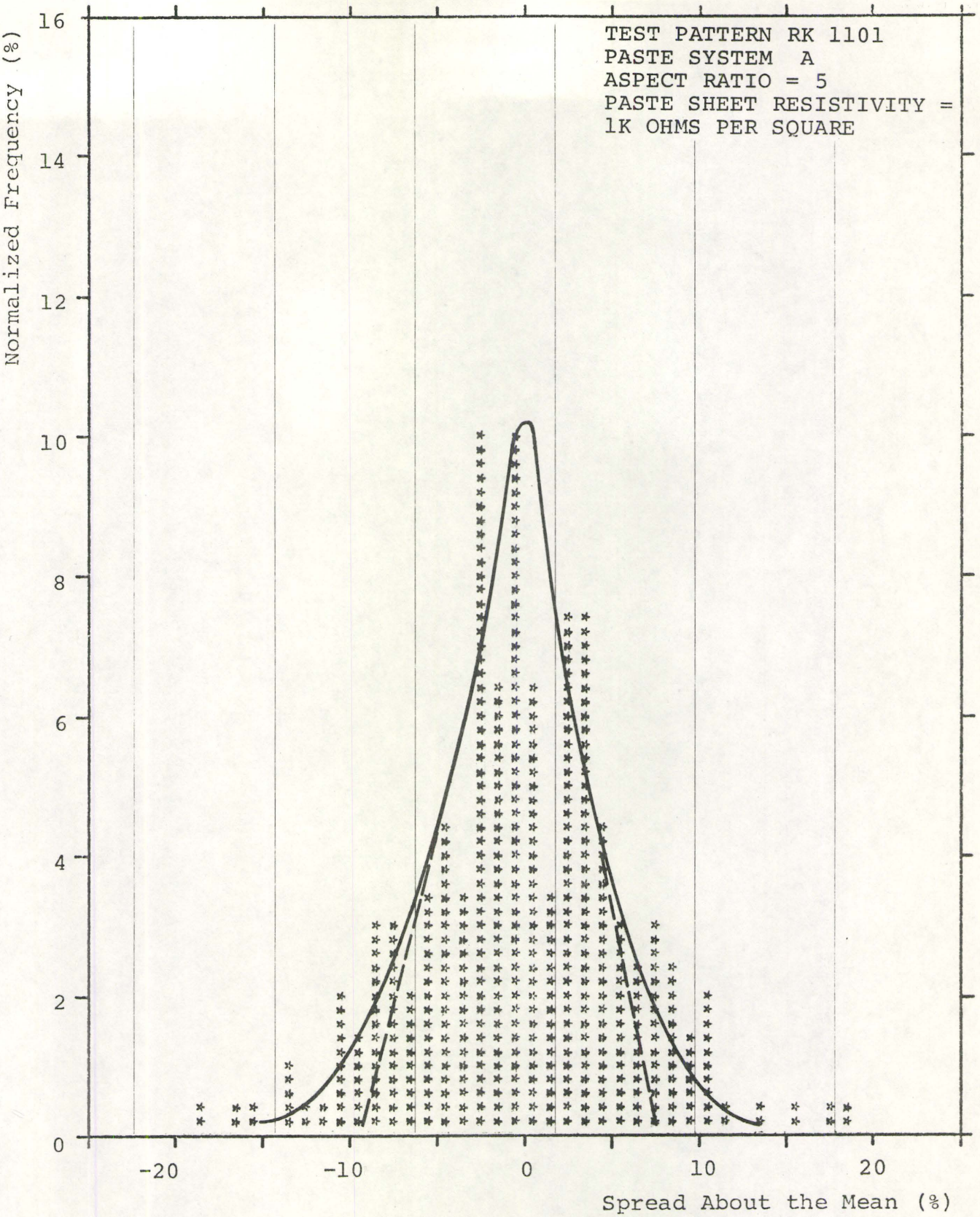

RESISTANCE DISTRIBUTION FOR ASPECT RATIO 5
AND 1K OHM PER SQUARE MATERIAL

FIGURE 19

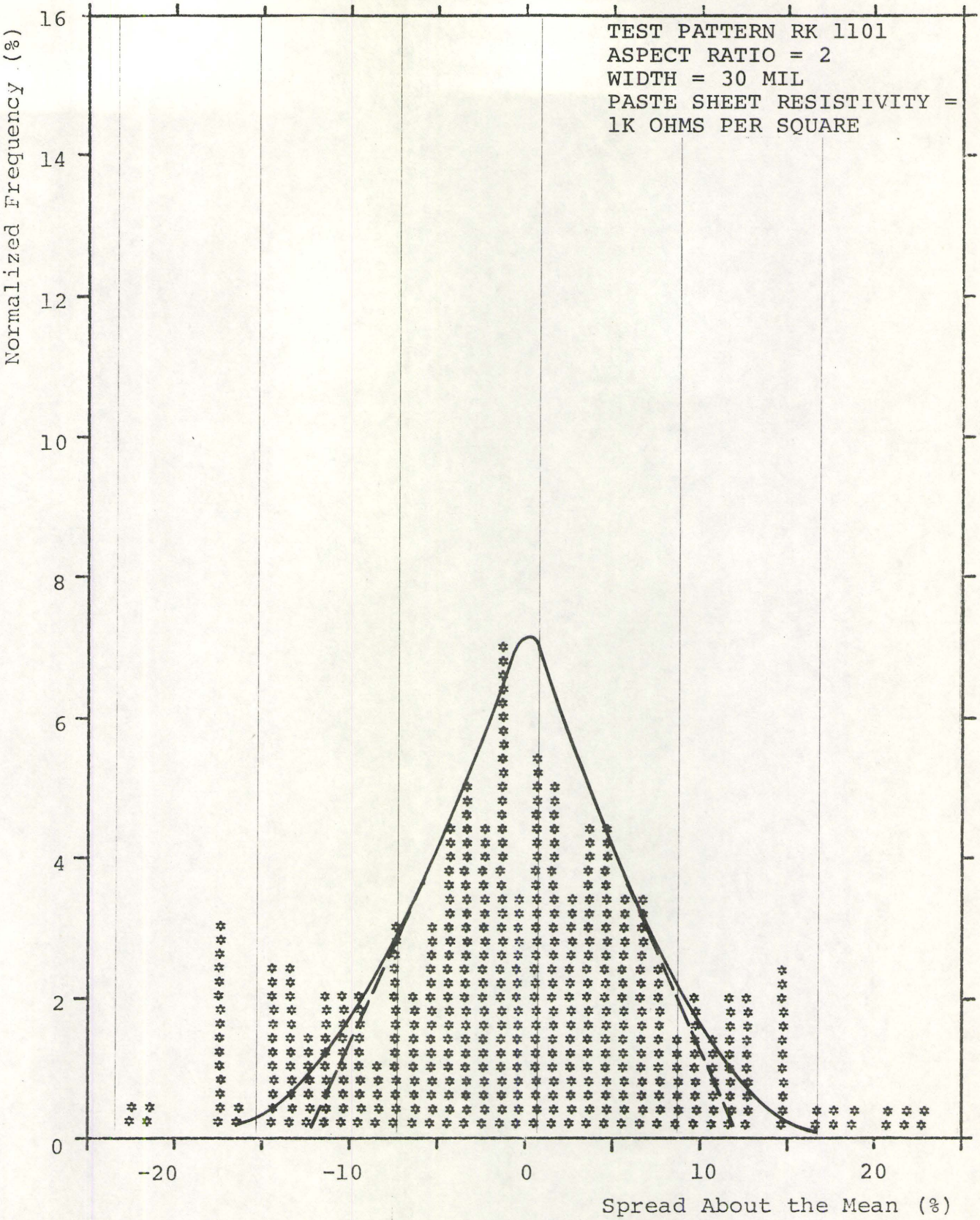

RESISTANCE DISTRIBUTION FOR ASPECT RATIO 2
AND 1K OHM PER SQUARE MATERIAL

FIGURE 20

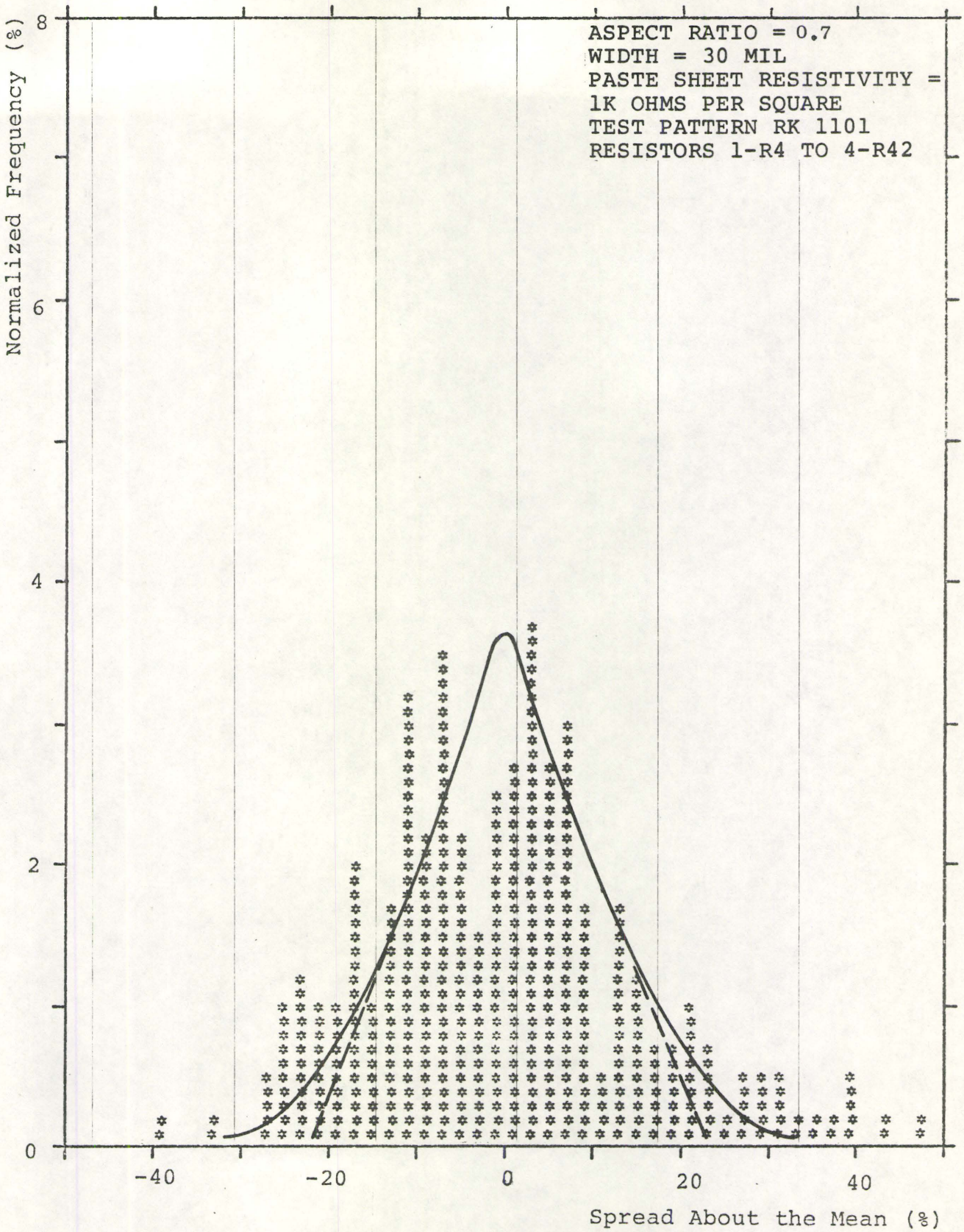

RESISTANCE DISTRIBUTION FOR ASPECT RATIO 0.7
AND 1K OHM PER SQUARE MATERIAL

FIGURE 21

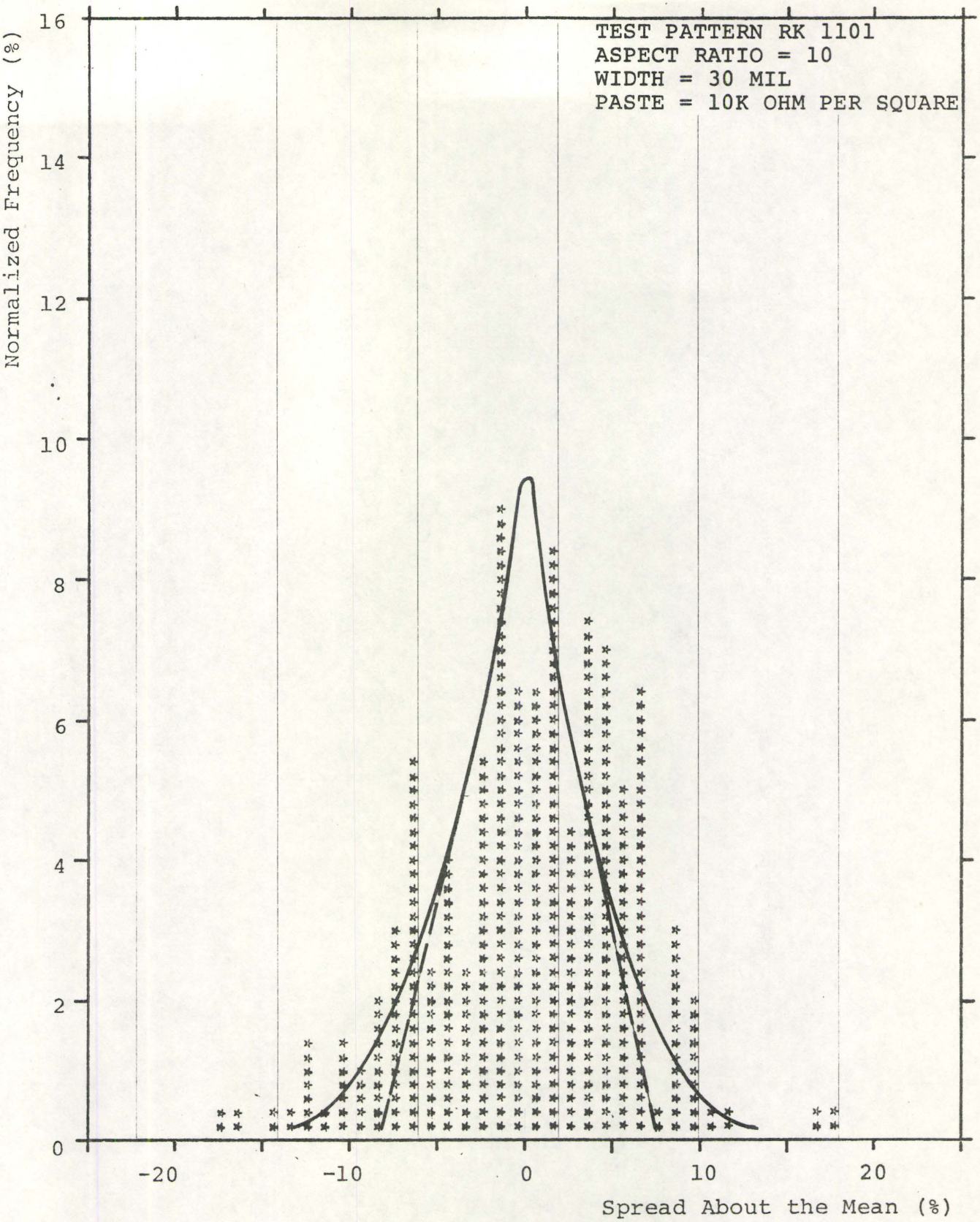

RESISTANCE DISTRIBUTION FOR ASPECT RATIO 10
AND 10K OHM PER SQUARE MATERIAL

FIGURE 22

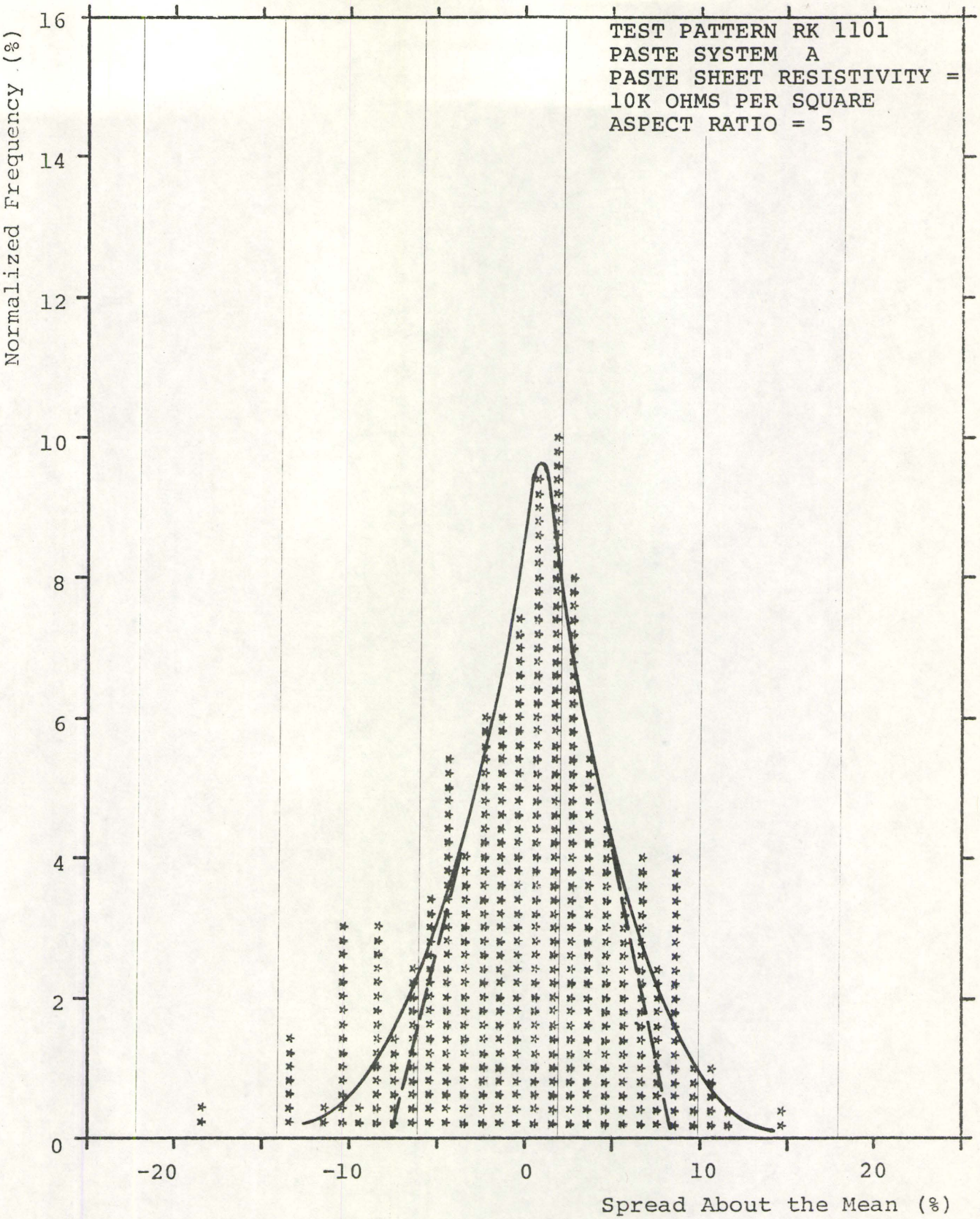

RESISTANCE DISTRIBUTION FOR ASPECT RATIO 5
AND 10K OHM PER SQUARE MATERIAL

FIGURE 23

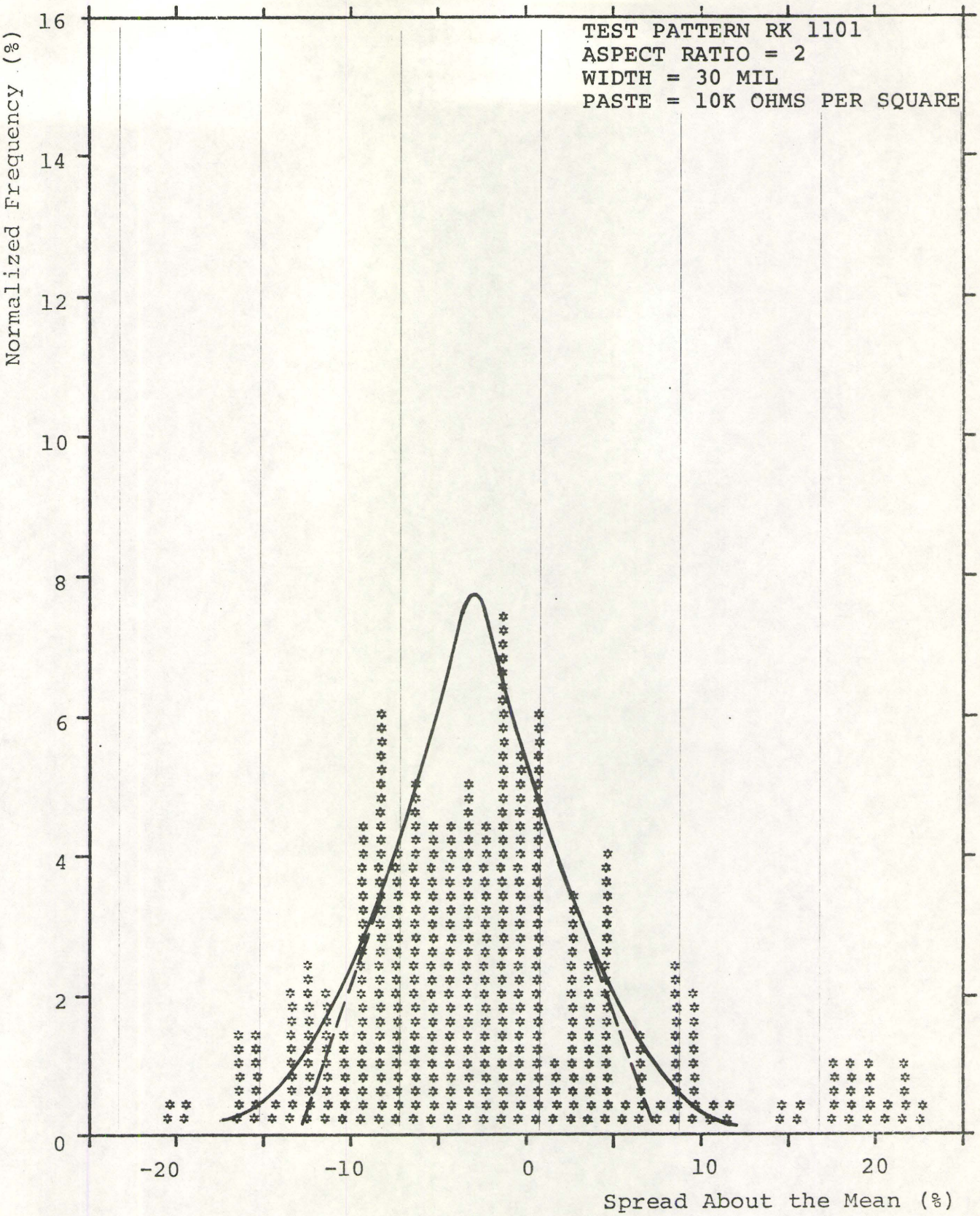

RESISTANCE DISTRIBUTION FOR ASPECT RATIO 2
AND 10K OHM PER SQUARE MATERIAL

FIGURE 24

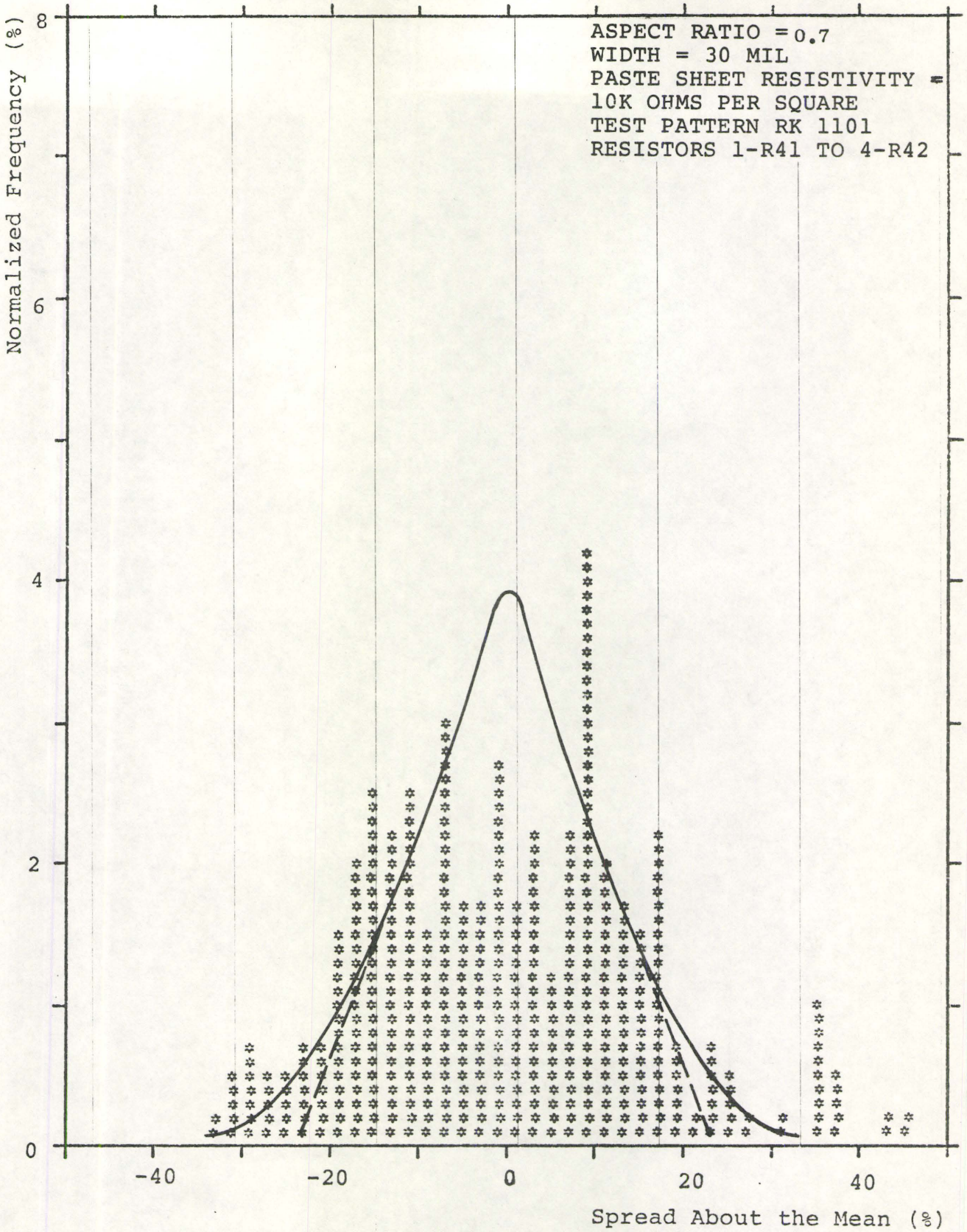

RESISTANCE DISTRIBUTION FOR ASPECT RATIO 0.7
AND 10K OHM PER SQUARE MATERIAL

FIGURE 25

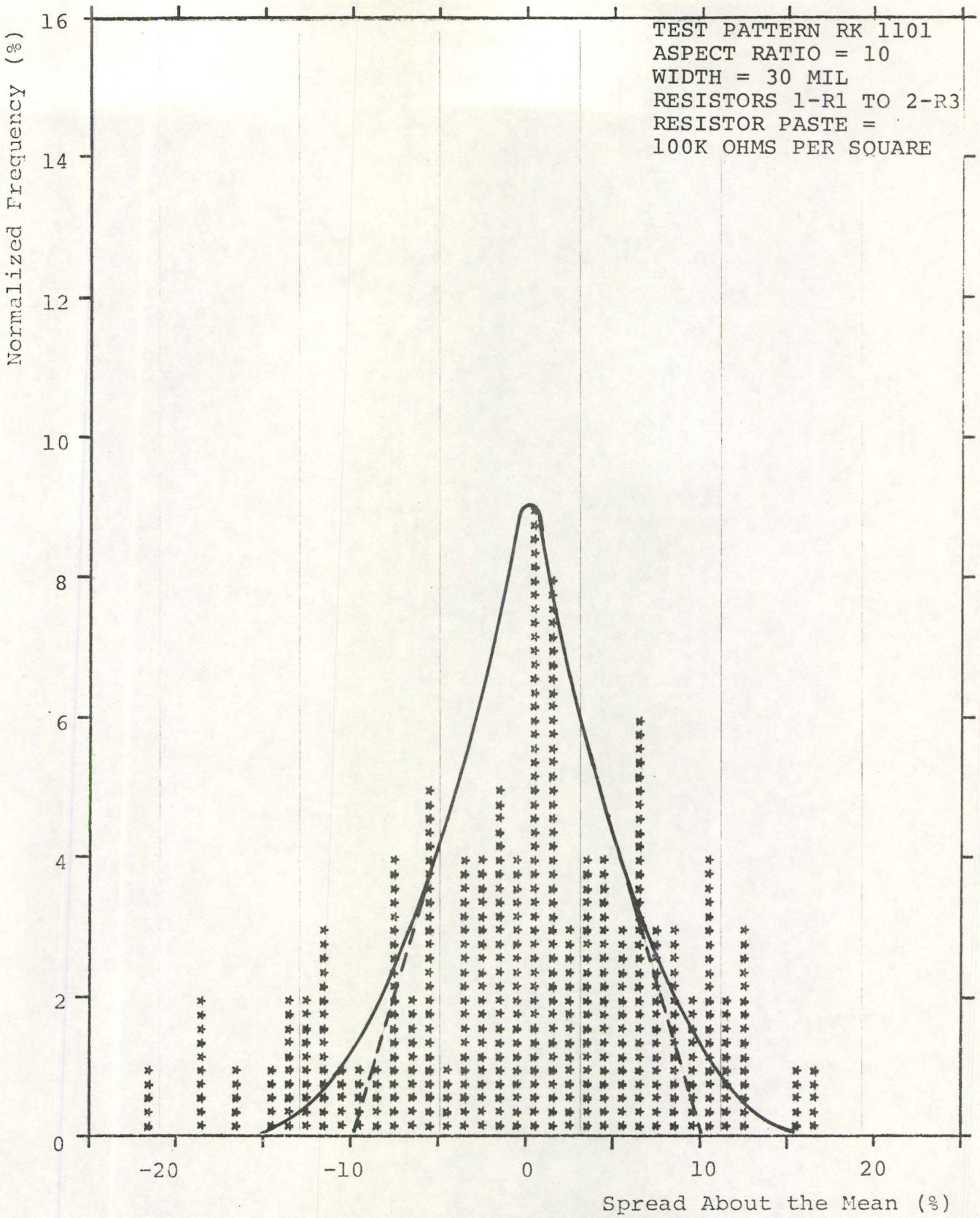

RESISTANCE DISTRIBUTION FOR ASPECT RATIO 10
AND 100K OHM PER SQUARE MATERIAL

FIGURE 26

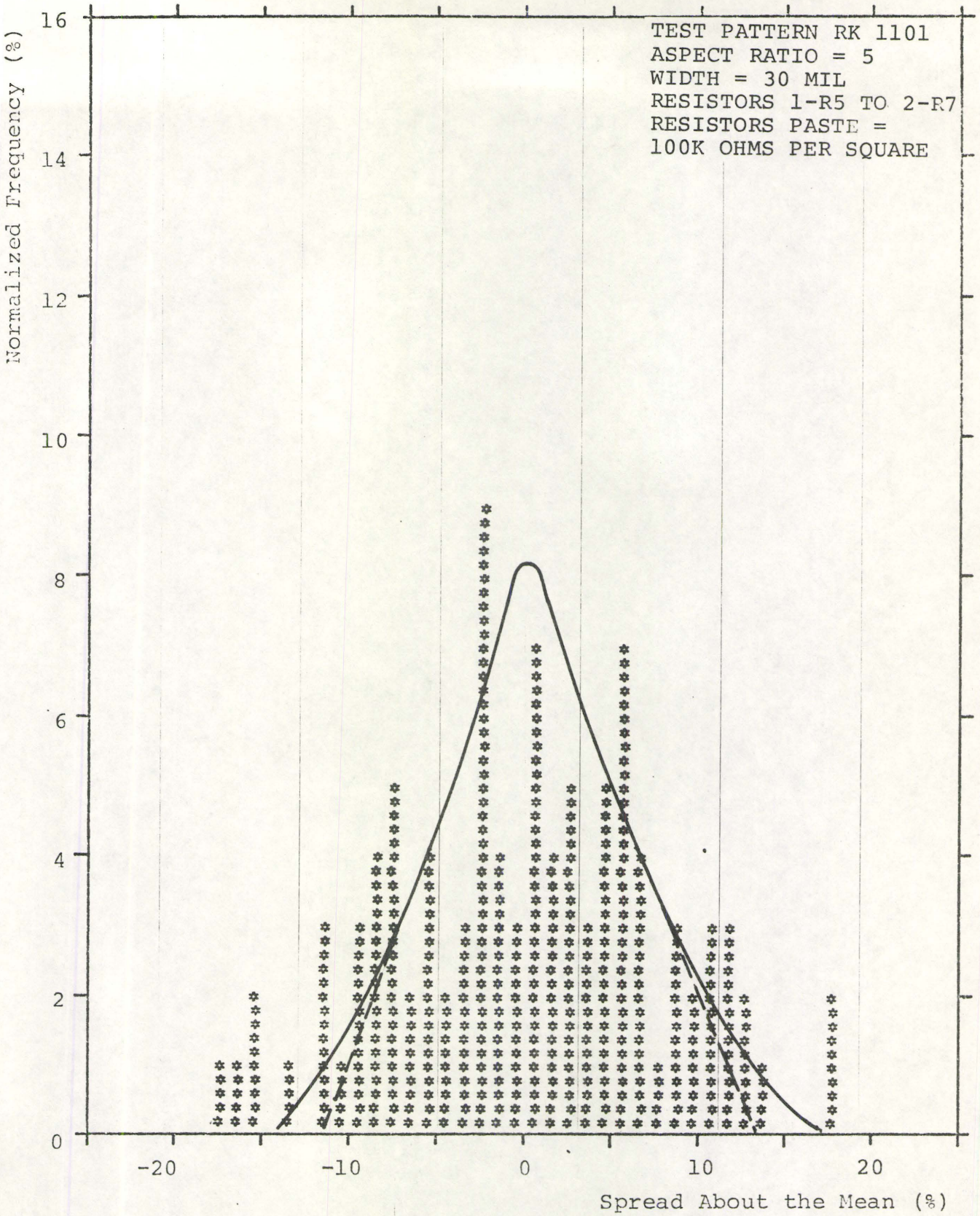

RESISTANCE DISTRIBUTION FOR ASPECT RATIO 5
AND 100K OHM PER SQUARE MATERIAL

FIGURE 27

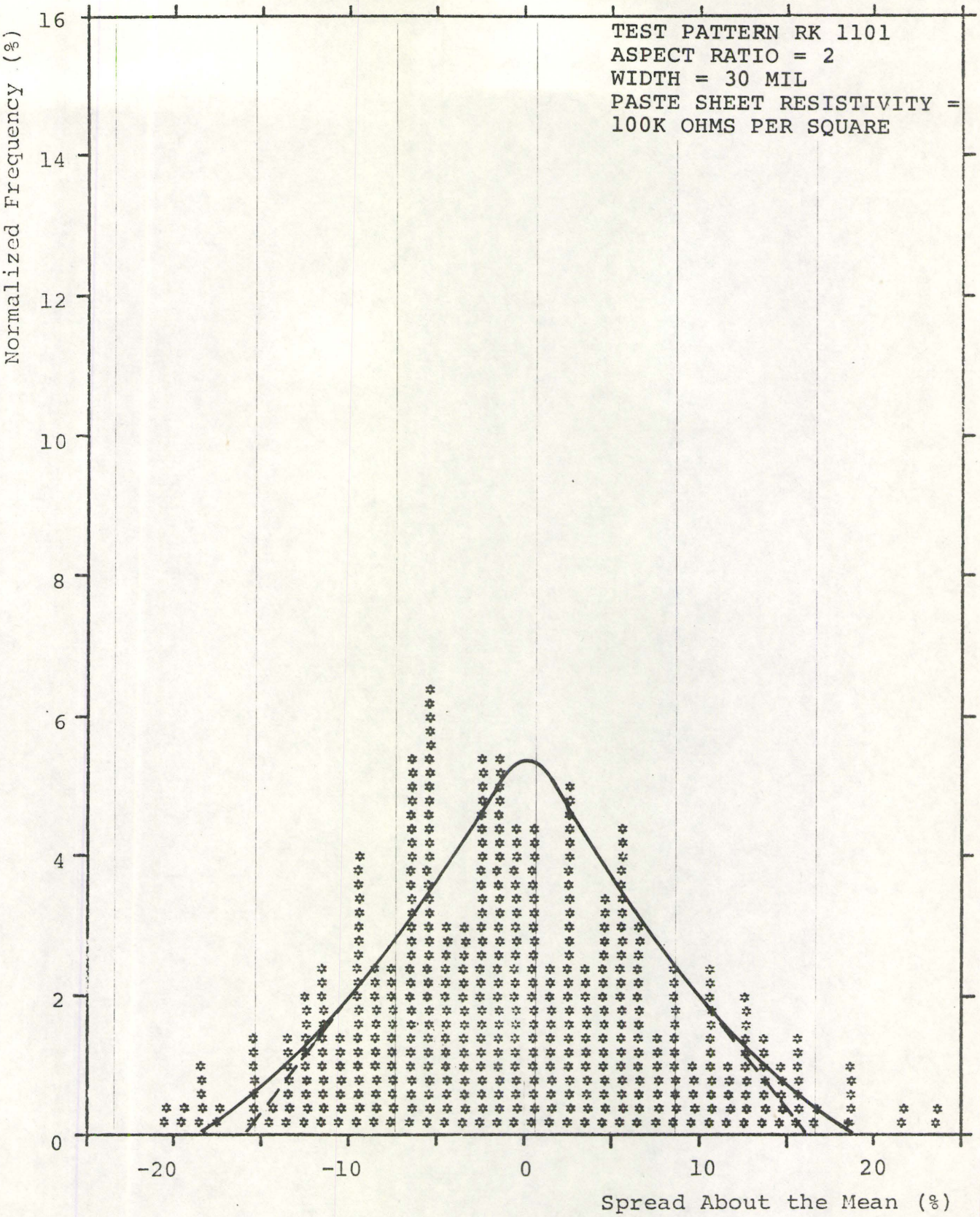

RESISTANCE DISTRIBUTION FOR ASPECT RATIO 2
AND 100K OHM PER SQUARE MATERIAL

FIGURE 28

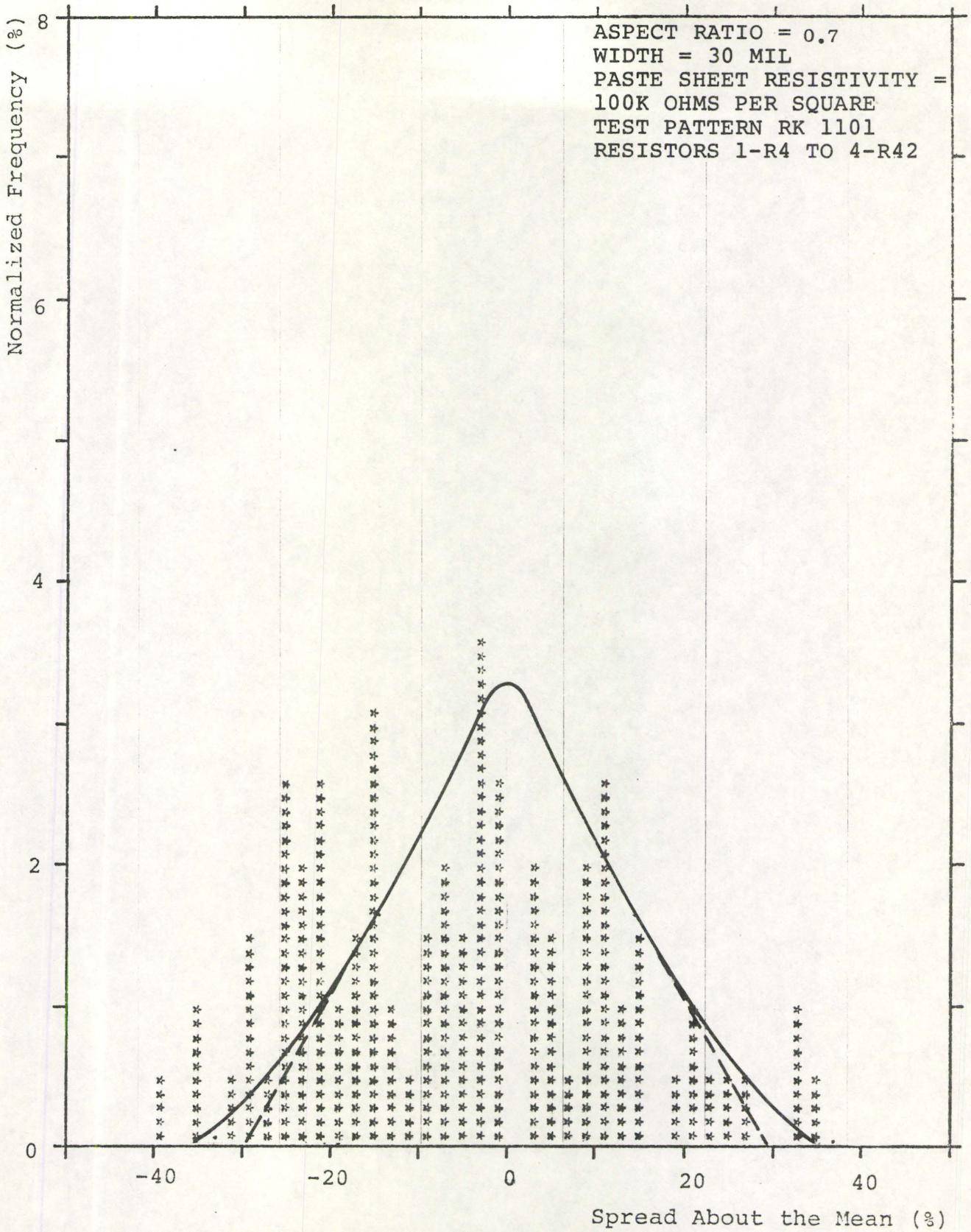

RESISTANCE DISTRIBUTION FOR ASPECT RATIO 0.7
AND 100K OHM PER SQUARE MATERIAL

FIGURE 29

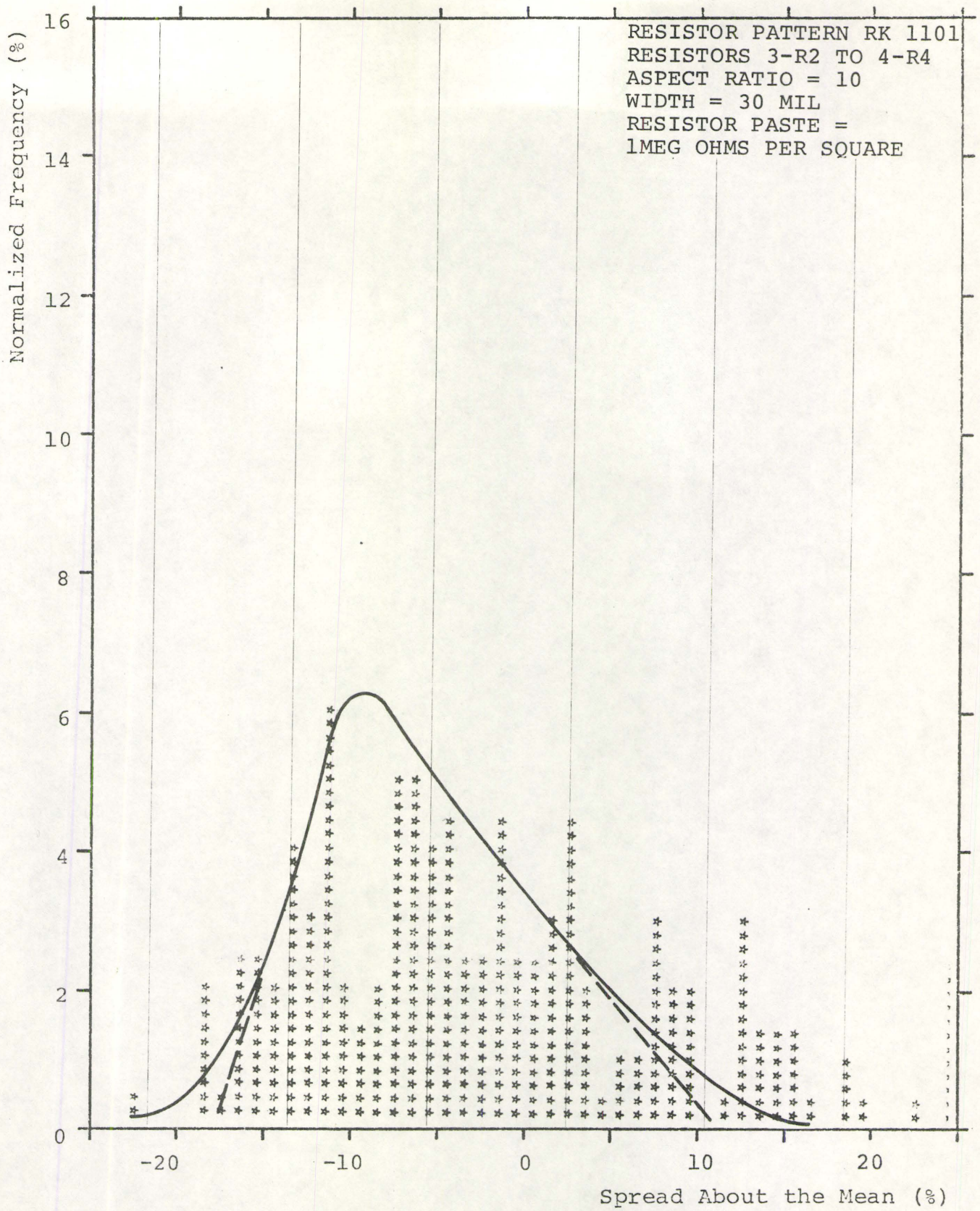

RESISTANCE DISTRIBUTION FOR ASPECT RATIO 0.7
AND 1M OHM PER SQUARE MATERIAL

FIGURE 30

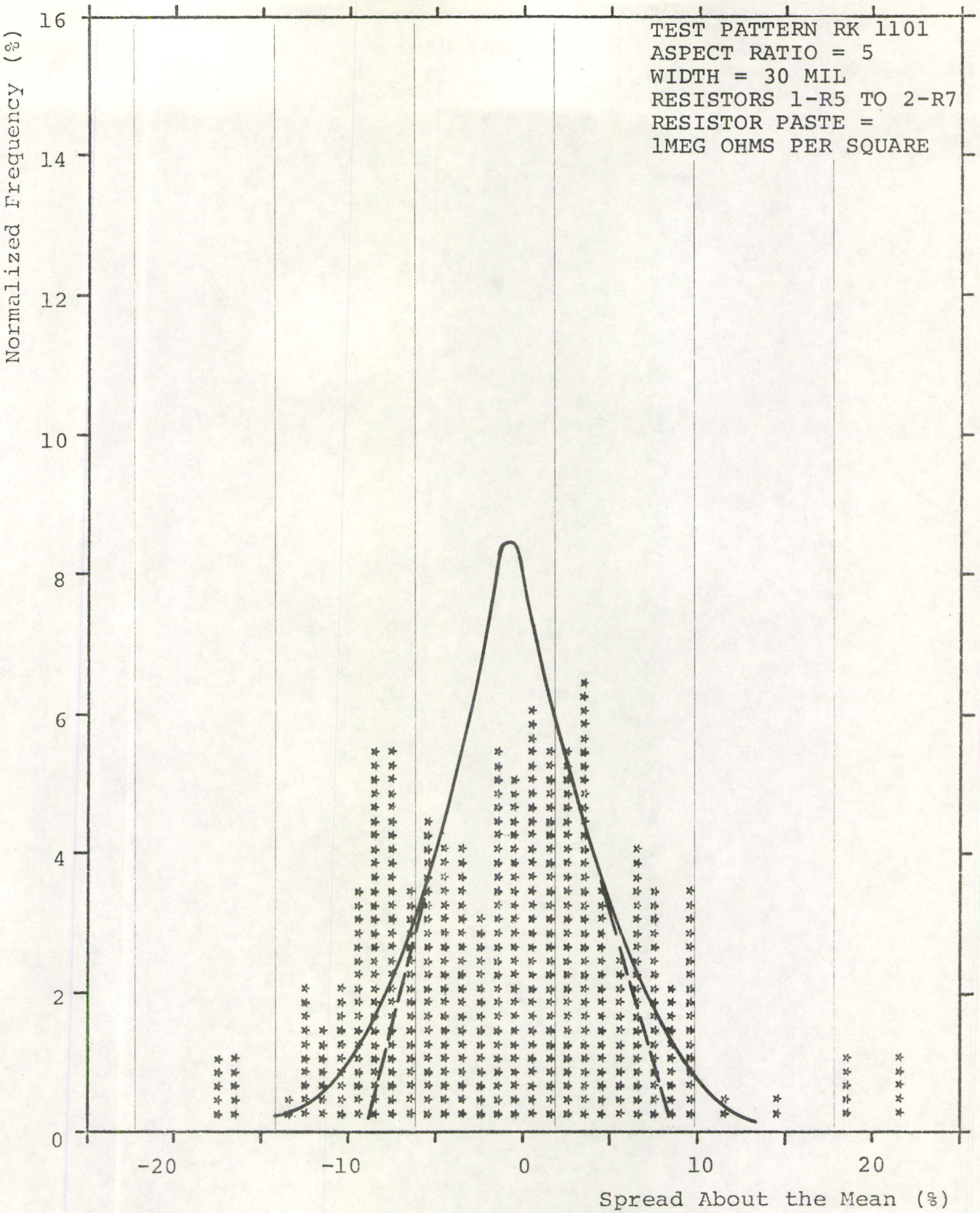

RESISTANCE DISTRIBUTION FOR ASPECT RATIO 5
AND 1M OHM PER SQUARE MATERIAL

FIGURE 31

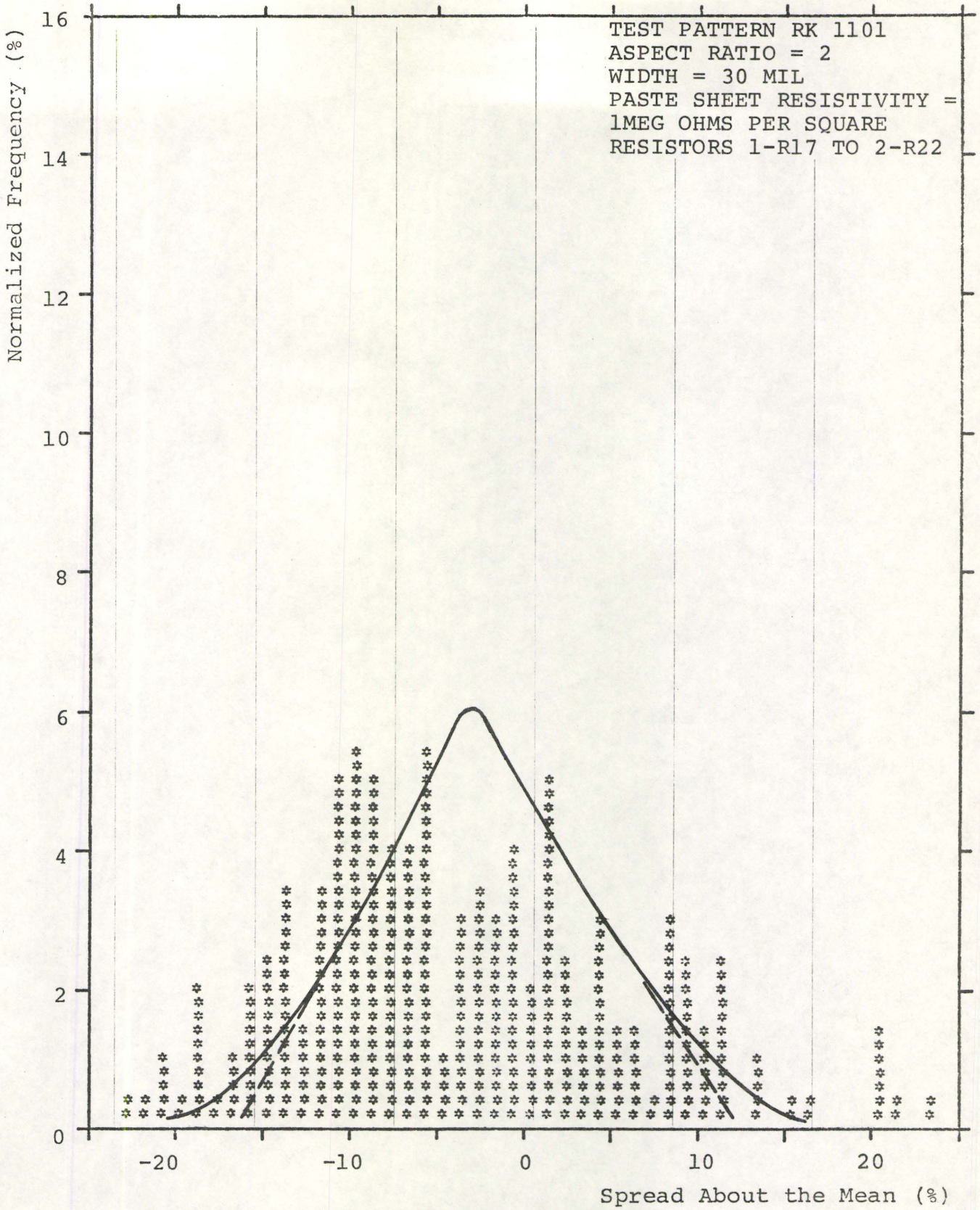

RESISTANCE DISTRIBUTION FOR ASPECT RATIO 2
AND 1M OHM PER SQUARE MATERIAL

FIGURE 32

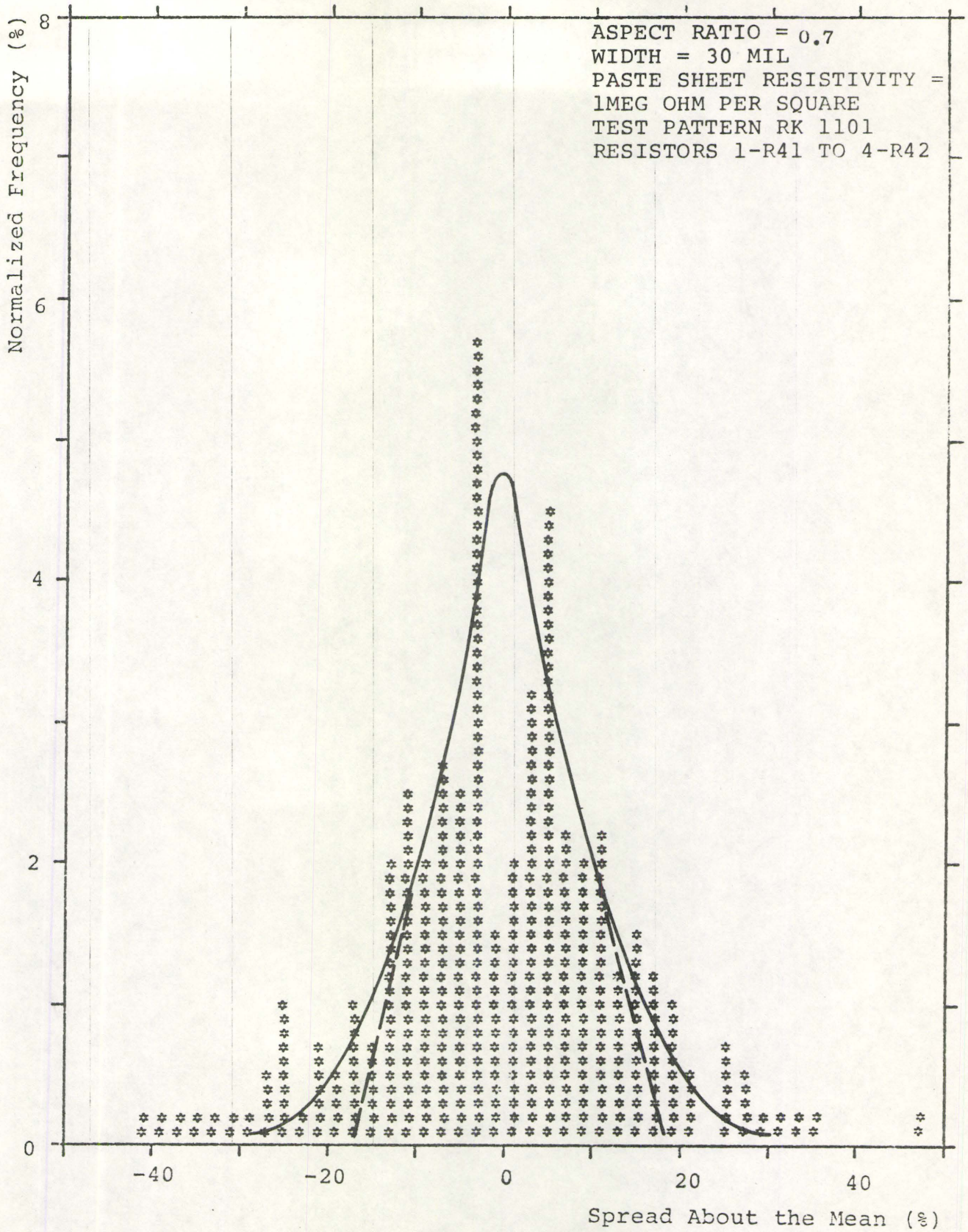

RESISTANCE DISTRIBUTION FOR ASPECT RATIO 0.7
AND 1M OHM PER SQUARE MATERIAL

FIGURE 33

Sheet Resistivity (ohm per square)	Aspect Ratio	Total-Spread (% of mean)	Tangent-Spread (% of mean)
100	10	24	15
	5	26	15.5
	2	31	20.5
	0.7	52	32.5
1K	10	23	14
	5	27.5	16.5
	2	33	24
	0.7	64	44
10K	10	26	15.5
	5	27	16
	2	30	20
	0.7	64	46
100K	10	30.5	19.5
	5	31	24.5
	2	36	31.5
	0.7	70	58
1M	10	38	28
	5	27	17
	2	36	28
	0.7	57	35

TOTAL-SPREADS AND TANGENT-SPREADS FOR THE AS-FIRED RESISTANCE DISTRIBUTION

FIGURE 34

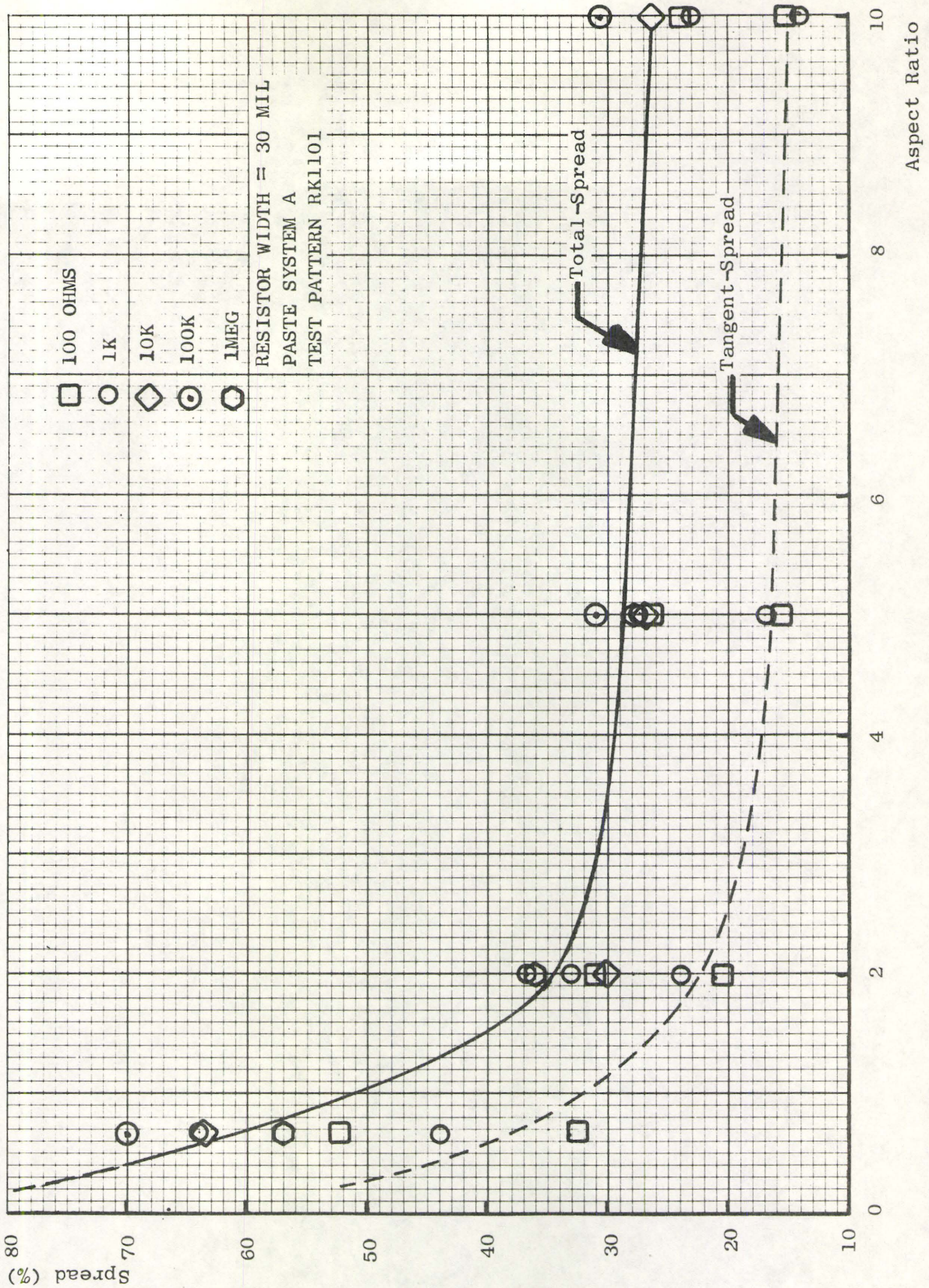

TOTAL-SPREAD AND TANGENT-SPREAD FOR
THE AS-FIRED DISTRIBUTIONS

FIGURE 35

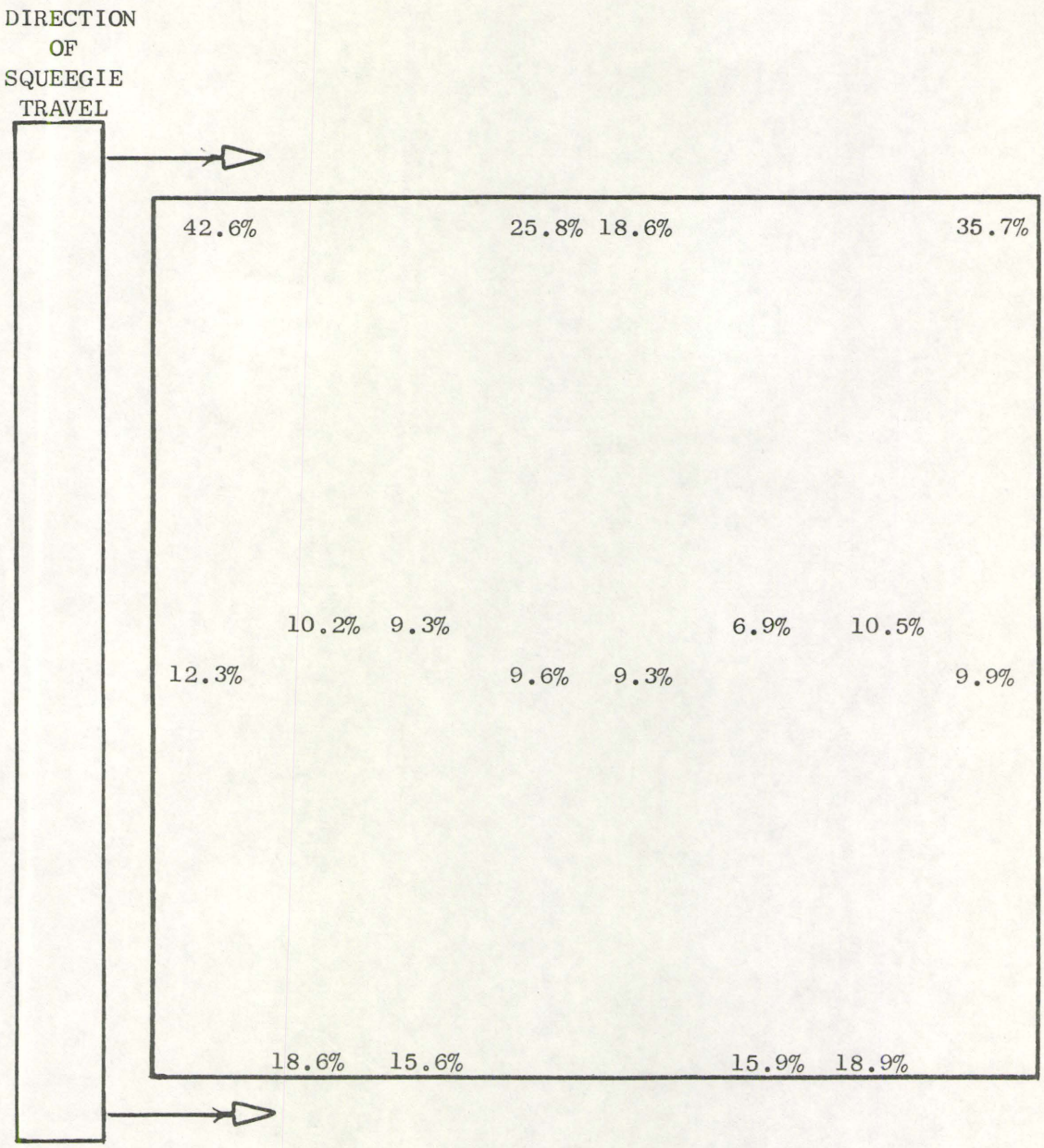

EFFECT OF RESISTOR POSITION ON RESISTANCE STATISTICAL VARIATION
FOR A RESISTOR WITH ASPECT RATIO OF 10
AND 100 OHM PER SQUARE PASTE

FIGURE 36

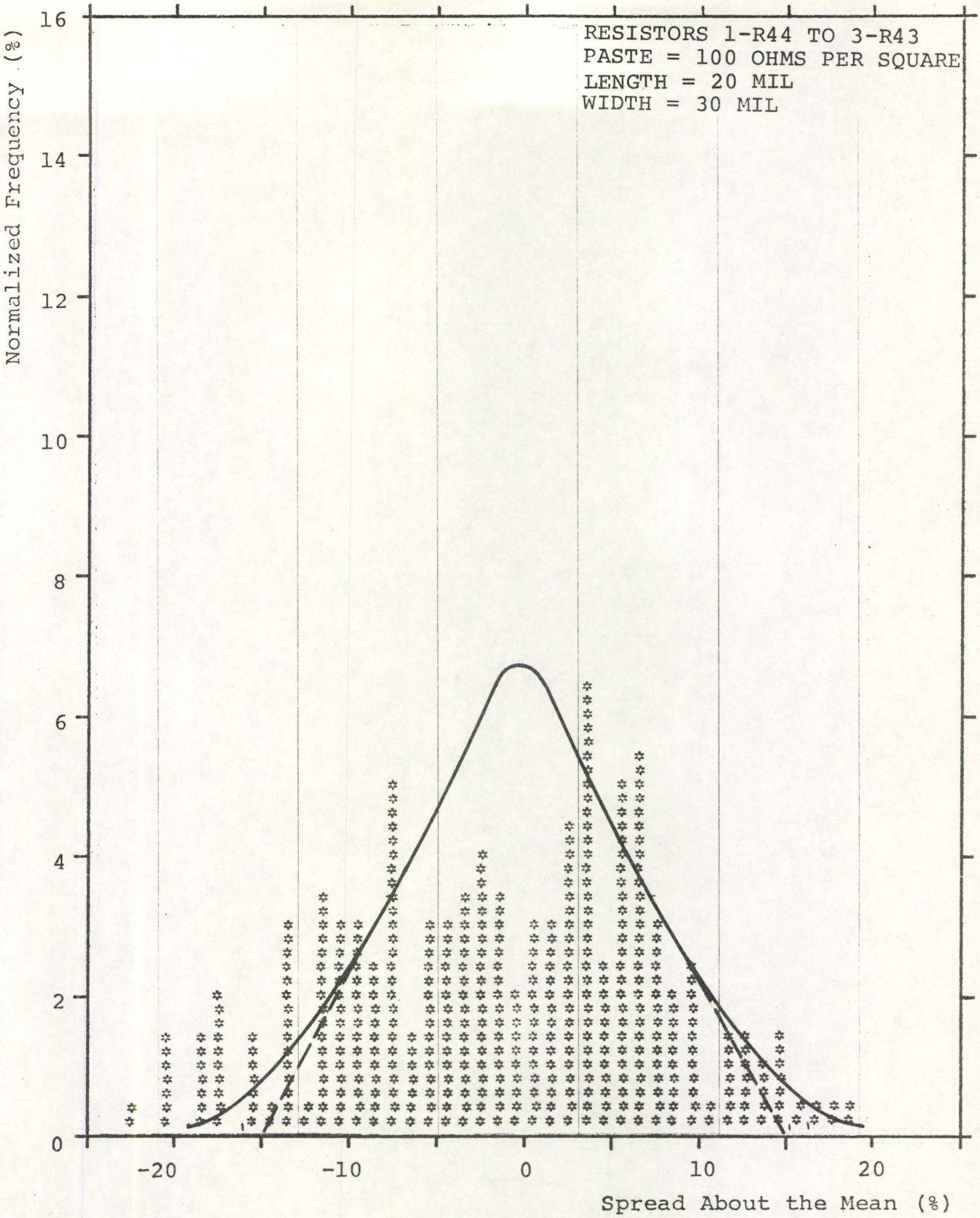

AS-FIRED RESISTANCE DISTRIBUTION FOR
RESISTOR WIDTH OF 30 MIL

FIGURE 37

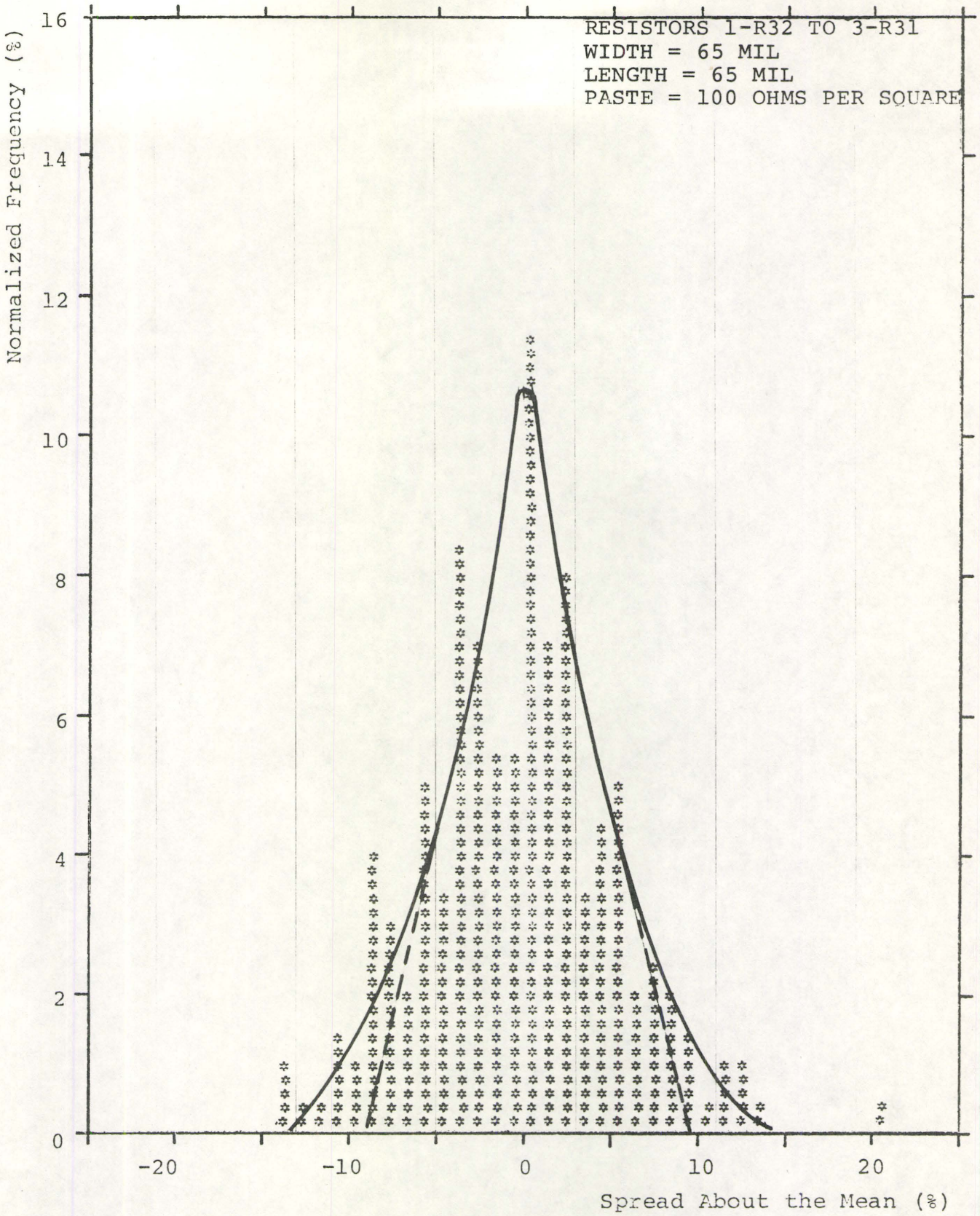

AS-FIRED RESISTANCE DISTRIBUTION FOR
RESISTOR WIDTH OF 65 MIL

FIGURE 38

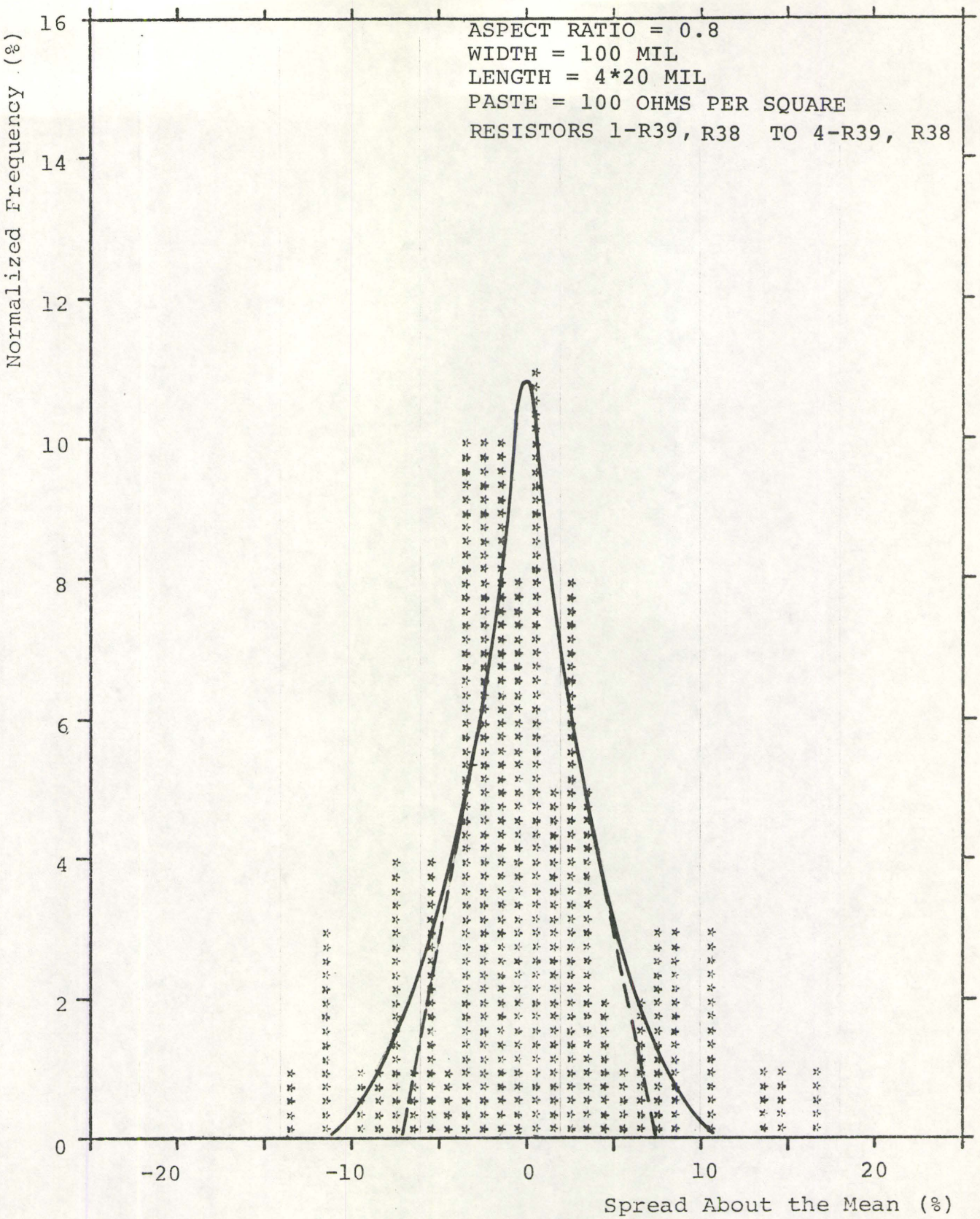

AS-FIRED RESISTANCE DISTRIBUTION FOR
RESISTOR WIDTH OF 100 MIL

FIGURE 39

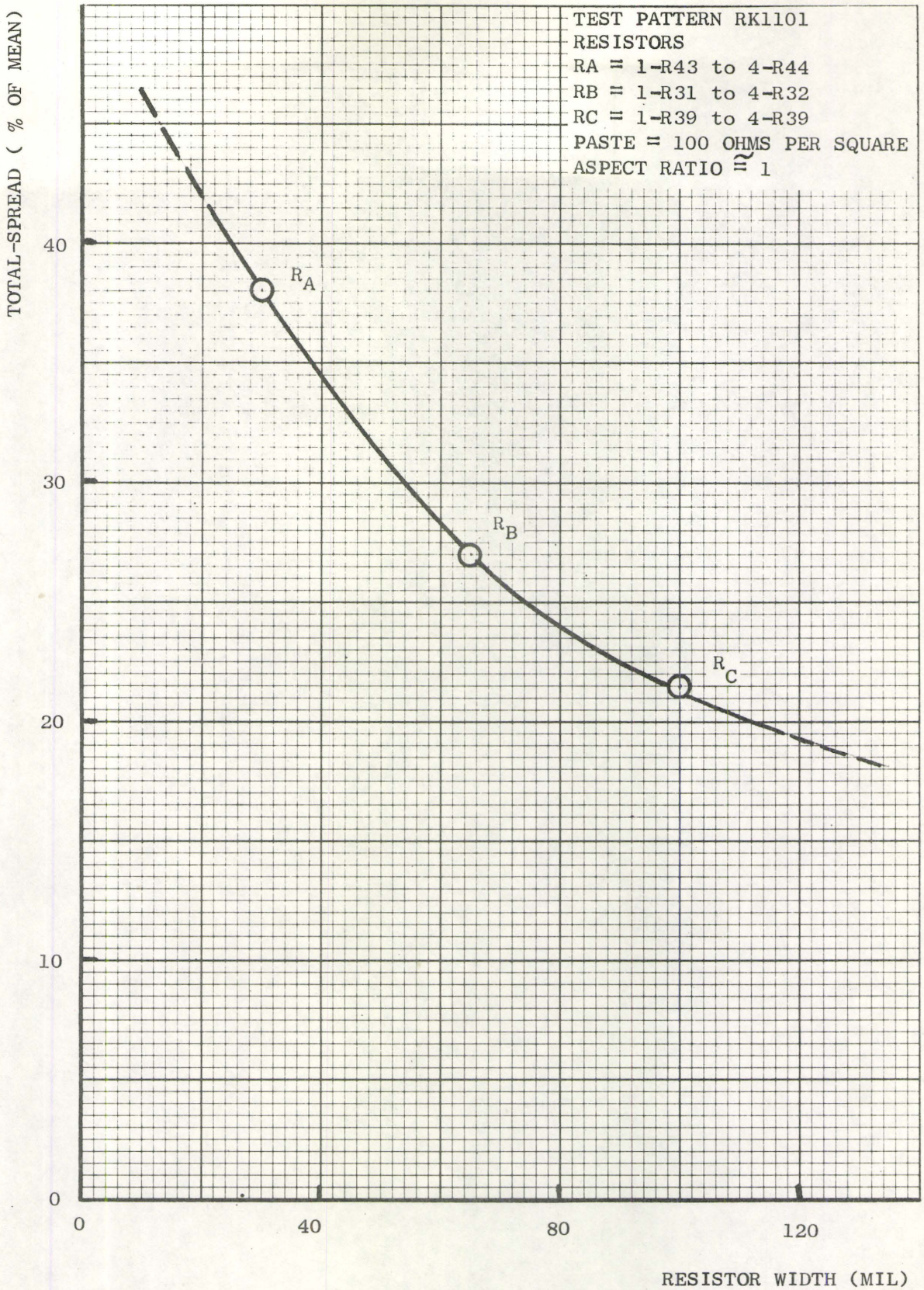

EFFECT OF RESISTOR WIDTH ON RESISTANCE SPREAD

FIGURE 40

Aspect Ratio	Sheet Resistivity (ohm/sq.)	Yield to Tolerance about Mean (%) ±1%	±2%	±5%	±10%	±15%	±20%
10	100	9.5	19.0	59.0	90.5	96.0	98.0
	1K	10.0	21.5	53.0	86.0	97.0	98.5
	10K	14.0	29.5	64.5	97.0	100.	100.
	100K	6.5	15.0	36.5	71.5	90.5	97.0
	1000K	5.0	12.5	29.0	55.5	79.0	90.0
5	100	14.0	27.0	62.5	86.0	93.0	96.0
	1K	16.5	26.5	64.0	89.5	96.5	99.5
	10K	17.0	33.0	66.5	92.5	99.5	100.0
	100K	3.5	8.5	22.0	47.0	73.5	89.0
	1000K	11.0	22.0	48.5	86.5	93.5	96.5
2	100	12.0	22.0	44.5	81.5	92.5	99.5
	1K	9.0	21.0	47.5	71.5	90.0	95.0
	10K	11.5	20.0	44.0	75.0	85.0	92.0
	100K	9.0	17.0	39.5	73.0	89.0	95.5
	1000K	6.0	14.0	28.5	61.5	82.5	89.5
0.7	100	6.5	13.0	31.0	60.0	77.0	89.0
	1K	4.5	10.5	26.5	52.0	70.0	80.0
	10K	3.0	9.0	19.0	45.0	66.5	83.0
	100K	4.6	7.8	17.7	32.8	47.3	58.3
	1000K	3.0	6.5	29.5	57.0	74.5	85.0

RESULTS FOR YIELD ANALYSIS OF RESISTOR DISTRIBUTIONS

FIGURE 41

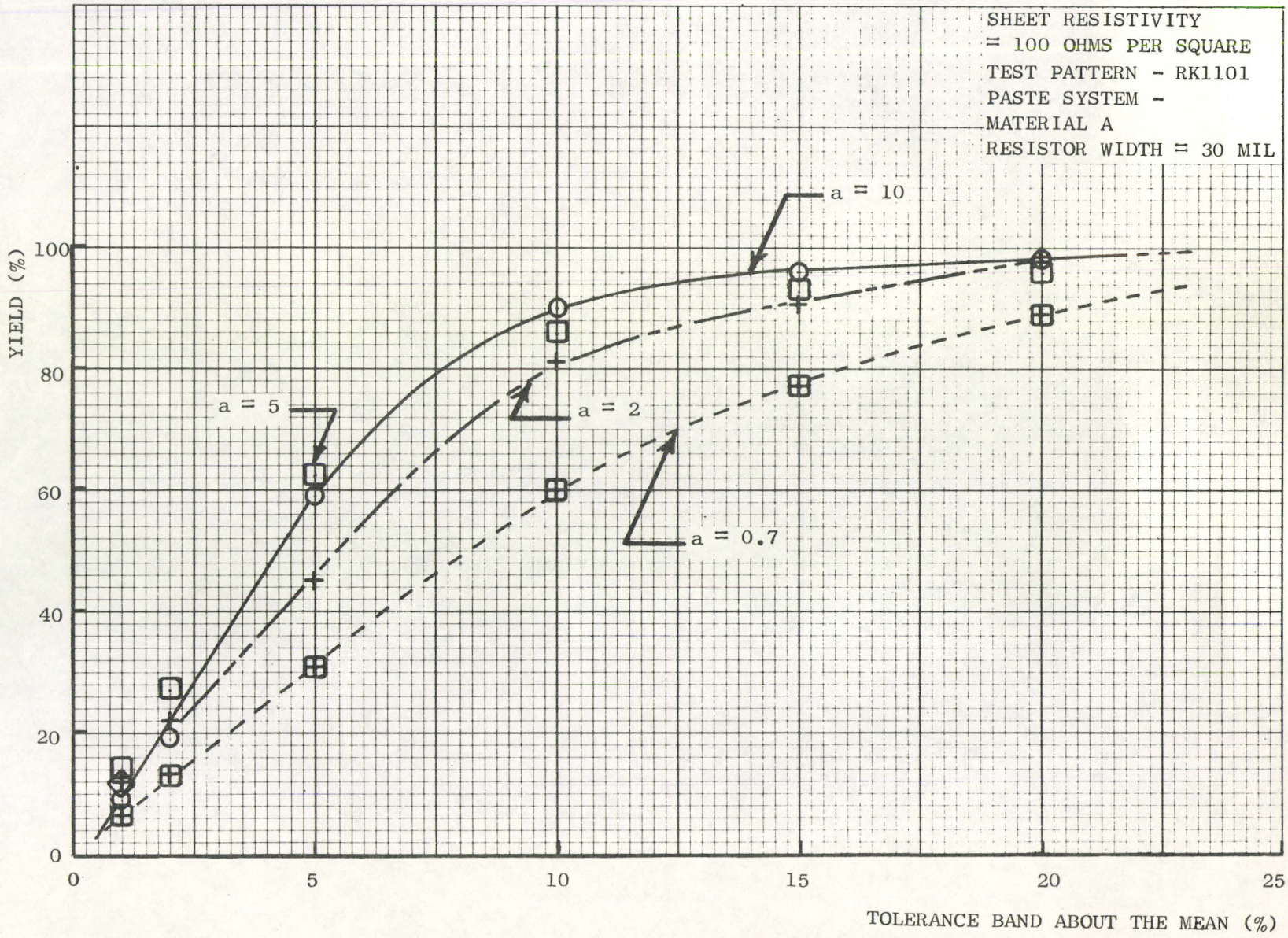

FIGURE 42

EFFECT OF ASPECT RATIO ON YIELD

(A) Case One - Aspect Ratio = 10

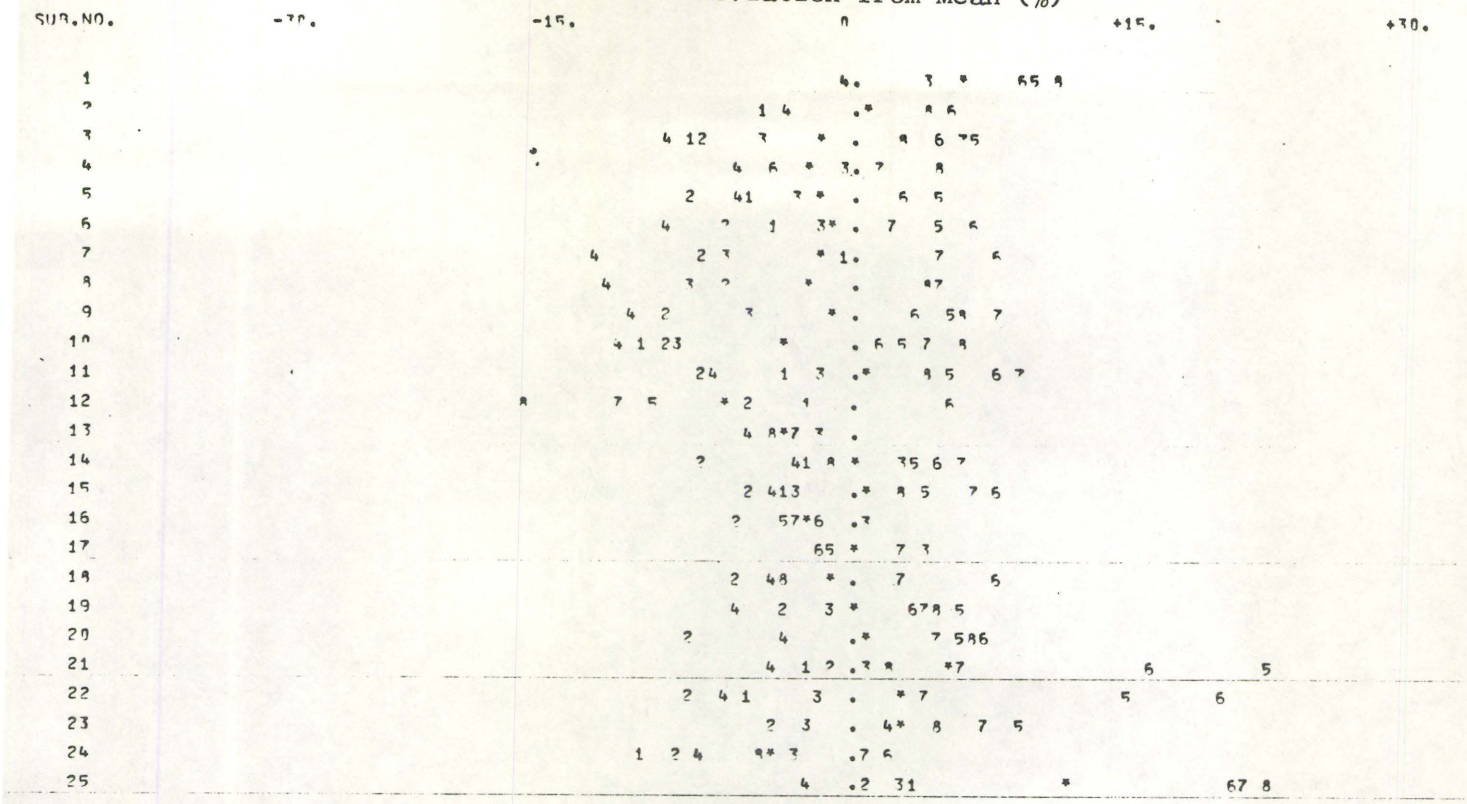

(B) Case Two - Aspect Ratio = 0.7

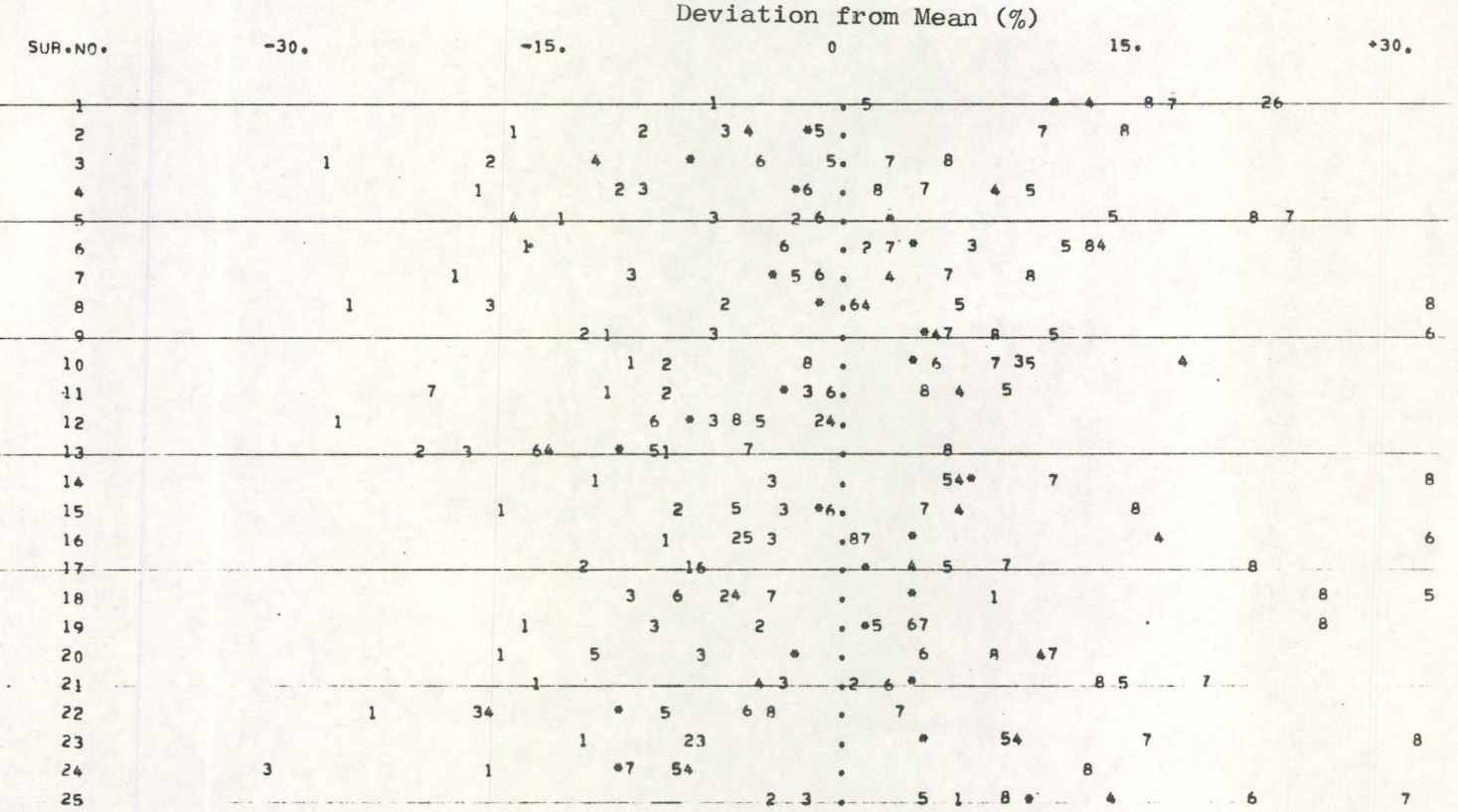

SUBSTRATE PLOT FOR 100 OHMS PER SQUARE PASTE

FIGURE 43

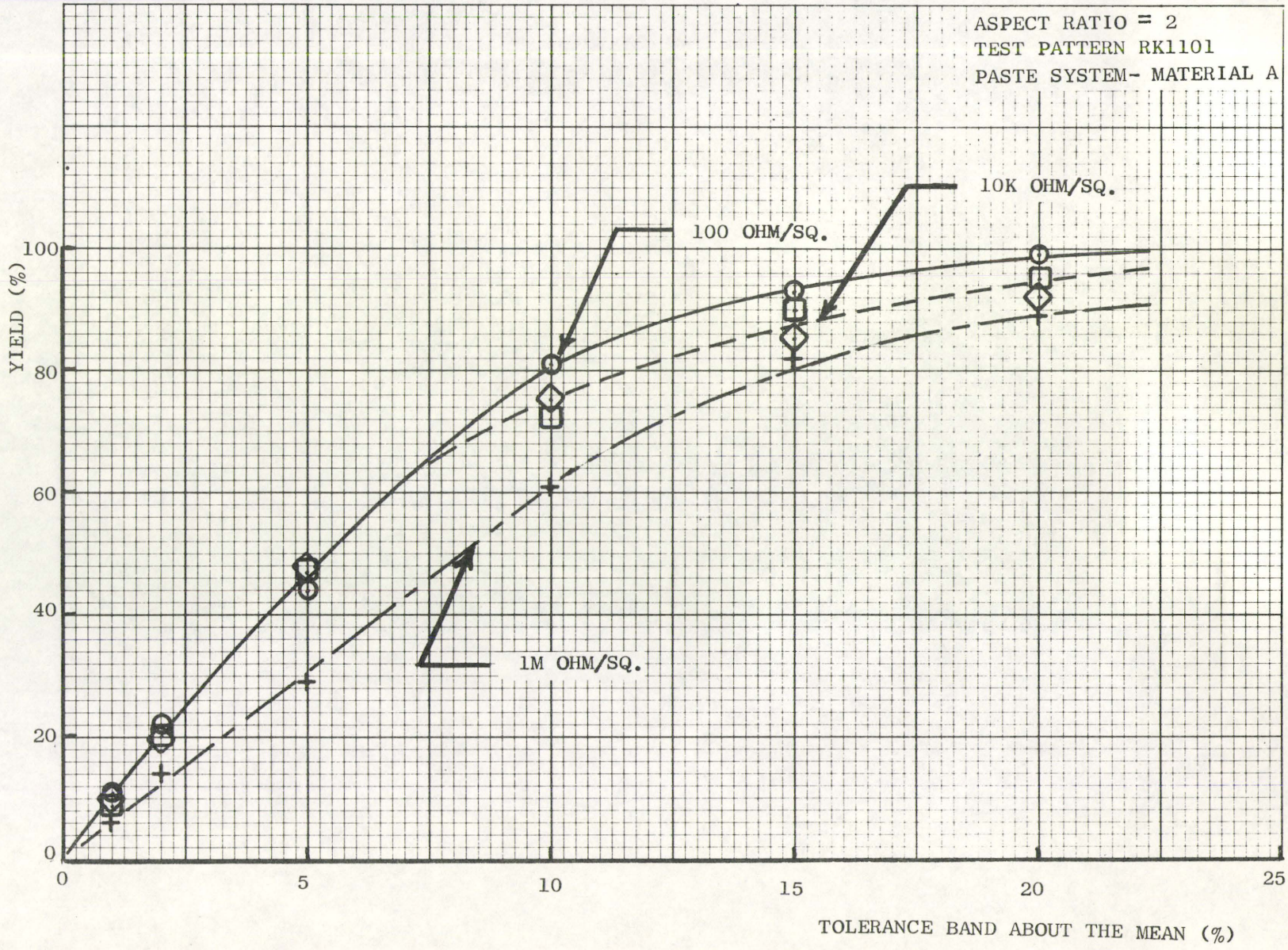

EFFECT OF SHEET RESISTIVITY ON YIELD

FIGURE 44

(A) CASE ONE - SHEET RESISTANCE = 100 OHMS PER SQUARE

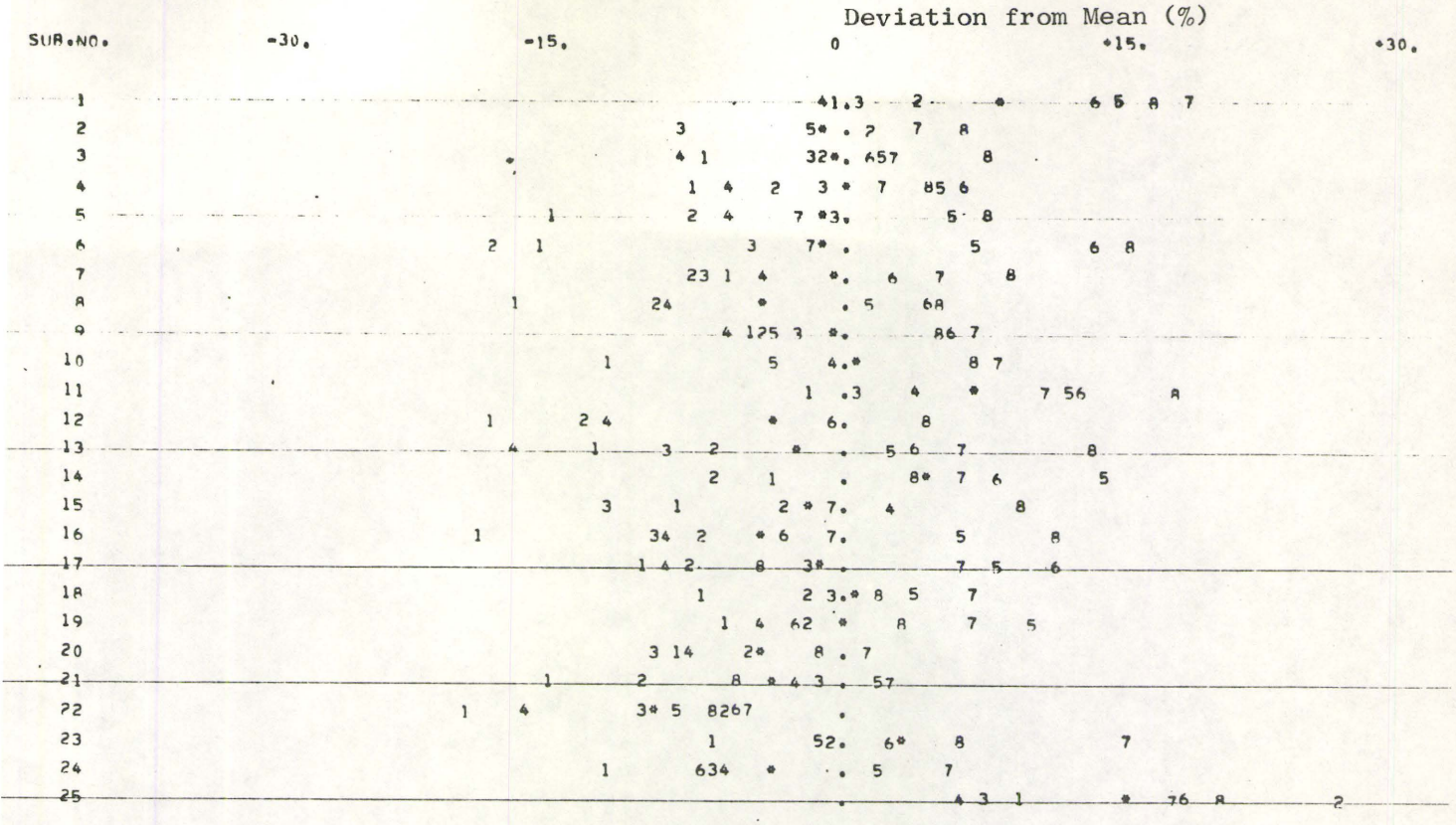

(B) CASE TWO - SHEET RESISTANCE = 1M OHMS PER SQUARE

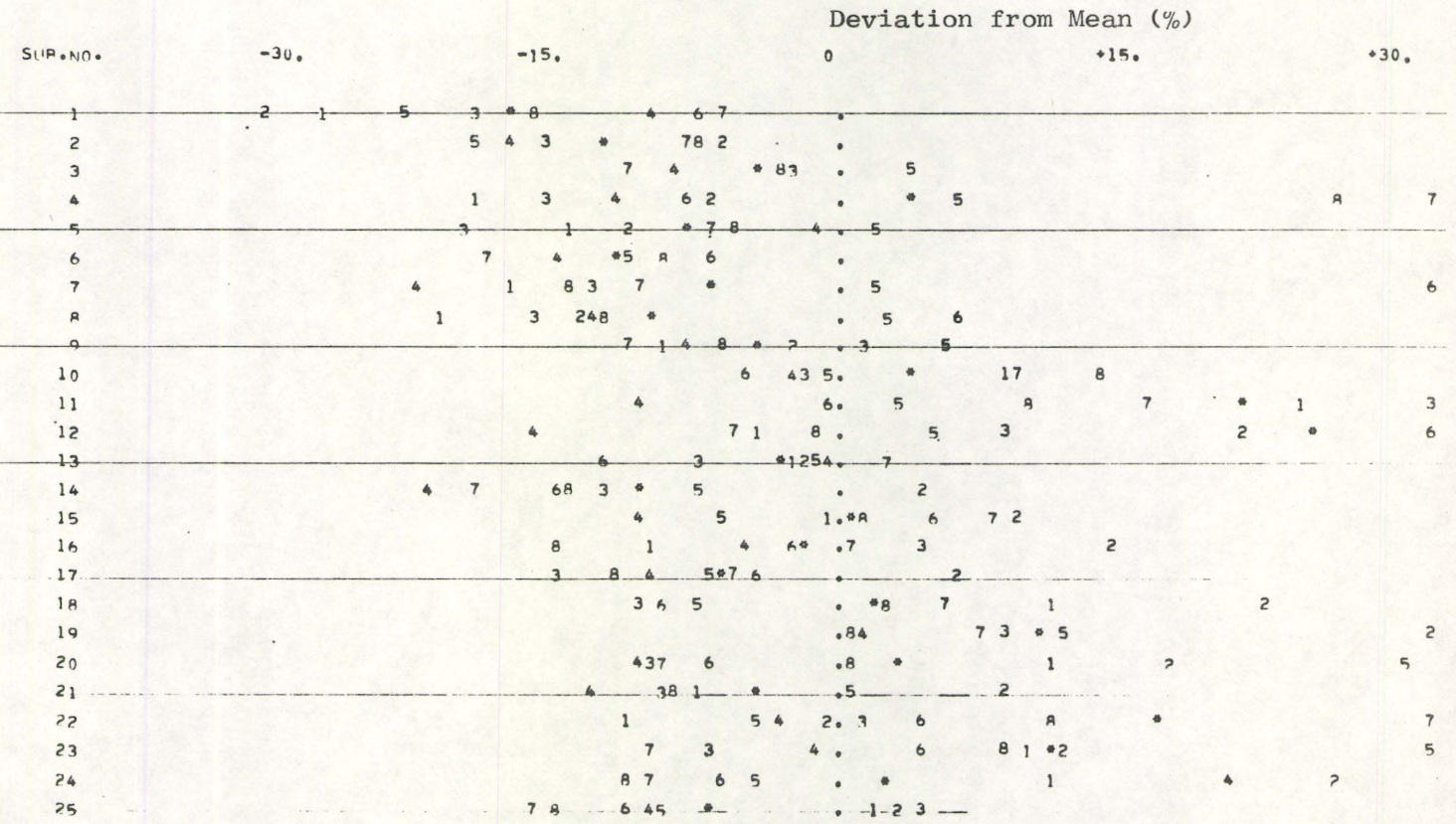

SUBSTRATE PLOTS FOR ASPECT RATIO 2

FIGURE 45

APPENDIX

APPENDIX A

AS-FIRED RESISTOR VALUES

FOR

TEST PATTERN RK1101

LIST OF FIGURES FOR APPENDIX A

Table	Sheet Resistivity (ohm per square)	Aspect Ratio	Resistors Investigated For Each Aspect Ratio	
1	100	10	1-R1	1-R2
2	100K	10	2-R1	2-R2
3	1K	10	1-R4	1-R3
4	10K	10	2-R4	2-R3
5	100	5	1-R5	1-R6
6	1K	5	2-R5	2-R6
7	10K	5	1-R8	1-R7
8	100K	5	2-R8	2-R7
9	1000K	5		
10	100	2	1-R17	1-R21
11	1K	2	1-R18	1-R22
12	10K	2	2-R17	2-R21
13	100K	2	2-R18	2-R22
14	1000K	2		
15	100	0.67	1-R41	1-R42
16	1K	0.67	2-R41	2-R42
17	10K	0.67	4-R41	4-R42
18	100K	0.67	3-R41	3-R42
19	1000K	0.67		
20	100	10	3-R2	3-R1
21	1K	10	4-R2	4-R1
22	10K	10	3-R3	3-R4
23	100K	10	4-R3	4-R4
24	1000K	10		
25	100	0.2	1-R40	1-R37
26	1K	0.2	1-R33	1-R36
27	10K	0.2	2-R40	2-R37
28	100K	0.2	2-R33	2-R36

continued....

LIST OF FIGURES FOR APPENDIX A (continued)

Table	Sheet Resistivity (ohm per square)	length x width (mil.)	Resistors Investigated For Each Aspect Ratio		
30	100	20 x 30	1-R44		1-R43
			2-R44		2-R43
			4-R44		4-R43
			3-R44		3-R43
31	100	65 x 65	1-R31		1-R32
			2-R31		2-R32
			3-R31		3-R32
			4-R31		4-R32
32	100	80 x 100	1-R39	to	1-R38
			2-R39	to	2-R38
			3-R39	to	3-R38
			4-R39	to	4-R38

TABLE ONE

TOLERANCE STUDY
TEST PATTERN RK 1101
ASPECT RATIO = 10
WIDTH = 30 MIL
RESISTORS 1-R1 TO 2-R3
RESISTOR PASTE = 100 OHMS PER SQUARE

AS-FIRED RESISTANCE $x10^0$ (ohm)

SUBSTRATE	1-R1	1-R2	2-R1	2-R2	1-R4	1-R3	2-R4	2-R3
1	1145.	1256.	1227.	1160.	1001.	1092.	1076.	1096.
2	1068.	1079.	1036.	1077.	1019.	1061.	1040.	1077.
3	1109.	1143.	1134.	1144.	980.	1030.	989.	1027.
4	784.	1052.	1001.	940.	1088.	1077.	1072.	1111.
5	980.	1073.	1035.	1008.	1019.	1074.	1052.	1034.
6	835.	898.	930.	913.	1018.	1058.	1067.	1111.
7	1140.	1217.	1145.	1138.	991.	1022.	1059.	1133.
8	1042.	1050.	1021.	892.	991.	1068.	1066.	1122.
9	1093.	1171.	1084.	939.	1010.	1051.	1048.	1116.
10	1082.	1017.	1016.	964.	1012.	1065.	1059.	1111.
11	815.	1038.	1090.	1095.	1056.	1083.	1054.	1159.
12	734.	942.	1052.	1059.	1027.	1033.	1086.	1117.
13	807.	956.	934.	865.	1018.	1099.	1041.	1072.
14	1063.	1165.	1137.	1030.	1097.	1126.	1049.	1115.
15	898.	1113.	1084.	1125.	1043.	1079.	1062.	1104.
16	1032.	1101.	1036.	1119.	1099.	1108.	1055.	1095.
17	837.	1084.	1076.	1011.	1081.	1112.	1106.	1128.
18	915.	1091.	1083.	837.	1072.	1064.	1069.	1065.
19	776.	993.	1049.	909.	1074.	1102.	1075.	1068.
20	1018.	1074.	1023.	968.	1054.	1097.	1045.	1083.
21	1143.	1215.	1075.	951.	1064.	1152.	1058.	1111.
22	1166.	1155.	1070.	855.	1045.	1053.	1048.	1053.
23	1105.	1046.	1094.	1039.	1076.	1077.	1075.	1011.
24	886.	997.	978.	766.	1054.	1065.	1011.	1070.
25	1186.	1278.	1149.	1278.	1089.	1153.	1102.	1179.

TABLE TWO

AS FIRED RESISTANCE STUDY
TEST PATTERN PK 1101
ASPECT RATIO = 1^0
WIDTH = 30 MIL
RESISTORS 1-R1 TO 2-R3
RESISTOR PASTE = 100K OHMS PER SQUARE

AS-FIRED RESISTANCE $x10^2$ (ohm)

Substrate	1-R1	1-R2	2-R1	2-R2	1-R4	1-R3	2-R4	2-R3
1	4936.	4896.	5206.	5416.	7621.	7787.	8049.	7878.
2	5587.	5572.	5677.	5617.	7158.	6495.	7925.	7104.
3	4879.	4735.	4807.	4749.	6490.	6714.	7089.	7357.
4	5171.	4982.	5259.	5031.	7063.	6286.	6919.	7016.
5	5259.	5516.	5528.	5487.	8648.	8388.	8928.	9036.
6	5332.	5779.	5436.	6233.	7699.	6891.	8084.	8509.
7	6280.	6663.	6392.	6409.	8665.	8332.	8539.	8893.
8	5356.	5479.	5541.	5520.	8035.	8070.	8365.	9011.
9	5877.	5537.	5406.	5441.	7825.	7787.	7405.	7768.
10	5607.	5447.	5486.	5540.	8059.	7495.	7967.	8105.
11	5453.	5887.	5479.	5962.	8833.	8558.	8767.	8881.
12	6108.	5875.	6407.	6373.	8776.	8559.	8894.	9376.
13	5541.	5193.	4634.	5479.	7861.	8137.	8114.	8489.
14	5289.	5703.	5625.	6003.	8316.	8019.	8701.	9044.
15	5444.	5426.	5393.	5519.	7840.	7601.	8519.	8147.
16	5190.	5529.	5487.	5833.	8051.	8314.	8617.	9237.
17	4950.	5681.	5556.	6074.	8163.	8135.	8589.	8944.
18	4824.	5062.	4717.	5536.	7749.	7567.	8234.	8242.
19	5283.	5504.	5526.	5935.	7902.	7963.	8378.	8536.
20	5107.	4995.	5301.	5177.	6949.	7029.	7438.	7758.
21	5409.	5362.	5218.	5105.	8050.	7946.	8336.	8501.
22	5568.	5742.	5347.	5584.	7597.	7525.	8107.	8133.
23	5680.	6122.	5716.	6211.	7419.	7605.	7908.	8196.
24	5779.	5826.	5726.	5846.	7247.	7416.	8161.	8432.
25	5318.	4995.	5348.	5268.	7986.	7593.	8379.	8476.

TABLE TWO (A)

AS FIRED RESISTANCE STUDY
TEST PATTERN PK 1101
ASPECT RATIO = 10
WIDTH = 30 MIL
RESISTORS 1-R4 TO 2-R3
RESISTOR PASTE = 100K OHMS PER SQUARE

AS-FIRED RESISTANCE $\times 10^2$ (ohm)

Substrate	1-R4	1-R3	2-R4	2-R3
1	7621.	7787.	8049.	7878.
2	7158.	6495.	7925.	7104.
3	6499.	6714.	7089.	7357.
4	7063.	6286.	6919.	7016.
5	8648.	8388.	8928.	9036.
6	7699.	6891.	8084.	8509.
7	8665.	8332.	8639.	8897.
8	8035.	8070.	8365.	9011.
9	7825.	7787.	7405.	7768.
10	8059.	7495.	7967.	8105.
11	8833.	8558.	8767.	8881.
12	8776.	8559.	8894.	9776.
13	7861.	8137.	8114.	8489.
14	8316.	8019.	8701.	9044.
15	7840.	7601.	8519.	8147.
16	8051.	8314.	8617.	9237.
17	8163.	8135.	8689.	8944.
18	7749.	7567.	8234.	8242.
19	7902.	7963.	8378.	8536.
20	6949.	7029.	7438.	7758.
21	8050.	7946.	8336.	8501.
22	7597.	7525.	8107.	8133.
23	7419.	7605.	7908.	8196.
24	7247.	7406.	8061.	8432.
25	7986.	7593.	8379.	8476.

T A B L E T H R E E

AS FIRED RESISTANCE STUDY
TEST PATTERN RK 1101
PASTE SYSTEM -A-
ASPECT RATIO = 10
WIDTH = 30 MIL
RESISTORS 1-R1 TO 2-R3
RESISTOR PASTE = 1K OHMS PER SQUARE

AS-FIRED RESISTANCE $x10^0$ (ohm)

Substrate	1-R1	1-R2	2-R1	2-R2	1-R4	1-R3	2-R4	2-R3
1	9373.	9219.	8578.	8524.	8756.	8458.	8758.	9560.
2	10681.	9876.	10209.	10046.	9404.	9765.	9565.	9369.
3	9536.	10317.	9250.	9838.	8146.	7975.	9540.	9581.
4	9799.	9512.	8793.	9411.	9646.	9431.	9547.	9685.
5	8862.	8107.	9212.	8977.	8951.	8749.	9172.	9830.
6	9519.	9059.	9611.	9234.	8974.	9978.	9600.	10000.
7	9540.	8818.	9071.	9293.	9689.	9400.	9342.	9765.
8	9502.	9024.	8176.	9361.	9351.	9055.	9191.	9610.
9	9398.	9387.	9293.	9101.	9489.	9112.	9031.	10051.
10	10150.	9685.	9028.	9686.	9491.	9689.	9367.	9637.
11	10098.	9620.	9455.	9682.	8717.	8551.	9364.	9318.
12	9988.	9897.	9337.	9841.	8788.	8436.	9231.	9965.
13	9510.	9454.	8724.	9485.	8749.	8983.	9962.	9974.
14	9618.	9062.	9048.	9744.	8888.	9028.	9330.	9851.
15	9856.	10113.	9510.	9575.	9748.	8961.	9558.	9517.
16	10211.	8645.	8507.	8977.	8616.	8236.	8931.	9584.
17	9817.	9578.	9450.	10248.	8885.	8891.	9079.	9817.
18	8909.	9272.	8825.	8922.	9290.	8873.	9843.	10124.
19	9813.	9793.	8992.	10038.	8541.	9341.	8605.	9768.
20	9718.	9256.	9202.	9824.	9523.	9296.	8911.	9541.
21	9614.	9476.	9573.	9584.	8755.	9024.	9287.	9588.
22	9503.	9489.	8845.	9659.	9127.	8988.	9181.	9473.
23	9464.	9797.	9258.	9867.	8745.	7892.	9318.	9194.
24	8839.	8878.	8835.	8617.	9129.	8466.	9519.	9723.
25	8933.	8824.	8604.	8950.	8661.	8934.	10540.	10000.

TABLE FOUR

AS FIRED RESTSTANCE STUDY
TEST PATTERN RK 1101
ASPECT RATIO = 10
WIDTH =30 MIL
PASTE = 10K OHMS PER SQUARE

AS-FIRED RESISTANCE $x10^{1}$ (ohm)

Substrate	1-R1	1-R2	2-R1	2-R2	1-R4	1-R3	2-R4	2-R3
1	9051.	8628.	8911.	7938.	9403.	9763.	9501.	10307.
2	9988.	9823.	9752.	10305.	9833.	9929.	10167.	9881.
3	8691.	10052.	9546.	9023.	9761.	10063.	10000.	10000.
4	9472.	10198.	9846.	8660.	10051.	10448.	10254.	10541.
5	9279.	9409.	9477.	9200.	10465.	10437.	10210.	10591.
6	9210.	10095.	9505.	9094.	9710.	9782.	9756.	10439.
7	9447.	9775.	8854.	9599.	9865.	10253.	10292.	11266.
8	9051.	10058.	9870.	9351.	9580.	10050.	10213.	10687.
9	9559.	9514.	9618.	8302.	9994.	10140.	10534.	10795.
10	9430.	10230.	9494.	9702.	9374.	9583.	9977.	9931.
11	9750.	10616.	11335.	10284.	9186.	9552.	10252.	10152.
12	9388.	9833.	9408.	9539.	9067.	10221.	10234.	10386.
13	9264.	8922.	8982.	8586.	9977.	9949.	10454.	10254.
14	10171.	9875.	9963.	9757.	10262.	10489.	10317.	10272.
15	10084.	9528.	9500.	8816.	9956.	9971.	9832.	10015.
16	9749.	9931.	9831.	9708.	9810.	10253.	10063.	10096.
17	9128.	9426.	8993.	9022.	9968.	9952.	10175.	10032.
18	9212.	9191.	9066.	8866.	9605.	9797.	9668.	9622.
19	9839.	9128.	9069.	9576.	9708.	9703.	9572.	10113.
20	8974.	8938.	8712.	8105.	9540.	10323.	9906.	10069.
21	9747.	9053.	8837.	9054.	9489.	9605.	9796.	9480.
22	9150.	9068.	8475.	8449.	9473.	9590.	9674.	9617.
23	9549.	9751.	9260.	9277.	9764.	10074.	9847.	9962.
24	10030.	9571.	9245.	8460.	9480.	9463.	9628.	10087.
25	8928.	9135.	8740.	8768.	9437.	10026.	9758.	9809.

TABLE FIVE

TOLERANCE STUDY -- AS FIRED RESISTORS ---
TEST PATTERN RK1101
ASPECT RATIO = 5
WIDTH = 30 MIL.
RESISTOR PASTE = 100 OHM/ SQUARE

AS-FIRED RESISTANCE $x10^0$ (ohm)

Substrate	1-R5	1-R6	2-R5	2-R6	1-R8	1-R7	2-R8	2-R7
1	608.	649.	604.	623.	548.	555.	562.	549.
2	536.	565.	511.	540.	524.	539.	540.	541.
3	430.	573.	543.	602.	507.	529.	507.	507.
4	445.	591.	539.	509.	550.	559.	544.	518.
5	478.	573.	527.	545.	531.	537.	549.	509.
6	504.	600.	526.	576.	542.	581.	562.	564.
7	590.	592.	543.	558.	507.	535.	551.	507.
8	431.	526.	521.	528.	508.	558.	561.	521.
9	588.	585.	525.	540.	521.	560.	544.	537.
10	492.	573.	532.	506.	513.	561.	566.	568.
11	450.	579.	537.	590.	536.	588.	570.	536.
12	353.	515.	519.	489.	531.	551.	554.	531.
13	556.	578.	528.	563.	520.	519.	562.	538.
14	518.	543.	539.	515.	520.	547.	559.	524.
15	523.	577.	536.	557.	542.	570.	550.	525.
16	522.	587.	529.	607.	561.	576.	567.	545.
17	387.	552.	535.	504.	555.	580.	565.	570.
18	359.	568.	525.	508.	558.	572.	542.	543.
19	463.	527.	514.	499.	539.	569.	545.	539.
20	575.	563.	538.	541.	534.	550.	518.	522.
21	551.	595.	524.	529.	559.	573.	531.	538.
22	587.	552.	536.	523.	530.	534.	546.	522.
23	632.	613.	578.	586.	579.	564.	558.	526.
24	406.	558.	465.	447.	521.	550.	531.	536.
25	625.	656.	602.	629.	654.	613.	610.	594.

TABLE STX
AS FIRED RESISTANCE SPREAD
L DALTON MOLSON
PASTE SYSTEM #A#
ASPECT RATIO = 5
PASTE SHEET RESISTIVITY = 1K OHMS PER SQUARE

AS-FIRED RESISTANCE $x10^0$ (ohm)

Substrate	1-R5	1-R6	2-R5	2-R6	1-R8	1-R7	2-R8	2-R7
1	4146.	4690.	4591.	4970.	4500.	3922.	4001.	4395.
2	5058.	5060.	5181.	5049.	5166.	4975.	4845.	4596.
3	4978.	4595.	4396.	6227.	4433.	4069.	4926.	5152.
4	4621.	4826.	4765.	4755.	4413.	4826.	5055.	4132.
5	3860.	4700.	5003.	4857.	4613.	4461.	4927.	4694.
6	4437.	4343.	4762.	4665.	4921.	4617.	5202.	4752.
7	4210.	4687.	4813.	4863.	5023.	4958.	5097.	4906.
8	4321.	5512.	4640.	4721.	4544.	4653.	4666.	4751.
9	4545.	4784.	4929.	5239.	4605.	4347.	4573.	4869.
10	5000.	4758.	4724.	5334.	4625.	4734.	4693.	4691.
11	5007.	4854.	4351.	5102.	4674.	4379.	4719.	4491.
12	4936.	5446.	4757.	5585.	4601.	4490.	4871.	4684.
13	4233.	4318.	4252.	4723.	4482.	4574.	4997.	4894.
14	4568.	4492.	4557.	4827.	4715.	4576.	4928.	4569.
15	4870.	4697.	4613.	5129.	4597.	4420.	4851.	4691.
16	4638.	4765.	4832.	4638.	4865.	4635.	5182.	5082.
17	4885.	4599.	4601.	5211.	4614.	4530.	4835.	4919.
18	4321.	4514.	4217.	4564.	4937.	4506.	4842.	4844.
19	4900.	4864.	4245.	4626.	4369.	4269.	4845.	4515.
20	4797.	4681.	4699.	4959.	4593.	4595.	4825.	4469.
21	4625.	4719.	4474.	4969.	4591.	4865.	5046.	4584.
22	4769.	4858.	4738.	4947.	4638.	4518.	4693.	4505.
23	4691.	4881.	4535.	5182.	4572.	4661.	4888.	4672.
24	4212.	4542.	4380.	4720.	4304.	4486.	5132.	4582.
25	4461.	4457.	4726.	4886.	4924.	4393.	5132.	4849.

T A B L E S E V E N

AS FIRED RESISTANCE STUDY
PASTE SYSTEM #A#
PASTE SHEET RESISTIVITY = 10K OHMS PER SQUARE
ASPECT RATIO = 5

AS-FIRED RESISTANCE $x10^{1}$ (ohm)

Substrate	1-R5	1-R6	2-R5	2-R6	1-R8	1-R7	2-R8	2-R7
1	4758.	4828.	5162.	4483.	4675.	5356.	5120.	5079.
2	5010.	5222.	5316.	4833.	5236.	4895.	5090.	4868.
3	4486.	5436.	5192.	4435.	5066.	5281.	4804.	4995.
4	5043.	5369.	5076.	4748.	5081.	5383.	5240.	5120.
5	4936.	4965.	4936.	4615.	5141.	5159.	5074.	5089.
6	4925.	5387.	5000.	4802.	5197.	4860.	5046.	4992.
7	5040.	5472.	4978.	5071.	5159.	4976.	5378.	5342.
8	5089.	5341.	5058.	5276.	4963.	5296.	4993.	5041.
9	5228.	5393.	5084.	4774.	5145.	5493.	5456.	5230.
10	4921.	5466.	4961.	4834.	5035.	5173.	5219.	5308.
11	5155.	5776.	5360.	5351.	4489.	4759.	5323.	5234.
12	4787.	5535.	4881.	5059.	4973.	5275.	5183.	5194.
13	4815.	5131.	4488.	4795.	5007.	5284.	5120.	5012.
14	5569.	5437.	5122.	5590.	5405.	5450.	5177.	5085.
15	5234.	5370.	4873.	4517.	5172.	5055.	5026.	5001.
16	5007.	5141.	4761.	4914.	5107.	5293.	5432.	5113.
17	5114.	5222.	4833.	4956.	5050.	4957.	5126.	4815.
18	5099.	5154.	4756.	4739.	4914.	5044.	4913.	4850.
19	5502.	5131.	5010.	5235.	5034.	5065.	5200.	5320.
20	4894.	5094.	4745.	4546.	5102.	5270.	5387.	4923.
21	5435.	5168.	4620.	4673.	4717.	4620.	4948.	4713.
22	4797.	4726.	4480.	4699.	5089.	4693.	5030.	4796.
23	5156.	5129.	5056.	5000.	4961.	5217.	5100.	4909.
24	5000.	5146.	4804.	4589.	4654.	4794.	4986.	4921.
25	4623.	4764.	4108.	4610.	4763.	4841.	5028.	4896.

T A B L E E I G H T

TOLERANCE STUDY -- AS FIRED RESISTORS --

TEST PATTERN PK 1101

ASPECT RATIO = 5

WIDTH = 30 MIL

RESISTORS 1-R5 TO 2-R7

RESISTOR PASTE = 100K OHMS PER SQUARE

AS-FIRED RESISTANCE $x10^2$ (ohm)

Substrate	1-R5	1-R6	2-R5	2-R6	1-R8	1-R7	2-R8	2-R7
1	3225.	3438.	3338.	3209.	3806.	3622.	4675.	3709.
2	2803.	2892.	2710.	2902.	3449.	3473.	3708.	3722.
3	2998.	2797.	3009.	2533.	3783.	3380.	3744.	3470.
4	3262.	3601.	3330.	3331.	4640.	4419.	4809.	4528.
5	3155.	3394.	3028.	3424.	4008.	3558.	4386.	3895.
6	3648.	3899.	3577.	3824.	4372.	4154.	4536.	4491.
7	3264.	3514.	3409.	3126.	4247.	3988.	3996.	4311.
8	3297.	3323.	3018.	3105.	4113.	3969.	3752.	3673.
9	3561.	3438.	3181.	3368.	3881.	3763.	4098.	4057.
10	3353.	3787.	3458.	3467.	4525.	4315.	4383.	4386.
11	3578.	3789.	3814.	3704.	4567.	4505.	4842.	4623.
12	3245.	3267.	2970.	3387.	4161.	4016.	4246.	4125.
13	3760.	3424.	3326.	3850.	4008.	3925.	4352.	4568.
14	3414.	3284.	3246.	3285.	3812.	3787.	4082.	4065.
15	3252.	3513.	3435.	3571.	4217.	4030.	4565.	4457.
16	3330.	3155.	3302.	3499.	4177.	4155.	4444.	4305.
17	3018.	3260.	2871.	3256.	4023.	3832.	4274.	4146.
18	3262.	3567.	3339.	3578.	4003.	4221.	4322.	4288.
19	3193.	3062.	3050.	3108.	3642.	3636.	3804.	3764.
20	3307.	3353.	3173.	3450.	4140.	4078.	4213.	4251.
21	3561.	3488.	3258.	3580.	4027.	3962.	4217.	4226.
22	3680.	3564.	3387.	3719.	4212.	4148.	4350.	4476.
23	3769.	3443.	3264.	3419.	3881.	3923.	4005.	4128.
24	3523.	3275.	3252.	3388.	3842.	3872.	4142.	4307.
25	3427.	3248.	3296.	3012.	3973.	4007.	4329.	4319.

TABLE EIGHT A

TOLERANCE STUDY -- AS FIRED RESISTORS --
TEST PATTERN RK 1101
ASPECT RATIO = 5
WIDTH = 30 MIL
RESISTORS 1-R8 TO 2-R7
RESISTOR PASTE = 10UK OHMS PER SQUARE

AS-FIRED RESISTANCE x 10^2 (ohm)

Substrate	1-R8	1-R7	2-R8	2-R7
1	3806.	3622.	4675.	3709.
2	3449.	3473.	3708.	3722.
3	3783.	3380.	3744.	3470.
4	4640.	4419.	4809.	4528.
5	4008.	3558.	4386.	3895.
6	4372.	4154.	4536.	4491.
7	4247.	3988.	3996.	4311.
8	4113.	3969.	3752.	3673.
9	3881.	3763.	4098.	4057.
10	4525.	4315.	4383.	4386.
11	4567.	4505.	4842.	4623.
12	4161.	4016.	4246.	4125.
13	4008.	3925.	4352.	4568.
14	3812.	3787.	4082.	4065.
15	4317.	4030.	4565.	4457.
16	4177.	4155.	4444.	4305.
17	4023.	3832.	4274.	4146.
18	4003.	4221.	4322.	4288.
19	3642.	3636.	3804.	3764.
20	4140.	4078.	4213.	4251.
21	4027.	3962.	4217.	4226.
22	4212.	4148.	4350.	4476.
23	3881.	3923.	4005.	4128.
24	3842.	3872.	4142.	4307.
25	3973.	4007.	4329.	4319.

TABLE NINE

TEST PATTERN PK 1101
ASPECT RATIO = 5
WIDTH = 30 MIL
RESISTORS 1-R5 TO 2-R7
RESISTOR PASTE = 17 OHMS PER SQUARE

AS-FIRED RESISTANCE $x10^3$ (ohm)

Substrate	1-R5	1-R6	2-R5	2-R6	1-R8	1-R7	2-R8	2-R7
1	6131.	6608.	6701.	7057.	6101.	6801.	7445.	7631.
2	6216.	6793.	6499.	7768.	6709.	6721.	6541.	7293.
3	7841.	6562.	6767.	8077.	6780.	7301.	7567.	7536.
4	7149.	6923.	6960.	7790.	6957.	8963.	7351.	7728.
5	6772.	7235.	6924.	8103.	7177.	7270.	7520.	7948.
6	6815.	6885.	6830.	6725.	7559.	7797.	7312.	7443.
7	7976.	7074.	7189.	8794.	6447.	6613.	7358.	7428.
8	7265.	7274.	6783.	7233.	7392.	6871.	7430.	6875.
9	7005.	7517.	7169.	7503.	7770.	7030.	7636.	7697.
10	7215.	7355.	6526.	6847.	7413.	8119.	7839.	7328.
11	7635.	7881.	7864.	8777.	7622.	7000.	7994.	7889.
12	7874.	7653.	7522.	10455.	8067.	7537.	7491.	7324.
13	7674.	7507.	7836.	8122.	7707.	7552.	7005.	8067.
14	7362.	6801.	6638.	7105.	7946.	8958.	7525.	7172.
15	8006.	7579.	7099.	6997.	9351.	8224.	7250.	7061.
16	7036.	6840.	6407.	6462.	7674.	7896.	7165.	7255.
17	6914.	6697.	6648.	7467.	7089.	7329.	7579.	7932.
18	7477.	6803.	6185.	6879.	7525.	7371.	7565.	7861.
19	7570.	7438.	7378.	8122.	7680.	7741.	7649.	7900.
20	6830.	7461.	6859.	7696.	7403.	7959.	7684.	7450.
21	6897.	6801.	6971.	6729.	7059.	7562.	7309.	7700.
22	6695.	7182.	6465.	7172.	6984.	7281.	7850.	7264.
23	7461.	6757.	6809.	6816.	7353.	8116.	7985.	7604.
24	9319.	7158.	6818.	7719.	7000.	8078.	9994.	7681.
25	7145.	7511.	6945.	10978.	7616.	7418.	8496.	7958.

TABLE TEN

AS FIRED RESISTANCE STUDY
ASPECT RATIO = 2
PASTE= 100 OHMS PER SQUARE
WIDTH = 30 MIL
TEST PATTERN = RK 1101

AS-FIRED RESISTANCE $x10^{-1}$ (ohm)

Substrate	1-R17	1-R21	1-R18	1-R22	2-R17	2-R21	2-R18	2-R22
1	2402.	2502.	2438.	2391.	2754.	2723.	2842.	2796.
2	2215.	2449.	2219.	2422.	2375.	2389.	2497.	2560.
3	2239.	2395.	2380.	2215.	2458.	2447.	2470.	2590.
4	2224.	2335.	2388.	2279.	2538.	2569.	2467.	2514.
5	2050.	2228.	2405.	2278.	2543.	2598.	2362.	2592.
6	2035.	1983.	2295.	2393.	2579.	2717.	2371.	2767.
7	2278.	2236.	2242.	2314.	2469.	2474.	2532.	2626.
8	2015.	2188.	2204.	2203.	2448.	2514.	2421.	2527.
9	2304.	2320.	2359.	2279.	2327.	2545.	2580.	2533.
10	2123.	2435.	2413.	2406.	2335.	2574.	2606.	2572.
11	2369.	2411.	2431.	2502.	2685.	2711.	2663.	2829.
12	1988.	2105.	2421.	2134.	2519.	2407.	2518.	2518.
13	2107.	2257.	2195.	2016.	2474.	2497.	2559.	2722.
14	2324.	2264.	2558.	2567.	2734.	2607.	2568.	2507.
15	2222.	2344.	2121.	2477.	2375.	2370.	2404.	2637.
16	1973.	2247.	2185.	2199.	2557.	2341.	2400.	2683.
17	2170.	2223.	2381.	2203.	2600.	2680.	2562.	2317.
18	2251.	2373.	2405.	2456.	2499.	2418.	2579.	2465.
19	2279.	2376.	2317.	2322.	2654.	2365.	2574.	2492.
20	2220.	2301.	2193.	2227.	2420.	2323.	2449.	2394.
21	2059.	2173.	2389.	2361.	2463.	2475.	2475.	2291.
22	1952.	2270.	2176.	2032.	2217.	2285.	2296.	2261.
23	2261.	2398.	2564.	2480.	2383.	2481.	2765.	2557.
24	2129.	2262.	2262.	2272.	2462.	2245.	2553.	2411.
25	2632.	3018.	2590.	2560.	2767.	2833.	2826.	2873.

TABLE ELEVEN

TOLERANCE STUDY - THICK FILM -
TEST PATTERN RK 1101
ASPECT RATIO = 2
WIDTH = 30 MIL
PASTE = 1K OHMS PER SQUARE

AS-FIRED RESISTANCE $\times 10^0$ (ohm)

Substrate	1-R17	1-R21	1-R18	1-R22	2-R17	2-R21	2-R18	2-R22
1	1571.	1542.	1909.	1681.	1608.	1773.	1622.	1882.
2	1976.	2205.	2526.	1768.	1823.	2108.	1994.	2538.
3	1863.	1880.	1612.	2053.	1860.	1857.	1679.	1906.
4	1933.	2085.	2018.	1889.	1908.	1881.	2143.	1957.
5	1698.	1745.	1976.	1665.	1655.	1889.	2062.	2098.
6	2012.	1905.	1958.	1804.	1847.	2112.	1986.	2197.
7	1806.	1827.	1840.	1756.	1548.	1911.	1965.	1981.
8	1685.	1795.	1556.	1387.	1932.	1607.	1897.	1976.
9	1880.	1948.	2287.	1734.	1940.	1891.	1857.	1956.
10	1981.	2107.	2081.	1859.	1957.	1947.	1934.	1810.
11	1634.	2016.	1932.	1643.	1819.	2217.	1891.	1849.
12	1851.	2065.	1774.	1759.	1799.	1969.	1831.	1938.
13	1650.	1735.	1606.	1458.	1768.	2004.	2099.	2087.
14	1851.	2048.	1733.	1670.	1827.	1820.	2033.	2118.
15	1992.	2008.	1755.	1720.	1964.	1914.	1906.	1953.
16	1978.	2150.	1824.	1857.	1909.	1853.	2147.	2294.
17	1897.	2150.	2028.	1480.	1848.	2261.	1934.	1874.
18	1649.	1842.	1691.	1616.	1942.	2465.	1883.	1875.
19	1807.	1996.	1932.	1794.	1769.	2358.	1795.	1821.
20	2074.	2027.	1840.	1828.	1693.	1968.	1798.	1683.
21	1885.	1845.	1557.	1543.	1553.	1775.	1836.	1865.
22	2148.	2034.	1894.	1629.	1818.	1943.	2039.	1743.
23	1802.	1996.	1746.	1863.	1760.	1875.	1805.	1967.
24	1799.	1797.	1600.	1623.	1657.	1948.	1951.	2072.
25	1853.	1994.	1820.	1698.	1933.	1842.	1711.	1791.

T A B L E T W E L V E

TOLERANCE STUDY- THICK FILM
TEST PATTERN RK 1101
ASPECT RATIO = 2
WIDTH = 30 MIL
PASTE = 10K OHMS PER SQUARE

AS-FIRED RESISTANCE $x10^1$ (ohm)

Substrate	1-R17	1-R21	1-R18	1-R22	2-R17	2-R21	2-R18	2-R22
1	1826.	2257.	1729.	1676.	1786.	1776.	1639.	1712.
2	1825.	2449.	1898.	1763.	2019.	1873.	2022.	1808.
3	1712.	2046.	1713.	1557.	1774.	1834.	1774.	1698.
4	1735.	2157.	1897.	1902.	2024.	1937.	1881.	1981.
5	1704.	2053.	1701.	1815.	2139.	1970.	1824.	1794.
6	1837.	2320.	1880.	1792.	1924.	1994.	1945.	1930.
7	1793.	2308.	1864.	1894.	2076.	2013.	1718.	1925.
8	1796.	2246.	1863.	1845.	2011.	1892.	1937.	1902.
9	1846.	2379.	1696.	1667.	1862.	1779.	2525.	1792.
10	1803.	2328.	1779.	1806.	1917.	1954.	1882.	1905.
11	1650.	2122.	1798.	1871.	2049.	2038.	2402.	2157.
12	1631.	2083.	1847.	1934.	1852.	1887.	2570.	1884.
13	1841.	2138.	1812.	1791.	1891.	2012.	1945.	1925.
14	1881.	2650.	1976.	1852.	1928.	2052.	2096.	2039.
15	1929.	2582.	2579.	1759.	1941.	1981.	2132.	1965.
16	1830.	2388.	2010.	1837.	1912.	2131.	2053.	2194.
17	1892.	2670.	1924.	1837.	1951.	1952.	2168.	1970.
18	2057.	2302.	1824.	1911.	1913.	2114.	1929.	1915.
19	1975.	2343.	1777.	1762.	1939.	2013.	2058.	2130.
20	1922.	2488.	1876.	1805.	2032.	1973.	1932.	1976.
21	1958.	2457.	1793.	1731.	1947.	1925.	1945.	1954.
22	1776.	2347.	1771.	1665.	1833.	1767.	1953.	1817.
23	1903.	2607.	2015.	1798.	2097.	2045.	1963.	2147.
24	3683.	2357.	1793.	1848.	1984.	1948.	1966.	1920.
25	1835.	1965.	1738.	1570.	1853.	1865.	1715.	1635.

TABLE THIRTEEN

TOLERANCE STUDY
TEST PATTERN RK 1101
ASPECT RATIO = 2
WIDTH = 30 MIL
PASTE SHEET RESISTIVITY = 100K OHMS PER SQUARE

AS-FIRED RESISTANCE $\times 10^2$ (ohm)

Substrate	1-R17	1-R21	1-R18	1-R22	2-R17	2-R21	2-R18	2-R22
1	1500.	1546.	1481.	1627.	1956.	1744.	1603.	1762.
2	1149.	1357.	1539.	1585.	1802.	1970.	1486.	1587.
3	1474.	1555.	1449.	1390.	1684.	1602.	1655.	1658.
4	1973.	2400.	1499.	1647.	1681.	1739.	1887.	1883.
5	1638.	1696.	1625.	1666.	1797.	1877.	1815.	1936.
6	1745.	1845.	1503.	1573.	1717.	2117.	2060.	1932.
7	1533.	1651.	1592.	1607.	1805.	1672.	1478.	1731.
8	1560.	1643.	1584.	1685.	1684.	1529.	1778.	1783.
9	1542.	1675.	1615.	1614.	1661.	1764.	1816.	1952.
10	1519.	1507.	1710.	1877.	1706.	1961.	1711.	1851.
11	1362.	1750.	1916.	1621.	1862.	2319.	1848.	1897.
12	1587.	1638.	1607.	1445.	1781.	1670.	1654.	1616.
13	1436.	1769.	1680.	1595.	1779.	1655.	2282.	2013.
14	1488.	1582.	1668.	1513.	1777.	1661.	1740.	1723.
15	1531.	1546.	1608.	1570.	1748.	1687.	1883.	1673.
16	1472.	1564.	1699.	1595.	1927.	1758.	1768.	1663.
17	1564.	1401.	1720.	1581.	1714.	1743.	1750.	1812.
18	1564.	1604.	1649.	1565.	1670.	1674.	1920.	1688.
19	1604.	1613.	1534.	1486.	1835.	1743.	1729.	1658.
20	1438.	1618.	1791.	1815.	1848.	1911.	1672.	1713.
21	1609.	1655.	1668.	1598.	1823.	1867.	2107.	2171.
22	1597.	1794.	1690.	1533.	1759.	1808.	1942.	1788.
23	1607.	1630.	1714.	1569.	1739.	1799.	1785.	1795.
24	1685.	1601.	1649.	1386.	1914.	1718.	1839.	1794.
25	1703.	1714.	1593.	1514.	1801.	1827.	2007.	1903.

TABLE FOURTEEN

TOLERANCE STUDY
TEST PATTERN RK 1101
ASPECT RATIO = 2
WIDTH = 30 MIL
PASTE SHEET RESISTIVITY = 1MEG OHMS PER SQUARE
RESISTORS 1-R17 TO 2-R22

AS-FIRED RESISTANCE $x10^3$ (ohm)

Substrate	1-R17	1-R21	1-R18	1-R22	2-R17	2-R21	2-R18	2-R22
1	1693.	1594.	1873.	2072.	1783.	2129.	2165.	1943.
2	1950.	2154.	1957.	1908.	1870.	2137.	2119.	2129.
3	2098.	2227.	2236.	2099.	2380.	2292.	2052.	2230.
4	1870.	2145.	1951.	2034.	2432.	2116.	3627.	2879.
5	1986.	2043.	1854.	2263.	2335.	2169.	2148.	2166.
6	2034.	2054.	2097.	1964.	2050.	2152.	1880.	2084.
7	1910.	2058.	2009.	1800.	2338.	3015.	2065.	1975.
8	1826.	1988.	1938.	2008.	2351.	2427.	2022.	2019.
9	2090.	2241.	2325.	2121.	2425.	2155.	2053.	2160.
10	2493.	2508.	2256.	2240.	2280.	2186.	2499.	2601.
11	2826.	2770.	4642.	2062.	2367.	2276.	2647.	2510.
12	2202.	2761.	2494.	1945.	2413.	6527.	2175.	2269.
13	2246.	2260.	2126.	2279.	2270.	2028.	2352.	2230.
14	2300.	2393.	2016.	1816.	2134.	1965.	1866.	1982.
15	2280.	2497.	2318.	2069.	2159.	2401.	2479.	2323.
16	2077.	2606.	2397.	2192.	2255.	2248.	2312.	1972.
17	2201.	2437.	1973.	2077.	2140.	2204.	2166.	2032.
18	2545.	2791.	2057.	2346.	2126.	2085.	2414.	2348.
19	2534.	3070.	2488.	2324.	2563.	2530.	2464.	2317.
20	2550.	2677.	2074.	2065.	2954.	2146.	2089.	2313.
21	2128.	2485.	2095.	2011.	2316.	2298.	2204.	2101.
22	2050.	2286.	2318.	2222.	2206.	2389.	5285.	2542.
23	2517.	2555.	2141.	2275.	3894.	2388.	2076.	2486.
24	2541.	2867.	2155.	2750.	2207.	2154.	2075.	2047.
25	2333.	2367.	2387.	2071.	2093.	2053.	1942.	1971.

TABLE FIFTEEN

RESISTOR SPREAD STUDY
ASPECT RATIO = 0.667
WIDTH = 30 MIL
PASTE SHEET RESISTIVITY = 100 OHMS PER SQUARE
RESISTORS 1-R41 TO 4-R42
TEST PATTERN RK 1101

AS-FIRED RESISTANCE $x10^{-2}$ (ohm)

Substrate	1-R41	1-R42	2-R41	2-R42	4-R41	4-R42	3-R41	3-R42
1	8658.	11240.	9363.	10410.	9340.	11310.	10790.	10680.
2	7678.	8315.	8699.	8806.	9161.	9097.	10170.	10590.
3	6814.	7598.	8527.	8071.	9203.	8879.	9452.	9752.
4	7556.	8227.	8317.	9998.	10130.	9099.	9614.	9393.
5	7946.	9008.	8660.	7714.	10550.	9153.	11380.	11170.
6	7784.	9387.	9883.	10480.	10290.	8973.	9496.	10410.
7	7403.	8276.	8233.	9492.	9005.	9131.	9770.	10160.
8	6951.	8695.	7579.	9337.	9790.	9316.	9248.	12390.
9	8140.	8050.	8669.	9668.	10260.	12670.	9777.	9987.
10	8270.	8448.	10060.	10880.	10130.	9674.	9960.	9059.
11	8118.	8442.	9096.	9796.	10020.	9219.	7314.	9616.
12	6887.	9133.	8643.	9182.	8864.	8379.	8550.	8731.
13	8449.	7280.	7474.	7856.	8376.	7818.	8818.	9738.
14	8082.	9790.	8929.	9799.	9723.	9849.	10270.	12480.
15	7648.	8458.	8978.	9798.	8748.	9198.	9648.	10630.
16	8401.	8750.	8910.	10760.	8816.	12170.	9338.	9323.
17	8553.	8040.	9261.	9571.	9772.	8612.	10020.	11190.
18	9969.	8698.	8234.	8767.	12270.	8490.	8911.	11530.
19	7774.	8865.	8367.	9627.	9443.	9570.	9646.	11520.
20	7669.	8114.	8587.	10180.	8090.	9629.	10240.	9954.
21	7838.	9300.	8957.	8887.	10600.	9496.	10990.	10450.
22	7037.	7531.	7513.	7568.	8425.	8833.	9544.	8942.
23	8022.	8546.	8593.	10080.	10040.	9239.	10670.	11960.
24	7587.	8272.	4717.	8543.	8504.	9279.	8248.	10430.
25	9812.	8912.	9092.	10540.	9641.	11210.	11920.	10000.

TABLE SIXTEEN

ASPECT RATIO = 0.667
WIDTH = 30 MIL.
PASTE SHEET RESISTIVITY = 1K OHMS PER SQUARE
TEST PATTERN RK 1101
RESISTORS 1-R41 TO 4-R42

AS-FIRED RESISTANCE $x10^{-1}$ (ohm)

Substrate	1-R41	1-R42	2-R41	2-R42	4-R41	4-R42	3-R41	3-R42
1	2960.	4205.	3962.	3526.	4519.	4314.	3952.	5879.
2	4798.	4396.	4865.	4291.	4815.	4588.	4386.	5468.
3	3771.	4108.	5515.	4881.	6077.	5149.	5168.	6227.
4	3905.	4604.	5124.	4545.	5086.	4356.	6260.	4414.
5	3693.	4464.	4200.	4869.	5095.	4499.	4214.	5252.
6	3496.	4998.	4500.	4453.	5051.	4638.	4336.	4512.
7	4466.	4325.	4265.	4425.	5700.	5473.	4343.	5289.
8	3690.	3598.	3722.	4118.	5176.	4005.	4617.	4778.
9	3832.	5223.	4635.	3774.	5485.	4565.	4359.	5011.
10	4810.	4874.	4615.	3932.	5885.	5131.	4732.	5367.
11	4326.	5172.	4956.	4118.	5145.	5196.	5053.	4274.
12	4742.	4741.	3591.	4806.	6720.	5748.	5143.	6251.
13	4014.	4275.	4952.	4604.	5813.	4282.	4522.	4986.
14	3973.	4579.	5328.	4029.	5490.	5131.	4833.	5467.
15	4246.	7370.	5435.	4456.	5791.	3974.	5267.	5608.
16	3713.	3742.	3941.	4068.	5925.	3923.	4252.	5574.
17	5473.	5733.	4901.	5080.	5661.	4952.	4288.	5228.
18	3658.	5173.	4979.	4549.	5500.	4526.	4215.	4831.
19	3650.	4679.	4017.	4167.	6430.	5031.	5065.	5493.
20	4251.	5443.	4882.	6032.	6260.	4975.	4943.	6600.
21	4854.	4950.	4889.	4646.	6102.	4932.	4472.	5799.
22	4675.	5165.	4520.	4734.	6675.	5086.	4977.	5861.
23	4987.	5209.	4493.	4640.	6467.	4958.	4865.	5067.
24	3264.	4333.	4355.	3770.	5272.	4486.	4158.	4798.
25	4922.	4165.	5620.	2195.	7056.	6900.	5000.	5025.

TABLE SEVENTEEN

ASPECT RATIO = 0.667
WIDTH = 30 MIL.
PASTE SHEET RESISTIVITY = 10K OHMS PER SQUARE
TEST PATTERN RK 1101
RESISTORS 1-R41 TO 4-R42

AS-FIRED RESISTANCE $x10^0$ (ohm)

Substrate	1-R41	1-R42	2-R41	2-R42	4-R41	4-R42	3-R41	3-R42
1	3093.	3772.	3655.	3512.	4061.	3903.	3865.	5047.
2	4212.	4611.	5788.	4935.	3488.	2098.	5030.	5777.
3	3298.	3954.	4159.	3954.	4179.	4231.	4904.	4159.
4	3369.	3847.	4195.	3770.	4410.	4246.	4722.	4667.
5	3851.	4074.	4038.	4068.	4989.	4339.	4457.	4406.
6	3458.	3903.	4170.	4295.	4220.	4064.	4376.	4747.
7	3685.	4205.	3876.	3913.	4502.	4994.	4825.	4353.
8	3542.	3748.	3957.	3613.	4669.	4682.	4575.	4550.
9	3673.	3661.	4166.	3854.	3508.	3496.	4021.	4701.
10	2984.	3035.	3545.	3220.	3773.	3619.	3534.	4757.
11	2960.	3122.	4245.	4002.	4240.	4486.	4289.	5372.
12	3545.	4069.	4680.	3138.	4641.	5423.	5067.	3605.
13	3560.	3443.	4994.	4615.	5914.	4690.	4837.	4270.
14	3691.	4346.	4864.	3914.	5800.	4761.	6171.	5407.
15	2879.	3799.	4438.	4318.	5323.	4852.	4507.	5064.
16	3648.	3861.	4731.	5060.	4783.	4980.	4975.	4666.
17	3804.	3994.	4705.	4343.	5841.	4244.	4047.	5049.
18	3773.	4678.	4728.	4865.	3036.	4911.	4652.	4022.
19	3258.	3979.	4574.	4662.	5172.	5120.	4863.	4657.
20	3615.	3656.	3982.	3764.	3721.	3394.	3924.	4736.
21	4272.	3785.	4388.	4094.	6260.	4416.	4729.	4592.
22	3322.	4007.	4650.	4663.	4974.	4441.	4876.	5150.
23	3599.	5649.	4582.	4341.	6432.	4623.	5082.	5253.
24	3294.	3537.	3852.	3383.	5316.	4611.	4654.	4413.
25	3759.	3776.	3814.	3987.	4513.	4703.	4461.	5850.

TABLE EIGHTEEN A

ASPECT RATIO = 0.667
WIDTH = 30 MIL.
PASTE SHEET RESISTIVITY = 100K OHMS PER SQUARE
TEST PATTERN RK 1101
RESISTORS 1-R41 TO 2-R42

AS FIRED RESISTANCE x 10^1 (ohm)

Substrate	1-R41	1-R42	2-R41	2-R42
1	3230.	2984.	4737.	3424.
2	3392.	4069.	3757.	3416.
3	5375.	3689.	4190.	3990.
4	2791.	3311.	3218.	4998.
5	4042.	3586.	4320.	4420.
6	2838.	3308.	4218.	4586.
7	2647.	4822.	4159.	3267.
8	3322.	5221.	4573.	6340.
9	3982.	4309.	5132.	5280.
10	4220.	7462.	6838.	4744.
11	3546.	4508.	4013.	3603.
12	7959.	5847.	5199.	7003.
13	5463.	5739.	4941.	4468.
14	4960.	3687.	3382.	4470.
15	3063.	4284.	4079.	4290.
16	5753.	4834.	8069.	3112.
17	3695.	3544.	4431.	4788.
18	3167.	4806.	4511.	4926.
19	4198.	6522.	4898.	3212.
20	4151.	4698.	3925.	3486.
21	3065.	3930.	3817.	4271.
22	3674.	3385.	4064.	3745.
23	3266.	3693.	4781.	4182.
24	3357.	3648.	3942.	4671.

TABLE EIGHTEEN

ASPECT RATIO = 0.667
WIDTH = 30 MIL.
PASTE SHEET RESISTIVITY = 100K OHMS PER SQUARE
TEST PATTERN RK 1101
RESISTORS 1-R41 TO 4-R42

AS-FIRED RESISTANCE $x10^{1}$ (ohm)

Substrate	1-R41	1-R42	2-R41	2-R42	4-R41	4-R42	3-R41	3-R42
1	3230.	2984.	4737.	3424.	5105.	5225.	5864.	4740.
2	3392.	4069.	3757.	3416.	5034.	8186.	6119.	5799.
3	5375.	3689.	4190.	3990.	6535.	5230.	5126.	4797.
4	2791.	3311.	3218.	4998.	5156.	4309.	6666.	3823.
5	4042.	3586.	4320.	4420.	5525.	4117.	4621.	3829.
6	2838.	3308.	4218.	4586.	3609.	5617.	5834.	6844.
7	2647.	4822.	4159.	3267.	4049.	4747.	5898.	4050.
8	3322.	5221.	4573.	6340.	3580.	5486.	7556.	5610.
9	3982.	4309.	5132.	5280.	7104.	5080.	5489.	4059.
10	4220.	7462.	6838.	4744.	9660.	5353.	4738.	9082.
11	3546.	4508.	4013.	3603.	6763.	4710.	4307.	3128.
12	7959.	5847.	5199.	7003.	4170.	4357.	6708.	6302.
13	5463.	5739.	4941.	4468.	7042.	3689.	6555.	4558.
14	4960.	3687.	3382.	4470.	4613.	4595.	3149.	6728.
15	3063.	4284.	4079.	4290.	5188.	5121.	4604.	3398.
16	5753.	4834.	8069.	3112.	5617.	4207.	3391.	4698.
17	3695.	3544.	4431.	4788.	6273.	5362.	5168.	4412.
18	3167.	4806.	4511.	4926.	3231.	5198.	4133.	5248.
19	4198.	6522.	4898.	3212.	4421.	4956.	4419.	3364.
20	4151.	4698.	3925.	3486.	1498.	5632.	7277.	5724.
21	3065.	3930.	3817.	4271.	7046.	5030.	5646.	4924.
22	3674.	3385.	4064.	3745.	2997.	3808.	4071.	4656.
23	3266.	3693.	4781.	4182.	4534.	4138.	9252.	4895.
24	3357.	3648.	3942.	4671.	5535.	4680.	3920.	4363.

TABLE NINTEEN

ASPECT RATIO = 0.667
WIDTH = 30 MIL.
PASTE SHEET RESISTIVITY = 1MEG OHM PER SQUARE
TEST PATTERN RK 1101
RESISTORS 1-R41 TO 4-R42

AS-FIRED RESISTANCE $x10^2$ (ohm)

Substrate	1-R41	1-R42	2-R41	2-R42	4-R41	4-R42	3-R41	3-R42
1	1639.	2415.	3121.	2356.	2256.	2681.	2258.	2024.
2	2059.	2492.	2751.	2504.	2174.	2572.	2685.	2396.
3	2451.	3030.	2939.	2874.	2471.	3050.	2793.	3037.
4	2140.	2725.	2616.	2223.	2232.	2657.	2504.	2704.
5	1772.	2484.	2986.	2207.	1886.	2471.	2629.	2425.
6	2253.	2367.	2850.	2477.	2188.	2768.	2498.	2341.
7	1934.	2475.	2652.	2530.	1969.	2293.	2486.	2624.
8	2478.	2469.	2759.	2307.	1820.	2829.	2657.	2396.
9	1504.	2983.	2508.	2288.	1557.	2701.	2511.	2166.
10	2220.	2643.	2681.	2488.	2534.	2944.	2629.	2433.
11	2110.	2670.	2579.	2632.	2580.	2967.	2996.	3280.
12	2525.	2386.	4978.	2247.	2261.	3306.	2441.	2414.
13	1910.	2956.	3005.	2363.	2568.	3237.	3473.	3053.
14	1847.	2777.	2918.	2022.	1933.	2320.	2347.	2109.
15	1884.	2345.	2658.	2270.	1599.	2273.	2431.	2199.
16	3430.	2911.	3208.	2354.	2806.	2410.	2590.	2108.
17	1729.	2244.	2705.	2237.	2372.	2315.	2084.	2400.
18	2483.	2500.	2842.	2478.	2489.	2537.	2822.	2800.
19	2950.	3274.	3792.	2650.	2319.	3374.	3083.	2770.
20	2290.	2646.	2610.	2328.	2421.	2694.	2793.	2670.
21	2010.	2797.	2822.	2459.	2548.	2506.	2729.	2365.
22	2460.	3221.	2694.	2259.	2650.	2887.	2900.	2843.
23	2709.	2713.	2864.	2797.	2831.	2764.	2826.	3027.
24	2736.	2507.	2707.	2613.	2600.	2703.	2958.	2688.
25	2386.	2496.	2709.	2718.	2679.	2714.	2722.	2433.

TABLE TWENTY

TEST PATTERN RK 1101
RESISTORS 3-R2 TO 4-R4
ASPECT RATIO = 10
WIDTH = 30 MIL.
SHEET RESISTIVITY = 100 OHMS PER SQUARE

AS-FIRED RESISTANCE $x10^0$ (ohm)

Substrate	3-R2	3-R1	4-R2	4-R1	3-R3	3-R4	4-R3	4-R4
1	1105.	1105.	1142.	1098.	1200.	1193.	1219.	1217.
2	1049.	1067.	1103.	1064.	1155.	1157.	1143.	1144.
3	1011.	1016.	1054.	998.	1167.	1151.	1160.	1129.
4	1039.	1036.	1096.	1040.	1076.	1059.	1118.	1147.
5	1044.	1014.	1071.	1037.	1153.	1127.	1104.	1106.
6	1055.	1032.	1083.	1001.	1147.	1169.	1124.	1104.
7	1098.	1017.	1032.	961.	1150.	1180.	1148.	1106.
8	1009.	1031.	1009.	966.	1147.	1147.	1148.	1145.
9	1042.	995.	1043.	980.	1158.	1139.	1184.	1163.
10	986.	999.	1005.	974.	1129.	1120.	1143.	1162.
11	1066.	1018.	1086.	1026.	1158.	1181.	1194.	1143.
12	1080.	1047.	1103.	989.	991.	1156.	970.	919.
13	1067.	1057.	1087.	1042.	1070.	1070.	1070.	1056.
14	1074.	1018.	1130.	1068.	1138.	1150.	1161.	1093.
15	1066.	1044.	1070.	1057.	1146.	1184.	1172.	1127.
16	1086.	1037.	1113.	1085.	1062.	1085.	1068.	1077.
17	1087.	1087.	1142.	1090.	1093.	1082.	1128.	1103.
18	1039.	1038.	1091.	1055.	1129.	1180.	1127.	1062.
19	1065.	1063.	1089.	1038.	1162.	1135.	1146.	1153.
20	1064.	1013.	1064.	1062.	1161.	1178.	1152.	1170.
21	1079.	1091.	1109.	1055.	1332.	1269.	1165.	1125.
22	1046.	1014.	1086.	1031.	1254.	1311.	1145.	1132.
23	1060.	1059.	1076.	1123.	1197.	1178.	1176.	1151.
24	982.	1004.	1072.	1019.	1112.	1121.	1108.	1054.
25	1136.	1112.	1128.	1076.	1334.	1314.	1321.	1337.

T A B L E T W E N T Y - O N E

RESISTOR PATTERN PK 1101
RESISTORS 3-R2 TO 4-R4
ASPECT RATIO = 10
WIDTH = 30 MIL.
PASTE SHEET RESISTIVITY = 1000 OHMS PER SQUARE

AS-FIRED RESISTANCE $x10^0$ (ohm)

Substrate	3-R2	3-R1	4-R2	4-R1	3-R3	3-R4	4-R3	4-R4
1	9013.	9018.	8856.	9709.	9650.	9064.	9412.	10550.
2	8973.	9485.	9381.	11110.	9840.	10010.	9637.	9962.
3	8154.	10070.	8890.	9156.	10200.	10840.	9756.	10250.
4	9492.	10070.	9565.	10910.	9134.	9307.	9774.	10120.
5	9015.	9671.	10180.	9773.	9327.	8554.	9523.	9789.
6	9242.	10270.	10310.	10380.	9362.	8568.	9771.	10190.
7	9125.	9340.	10564.	10140.	9429.	8956.	10310.	9820.
8	9154.	9211.	10220.	10330.	9253.	8843.	9889.	9753.
9	9405.	9348.	9607.	10740.	9460.	9167.	9321.	9969.
10	8737.	9263.	10420.	10780.	9794.	10090.	10590.	10750.
11	8879.	9188.	9370.	9845.	10160.	10160.	10110.	10410.
12	9521.	8900.	8630.	10060.	10690.	10190.	10600.	10510.
13	9240.	9035.	9353.	10230.	8184.	9319.	9637.	10360.
14	9434.	9333.	9759.	9973.	9317.	8624.	10520.	10020.
15	9010.	9406.	9865.	10690.	10000.	9385.	9865.	10530.
16	8683.	8837.	9479.	9683.	9305.	8397.	9621.	10200.
17	9486.	8788.	9772.	9997.	10440.	9887.	10580.	11270.
18	9236.	8912.	9581.	1007.	8925.	8968.	9222.	9869.
19	8753.	8478.	9813.	9505.	9620.	9860.	10030.	10260.
20	8886.	8635.	9794.	10390.	14340.	9461.	10550.	10580.
21	8789.	8625.	9629.	9567.	9528.	9412.	9914.	10360.
22	8748.	8835.	9694.	10160.	9543.	9286.	9681.	10440.
23	8632.	9088.	9141.	10030.	9726.	9855.	10470.	10880.
24	9002.	9402.	9934.	9889.	8703.	9276.	9745.	9924.
25	8671.	8843.	9698.	10540.	6237.	9597.	9273.	9489.

TABLE TWENTY-TWO

RESISTOR PATTERN RK 1101
RESISTORS 3-R2 TO 4-R4
ASPECT RATIO = 10
WIDTH = 30 MIL
PASTE SHEET RESISTIVITY = 10K OHMS PER SQUARE

AS-FIRED RESISTANCE $x10^{1}$ (ohm)

Substrate	3-R2	3-R1	4-R2	4-R1	3-R3	3-R4	4-R3	4-R4
1	9211.	9543.	9990.	9820.	10800.	10270.	11160.	10880.
2	9318.	9450.	10000.	9924.	9950.	10710.	9482.	10000.
3	9038.	9301.	9731.	9946.	10096.	10150.	10570.	10550.
4	9590.	10120.	10430.	10340.	9851.	9979.	10590.	10170.
5	9756.	9667.	10390.	10770.	9476.	9855.	10640.	10080.
6	9481.	9583.	9787.	10320.	9968.	9653.	10490.	10270.
7	9781.	10110.	10310.	10440.	10250.	9827.	10490.	10860.
8	10090.	10100.	9940.	10530.	10520.	10510.	10570.	10690.
9	9950.	10360.	10250.	10580.	10080.	9770.	10350.	10410.
10	9197.	9989.	9621.	9984.	9987.	10390.	10230.	10280.
11	9522.	9837.	9357.	9901.	11370.	10560.	10930.	10900.
12	9705.	9961.	10580.	9620.	9987.	9398.	10520.	10210.
13	9290.	9885.	9830.	10030.	9559.	9597.	9482.	9923.
14	9926.	10240.	10280.	10770.	10840.	10570.	11040.	11210.
15	9389.	10210.	10170.	10290.	10120.	9438.	10530.	10810.
16	9679.	9812.	10180.	10130.	9531.	9460.	9975.	9849.
17	9399.	9759.	9723.	10340.	10460.	10540.	10280.	10650.
18	9378.	9147.	9617.	9785.	9395.	9272.	9188.	9667.
19	9542.	9430.	9840.	10270.	9572.	9363.	9900.	9750.
20	9206.	9941.	10155.	10341.	9726.	9283.	10310.	10470.
21	8855.	9137.	9376.	10080.	9492.	9382.	9863.	9875.
22	8651.	9010.	9527.	9535.	9554.	9468.	9985.	9942.
23	9303.	9700.	10030.	10210.	10230.	10030.	10120.	10120.
24	9427.	9414.	9323.	9720.	9110.	9272.	10270.	10800.
25	9271.	9793.	9855.	9790.	9605.	9568.	10310.	10250.

TABLE TWENTY-THREE

RESISTOR PATTERN RK 1101
RESISTORS 3-R2 TO 4-R4
ASPECT RATIO = 10
WIDTH = 30 MIL.
RESISTOR PASTE = 100K OHMS PER SQUARE

AS-FIRED RESISTANCE $x10^2$ (ohm)

Substrate	3-R2	3-R1	4-R2	4-R1	3-R3	3-R4	4-R3	4-R4
1	6676.	7923.	7219.	7605.	6785.	6721.	6356.	7251.
2	6922.	7268.	7167.	6665.	5368.	5873.	5457.	5234.
3	6957.	7002.	6374.	7539.	6180.	5400.	5806.	5900.
4	8741.	8998.	8742.	8962.	7498.	7044.	7283.	7046.
5	7799.	8114.	7414.	8028.	6945.	6674.	6751.	6315.
6	8232.	8586.	8692.	8881.	6988.	6809.	7215.	7144.
7	8196.	8249.	7914.	8335.	6592.	6371.	6611.	7093.
8	7411.	7404.	7860.	8052.	6509.	6415.	5425.	6582.
9	8068.	7836.	7905.	8282.	6651.	6412.	6656.	6855.
10	8200.	9144.	8972.	8907.	7313.	6949.	7113.	7057.
11	8690.	9195.	9065.	9034.	7383.	6674.	6321.	6790.
12	8157.	8300.	8120.	8489.	7000.	6256.	5577.	7000.
13	8299.	8427.	8250.	8622.	6990.	6711.	6528.	6421.
14	7759.	8307.	8053.	7931.	6578.	6562.	6489.	6470.
15	8303.	8593.	8462.	8206.	6940.	6822.	6781.	6652.
16	8535.	8582.	8299.	8247.	7006.	6496.	6961.	6984.
17	7761.	7960.	8114.	8077.	6438.	6231.	6050.	6602.
18	8001.	8349.	8468.	7981.	6949.	6565.	6246.	6605.
19	7123.	7418.	7188.	7224.	6338.	6041.	5876.	6359.
20	7914.	8218.	8528.	7372.	6841.	6584.	6321.	6441.
21	7893.	7864.	7617.	7760.	7038.	6617.	6518.	6468.
22	8417.	8349.	8291.	8216.	7398.	6950.	7233.	7191.
23	7615.	7706.	7626.	7780.	6655.	6407.	6572.	6226.
24	8085.	8040.	7560.	7724.	6358.	5973.	6730.	6971.
25	8196.	8245.	8013.	8093.	6623.	6914.	6621.	6908.

TABLE TWENTY-FOUR

RESISTOR PATTERN RK 1101
RESISTORS 3-R2 TO 4-R4
ASPECT RATIO = 10
WIDTH = 30 MIL.
PASTE 1MEGOHM PER SQUARE

AS-FIRED RESISTANCE $x10^3$ (ohm)

Substrate	3-R2	3-R1	4-R2	4-R1	3-R3	3-R4	4-R3	4-R4
1	1319.	1568.	1435.	1595.	1196.	1250.	1570.	1675.
2	1364.	1420.	1433.	1415.	1430.	1453.	1845.	1849.
3	1389.	1375.	1407.	1530.	1431.	1402.	1635.	1827.
4	1362.	1470.	1521.	1376.	1499.	1514.	1704.	1738.
5	1402.	1459.	1474.	1460.	1465.	1528.	1730.	1738.
6	1444.	1435.	1502.	1507.	1365.	1358.	1775.	1825.
7	1351.	1430.	1426.	1355.	1344.	1406.	1766.	1633.
8	1507.	1400.	1318.	1590.	1400.	1450.	1678.	1753.
9	1378.	1515.	1482.	1497.	1372.	1392.	1600.	1862.
10	1395.	1482.	1500.	1500.	1498.	1541.	1914.	1770.
11	1175.	1427.	1501.	1340.	1744.	2024.	2084.	2089.
12	1318.	1518.	1492.	1426.	1552.	1556.	1820.	1868.
13	1418.	1519.	1549.	1516.	1532.	1647.	2008.	1763.
14	1347.	1517.	1543.	1526.	1402.	1428.	1748.	1938.
15	1539.	1607.	1553.	1533.	1582.	1749.	1652.	1717.
16	1310.	1584.	1543.	1528.	1341.	1378.	1727.	1807.
17	1374.	1572.	1578.	1573.	1430.	1592.	1707.	1814.
18	1408.	1547.	1653.	1745.	1508.	1583.	2071.	2010.
19	1497.	1654.	2693.	1657.	1562.	1588.	2015.	1974.
20	1597.	1596.	1612.	1670.	1512.	1545.	2045.	1835.
21	1509.	1663.	1621.	1653.	1492.	1628.	1832.	1821.
22	1536.	2187.	1655.	1743.	1507.	1529.	1869.	1810.
23	1626.	1628.	1659.	1814.	1634.	2678.	2009.	2093.
24	1549.	1535.	1559.	1919.	1734.	1682.	2018.	2213.
25	1424.	1525.	1592.	1549.	1448.	1499.	1854.	2344.

TABLE TWENTY-FIVE

RESISTOR PATTERN RK 1101
RESISTORS 1-R40 TO 2-R36
ASPECT RATIO = 0.2
WIDTH = 100 MIL.
SHEET RESISTIVITY = 100 OHMS PER SQUARE

AS-FIRED RESISTANCE $x10^{-2}$ (ohm)

Substrate	1-R40	1-R37	1-R33	1-R36	2-R40	2-R37	2-R33	2-R36
1	3149.	3278.	2861.	2403.	3297.	3145.	3085.	2546.
2	2674.	2708.	2631.	2531.	2909.	2858.	2711.	2525.
3	2874.	2935.	2704.	2496.	3118.	3216.	2804.	2458.
4	2816.	2886.	2815.	2366.	3109.	3356.	2908.	2523.
5	2915.	2870.	2625.	2524.	3019.	2950.	2602.	2456.
6	3065.	2946.	2845.	2769.	3192.	3281.	3076.	2789.
7	2880.	2953.	2491.	2428.	3053.	2994.	2717.	2536.
8	3321.	2993.	2575.	2502.	3343.	3248.	2608.	2780.
9	3029.	3099.	2651.	2613.	3198.	3038.	2769.	3010.
10	2886.	2981.	2732.	2451.	3117.	3010.	2512.	2848.
11	2816.	2791.	2722.	2194.	3096.	3065.	2593.	2575.
12	2799.	3233.	3047.	2432.	2797.	2986.	2819.	2629.
13	2663.	2735.	2653.	2253.	2926.	2941.	2657.	2375.
14	3091.	3010.	2940.	2704.	3118.	3080.	2808.	2700.
15	2838.	2976.	2761.	2582.	3123.	3107.	3131.	2566.
16	3013.	2843.	2964.	2518.	3387.	3129.	2914.	3003.
17	3221.	2831.	2973.	2671.	3360.	3119.	2829.	2858.
18	2905.	3092.	2538.	2505.	3055.	3075.	2784.	2926.
19	2800.	2982.	2764.	2658.	3162.	2986.	2910.	2803.
20	2998.	2955.	2625.	2587.	3210.	3108.	3023.	2556.
21	2952.	2891.	2723.	2611.	2980.	3087.	2998.	2846.
22	2678.	2494.	2159.	2254.	2696.	2791.	2513.	2413.
23	2948.	2980.	2800.	2534.	3098.	2966.	2749.	2598.
24	2658.	2604.	2870.	2444.	3034.	2536.	2508.	2427.
25	3199.	3355.	3719.	2749.	3595.	3271.	3011.	3361.

TABLE TWENTY-SIX

RESISTOR PATTERN RK1101
RESISTORS 1-R40 TO 2-R36
ASPECT RATIO = 0.2
WIDTH = 100 MIL.
SHEET RESISTIVITY = 1K OHMS PER SQUARE

8 25

1	9707.	7813.	6122.	5900.	8288.	7808.	10430.	6679.
2	14120.	14760.	13480.	7716.	13750.	10060.	7112.	12190.
3	11420.	10450.	13580.	7764.	11720.	10810.	13020.	12590.
4	11950.	6678.	11820.	11860.	15200.	15120.	13140.	8864.
5	13690.	9691.	9703.	7491.	11790.	10220.	11640.	11350.
6	11890.	11970.	10780.	15080.	10420.	11540.	13150.	9528.
7	9320.	10360.	10720.	9970.	12520.	10640.	8147.	11170.
8	11640.	10530.	8447.	9484.	10390.	8461.	12490.	11190.
9	18160.	8766.	11220.	8495.	11710.	11200.	13520.	10140.
10	13670.	8509.	13710.	10330.	13080.	11560.	12820.	11250.
11	12380.	14070.	10770.	10220.	16220.	17370.	12420.	11500.
12	9146.	14510.	11770.	9311.	11190.	11650.	11160.	14580.
13	13640.	8161.	8527.	7408.	13160.	10780.	10890.	9193.
14	14240.	12250.	10980.	6758.	11170.	11000.	18850.	10880.
15	19170.	12760.	13070.	12640.	13120.	12210.	20110.	12980.
16	16780.	10600.	8810.	7124.	10060.	21540.	12700.	11420.
17	19570.	14670.	13330.	8423.	11620.	11650.	19170.	11020.
18	16840.	10020.	7685.	9205.	17540.	8680.	13530.	9984.
19	19950.	12750.	10660.	9218.	15560.	15190.	12460.	11320.
20	17650.	10530.	14410.	8794.	18400.	9819.	11570.	14420.
21	16770.	10890.	13100.	11050.	13420.	12090.	12900.	12980.
22	17860.	11220.	12750.	11030.	17880.	10540.	15030.	16150.
23	15270.	11540.	16420.	11220.	15960.	12780.	13220.	13120.
24	17910.	10980.	7840.	7056.	11270.	8882.	11460.	8964.
25	18030.	10940.	12870.	13110.	14840.	11140.	10840.	9601.

TABLE TWENTY-SEVEN

ASPECT RATIO = 0.2
WIDTH = 100 MIL.
RESISTORS 1-R40 TO 2-R36
PASTE = 10 K OHMS PER SQUARE

AS-FIRED RESISTANCE $x10^0$ (ohm)

Substrate	1-R40	1-R37	1-R33	1-R36	2-R40	2-R37	2-R33	2-R36
1	1448.	1288.	1662.	968.	1215.	1423.	1434.	1284.
2	1842.	1538.	1900.	1439.	1771.	1791.	2019.	1644.
3	1724.	1570.	1927.	1178.	1205.	1482.	1593.	1234.
4	1768.	1474.	1893.	1137.	1747.	1672.	1849.	1351.
5	1531.	1282.	1934.	1168.	1410.	1159.	1664.	1261.
6	1733.	1516.	1839.	1024.	1714.	1448.	1596.	1329.
7	1827.	1636.	1962.	1179.	1595.	1509.	1542.	1488.
8	1458.	1363.	2017.	1125.	1729.	1431.	1527.	1383.
9	1468.	1344.	1787.	888.	1477.	1480.	1547.	1342.
10	1335.	1190.	1647.	887.	1663.	1223.	1533.	1065.
11	1557.	1450.	1718.	845.	1583.	1579.	1425.	1265.
12	1636.	1440.	1912.	1124.	1679.	1720.	1650.	1341.
13	1829.	1561.	1925.	1153.	1692.	1441.	1686.	1603.
14	1780.	1500.	2088.	1231.	1754.	1654.	1604.	1592.
15	1595.	1176.	1809.	907.	1753.	1417.	1647.	1313.
16	1450.	1393.	2013.	1139.	1734.	1555.	1521.	1667.
17	1766.	1576.	1993.	1113.	1718.	1659.	1734.	1300.
18	2028.	1806.	2009.	1329.	1698.	1703.	1599.	1555.
19	1428.	1303.	1866.	1147.	1479.	1427.	1275.	1634.
20	1557.	1348.	1889.	1103.	1484.	1714.	1622.	1381.
21	1692.	1426.	1976.	1090.	1561.	1414.	1618.	1483.
22	1733.	1462.	1828.	1052.	1433.	1216.	1348.	1489.
23	1529.	1429.	1941.	1164.	1646.	1699.	1904.	1578.
24	1487.	1274.	1726.	875.	1634.	1433.	1446.	1245.
25	1742.	1488.	2012.	1107.	1578.	1484.	1507.	1277.

TABLE TWENTY-EIGHT

ASPECT RATIO = 1.2
WIDTH = 100 MIL.
RESISTORS 1-R40 TO 2-R36
PASTE = 100K OHMS PER SQUARE

AS-FIRED RESISTANCE $x10^0$ (ohm)

Substrate	1-R40	1-R37	1-R33	1-R36	2-R40	2-R37	2-R33	2-R36
1	7875.	7230.	10940.	4586.	6696.	6280.	7577.	5872.
2	6533.	3659.	8712.	3773.	6072.	5182.	9512.	6355.
3	7659.	6194.	10530.	5560.	6679.	5982.	7468.	6428.
4	7693.	6888.	11620.	4911.	7195.	7298.	8189.	7892.
5	6396.	5618.	8440.	4840.	5295.	5085.	7484.	7286.
6	7510.	7604.	11400.	4876.	6582.	6340.	7747.	8765.
7	7139.	6472.	11030.	3914.	8787.	6611.	6833.	6770.
8	7878.	6970.	10860.	6821.	8200.	7683.	10450.	10120.
9	7510.	6552.	11350.	5532.	5938.	5251.	7989.	10170.
10	7919.	7548.	12170.	8361.	8667.	8362.	11960.	8944.
11	7374.	6343.	13170.	5823.	9760.	8796.	10080.	7241.
12	7103.	5667.	11350.	6147.	6527.	5003.	9276.	7116.
13	7450.	6756.	13480.	6540.	7858.	6490.	9836.	9238.
14	8339.	7702.	12090.	6652.	8340.	8232.	10670.	8125.
15	7666.	6695.	11940.	6772.	8442.	6495.	10290.	7546.
16	7767.	6458.	10930.	5750.	6141.	6777.	9817.	7611.
17	6826.	6261.	11580.	6654.	8442.	7172.	10870.	5633.
18	8801.	7378.	12320.	7819.	7805.	7361.	10460.	9194.
19	9126.	8089.	12290.	6923.	9041.	8718.	9569.	8254.
20	6525.	7790.	15200.	5911.	8148.	7815.	9895.	6217.
21	9823.	8109.	16480.	6901.	8367.	7462.	10780.	7863.
22	8480.	7029.	10970.	5395.	8081.	7592.	6554.	8176.
23	7451.	6918.	12440.	7925.	7600.	7770.	10940.	7369.
24	8249.	6605.	11990.	5083.	10180.	10480.	7883.	9900.
25	6655.	5974.	8746.	6312.	6396.	6597.	9660.	9031.

TABLE TWENTY-NINE

ASPECT RATIO = 0.2
WIDTH = 100 MIL.
PASTE = 1M. OHMS PER SQUARE
RESISTORS 1-R40 T/ 2-R36

AS-FIRED RESISTANCE $x10^1$ (ohm)

Substrate	1-R40	1-R37	1-R33	1-R36	2-R40	2-R37	2-R33	2-R36
1	7523.	6488.	6236.	8482.	9382.	11430.	7821.	6286.
2	7646.	6937.	7448.	6740.	8209.	8333.	9605.	6488.
3	7985.	6978.	7966.	6593.	8634.	8143.	8393.	6739.
4	7383.	6582.	8240.	6227.	8851.	7951.	8763.	5998.
5	7338.	6786.	7284.	5830.	8408.	7442.	7560.	6093.
6	7930.	7288.	8130.	6020.	8210.	9032.	8190.	6145.
7	7415.	6747.	7404.	5712.	8013.	8131.	7230.	5761.
8	7440.	7746.	8594.	5623.	8175.	7983.	7450.	4568.
9	7037.	6580.	7267.	5372.	9058.	9048.	5983.	5171.
10	7519.	6394.	10580.	6052.	8462.	8090.	7614.	6427.
11	7960.	6524.	7502.	8130.	9242.	8863.	10130.	6369.
12	8010.	6737.	7584.	5874.	10040.	9213.	8644.	5242.
13	8398.	7427.	6831.	7506.	9964.	8364.	9084.	6188.
14	6936.	6312.	8494.	5377.	8566.	7692.	7337.	4424.
15	6601.	6325.	9114.	5581.	7942.	8085.	7676.	5565.
16	9835.	8080.	10880.	7606.	7045.	6669.	9172.	5402.
17	6956.	6359.	7660.	5257.	7030.	6694.	8332.	4912.
18	8110.	6870.	8648.	6302.	9351.	9113.	8288.	5900.
19	8846.	8258.	10420.	7012.	10630.	10190.	9276.	6690.
20	7157.	6907.	8775.	6120.	8104.	7665.	9557.	5827.
21	8060.	6705.	8452.	5467.	7407.	7603.	10680.	5572.
22	7731.	7121.	9177.	6602.	8107.	8241.	10030.	8065.
23	7912.	7136.	9016.	5732.	8198.	7622.	7772.	6339.
24	7380.	6814.	9777.	5429.	8484.	8187.	9756.	5484.
25	7085.	7494.	9062.	6056.	8581.	8402.	7355.	6171.

TABLE THIRTY

RESISTORS 1-R44 TO 3-R43
PASTE = 100 OHMS PER SQUARE
ASPECT RATIO = 0.667
WIDTH = 30 MIL.

AS-FIRED RESISTANCE $x10^{+1}$ (ohm)

Substrate	1-R44	1-R43	2-R44	2-R43	4-R44	4-R43	3-R44	3-R43
1	1207.	1134.	1103.	1204.	1070.	946.	930.	864.
2	884.	894.	968.	986.	934.	918.	983.	787.
3	924.	958.	1107.	902.	803.	951.	879.	788.
4	1087.	855.	989.	862.	1025.	994.	917.	807.
5	965.	901.	912.	911.	977.	967.	829.	865.
6	912.	864.	1133.	1010.	978.	944.	898.	917.
7	924.	881.	911.	977.	806.	823.	833.	761.
8	852.	859.	894.	1196.	858.	1134.	837.	839.
9	962.	967.	903.	1024.	866.	942.	758.	812.
10	1026.	937.	1013.	960.	1013.	892.	865.	824.
11	892.	844.	947.	916.	978.	879.	954.	861.
12	966.	918.	902.	1008.	972.	1048.	934.	847.
13	770.	720.	812.	812.	972.	936.	836.	673.
14	958.	1008.	1035.	1074.	1045.	962.	986.	890.
15	1084.	995.	984.	940.	1048.	843.	945.	896.
16	999.	900.	982.	996.	1059.	872.	982.	775.
17	992.	867.	1008.	1019.	1048.	983.	970.	904.
18	999.	997.	875.	1013.	1071.	945.	966.	845.
19	771.	839.	950.	1000.	965.	1009.	868.	826.
20	956.	992.	885.	1159.	848.	805.	916.	863.
21	1009.	944.	1040.	1145.	956.	1038.	970.	966.
22	956.	828.	744.	888.	767.	859.	742.	746.
23	919.	832.	1002.	992.	998.	827.	1165.	764.
24	980.	875.	912.	786.	984.	848.	934.	821.
25	1123.	990.	1057.	1022.	1224.	908.	964.	824.

TABLE THIRTY-ONE

RESISTORS 1-R32 TO 3-R31
WIDTH = 65 MIL.
LENGTH = 65 MIL.
PASTE = 100 OHMS PER SQUARE

AS-FIRED RESISTANCE $x10^{+1}$ (ohm)

Substrate	1-R32	1-R31	2-R32	2-R31	4-R32	4-R31	3-R32	3-R31
1	1315.	1330.	1237.	1270.	1195.	1231.	1218.	1194.
2	1238.	1218.	1177.	1239.	1257.	1166.	1247.	1230.
3	1165.	1197.	1257.	1186.	1190.	1170.	1124.	1198.
4	1055.	1170.	1248.	1225.	1207.	1156.	1146.	1172.
5	1050.	1181.	1080.	1176.	1230.	1152.	1105.	1168.
6	1269.	1205.	1265.	1227.	1117.	1181.	1085.	1089.
7	1227.	1277.	1174.	1183.	1153.	1189.	1110.	1176.
8	1264.	1280.	1265.	1212.	1153.	1190.	1098.	1194.
9	1255.	1281.	1172.	1245.	1174.	1183.	1108.	1178.
10	1240.	1278.	1294.	1232.	1168.	1203.	1115.	1153.
11	1220.	1181.	1243.	1200.	1146.	1128.	1069.	1107.
12	1222.	1269.	1358.	1164.	1289.	1297.	1251.	1218.
13	1134.	1126.	1162.	1180.	1214.	1173.	1092.	1114.
14	1168.	1194.	1324.	1232.	1356.	1364.	1282.	1249.
15	1116.	1123.	1125.	1157.	1304.	1202.	1209.	1181.
16	1201.	1140.	1250.	1207.	1210.	1253.	1226.	1185.
17	1252.	1251.	1338.	1264.	1309.	1243.	1221.	1243.
18	1224.	1226.	1203.	1227.	1274.	1278.	1239.	1273.
19	1222.	1251.	1311.	1276.	1305.	1378.	1248.	1239.
20	1154.	1222.	1168.	1251.	1278.	1281.	1218.	1223.
21	1256.	1229.	1169.	1233.	1225.	1250.	1193.	1285.
22	1213.	1134.	1118.	1152.	1233.	1167.	1112.	1187.
23	1216.	1254.	1219.	1219.	1296.	1251.	1223.	1224.
24	1157.	1215.	1147.	1134.	1239.	1180.	1154.	1198.
25	1327.	1331.	1320.	1324.	1554.	1470.	1367.	1311.

TABLE THIRTY-TWO

ASPECT RATIO = 0.8
WIDTH = 100 MIL
LENGTH = 4 * 20 MIL.
PASTE = 100 OHMS PER SQUARE
RESISTORS 1-R39 ,<83 TO 3-R39,R38

AS-FIRED FESISTANCE $x10^{+1}$ (ohm)

Substrate	1-R39	2-R39	4-R39	3-R39
1	897.	884.	859.	885.
2	775.	807.	862.	858.
3	804.	850.	818.	867.
4	824.	875.	829.	832.
5	835.	807.	855.	823.
6	846.	916.	837.	944.
7	824.	825.	837.	839.
8	871.	859.	858.	870.
9	869.	824.	842.	849.
10	864.	828.	839.	850.
11	788.	833.	806.	851.
12	836.	828.	877.	848.
13	769.	794.	828.	824.
14	882.	860.	945.	908.
15	833.	830.	859.	857.
16	831.	876.	886.	924.
17	832.	863.	914.	909.
18	858.	837.	890.	915.
19	816.	847.	877.	941.
20	819.	854.	884.	845.
21	835.	872.	839.	922.
22	739.	756.	790.	787.
23	824.	863.	856.	881.
24	757.	755.	826.	791.
25	973.	927.	989.	963.

APPENDIX B

FORTRAN STATEMENTS FOR

COMPUTER PROGRAM

```
      PROGRAM TST (INPUT,OUTPUT,TAPE5=INPUT,TAPE6=OUTPUT)
      REAL VALUE(8,250),TOTAL(2000),SMEAN(250),SSD(250)
      REAL MEANR(250), SDR(250)
      EQUIVALENCE(VALUE(1,1),TOTAL(1))
      DATA INDEV/5/,LP/6/
20    FORMAT(1H0/1H ,12HTOTAL MEAN =,F8.0,9X,16HTOTAL STAN.DEV.= ,F10.0)
30    FORMAT(1H1,10X,     7HSUB.NO.,13X1H-,F3.0,18X1H-,F3.0,1H ,21X,2H0
     121X1H+,F3.0,1H ,18X1H+,F3.0,1H    )
40    FORMAT(1H1)
10    FORMAT(4F10.0)
      DO 102 IR=1,8
      DO 102 IC=1,250
102   VALUE(IR,IC)=0.
      DO 103 IR=1,250
      SMEAN(IR)=0.
      SSD(IR)=0.
      MEANR(IR)=0.
      SDR(IR)=0.
103   CONTINUE
      DO 104 IT=1,2000
104   TOTAL(IT)=0.
1     CALL INRES(VALUE,N,L,INDEV,LP)
      READ (INDEV,10) HFS,PMFS, HINT, HCV
C        HFS - HISTOGRAM FULL SCALE AS  OF TOTAL MEAN  (25)
C        PMFS - SPLOT FULL SCALE AS OF TOTAL MEAN +/-   (25)
C        HINT - HISTOGRAM INTERVAL IN RESISTANCE UNITS  ( 1 TOTAL MEAN )
C        HCV - HISTOGRAM CENTER VALUE IN RESISTANCE UNITS ( TOTAL MEAN )
C        NOTE VALUES IN BRACKETS TAKEN IF READ IN NEG OR ZERO VALUE.
C
C
      J=N*L
      IF(HFS) 11,11,12
11    HFS=25.
12    IF(PMFS)13,13,14
13    PMFS=25.
14    CALL SDMEA(TOTAL,J,TSD,TMEAN)
      IF(HINT)15,15,16
15    HINT=TMEAN/100
16    IF(HCV)17,17,18
17    HCV=TMEAN
18    WRITE(LP,20)TMEAN,TSD
      CALL SUMSD(VALUE,N,L,SMEAN,SSD,LP)
      CALL SUMSR(VALUE,N,L,MEANR,SDR,LP)
      NPTS=10000/HFS
      CALL HISTO(TOTAL,J,HCV,HINT,60,NPTS,LP)
      RMFS=PMFS*TMEAN/100
      RMAX=TMEAN+RMFS
      RMIN=TMEAN-RMFS
      PMFSH=PMFS*0.5
      WRITE(LP,30)PMFS,PMFSH,PMFSH,PMFS
      CALL SPLOT(VALUE,N,L,SMEAN,RMAX,RMIN,LP)
      WRITE(LP,40)
      CALL YIELD(TOTAL,J,TMEAN,LP)
100   CONTINUE
      STOP
      END
```

```
      SUBROUTINE INRES(VALUE,N,L,INDEV,LP)
C           THIS SUBROUTINE COPIES EIGHT CARDS TO THE OUTPUT
C     CHANNEL LP FROM INPUT CHANNEL INDEV. IT THEN READS TWO INTEGERS
C     N AND L IN 10 FORMAT AND NXL REAL NUMBERS (VALUE) IN F0.0 FORMAT
      REAL VALUE (8,250), COMMT (80)
10    FORMAT(2I10)
20    FORMAT(8F5.0)
30    FORMAT(7(10A8/),10A8)
70    FORMAT(1H ,I5,4X,10(F8.0,2X))
40    FORMAT(1H1,////////,8(1H ,10A8/))
50    FORMAT(1H0,I5,10X,I5/1H0)
      READ(INDEV,30)COMMT
      READ(INDEV,10)N,L
60    FORMAT(1H1,          12HNO.RESISTORS  ,5X,13HNO.SUBSTRATES  , 1H ,
     12X,13HPER SUBSTRATE     )
      WRITE(LP,40) COMMT
      WRITE(LP,50)N,L
61    FORMAT(1H1,////////)
      DO 12 J=1,L
      DO 12 I=1,N
      CALL READX(VALUE(I,J))
12    CONTINUE
      DO 13 J=1,L
      WRITE(LP,70)J,(VALUE(I,J),I=1,N)
13    CONTINUE
      WRITE(LP,61)
      WRITE(LP,40)COMMT
      WRITE(LP,40) COMMT
      WRITE(LP,40) COMMT
      RETURN
      END
```

```
      SUBROUTINE SPLOT (VALUE,N,L, MEAN,RMAX,RMIN,LP)
C
C
C           THIS ROUTINE PLOTS RESISTOR VALUE AGAINST SUBSTRATE
C     NUMBER UP TO L
C     NUMBER UP TO 10 RESISTORS (EACH A DIFFERENT CURVE) MAY BE
C     PLOTTED AND THE MEAN RESISTANCE OF THE SUBSTRATE (IN MEAN) WILL
C     ALSO BE PLOTTED THE RESISTANCE SCALE IS 100 CHARACTERS FROM RMIN
C     TO RMAX THE LINEPRINTER USED IS OUTPUT LP  L IS THE NUMBER OF
C     SUBSTRATES N THE NUMBER OF RESISTORS PER SUBSTRATE. THE RESISTOR
C     VALUES ARE CONTAINED IN VALUE(N,L)  NOTE MEAN IS A REAL ARRAY
C
C
      REAL VALUE(N,L), MEAN(L)
      INTEGER BLANK
      INTEGER LINE(100),SYMBOL(12)
      DATA SYMBOL/1H1,1H2,1H3,1H4,1H5,1H6,1H7,1H8,1H.,1H0,1H*,1H./
      DATA BLANK /1H /
      RPC=(RMAX-RMIN)/100
      DO 17 J=1,100
17    LINE(J)=BLANK
      WRITE (LP,20)
      DO 11 IL=1,L
      J=-2
      DO 12 IN=1,N
      I=(VALUE(IN,IL)-RMIN)/RPC
13    IF(I-1)21,22,22
21    I=1
22    IF(I-100)12,24,24
24    I=100
12    LINE(I)=SYMBOL(IN)
131   CONTINUE
      J=J+1
      IF(J) 15,14,16
14    I=(MEAN(IL)-RMIN)/RPC
      IN=11
130   IF(I-1) 210,220,220
210   I=1
220   IF(I-100) 120,240,240
240   I=100
120   LINE(I)=SYMBOL(IN)
      GO TO 131
15    I=50
      GO TO 130
16    WRITE(LP,10)IL,LINE
      DO 11 J=1,100
11    LINE(J)=BLANK
      WRITE(LP,20)
20    FORMAT(1H0)
10    FORMAT(1H0,I15,15X,100A1)
      RETURN
      END
```

```
      SUBROUTINE HISTO(VALUE, N,RMEAN,RINT,NINT,NPTS,LP)
C
C
C           THIS ROUTINE PLOTS A HISTOGRAM OF THE N NUMBERS CONTAINED
C     IN VALJE. THE HISTOGRAM IS CENTERED ABOUT RMAEN AND HAS NINT
C     INTERVALS EACH OF SIZE RINT. THE NUMBER FO SQUARES
C     (OR CHARACTERS ) UNDER THE HISTOGRAM ARE NPTS AND THE
C     LINEPRINTER USED IS OUTPUT NUMBER LP.     NOTE IF 1000 SQJARES ARE
C     JNDER THE CJRVE ( NPTS=1000 ) THEN AN INTERVAL 76 CHARACTERS HIGH
C     MEANS ( 76*N ) / 1000 OF OF THE VALUES ARE WITHIN THAT INTERVAL.
C
      REAL VALUE(N)
      INTEGER LINE(100),BLANK,SYMBOL,HFS
      DATA BLANK/1H /, SYMBOL/1H*/
10    FORMAT(1H ,F8.0,3H / ,F8.0,1H ,100A1 )
      DO 25 J=1,100
25    LINE(J)=BLANK
      NINTH = NINT*0.5
      ILESS=0
      HFS=10000/NPTS
      WRITE(LP,201)
201   FORMAT(1H1,////)
      WRITE(LP,20) HFS
20    FORMAT(1HO,21HFULL SCALE REPRESENTS,I5,39H  PERCENT OF RESISTORS I
     1N THAT INTERVAL   )
30    FORMAT(1H1)
      DO 24 I=1,NINT
      JLESS=ILESS
      AINT=(I-NINTH)*RINT+RMEAN
      BINT=AINT+RINT
      ILESS=0
      DO 22 J=1,N
      IF(VALUE(J)-BINT) 21,22,22
21    ILESS=ILESS+1
22    CONTINUE
      IVAL=(ILESS-JLESS)*NPTS/N
      IF(IVAL-100) 27,27,26
26    IVAL=100
27    IF(IVAL) 28,28,29
29    DO 23 J=1,IVAL
23    LINE(J)=SYMBOL
28    CONTINUE
      WRITE(LP,10) AINT, BINT, LINE
      DO 24 J=1,100
24    LINE(J)=BLANK
      WRITE(LP,30)
      RETURN
      END
```

```
      SUBROUTINE SJMSD (VALUE,N,L,MEAN,SD,LP)
C
C           THIS ROUTINE FINDS THE MEAN AND STANDARD DEVIATION OF
C     RESISTORSON EACH SUBSTRATE LISTS THEM ON THE LINEPRINTER
C     (OUTPUT LP) AND RETURNS THEM IN MEAN AND SD (BOTH REAL ARRAYS)
C     VALUE(N,L)CONTAINS THE RESISTOR VALUES. L SUBSTRATES N RESISTORS
C     EACH THE SJBROUTINE SDMEA IS USED BY THIS SUBROUTINE
C
      REAL VALUE(N,L),MEAN(L),SD(L),SUB(10)
      WRITE (LP,20)
      DO 11 I=1,L
      DO 12 J=1,N
12    SUB(J)=VALUE(J,I)
      CALL SDMEA (SUB,N,SD(I),MEAN(I))
11    WRITE (LP,10)I,MEAN(I),SD(I)
20    FORMAT(1H0,13HSUBSTRATE NO.,5X,4HMEAN,10X,10HSTAN. DEV.)
10    FORMAT(1H ,3X,I5,6X,F12.0,4X,F12.0  )
      RETURN
      END
```

```
      SUBROUTINE SUMSR(VALUE,N,L,MEANR,SDR,LP)
C
C              THIS ROUTINE FINDS THE MEAN AND STANDARD
C       DEVIATION FOR EACH RESISTOR IN THE SAME POSITION ON ALL
C        THE SUBSTRATES.  IT THEN LISTS THEM ON THE LINEPRINTER
C        AND RETURNS THEM IN ≠MEANR≠ AND≠SDR ( BOTH REAL ARRAYS)
C
      REAL VALUE(N,L), MEANR(L),SDR(L),SUBR(25)
      WRITE(LP,20)
20    FORMAT(1H0,13H RESISTOR NO.,5X,4HMEAN,10X,10HSTAN. DEV.)
      DO 11 J=1,N
      DO 12 I=1,L
12    SUBR(I)=VALUE(J,I)
      CALL SDMEA(SUBR,L,SDR(J),MEANR(J))
11    WRITE(LP,10) J, MEANR(J),SDR(J)
10    FORMAT(1H ,3X,I5,6X,F12.0,4X,F12.0  )
      RETURN
      END
```

```
      SUBROUTINE SDMEA (VALUE,N,SD,RMEAN)
C
C           THIS ROUTINE FINDS THE MEAN AND STANDARD DEVIATION OF THE
C     N QUANTITIES IN VALUE AND RETURNS THEM IN RMEAN AND SD
C
      REAL VALUE(N)
      X2=0
      X=0
      DO 11 I=1,N
      X=VALUE(I)+X
11    X2=VALUE(I)**2+X2
      RMEAN=X/N
      SD=(X2/N-(X/N)**2)**0.5
      RETURN
      END


      SUBROUTINE YIELD(VALUE,N,RMEAN,LP)
C
C           THIS ROUTINE FINDS THE YIELD ASSOCIATED
C           WITH 1, 2, 5, 10, 15, AND 20 PERCENT BANDS.
C
      REAL VALUE(N)
      I1=0
      I2=0
      I5=0
      I10=0
      I15=0
      I20=0
      T1=0.01*RMEAN
      T2=0.02*RMEAN
      T5=0.05*RMEAN
      T10=0.10*RMEAN
      T15=0.15*RMEAN
      T20=0.20*RMEAN
      DO 11 I=1,N
      A=ABS(VALUE(I)-RMEAN)
      IF(A.LE.T1) I1=I1+1
      IF(A.LE.T2) I2=I2+1
      IF(A.LE.T5) I5=I5+1
      IF(A.LE.T10)  I10=I10+1
      IF(A.LE.T15) I15=I15+1
      IF(A.LE.T20) I20=I20+1
11    CONTINUE
      I1P=I1*1000/N
      I2P=I2*1000/N
      I5P=I5*1000/N
      I10P=I10*1000/N
      I15P=I15*1000/N
      I20P=I20*1000/N
      WRITE(LP,100)
100   FORMAT(1H1,////////,20X14HYIELD ANALYSIS  ///)
      WRITE(LP,101)
101   FORMAT(1H0,15X,12HTOL. BAND( ) 4X1HI,4X,1H2,4X1H53X2H103X2H153X2H2
     10 )
      WRITE(LP,102) I1P,I2P,I5P,I10P,I15P,I20P
102   FORMAT(1H0,15X13HYIELD * 10( ), I4,5I5)
      WRITE(LP,103)
103   FORMAT(1H1)
      RETURN
      END
```

"RADIATION CONVERSION ENHANCEMENT"

WITH INHOMOGENEOUS CONVERTERS

by

L. DALTON MOLSON

"PART B: McMASTER (ON-CAMPUS)

PROJECT*"

A project report submitted in partial fulfillment
of the requirements for the degree of

Master of Engineering

Dept. of Engineering Physics

McMaster University

Hamilton, Ontario

1974

*One of the two project reports. The other part is designated PART A: INDUSTRIAL PROJECT

TITLE (PART B) : Radiation Conversion Enhancement with Inhomogeneous Converters

AUTHOR : L. Dalton Molson, B.Sc. (Waterloo)

Supervisor: Professor A.A. Harms

Number of Pages i, 88

MASTER OF ENGINEERING
(Engineering Physics)

McMaster University
Hamilton, Ontario

RADIATION CONVERSION ENHANCEMENT WITH INHOMOGENEOUS CONVERTERS

ABSTRACT

The possibility of radiation conversion enhancement with inhomogeneous converters has been investigated. Of particular interest is the radiation conversion in the neutron radiographic process. The investigation has centered on two techniques for enhancement.

One approach relies on isotopic and density variations in the converter. An analytical investigation has indicated that significant enhancement can be achieved for gadolinium converters that are isotopically enriched with gadolinium - 157. Further investigation using linear spatial variations of both the thermal neutron cross-sections, $\Sigma(x)$, and the electron attenuation coefficients, $\alpha(x)$, for a converter has produced enhancement as well. Enhancement values calculated with reference to a natural gadolinium converter foil 25 μm thick were found to be in excess of 2 for some inhomogeneous converter configurations.

A second approach to enhanced radiation conversion has been based on the field-enhanced secondary emission mechanisms. A natural gadolinium converter was used as a substrate for a low density granular insulator coating to produce a composite converter. Enhancement is obtained when primary internal conversion electrons produced in the (n,e^-) reaction create secondary emission in the insulator. Insulators of MgO and KCl were investigated. The degree of enhancement

was based on the amount of optical density observed in the exposed neutron radiographs. The MgO-Gd converters were found to have a positive optical density enhancement for increasing field values. However, a negative enhancement was observed for increasing MgO thicknesses for thicknesses in the range of 5 μm to 15 μm. The KCl-Gd converters showed a positive enhancement for increasing values of KCl thickness. Optical enhancements of 0.5% per μm were observed for KCl thicknesses in the range 5 μm to 30 μm. The effect of an applied electric field on the Gd-KCl converter was to produce enhancement at two potentials. A peak in the optical density was observed at 150 volts and another was observed at 600 volts. An increase in optical density of 18% was observed for the peaks. The effect of placing a thick protective layer of aluminum on the KCl coating proved to be disasterous for optical density enhancement. The ratio of optical densities for no coating to coating of aluminum was 2.2 for the 600 volt peak in the density curves. This effect indicates that the secondary electrons emitted from the KCl coating could be of very low energy, possibly in the electron volt range.

ACKNOWLEDGEMENTS

The author wishes to express his appreciation to Dr. A.A. Harms of the Engineering Physics Department for his interest and guidance throughout the project. Thanks also go to Dr. J.P. Marton (Welwyn Canada Ltd., London, Ontario) for advice on electron multiplication phenomena and for preparation of the converter coatings without which the experiments could not have been performed.

The author wishes to acknowledge receipt of a Province of Ontario Graduate Fellowship and a McMaster University Fellowship.

TABLE OF CONTENTS

LIST OF ILLUSTRATIONS

LIST OF ILLUSTRATIONS

LIST OF ILLUSTRATIONS

1. INTRODUCTION

Neutron radiography has been found to be a valuable tool in many areas of research and development.[1-3]

The nuclear industry now employs neutron radiography for inspection and non-destructive testing of items such as reactor fuel material that could not be evaluated by convential techniques. The aerospace industry is rapidly increasing its use of neutron radiography. Poor resin-bonding in the aluminum honeycomb structures for aircraft can be detected using this technique. Neutron radiography can, in general, be applied as a nondestructive test method in many areas involving brazings, adhesives, gasket locations and electronic components to mention a few. Reasons for the advantages that neutrons exhibit in radiographic inspection are discussed in the next section.

1.1. Principles in Neutron Radiography

Neutron radiography can be applied to situations where the more conventional x-radiation radiography is inapplicable. The ability for neutrons to work where x-rays fail is based on the fact that neutron interaction with materials is considerably different from x-ray interaction. X-rays interact with the clouds of electrons surrounding the atomic nucleus. As the cloud increases in density it has a greater absorbing effect on the x-radiation. The density of the electron cloud is determined by the atomic number

of the element; an increase in atomic number implies an increase in the electron density and a corresponding increase in the absorption of x-radiation. This effect is shown for 130 keV x-rays in Fig. 1 where the mass absorption coefficient is shown to be a smooth continuous function of the atomic number of the elements.

The neutrons, however, interact with the nuclei and are relatively unaffected by the electron clouds. The interaction depends on the exact makeup of each individual nucleus and is independent of the atomic number as illustrated in Fig. 1. The extent of neutron absorption depends on the neutron cross-section for the material. This property of "random" absorption can be used to identify elements that have a differing neutron cross-section but may be very similar in atomic number. It would be difficult to differentiate these elements using x-ray radiography. Neutron radiography can even be used to identify different isotopes of the same element that differ in neutron cross-sections.

1.2. Imaging Technique

In order to obtain a neutron radiograph of an object, a source of neutrons and a neutron detection system are required. First consider the source of neutrons.

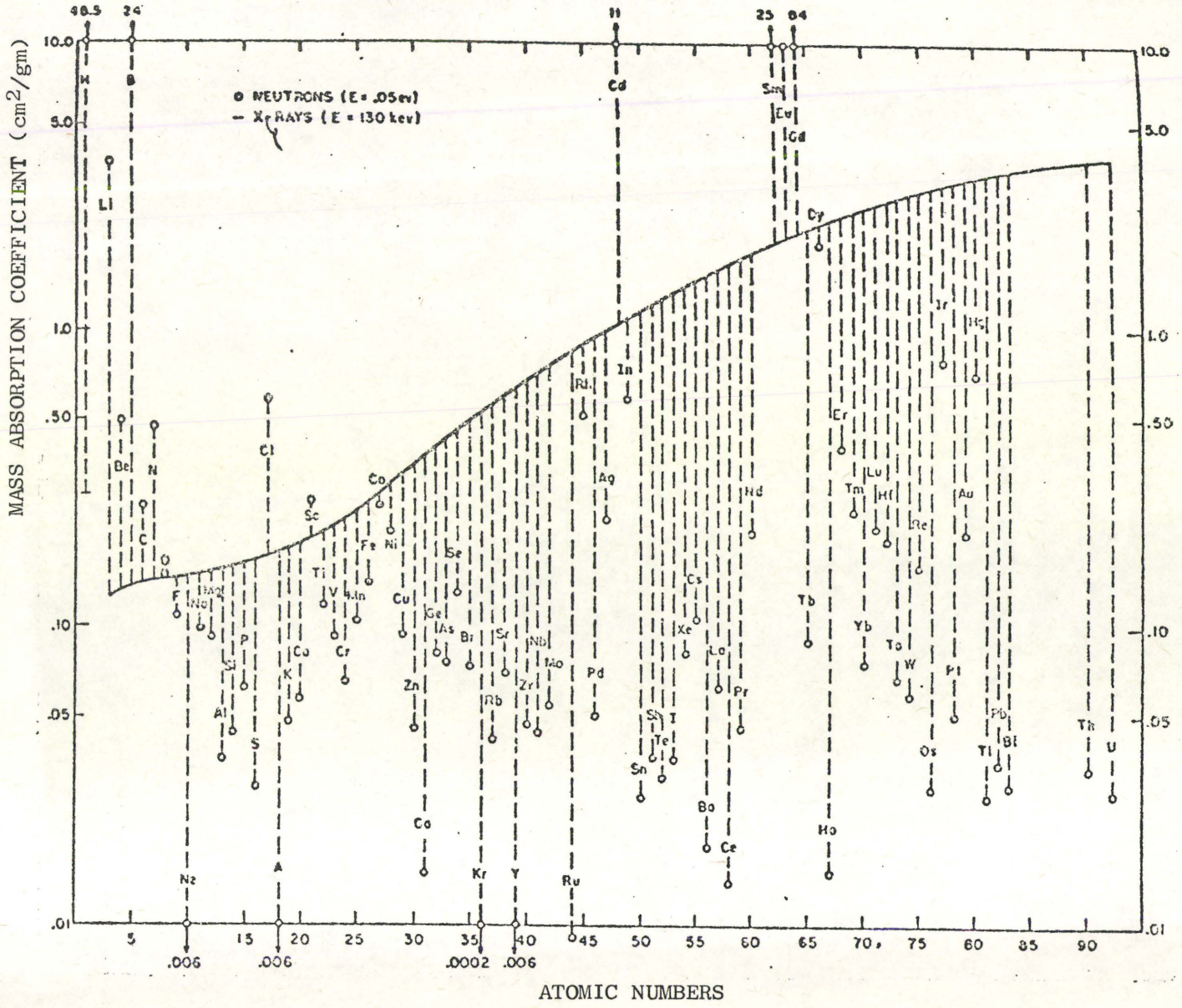

Mass Absorption Coefficients of the Elements For Thermal Neutrons and 130 kev X-rays.

FIGURE 1

1.2.1. Neutron Sources

Accelerator sources or isotopic neutron sources could be used for radiography. However, the neutrons obtained from these sources are primarily high energy and must be collimated and thermalized before they become useful. Thermal neutrons (0.01 to 0.3 ev) are more practical to use in radiography due to the fact that, although the cross-sections vary randomly with neutron energy, on the average fast neutrons have a lower cross-section than thermal neutrons.

The beam shaping in direction and energy that is required by the fast neutrons has a detrimental effect on the neutron flux. Accelerators have been able to produce fast neutron fluxes of the order 10^6 to 10^{12} neutrons per cm^2 per sec. but after collimation and thermalization the useable flux is reduced to typically 10^5 neutrons per cm^2 per second.

A similar problem exists for isotope sources. Good isotopic neutron sources can yield of the order of 10^7 fast neutrons per second for every curie of activity. This figure, however, is reduced by collimation and thermalization to produce a beam of thermal neutrons with a flux of the order of 10^2 to 10^3 neutrons per cm^2 per sec. for every curie of activity.

Nuclear reactors have been found to produce a very high thermal neutron flux and many reactors are capable of yielding a collimated thermal neutron beam with a flux of the order of 10^6 to 10^8 neutrons per cm^2 per sec. These beams can be used to produce high quality neutron radiographs with good resolution capabilities.

1.2.2. Neutron Detection System

When the thermal beam of neutrons has passed through the object to be radiographed, the remaining neutrons in the beam determine the neutron image. One of the standard techniques for obtaining the neutron image is to employ a neutron converter and a photographic film.

A neutron converter is required since the neutrons have little effect on the film emulsion. The thermal neutron beam passes through the object to be radiographed and is attenuated according to

$$\frac{dI(x)}{dx} = -\Sigma_t I(x)$$

where $I(x)$ is the neutron beam intensity and Σ_t is the macroscopic neutron cross section. The transmitted beam of neutrons then interacts with the converter screen.

There are two converter techniques that can be used to obtain the radiograph. One technique is the transfer exposure method as illustrated in Fig. 2(A). In this case the screen is made of material such as silver or gold

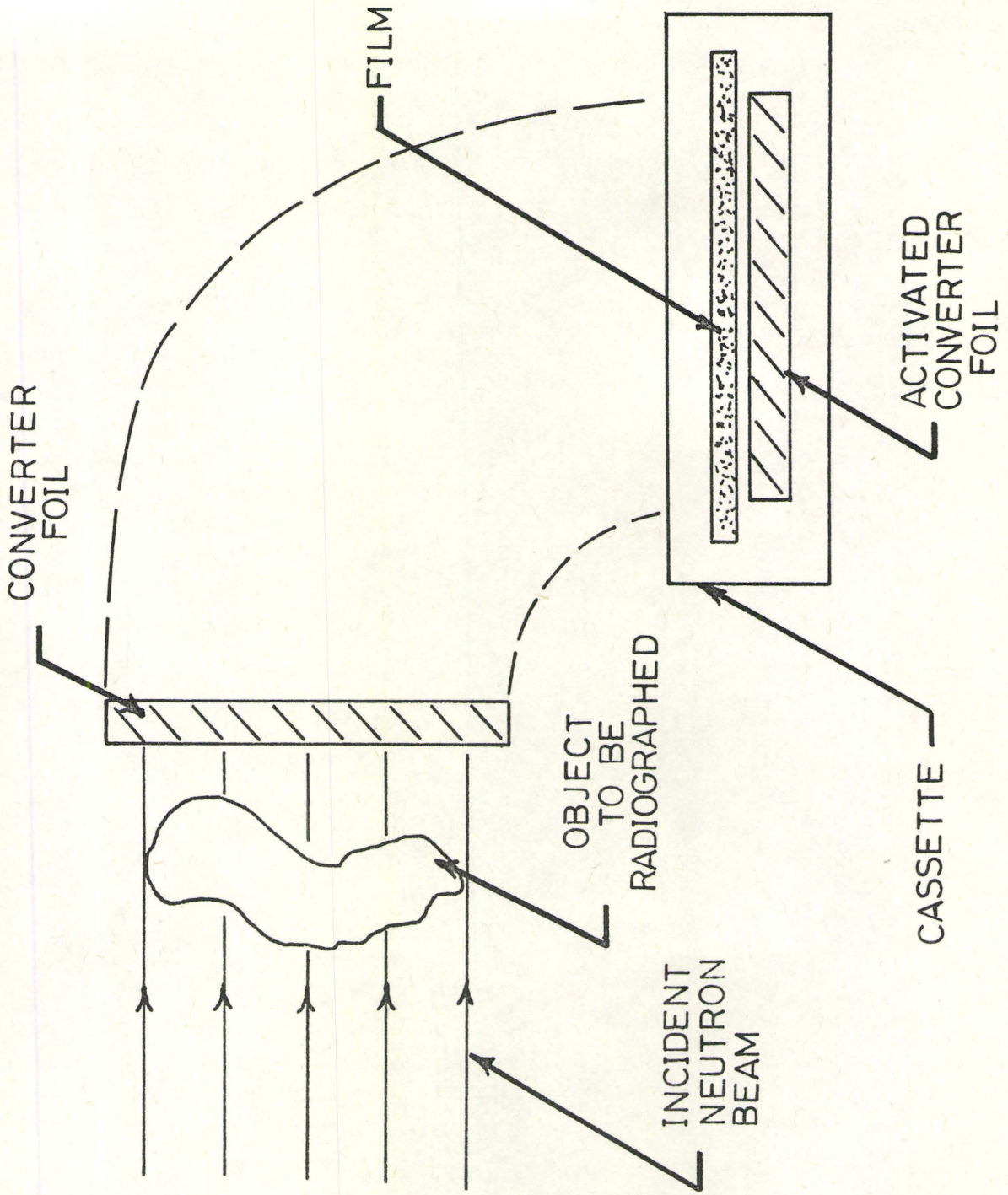

FIG. 2(a). Transfer exposure for neutron imaging. After neutron exposure the activated converter is removed to a film cassette for neutron imaging.

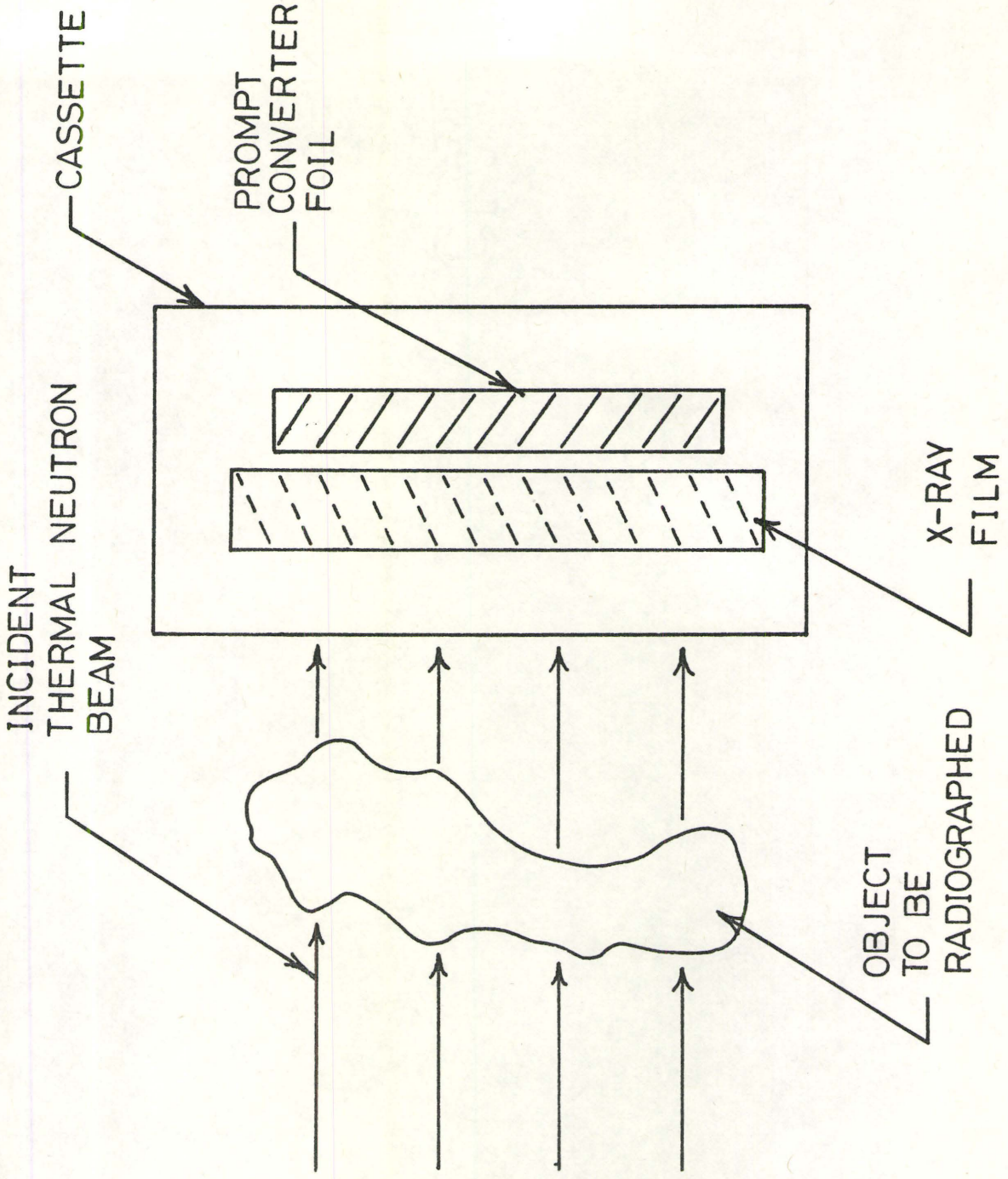

FIG. 2(b). Direct exposure technique for neutron imaging.

that can be activated by the neutrons. The screen is activated to an amount corresponding to the neutron flux at each position on the converter. The activated converter is then removed from the neutron beam and placed in a cassette containing photographic film. The radiation emitted by the converter then produces an image on the film.

Another technique for obtaining the radiograph is the direct exposure method as illustrated in Fig. 2(B). Instead of using a converter that is activated by the neutron beam, one uses a converter which emits prompt radiation and is not activated to any significant degree. Materials that can be used for this type of converter include lithium, cadmium and gadolinium. The prompt radiation is usually in the form of gamma radiation or electron emission. The neutron beam, after passing through the object to be radiographed, is incident on the cassette. The beam passes through the film with only a small amount of attenuation and then interacts with the converter to produce the prompt radiation. This radiation is detected by the photographic film to produce the neutron radiograph.

The high resolution capabilities associated with the prompt converters has been established.[4,5]

However, the associated conversion efficiency presents some limitations on the degree of versatility that could be achieved in neutron radiographic investigations. A low conversion efficiency requires either an increased neutron flux or an increase in the exposure time or both to produce satisfactory radiographs.

The possibility of increasing the efficiency of the radiation converter must be considered a highly desirable alternative to either of these possibilities. First consider the conversion process in the converter.

1.3. Gadolinium Converter Process

Of specific interest is the conversion of the neutron image for the gadolinium (Gd) foil converters. The conversion process in Gd is illustrated in Fig. 3. for a standard "backscreen" configuration. There are essentially two transport processes that must be considered for the converter. One involves the transport of the incident neutron to the point of absorption. At this point, the neutron is absorbed by the Gd nucleus and conversion radiation in the form of internal-conversion electrons is emitted. The second process involves the transport of this conversion radiation out of the Gd foil. The radiation is then free to interact with the film emulsion and produce the radiographic image.

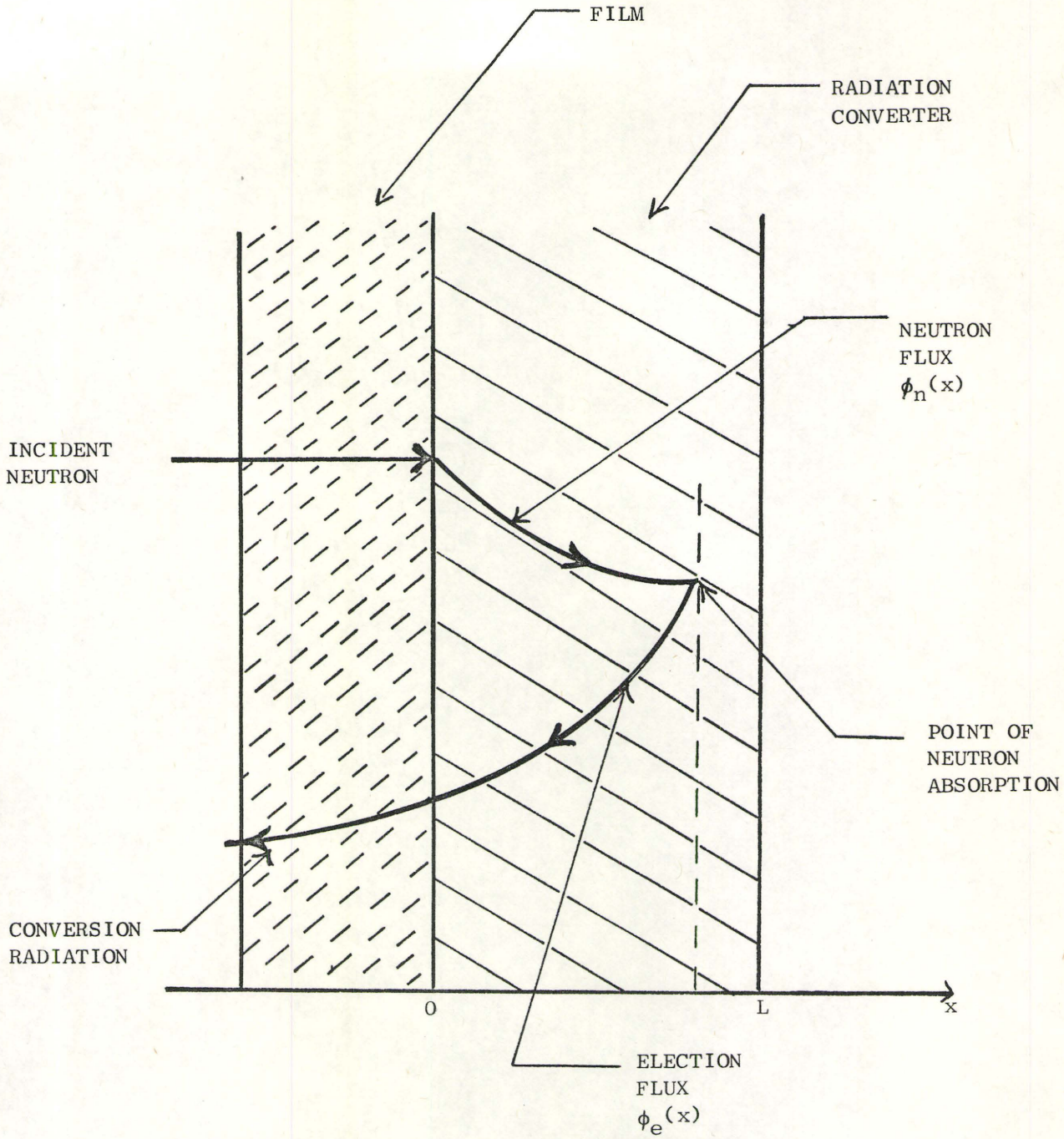

ILLUSTRATION OF THE NEUTRON CONVERSION PROCESS

FIGURE 3

2. CONVERSION ENHANCEMENT FOR A VARIABLE DENSITY CONVERTER

2.1. The Transport Model for the Converter

The transport of neutrons and electrons in the Gd converter play an important role in determining the conversion efficiency of the radiographic process. Each transport phenomenon can be considered independently since the interaction of neutrons with matter differs dramatically from the interaction of electrons with matter.

2.1.1. Neutron Transport Process

The neutron beam is attenuated as it passes through the converter. The fractional attenuation per unit distance is given by

$$\frac{d}{dx}\phi_n(x) = -\Sigma(x)\,\phi_n(x) \qquad (1)$$

where $\phi_n(x)$ is the space dependent neutron flux and $\Sigma(x)$ is the energy-averaged space dependent macroscopic absorption cross section for the neutron absorption process. The quantity $d\phi_n(x)/\phi_n(x)$ from equation (1) represents the fraction of neutrons that have penetrated the distance x into the converter without interacting and then interact in the distance dx. Clearly then the quantity $\Sigma(x)dx$ is the probability that a neutron interacts in dx and therefore can be considered as a probability per unit length for neutron interaction. Equation (1) can be intergrated directly to obtain an expression for the neutron flux

$$\phi_n(x) = \phi_{no}\exp\left(-\int_o^x \Sigma(x')dx'\right) \qquad (2)$$

where $\phi_{no}(x)$ is the flux of neutrons incident on the converter. Then the probability that a neutron can move through a distance x without interacting is given by

$$\frac{\phi_n(x)}{\phi} = \exp\left(-\int_o^x \Sigma(x')dx'\right) \qquad (3)$$

The probability that a neutron will move through the distance x and then have its first interaction in dx of x is then

$$p_n(x)dx = \Sigma(x)\ \exp\left(-\int_o^x \Sigma(x')dx'\right)dx \qquad (4)$$

In the interaction of the neutron and the nucleus of the Gd atom, the neutron is absorbed and conversion electrons are emitted. If γ represents the number of conversion electrons that are emitted for every neutron absorbed, then the probability that γ electrons are produced in dx of x is just

$$p_{ne}(x)\ dx = \gamma p_n(x)\ dx$$

$$= \gamma\Sigma(x)\ \exp\left(-\int_o^x \Sigma(x')dx'\right)dx \qquad (5)$$

Equation (5) represents the transport of neutrons incident on the converter to the point of absorption and the subsequent production of conversion electrons. Now consider the transport of these electrons out of the converter.

2.1.2. Electron Transport Process

The transport of the electrons in the converter is characterized by an attenuation constant. The fractional attenuation per unit distance that the electrons travel in the converter is given by

$$\frac{d}{dx}\,\phi_e(x) = \alpha(x)\;\phi_e(x) \qquad (6)$$

where $\phi_e(x)$ is the electron flux at the point x in the converter and $\alpha(x)$ is the space-dependent linear attenuation coefficient of the emitted internal-conversion electrons. Equation (6) can be integrated directly to yield the electron flux that reaches the x = o edge of the converter.

$$\begin{aligned}\phi_e(0) &= \phi_e(x)\;\exp\left(\int_x^o \alpha(x')dx'\right)\\ &= \phi_e(x)\;\exp\left(-\int_o^x \alpha(x')dx'\right)\end{aligned} \qquad (7)$$

Then the probability that the electron formed at dx of x will reach the edge of the converter is

$$p_e(x) = \frac{\phi_e(0)}{\phi_e(x)} = \exp\left(-\int_o^x \alpha(x')dx'\right) \qquad (8)$$

Equation (8) represents the transport of the internal conversion electrons from the point of neutron absorption to the edge of the converter foil as indicated in Fig. 3.

The two transport phenomenon can be combined so that the probability that a neutron is absorbed in dx of x, produces internal conversion electrons, and the electrons are transported to the film emulsion edge of the converter is given by

$$p(x)dx = p_e(x) \cdot p_{ne}(x)dx \qquad (9)$$

$$= \exp\left(-\int_0^x \alpha(x')dx'\right) \gamma\, \Sigma(x) \exp\left(-\int_0^x \Sigma(x')dx'\right)dx$$

$$= \gamma\, \Sigma(x) \exp\left(-\int_0^x [\Sigma(x') + \alpha(x')]dx'\right)dx$$

The total probability for the neutron-electron transport is a converter of thickness L is then given by

$$P(0,L) = \int_0^L p(x)dx \qquad (10)$$

$$= \gamma \int_0^L \Sigma(x) \exp\left(-\int_0^x [\Sigma(x') + \alpha(x')]dx'\right)dx$$

Let the flux of incident neutrons onto the converter be ϕ_{no}. Then the electron flux reaching the film emulsion side of the converter is

$$\phi_e(0) = \phi_{no}\, P(0,L) \qquad (11)$$

$$= \phi_{no}\, \gamma \int_0^L \Sigma(x) \exp\left(-\int_0^x [\Sigma(x') + \alpha(x')]dx'\right)dx$$

Equation (11) represents the conversion-transport phenomenon for a converter with a space-dependent neutron cross-section and electron attenuation coefficient.

2.1.3. Conversion Enhancement Ratio

Consider the possibility of increasing the efficiency of the conversion-transport process by means of variations in the neutron cross section and electron attenuation coefficient. It is convenient to compare the spatially dependent composition converter with a reference converter. The reference converter, in this case, is one which has spatially independent attenuation parameters, i.e.

$$\Sigma(x) = \Sigma_r \tag{12}$$

and

$$\alpha(x) = \alpha_r \tag{13}$$

The electron flux for the reference converter is then determined from equation (11) as

$$\phi_{er}(0) = \phi_{no}\,\gamma \int_o^L \Sigma_r \exp\left(-\int_o^x [\Sigma_r + \alpha_r]dx'\right)dx \tag{14}$$

$$= \phi_{no}\,\gamma\,\frac{\Sigma_r}{(\Sigma_r + \alpha_r)}\left(1 - \exp\,-[\Sigma_r + \alpha_r]L\right)$$

This reference electron flux can be compared with the electron flux for the variable composition converter to evaluate the conversion enhancement attained. For this purpose, a conversion enhancement ratio, ψ , can be defined. The enhancement ratio is given as

$$\psi = \frac{\phi_e(o)}{\phi_{er}(o)} = \frac{\phi_{no}\,\gamma \int_o^L \Sigma(x)\,\exp\left(-\int_o^x [\Sigma(x')+\alpha(x')]dx'\right)dx}{\phi_{no}\,\gamma\,\frac{\Sigma_r}{(\Sigma_r+\alpha_r)}\left(1-\exp\left\{-[\Sigma_r+\alpha_r]L\right\}\right)}$$

$$= \left(\frac{\Sigma_r+\alpha_r}{\Sigma_r}\right)\left(\frac{1}{1-\exp\left\{-[\Sigma_r+\alpha_r]L\right\}}\right) \cdot$$

$$\int_o^L \Sigma(x)\,\exp\left(-\int_o^x [\Sigma(x')+\alpha(x')]dx'\right)dx \qquad (15)$$

Equation (15) represents the enhancement that can be obtained by employing a variable density converter; a ψ value greater than unity represents an increase in the conversion efficiency.

2.2. Model Analysis

The conversion enhancement ratio can be evaluated for converters with space dependent neutron cross-sections and electron linear attenuation coefficients.

2.2.1. Uniform Isotopic Enrichment

First consider a converter with a uniform isotopic enrichment. This affects the neutron cross-section of the converter but not the electron attenuation coefficent since the density of the converter foil is unchanged. Therefore for this case we have

$$\Sigma(x) = \Sigma \qquad (16)$$

and

$$\alpha(x) = \alpha_r \qquad (17)$$

The conversion enhancement is thus given by

$$\psi = \left(\frac{\Sigma_r + \alpha_r}{\Sigma_r}\right) \frac{\Sigma}{(\Sigma + \alpha_r)} \frac{(1 - \exp\{-[\Sigma + \alpha_r]L\})}{1 - \exp\{-[\Sigma_r + \alpha_r]L\}}) \qquad (18)$$

A standard gadolinium converter foil possessing the various gadolinium isotopes in their natural abundances is used as the reference converter. For such a converter it has been found that[3,4]

$$\Sigma_r = 0.14\ \mu m^{-1} \qquad (19)$$

and

$$\alpha_r = 0.20\ \mu m^{-1} \qquad (20)$$

yields generally good agreement with experimental results if a thermal neutron source is used.

The conversion enhancement ratio as given by equation (18) has been evaluated for a range of Σ and a series of converter thicknesses. Results are shown graphically in Fig. 4. It is of interest to note that a significant conversion enhancement is possible with decreasing converter thickness. This does not imply that a decreasing converter thickness possessing higher enrichment will contribute to an increased conversion enhancement when compared to some standard natural gadolinium converter with a standard reference

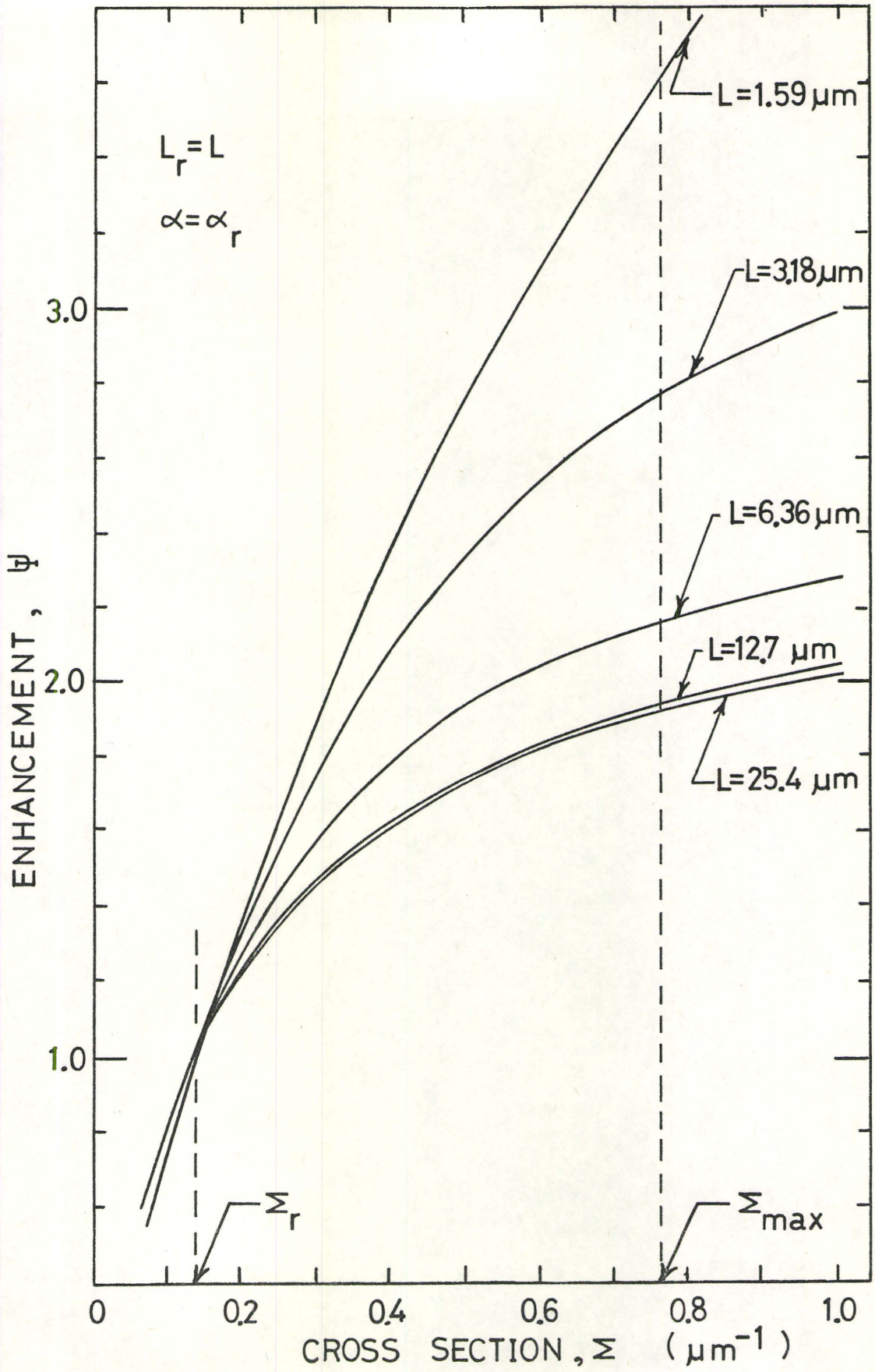

FIG. 4. Conversion enhancement for a uniform isotopically enriched converter.

thickness, L_r. When the reference converter has a constant thickness associated with it, the conversion enhancement ratio as given by equation (18) then becomes

$$\psi = \frac{(\Sigma_r+\alpha_r)}{\Sigma_r} \frac{\Sigma}{(\Sigma+\alpha_r)} \frac{(1-\exp\{-[\Sigma+\alpha_r]L\})}{(1-\exp\{-[\Sigma_r+\alpha_r]L_r\})} \quad (21)$$

The reference gadolinium converter foil to be used in this analysis has a thickness of

$$L_r = 25.4\ \mu m \quad (22)$$

Results for the conversion enhancement ratio as defined by equation (21) for a range of Σ are shown graphically in Fig. 5. An enhancement in excess of $\psi = 2.0$ is not possible. However, the break-even point, $\psi = 1$, is possible for very thin and enriched converters. This clearly suggests that some gain in both conversion enhancement and resolution[5] are possible for thin but highly enriched converter foils.

2.2.2. Linear Variations in Sigma and Alpha

In the preceding section the effect of uniform isotopic enrichment on the conversion enhancement has been evaluated. Consider, now, the effect of changes

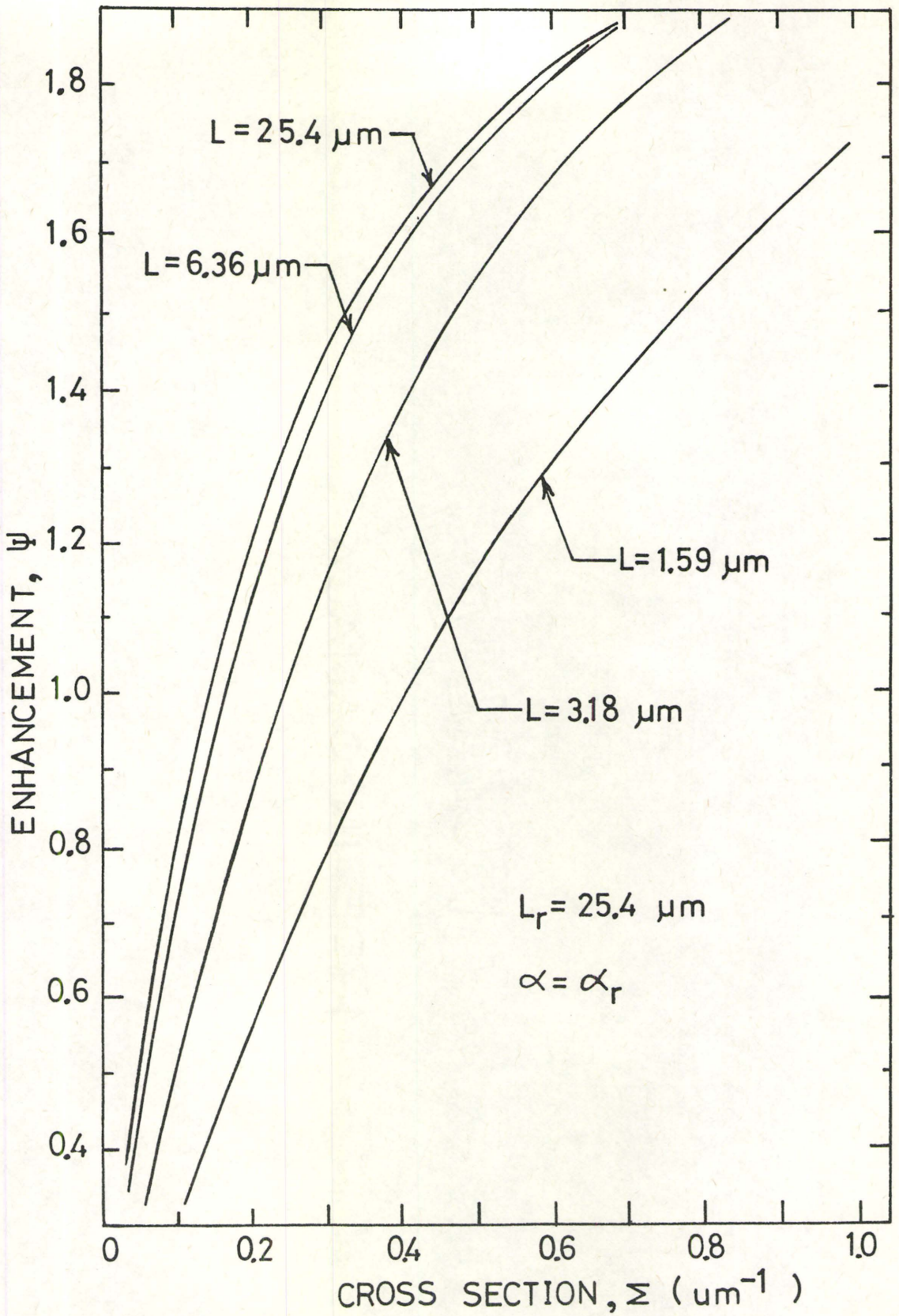

FIG. 5. Conversion enhancement for a uniform isotopically enrighed converter referenced to a standard converter thickness L_r = 25.4 μm.

in material density as well.

As a first approximation, consider linear variations in neutron absorption and electron attenuation with respect to position in the converter. Then

$$\Sigma(x) = \Sigma_o + \Sigma_1 x \tag{23}$$

and

$$\alpha(x) = \alpha_o + \alpha_1 x \tag{24}$$

The conversion enhancement ratio can then be written as

$$\psi = \frac{(\Sigma_r+\alpha_r)}{\Sigma_r} \frac{\int_o^L [\Sigma_o+\Sigma_1 x) \exp -\left\{[\Sigma_o+\alpha_o]x + \frac{[\Sigma_1+\alpha_1]x^2}{2}\right\} dx}{(1 - \exp -\{[\Sigma_r + \alpha_r]\ L_r\})} \tag{25}$$

Before this function can be evaluated, some realistic ranges for the variables must be defined.

Consider the neutron cross-section. The largest value that this parameter can physically attain is associated with the isotope of gadolinium, Gd - 157, which has a cross-section of

$$\Sigma_{Gd-157} = \Sigma_{max} = 0.77\ \mu m^{-1} \tag{26}$$

Then the range of values that $\Sigma(x)$ can have is given by

$$0 \leq \Sigma(x) \leq 0.77\ \mu m^{-1} \tag{27}$$

The electron attenuation coefficient for natural gadolinium is given in equation (20) as $\alpha_r = 0.2\ \mu m^{-1}$. Based on this value the maximum α has been set to

$$\alpha_{max} = 0.3 \mu m^{-1} \tag{28}$$

and a realistic range for $\alpha(x)$ is then

$$0 \leq \alpha(x) \leq 0.3\ \mu m^{-1} \tag{29}$$

Although the reference converter thickness has been maintained at $L_r = 25.4\ \mu m$, the conversion enhancement ratios associated with converters having thicknesses in the range

$$1.59 \leq L\ (\mu m) \leq 25.4 \tag{30}$$

have been evaluated for the various converter parameter configurations as defined by equations (23) and (24). Consider these configurations.

Case One:

$$\Sigma_o = \alpha_o = 0$$

First consider a converter with a space dependent neutron absorption cross-section given by

$$\Sigma(x) = \Sigma_1 x \quad ; \quad 0 \leq x \leq L \tag{31}$$

with

$$0 \leq \Sigma\ (L) \leq \Sigma_{max} \tag{32}$$

and an electron attenuation coefficient given by

$$\alpha(x) = \alpha_1 x \quad ; \; 0 \leq x \leq L \tag{33}$$

with

$$0 \leq \alpha(L) \leq \alpha_{max} \tag{34}$$

Physically this represents a converter with an increasing neutron absorption cross-section and an electron attenuation coefficient with penetration into the converter.

The conversion enhancement ratio associated with this converter has been evaluated for the range of converter thickness of interest. The results for $L = 25.4$ μm are given in Fig. 6. It has been found convenient to display the results in terms of the parameters Σ_T and α_T. They are defined as

$$\alpha_T = \alpha_o + \alpha_1 L = \alpha(L) \tag{35}$$

and

$$\Sigma_T = \Sigma_o + \Sigma_1 L = \Sigma(L) \tag{36}$$

Results of the conversion enhancement evaluation for $L = 12.7, 6.35, 1.59$ μm are found in Fig. 7, Fig. 8 and Fig. 9 respectively.

For all converter thicknesses, the largest conversion enhancement has been obtained for large values of Σ_T and small values of α_T.

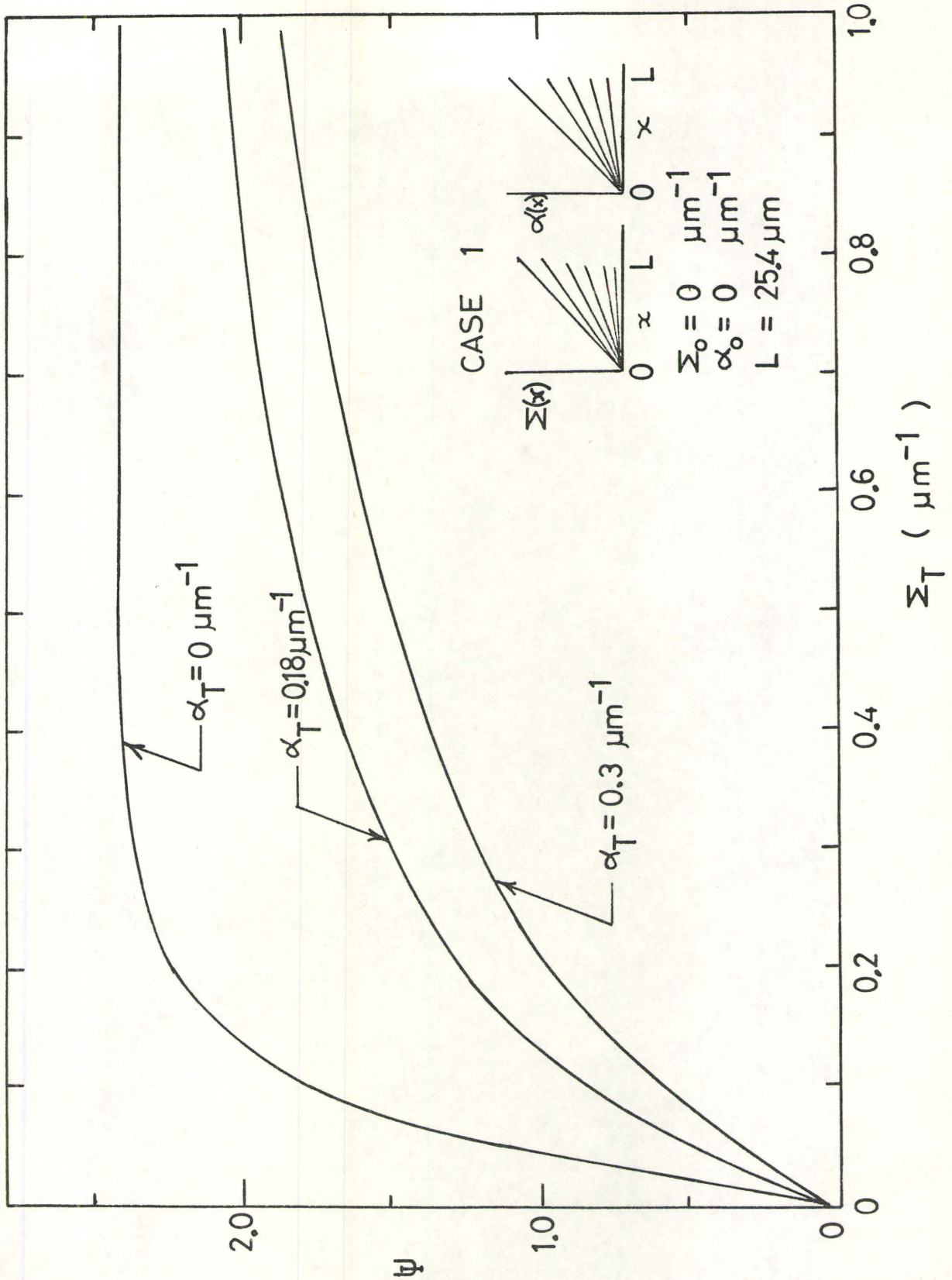

FIG. 6. Case One: Conversion enhancement ratio for $\Sigma_o = \alpha_o = 0$ and L = 25.4 um.

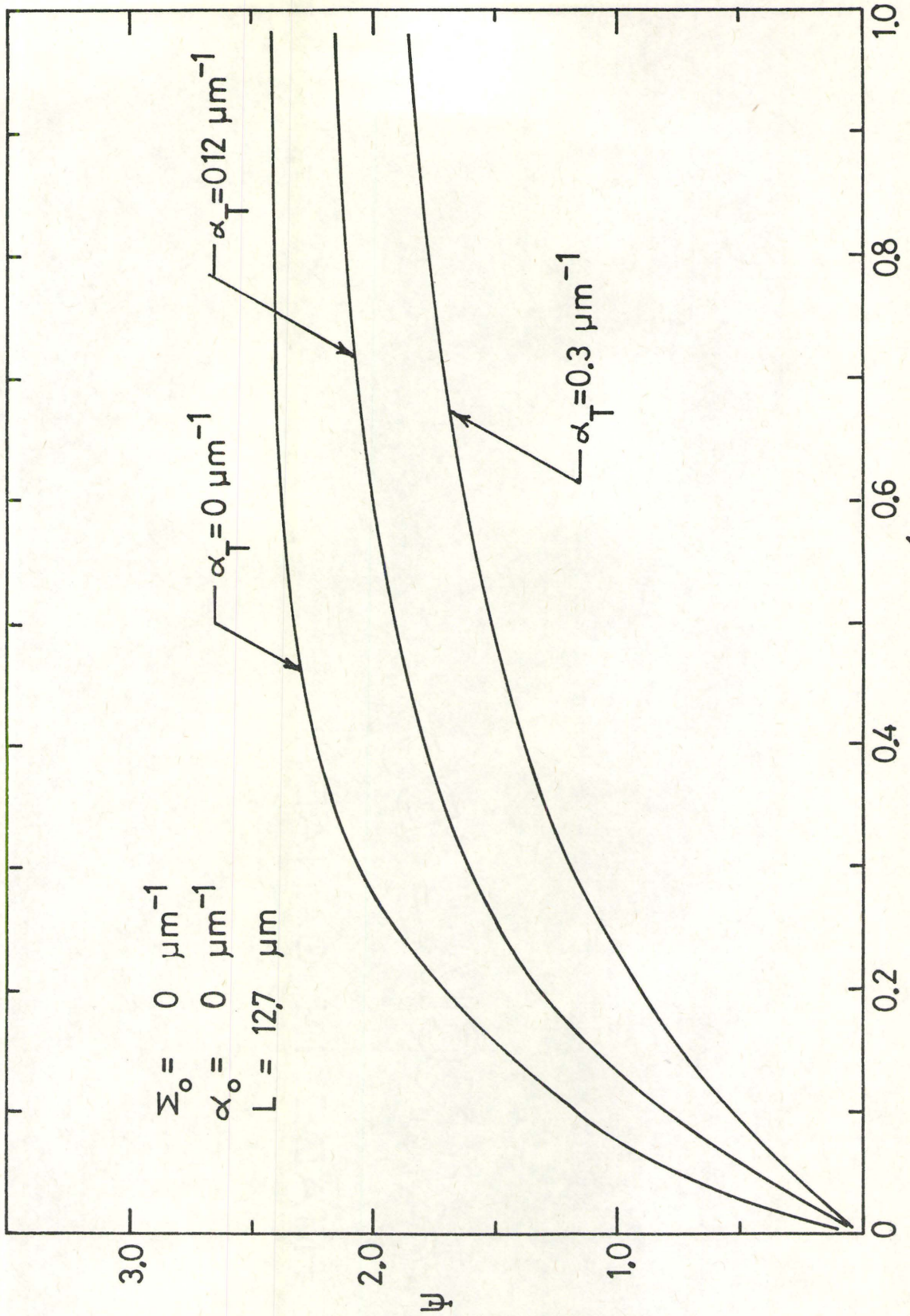

FIG. 7. Case One: Conversion enhancement ratio for $\Sigma_o = \alpha_o = 0$ and L = 12.7 μm.

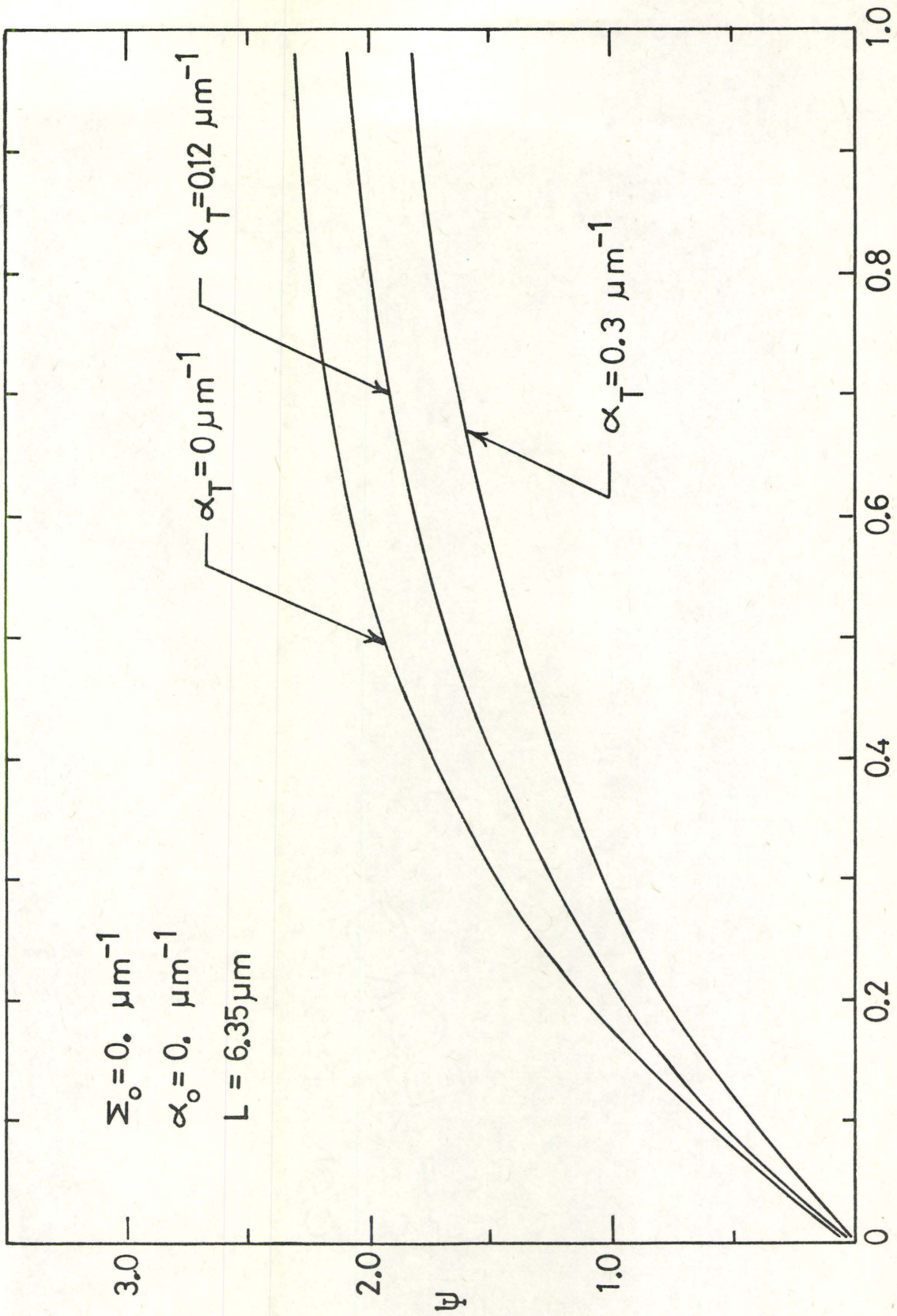

FIG. 8. Case One: Conversion enhancement ratio for $M_o =$ $\alpha_o = 0$ and L = 6.35 μm.

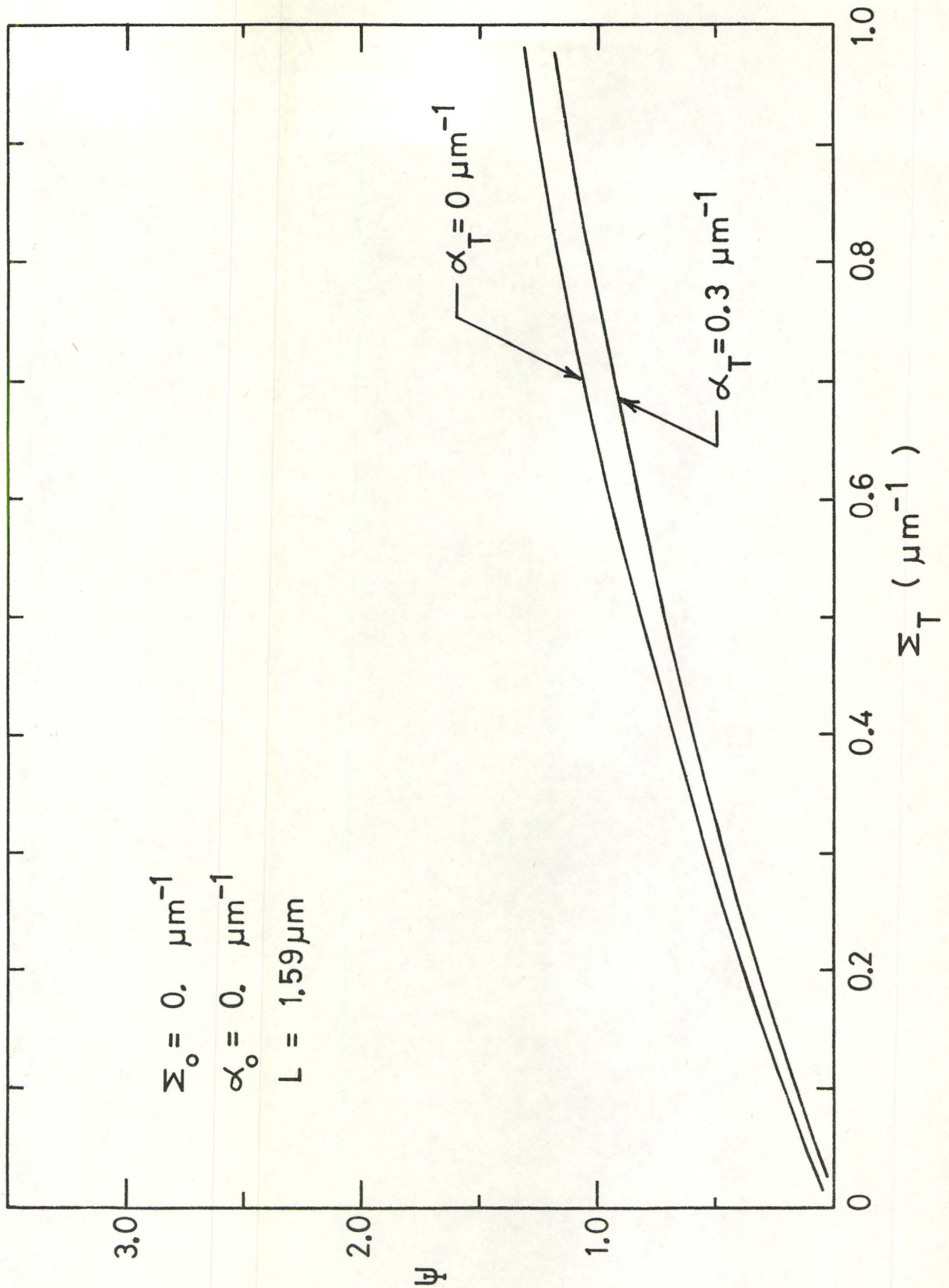

FIG. 9. Case One: Conversion enhancement ratio for $\Sigma_o = \alpha_o = 0$ and L = 1.59 μm.

Case Two:

$$\Sigma_o = 1.0\mu^{-1} \quad ; \quad \alpha_o = 0$$

Now consider a converter with the following neutron absorption characteristic

$$\Sigma(x) = \Sigma_{max} + \Sigma_1 x \quad ; \quad 0 \leq x \leq L \qquad (37)$$
$$= 1.0 + \Sigma_1 x$$

with $\Sigma(L)$ having the range of values given by equation 32. The electron attenuation is the same as defined for case one.

The results for L = 25.4 μm have been plotted in Fig. 10 for $\alpha_T = 0.3\ \mu m^{-1}$ and $0\ \mu m^{-1}$. The conversion enhancement ratio reaches a maximum value of $\psi = 2.42$ when $\alpha_T = 0\ \mu m^{-1}$. Since with $\alpha_T = 0.3\ \mu m^{-1}$ the conversion enhancement reaches a value of $\psi = 2.40$, enhancement is relatively independent of the electron attenuation coefficient for this converter configuration.

The effect of varying the converter thickness is illustrated in Fig. 11 for $\alpha_T = 0.3\ \mu m^{-1}$. As the converter thickness is decreased the conversion enhancement deteriorates as well. However, the enhancement only

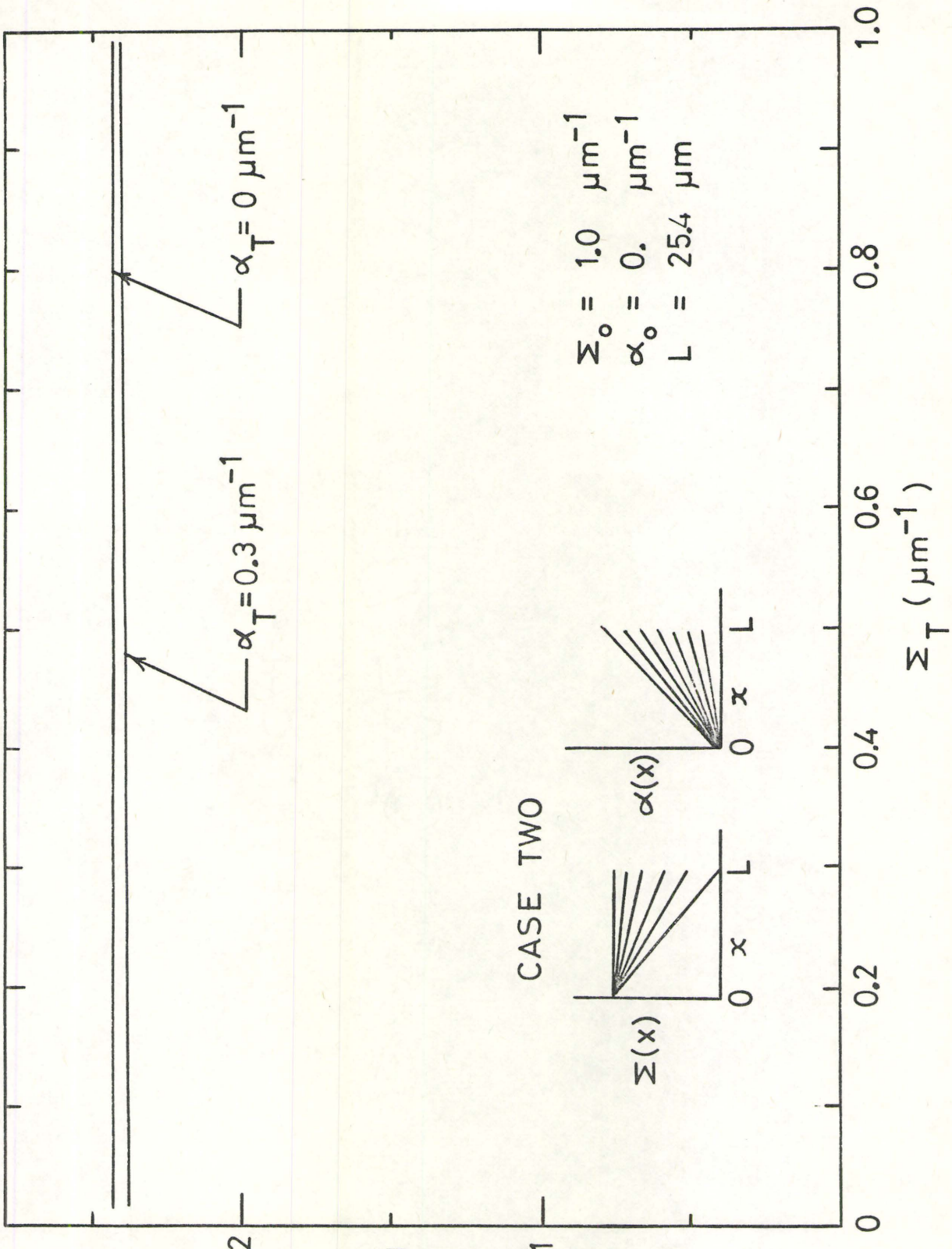

FIG. 10. Case Two: Conversion enhancement ratio for Σ_o = 1.0 ; α_o = 0 and L = 25.4 μm.

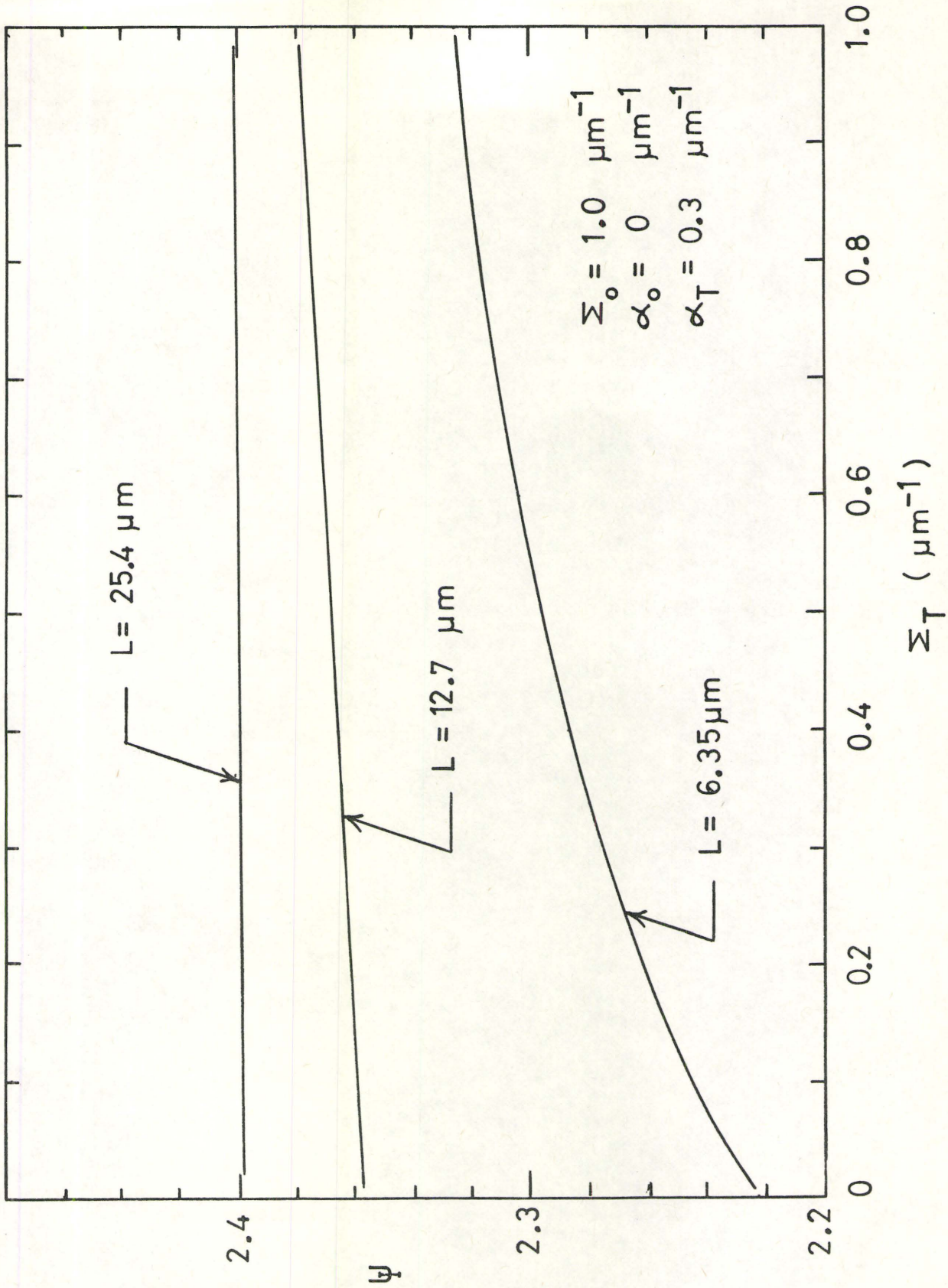

FIG. 11. Case Two: Effect of converter thickness on Conversion Enhancement for $\alpha_T = 0.3\ \mu m^{-1}$

only decreases by 5% when the converter thickness is decreased from 25.4 μm to 6.35 μm. This indicates that for this converter configuration most of the conversion takes place in the initial 6 μm of the converter.

Case Three:

$$\Sigma_o = 0 \ , \quad \alpha_o = 0.3$$

Consider now a converter that has a space-dependent neutron absorption cross-section given by equation (31) and equation (32) but with an electron attenuation given by

$$\alpha(x) = 0.3\ \mu m^{-1} + \alpha_1 x \qquad (38)$$

with $\alpha(L)$ in the range given by equation (34). Physically this represents a converter with an increasing neutron absorption cross-section with a decreasing electron attenuation coefficient with penetration into the converter.

The conversion enhancement ratios associated with this converter configuration have been calculated for the range of Σ_T and α_T of interest.

The results for L = 25.4 μm and L = 3.17 μm are shown in Fig. 12. The shaded areas represent the family of curves for the conversion enhancement for the range

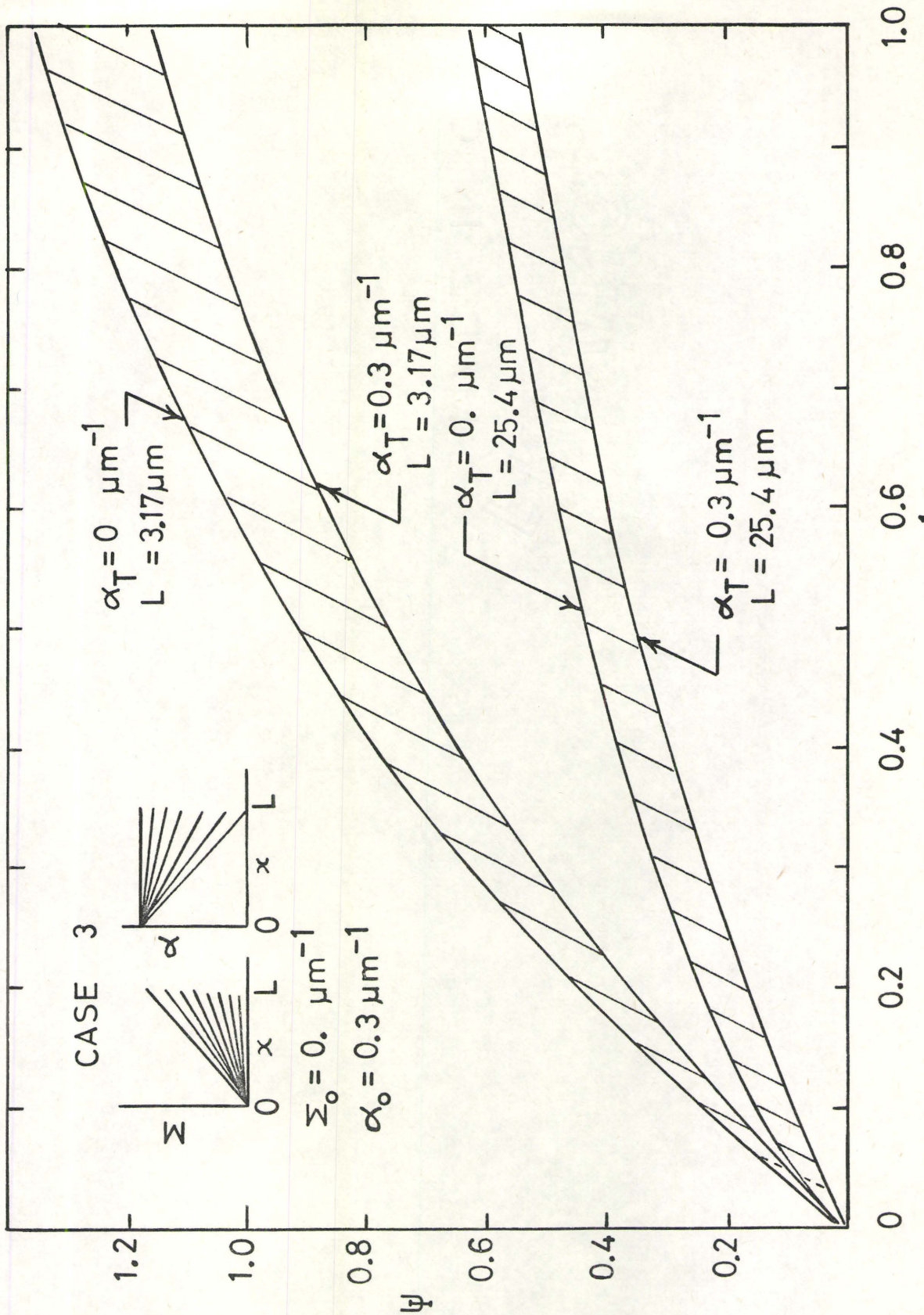

FIG. 12. Case Three: Conversion enhancement ratio for $\Sigma_o = 0$ and $\alpha_o = 0.3\ \mu m$.

of α_T from 0.3 μm^{-1} to 0 μm^{-1}. The enhancement for this converter increases as α_T decreases but never achieves an enhancement ratio in excess of $\psi = 1.4$.

The effect of converter thickness on conversion enhancement is illustrated in Fig. 13 for $\alpha_T = 0\ \mu m^{-1}$. The best enhancement is obtained for converter thicknesses from 3 μm to 6 μm.

Case Four:

$$\Sigma_o = 1.0 \mu m^{-1} \quad ; \quad \alpha_o = 0.3 \mu m^{-1}$$

Next consider a converter with the space dependent neutron absorption cross-section given by equation (37) and an electron absorption coefficient given by equation (38). This physically represents a converter that has large neutron absorption as well as electron absorption on the incident neutron (x = 0) edge of the converter. The neutron absorption as well as the electron absorption then decreases with penetration into the converter.

The results for L = 25.4 μm are plotted in Fig. 14. The shaded area represents the family of curves for the conversion enhancement for values of α_T between 0.3 μm^{-1} and 0 μm^{-1}. The enhancement

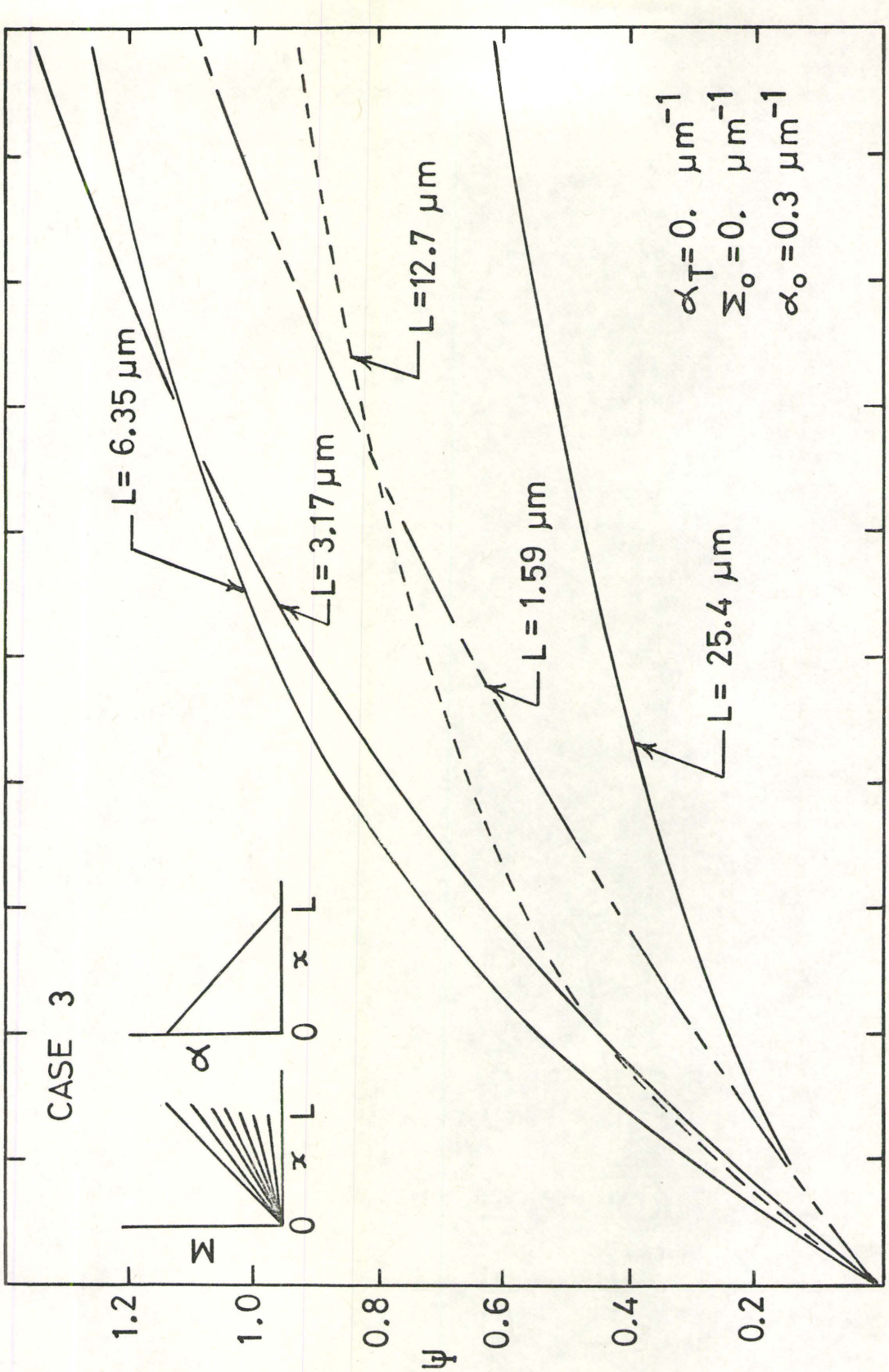

FIG. 13. Case Three: Effect of converter thickness on conversion enhancement for α_T = 0 μm.

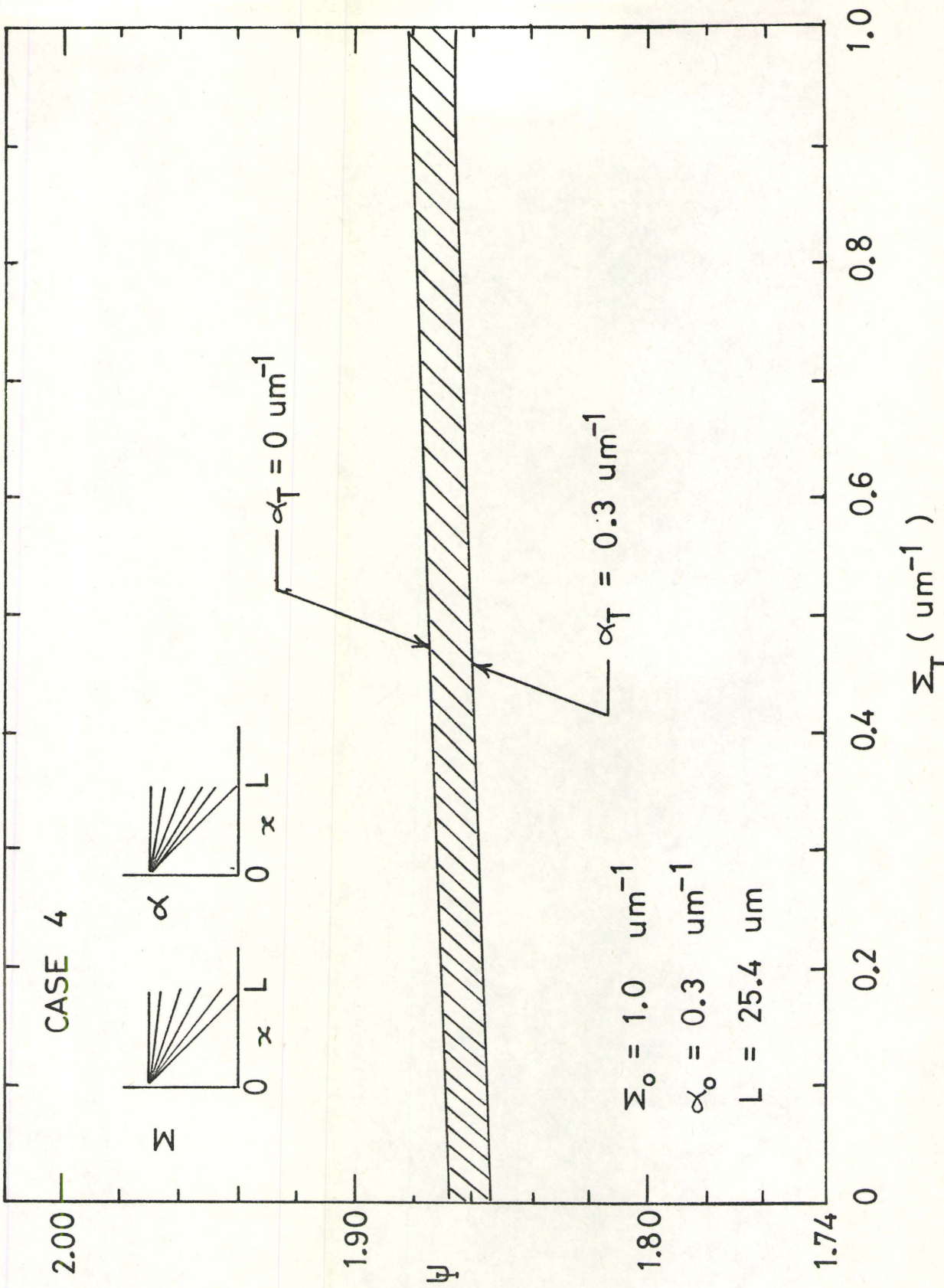

FIG. 14. Conversion enhancement ratio for Σ_o = 1.0 μm^{-1} and α_o = 0.3 μm^{-1}.

ratio increases as α_T decreases. The enhancement for this converter configuration is in the range from $\psi = 1.86$ to $\psi = 1.88$ for the values of Σ_T and α_T of interest.

The conversion enhancement associated with converter thicknesses of L = 25.4, 12.7 and 6.35 μm are illustrated in Fig. 15 for the case when $\alpha_T = 0\ \mu m^{-1}$. This converter configuration is relatively independent of converter thickness for the values of thickness investigated; the enhancement changes only by ~5% for a thickness change from 25.4 μm to 6.35 μm.

2.2.3. Effect of Converter Thickness on Conversion Enhancement

The effect of varying the converter thickness has been evaluated for the various converter configurations. The results are summarized in Fig. 16. The space dependent neutron absorption cross-section and electron attenuation that is used to generate each curve is indicated in the figure. For all the curves the extreme variations in both these parameters were used to emphasize the effect of varying the thickness. For example, the converter in case one is identified by $\Sigma_0 = \alpha_0 = 0$. The extreme variation occurs when $\Sigma_T = 0.7\ \mu m^{-1}$ and $\alpha_T = 0.3\ m^{-1}$. The value of $\Sigma_T = 0.7\ \mu m^{-1}$ was used to comply with the maximum value of the neutron absorption

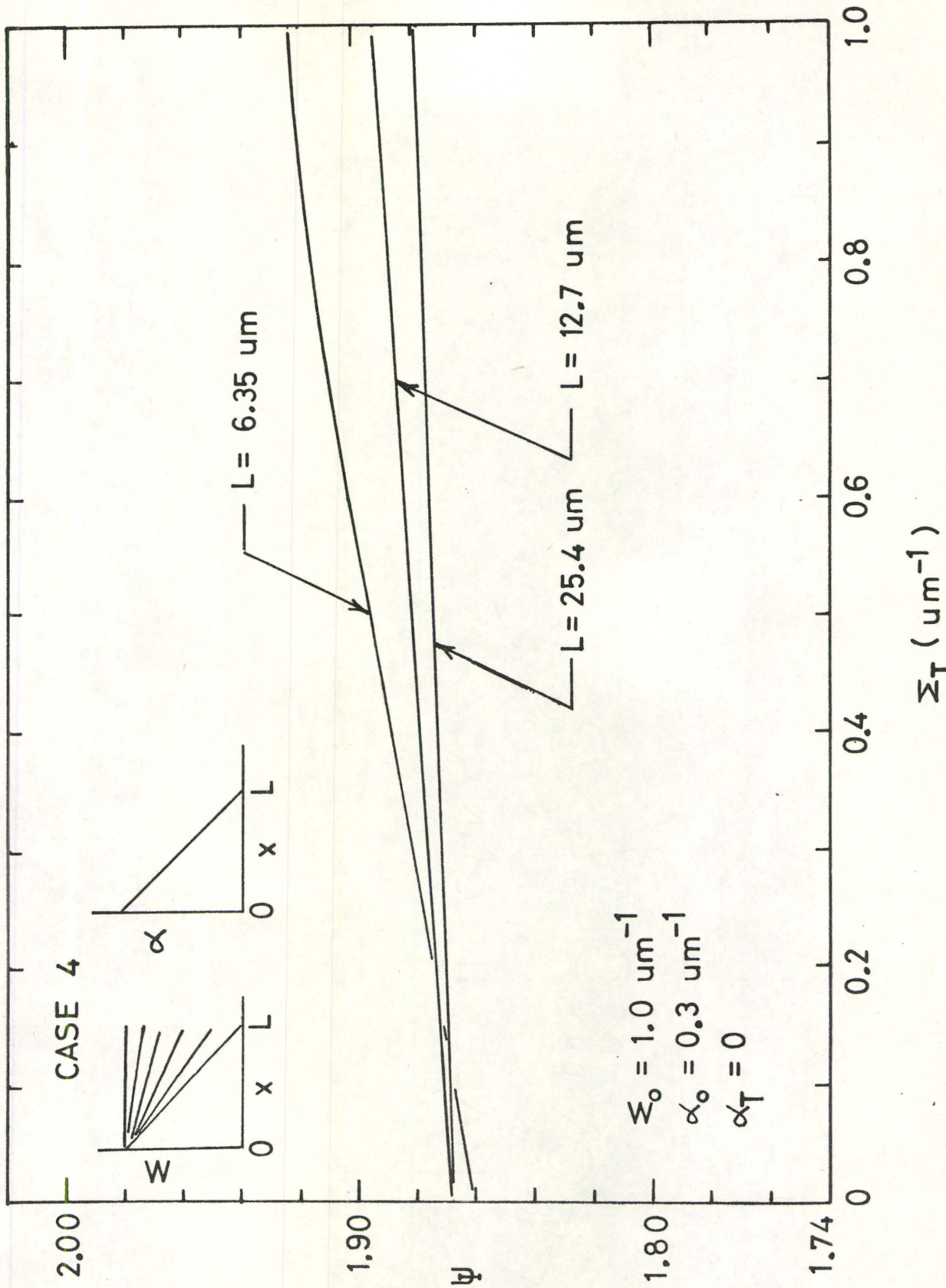

FIG. 15. Case 4: Variation in conversion enhancement for various converter thicknesses for $\alpha_T = 0\ \mu m^{-1}$

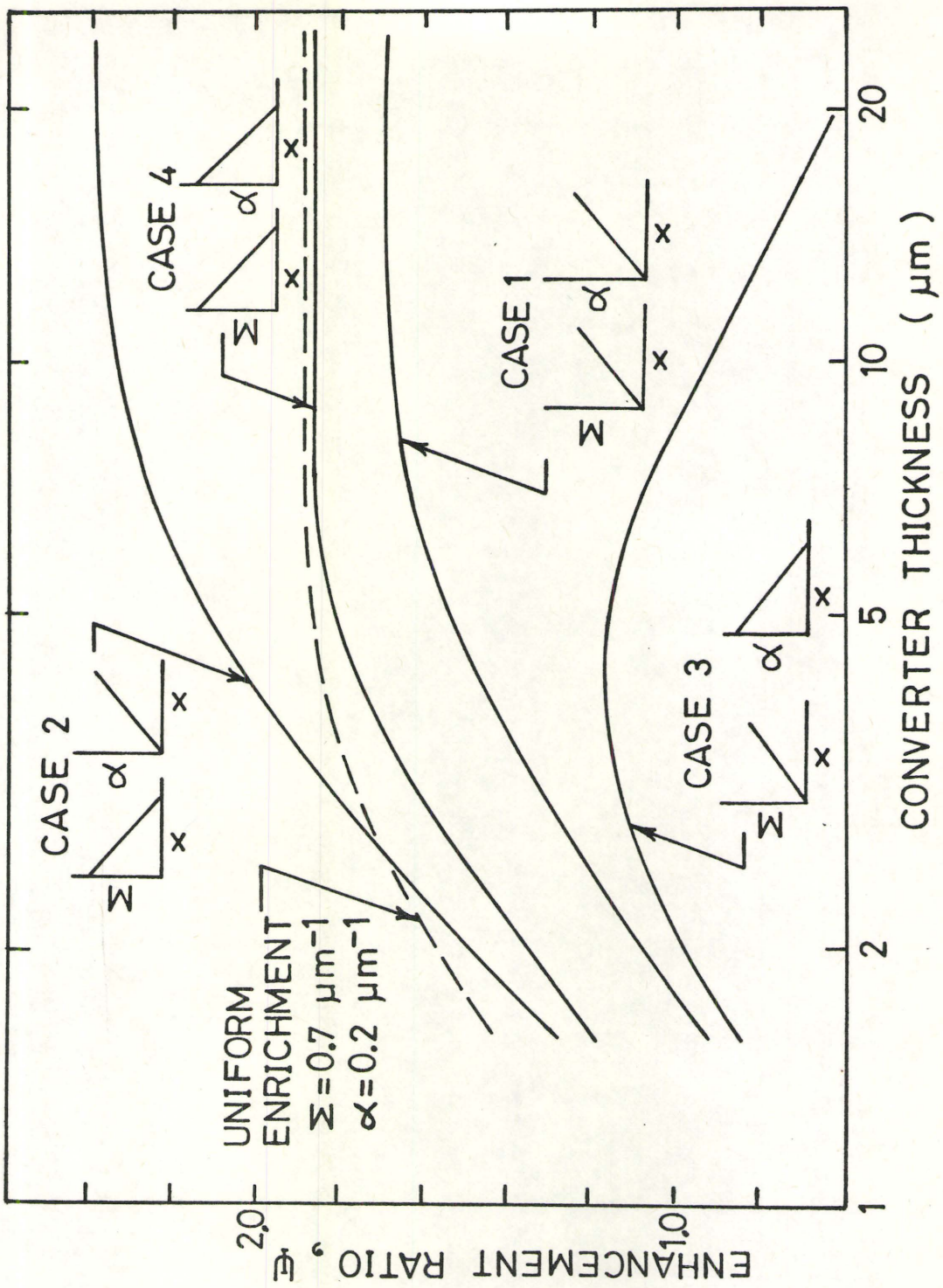

FIG. 16. Effect of converter thickness on conversion enhancement for the various converter configurations.

cross-section for the gadolinium - 157 isotope.

All curves of enhancement ratio versus converter thickness except for case three with $\Sigma_0 = 0$ and $a_0 = 0.3\ \mu m^{-1}$ exhibited a positive slope. These curves tend to reach an asymptote for thicknesses less than or equal to 25.4 μm. The curve case three reaches a maximum for a converter thickness near 4.5 μm and the enhancement decreases for larger values of thickness. The curve for the uniform isotopically enriched converter is also given. This curve becomes asymptotic to $\psi = 1.88$ for thicknesses greater than 6 μm.

2.3. Discussion of Results

The conversion enhancement ratios for several converter configurations have been evaluated. Significant improvement in the conversion process is possible by increasing the neutron absorption cross-section for the converter material. Natural gadolinium is used for the converter at present. If the concentration of the gadolinium - 157 isotope is increased in the converter, an increase in the neutron absorption cross-section from $\Sigma = 0.14\ \mu m^{-1}$ to $\Sigma = 0.77\ \mu m^{-1}$ is possible. The radiographic conversion process using a gadolinium - 157 converter has an associated conversion efficiency that is almost a factor of two better than a natural gadolinium converter.

For all the converter configurations investigated the enhancement ratio was improved by decreasing the value for the electron attenuation coefficient, α . This result coincides with anticipated results since this parameter represents a deterrant in the conversion process. It must be noted, however, that for case two and case four converter configurations, the effect of this parameter is minimal. The feature common to both these configurations is the space dependent neutron absorption cross-section. On the neutron incident edge of the converter (x = 0) it has a very large cross-section ($\Sigma(0) = \Sigma_{max}$). The fact that the electron attenuation coefficient is relatively insignificant for these configurations can be reasoned as follows. As the neutron beam in the radiographic process enters the converter, it encounters the very large neutron absorption material. The beam is attenuated significantly in the first few micrometers with very few neutrons able to penetrate to any depth into the converter. Hence, most of the conversion electrons that are produced in the interaction do not have to travel far in the converter to escape and then are not affected to a large degree by the electron attenuation coefficient.

This point is further emphasized by the fact that

for both these converter configurations a decrease in the converter thickness from 25.4 μm to 6.35 μm has little effect on the enhancement ratio.

Special mention should be given to the uniform isotopically enriched converter configuration. The enhancement ratio of 1.88 for a neutron absorption cross-section of 0.7 μm^{-1} represents a significant improvement over the standard natural gadolinium converter. The attractive element for this configuration is the availability of isotopically enriched gadolinium. Such a converter can be readily fabricated and used to verify the enhancement ratios obtained with the model analysis.

3. CONVERSION ENHANCEMENT BY ELECTRON MULTIPLICATION

3.1. Introduction

The formation of a neutron radiographic image using a gadolinium converter is based on the emission of internal conversion electrons. The possibility of using these electrons to create showers of secondary electrons is a very appealing approach to the problem of conversion enhancement.

The techniques and mechanisms for obtaining secondary emission using low density films of some insulators has already been investigated in reference to transmission dynodes and electron multiplication devices.[9][10][11][12][13] Garwin and Llacer[12] discuss the mechanism for low density films of CsI and KCl in which excited electrons produced in the KCl grains by the primary electrons diffuse through the film and are emitted as secondary electrons.

Garwin and Llacer also found that there is a unique relationship between yield of secondary electrons and the surface potential of the KCl dynode as indicated in Fig. 17. This relationship is independent of the primary electron energy and can be divided into two basic regions, region I and region II. The secondary yield in region one is determined by several phenomenon including mechanisms involving hole trapping, the drift of the electrons under the action of the electric field

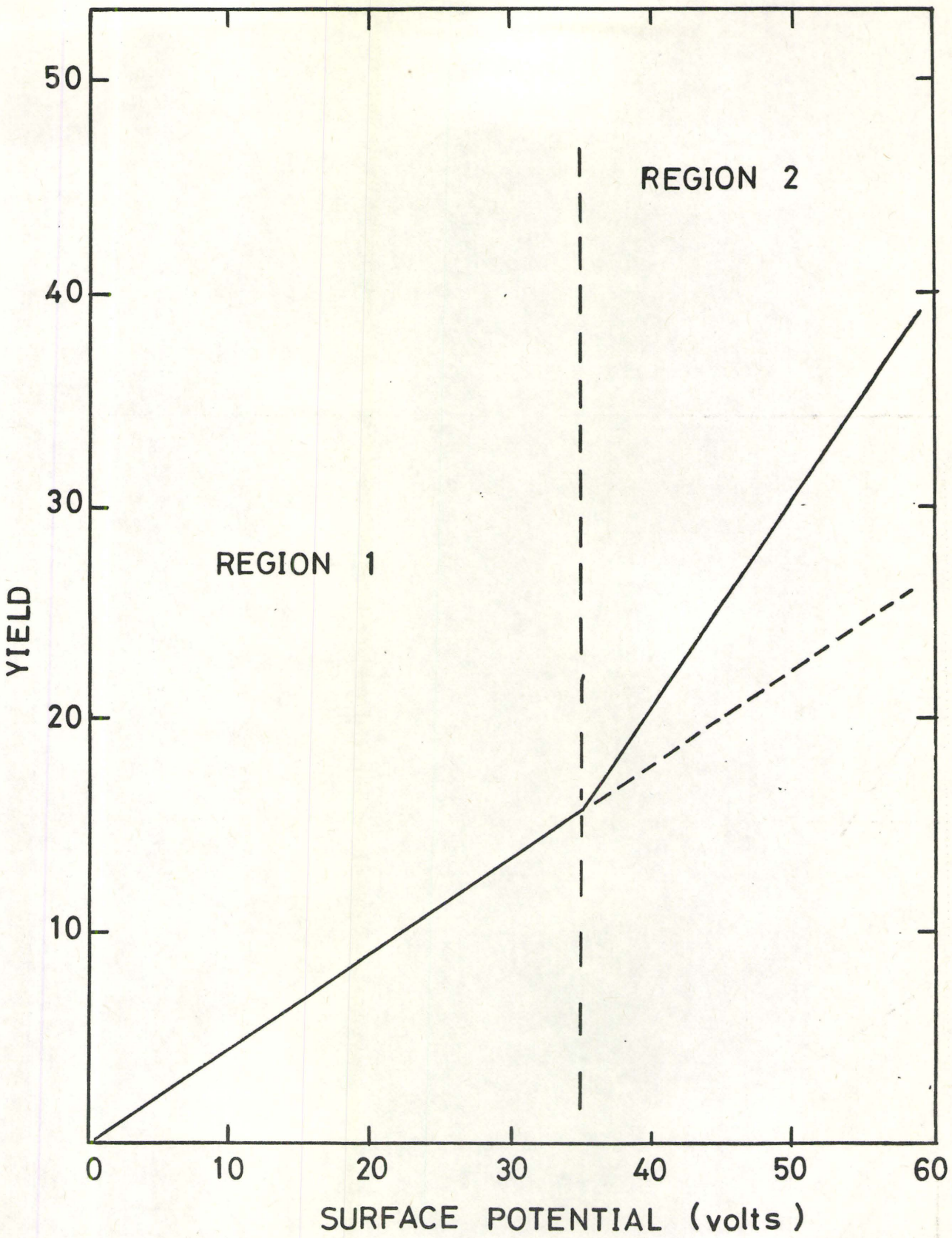

FIG. 17. Illustration of the unique relationship between Yield of secondary electrons and the surface potential for a KCl dynode.

produced by an applied surface potential and recombination of electron-hole pairs. It is anticipated that the primary effect that these mechanisms have is to enhance the depth from which electrons can escape thereby increasing the yield for secondary emission.

In region two the slope of the yield versus surface potential curve is twice that of region one. This increase can be attributed to the continuing yield enhancement mechanism of region one but with an increasing fraction of the secondary electrons undergoing multiplication by a factor of two.

Jacobs et al[9] have found that magnesium oxide secondary emission layers exhibit similar field enhanced secondary emission yields. Their results indicate that yields as large as 10,000 to 1 are possible with MgO. The mechanism responsible has been attributed to an avalanche type process. As the surface of the dielectric film is bombarded with primary electrons the surface is charged to a high potential. This produces a high field within the dielectric and electrons released within the material can then gain enough energy to liberate additional electrons.

Experimentation using KCl and MgO secondary emission film has been initiated to investigate the possibility of employing these secondary emission electrons to increase the neutron image intensity in a radiograph.

Consider the experimental conditions for evaluation of this phenomenon as it is applied to the neutron radiographic process.

3.2. Experimental Conditions

The Radiography Apparatus

The two essential items required to obtain a neutron image are a source of neutrons and a detector to translate the transmitted neutron beam into an observable image.

Neutron Source

The reactor facility at McMaster University has been found to be a good source of neutrons for radiographic work. A vertical through-tube of cadmium having a length of approximately 25 feet is used to transport thermal neutrons near the reactor core to the experimental area. The resulting neutron beam is well collimated and has a useful beam diameter of approximately 2.5 inches.

The neutron beam intensity can be varied by raising or lowering the water level in the vertical through-tube as indicated in Fig. 18. The beam intensity is measured in terms of the level of radiation as observed using a SNOOPY neutron detector. The detector is placed on the floor of the experimental deck with its active surface in contact with the wall of the vertical through-tube. The radiation level at this surface increased as the water level in the vertical through-tube is lowered. Typical operating radiation levels for neutron radiography experiments are in the range 20 to 25 mR/hr. These levels have been found adequate for this investigation and exposures of approximately two minutes yields radiographs

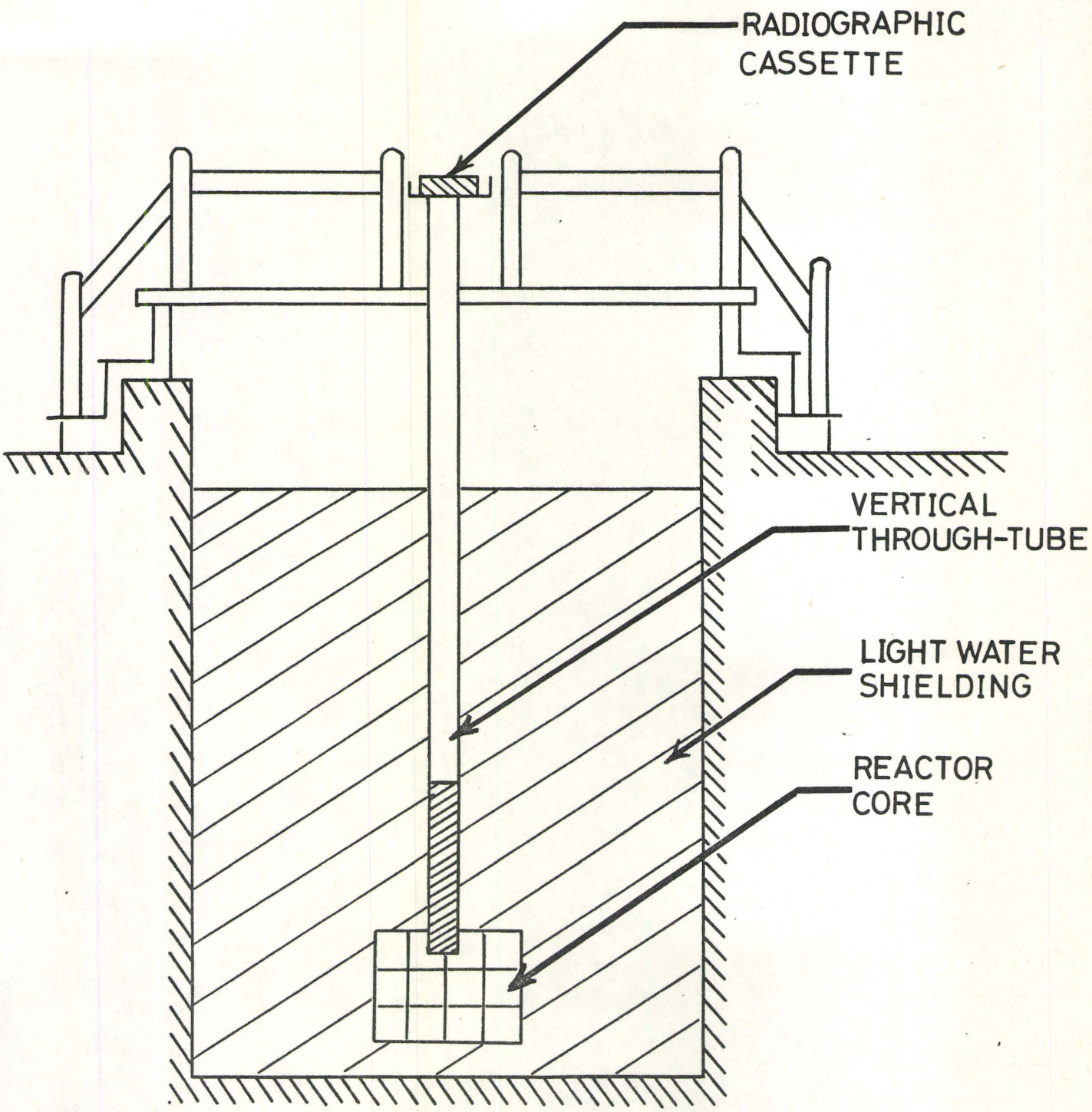

FIG. 18. Schematic of the neutron vertical through-tube radiography facility at the McMaster reactor.

with adequate film blackening.

Imaging Apparatus

The actual radiographs are obtained using a vacuum type x-ray film cassette. This cassette is commercially available by the name VAC-K-Set and can be evacuated to 30 mm of Hg.

The Cassette is loaded with x-ray film suitable for neutron radiographic applications; Kodac type AA double sided film has been used for these experiments. The cassette is also fitted with the gadolinium converter screen containing the appropriate secondary emission layer. Field plates of aluminum are also placed inside the cassette. These plates are used as electrodes to create surface charges appropriate for the secondary emission layers. An illustration of the cross-sectional view for a loaded cassette is shown in Fig. 19. The field plates are connected to a power supply (3KV range) to create a static electric field. A cardboard mask is placed between the x-ray film and the field plate as illustrated for two reasons. The mask protects the secondary emission layer from the x-ray film when a vacuum is introduced into the cassette. It also serves to decrease the applied electric field in the volume between the plates except in the region containing the converter and secondary emission layer.

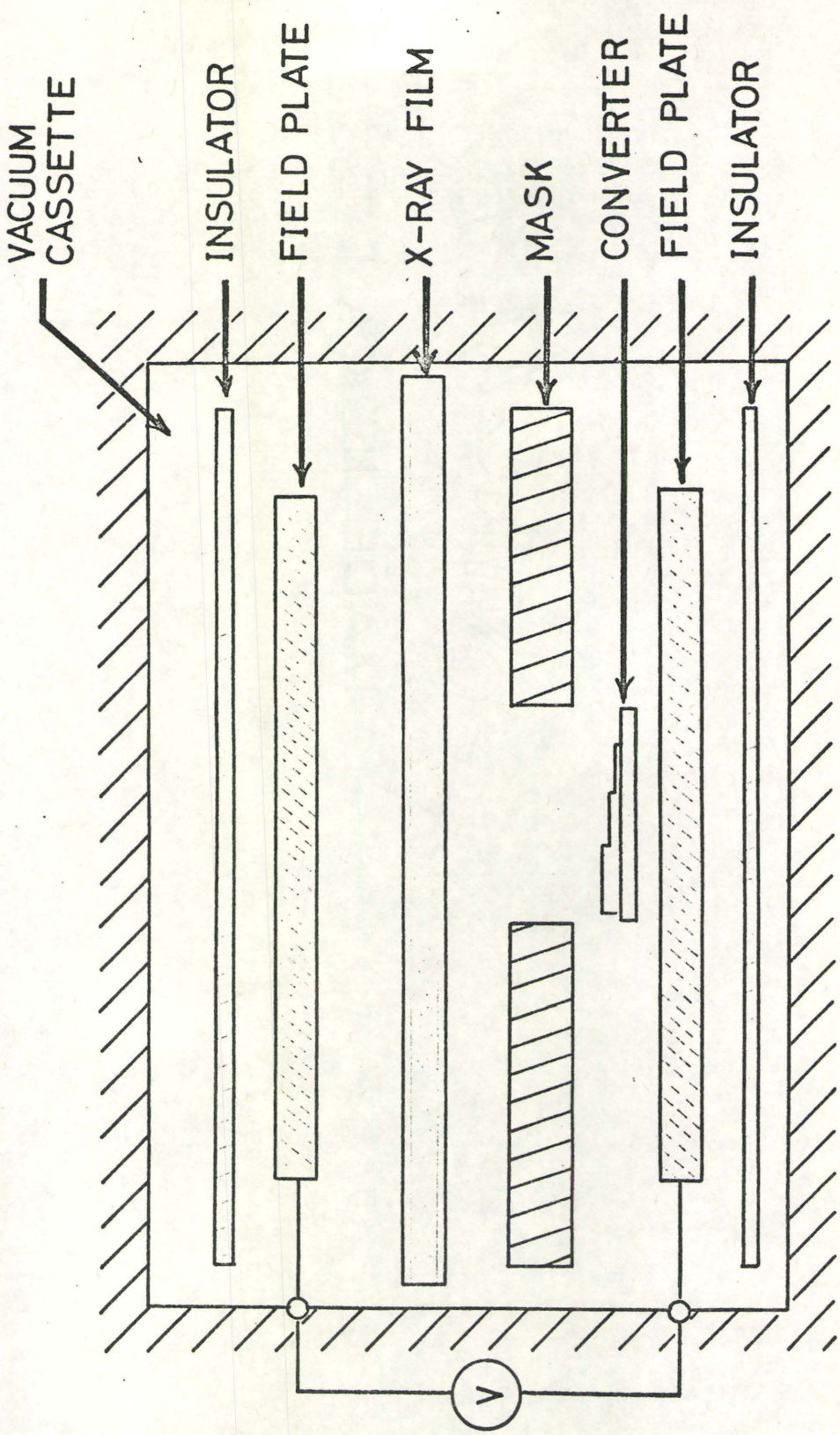

FIG.19. Cross sectional view of a loaded radiography cassette.

The Secondary Emission Converter

The converter for these experiements consists of a substrate of natural gadolinium metal and a secondary emission layer of either magnesium oxide (MgO) or potassium chloride (KCl). The gadolinium substrate is a foil having dimensions of 2.5 centimeters square and a thickness of approximately 25 microns.

The secondary emission layer is vacuum deposited onto the substrate. The surface of the gadolinium is first prepared by depositing a thin layer of aluminum less than 100 angstroms thick. This layer is then oxidized to provide a layer of aluminum oxide that is to increase the adhesion of the secondary emission layer to the gadolinium substrate. The secondary emission layer is deposited to have a deposited density in the range 0.10 to 0.25 per cent of the normal material density.

Various thicknesses of the secondary emission layer can be achieved on a single gadolinium substrate. This is done by first depositing a layer of the material over most of the substrate surface, and then masking off a band of substrate so that any subsequent depositions do not occur in that band. In this way several bands of different thicknesses for the secondary emission layer can be achieved. An example of the secondary emission converter produced using this technique is illustrated in Fig. 20. In this converter there are three different thicknesses of magnesium oxide material. One band consists

of a single deposited thickness of the magnesium oxide while a second band consists of double the thickness and the third band is three thicknesses of deposited magnesium oxide. Such a converter can be used to evaluate the effect of thickness of the secondary emission layer independent of experimental variables such as exposure time and neutron flux.

Now consider the techniques that have been used in evaluating the conversion enhancement obtained with the secondary emission converter.

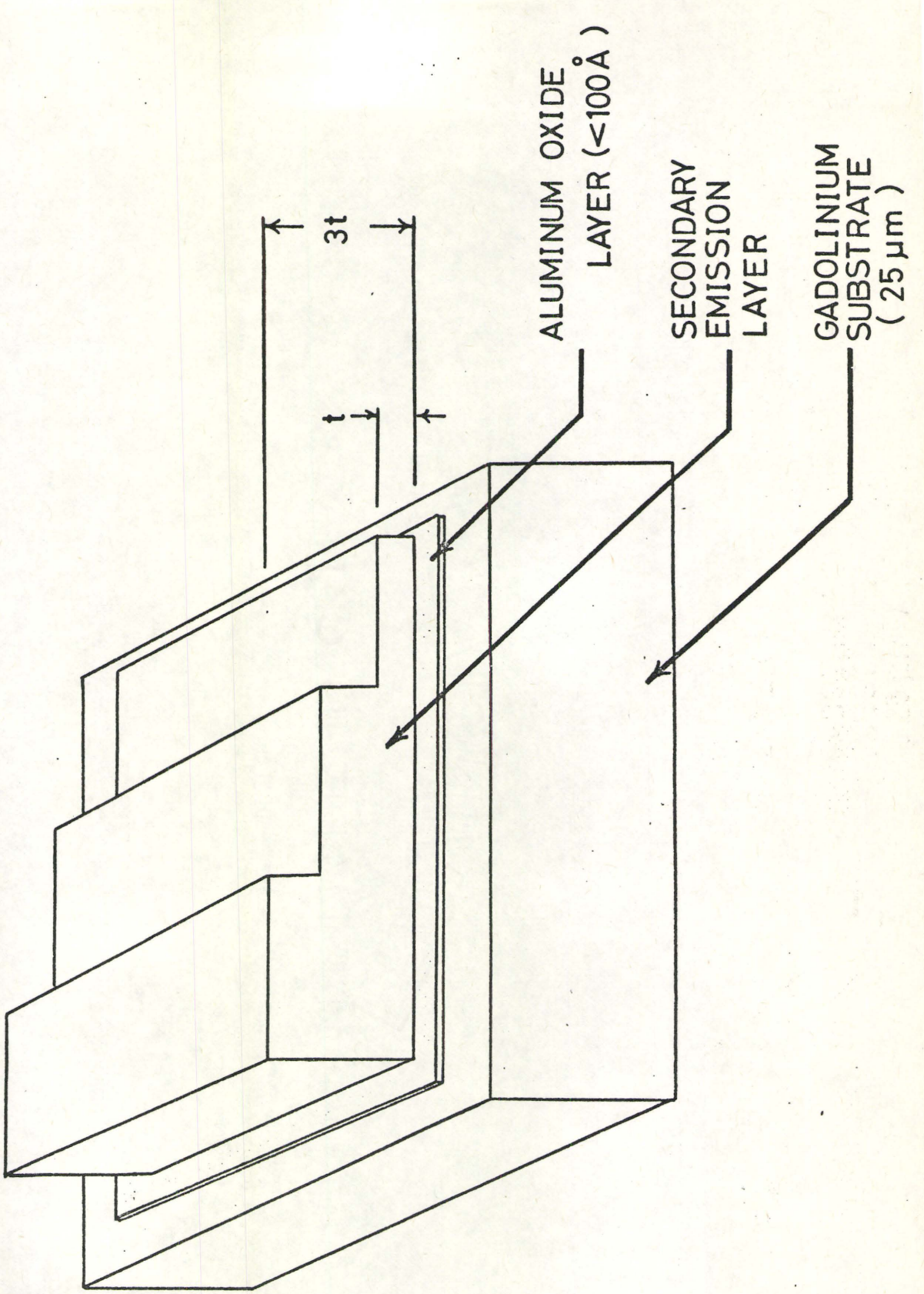

FIG. 20. Illustration of the Secondary Emission converter.

3.3. Enhancement Evaluation Techniques

3.3.1. Process for Obtaining a Radiograph

A standardized approach for obtaining the radiograph was developed to minimize the effects of variation in experimental parameters that can be introduced from one exposure to the next. One of the most critical parameters that should be kept constant when a comparison of exposures is required is the exposure time.

A routine for placing the cassette onto the holder in the neutron beam, turning on the high voltage for the static field, exposing under high voltage, turning the applied voltage off and removing the cassette from the beam was determined. An evaluation of exposure times with a "SNOOPY" radiation level of 20-25 mR/hr on contact with the vertical through-tube wall revealed that a total exposure of 2.0 minutes was adequate for converter enhancement evaluation. It was also found that 15 seconds was required for incrementing the high voltage power supply to the maximum required value. Injection and removal time of the cassette to and from the neutron beam was neglible compared to the total exposure time. This left 1.5 minutes for exposure at the designated field conditions.

The x-ray film was loaded and unloaded in dark room facilities in the reactor hall. Facilities for producing

a vacuum of 29-30 millimeters of mercury were also installed in this dark room so that the entire loading process could be achieved in a minimum of time. The exposures for each experiment were processed as a batch to minimize variations introduced by different developer conditions.

The resulting radiographs had light areas and dark areas depending on the neutron-electron interactions in the gadolinium substrate and the electron-electron interactions in the secondary emission layers. These radiographs must be evaluated to determine the enhancement obtained.

3.3.2. Radiograph Evaluation Technique

A typical radiograph is illustrated in Fig. 21. Without the converter a background beam shape as indicated in Fig. 21(a) is obtained. This shape is determined by the cadmium vertical through-tube. The image is produced by interaction of neutrons with the film and through (n,γ) reactions that occur when neutrons pass through the x-ray cassette. When the converter screen is used additional film blackening is produced.

Some care must be taken in evaluating the degree of film blackening that is caused by a difference in the converter composition. It has been observed that the background beam does not produce a uniform blackening over the entire shape of the beam. A way to overcome this problem when comparing the same area of different radiographs is illustrated in Fig. 21(b).

The process is based on the fact that once the beam shape has been defined, it remains relatively constant. The beam changes shape only if the position of the vertical through-tube is altered; this position is not altered for normal operating conditions.

Reference points or areas can be defined on the radiograph to be investigated relative to the beam shape. The intensity of a transmitted light beam at these reference points or areas can then be compared from one radiograph to the next.

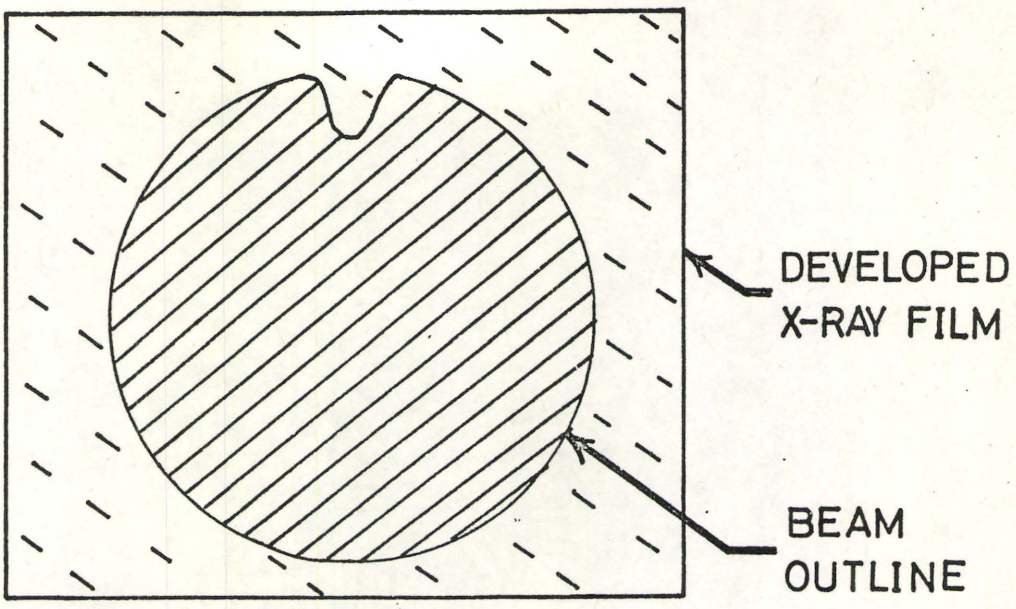

(A) ILLUSTRATION OF BACKGROUND BEAM SHAPE

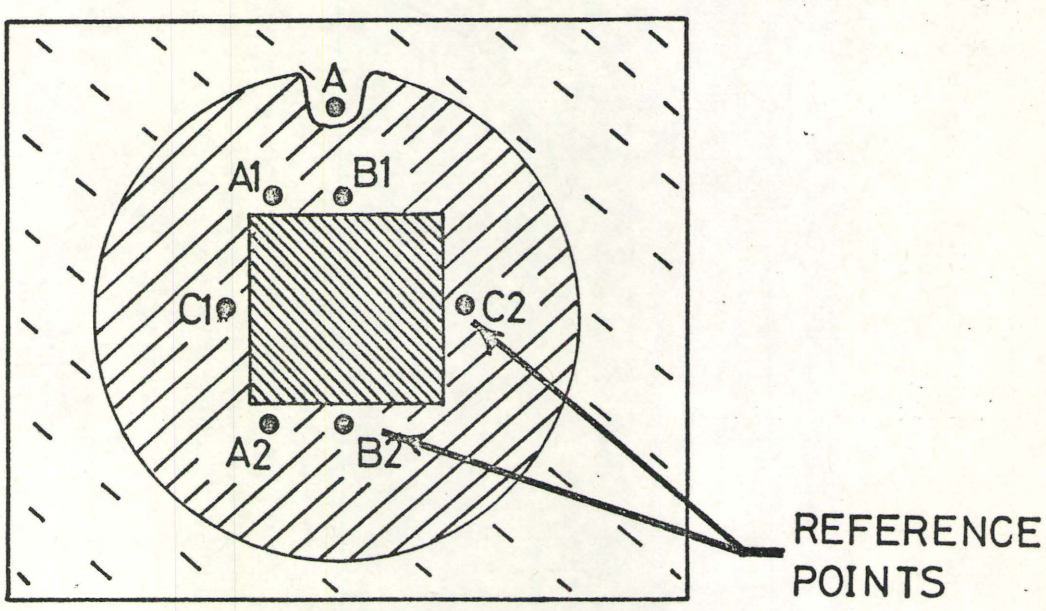

(B) REFERENCE POINTS ARE PLACED ON EACH RADIOGRAPH TO BE EVALUATED.

FIG. 21. Illustration of an exposed neutron radiograph.

Transmission intensities can be measured quickly by using a portable densitometer on a light box. The position "A" in Fig. 21(b) is used as the unity transmission reference point.

A more accurate way of measuring the intensity of a transmitted light beam is to employ a scanning microscope densitometer with a strip chart recorder. Two techniques for comparing radiographic results on the scanning densitometer have been developed. They are:

(1) Reference Intensity Technique

(2) Scan Comparison Technique

Both techniques have some common features. If care is taken so that the film in the cassette is essentially in a constant position for all exposures and the cassette is in a fixed position relative to the neutron beam, then reference points such as A1, A2, B1, B2, C1 and C2 in Fig. 21(b) can be determined for each radiograph. Scans between reference points A1 and A2, B1 and B2 and C1 and C2 can be recorded and evaluated according to one or both of the techniques listed above. Consider now, the reference intensity technique.

Reference Intensity Technique

The microscope densitometer is set up to scan between the reference points. The gain of the densitometer is set at a constant value. The only adjustment

made in the densitometer system is the zero adjust on the strip chart recorder. The process for taking results then is

(1) Define reference points on radiograph.

(2) A reference density plate is positioned in the beam of the densitometer to indicate a relative zero position. The reference plate is then removed.

(3) The radiograph to be analyzed is placed in the densitometer beam and lined up for a scan from one reference point to the next. The radiograph is scanned.

(4) Should the strip chart recorder go off scale, an estimate of the compensation required to bring the pen back on scale is obtained. The reference density plate is put into the densitometer beam and the zero is adjusted. The new zero position is noted and the scan is repeated.

In this way a different technique can be employed to obtain relative density values for radiographs. This technique also enables comparison of densities in specific areas of the radiograph with more accuracy than using a portable densitometer.

Scan Comparison Technique

This method makes use of the reference points on the radiograph as well as the profile of the scan obtained using the reference intensity technique to obtain

data on densities of a particular radiograph referenced to another scan. The comparison is uaually made between a background scan taken from a radiograph made without a converter in the cassette and the radiograph under investigation. When comparing scans, the most important features to be considered are:

(1) Area of the scan representing the background-converter interface (i.e. the rise and fall edges of the scan).

(2) Peaks of the scan associated with the reference points.

(3) Background in the scan.

Once these items have been matched for each scan, then a comparison of the amplitudes of the density can be obtained for any region across the scan. Fig. 22 illustrates the application of this approach to comparing results. Two peaks on the scan are obtained for the reference points placed on the radiograph. The remaining contribution on the scan is due to the converter. The two reference peaks and the rise and fall edges of the converter contribution are matched for the traces to be compared. Then a comparison of the scan amplitudes for the different areas of the converter can be directly determined.

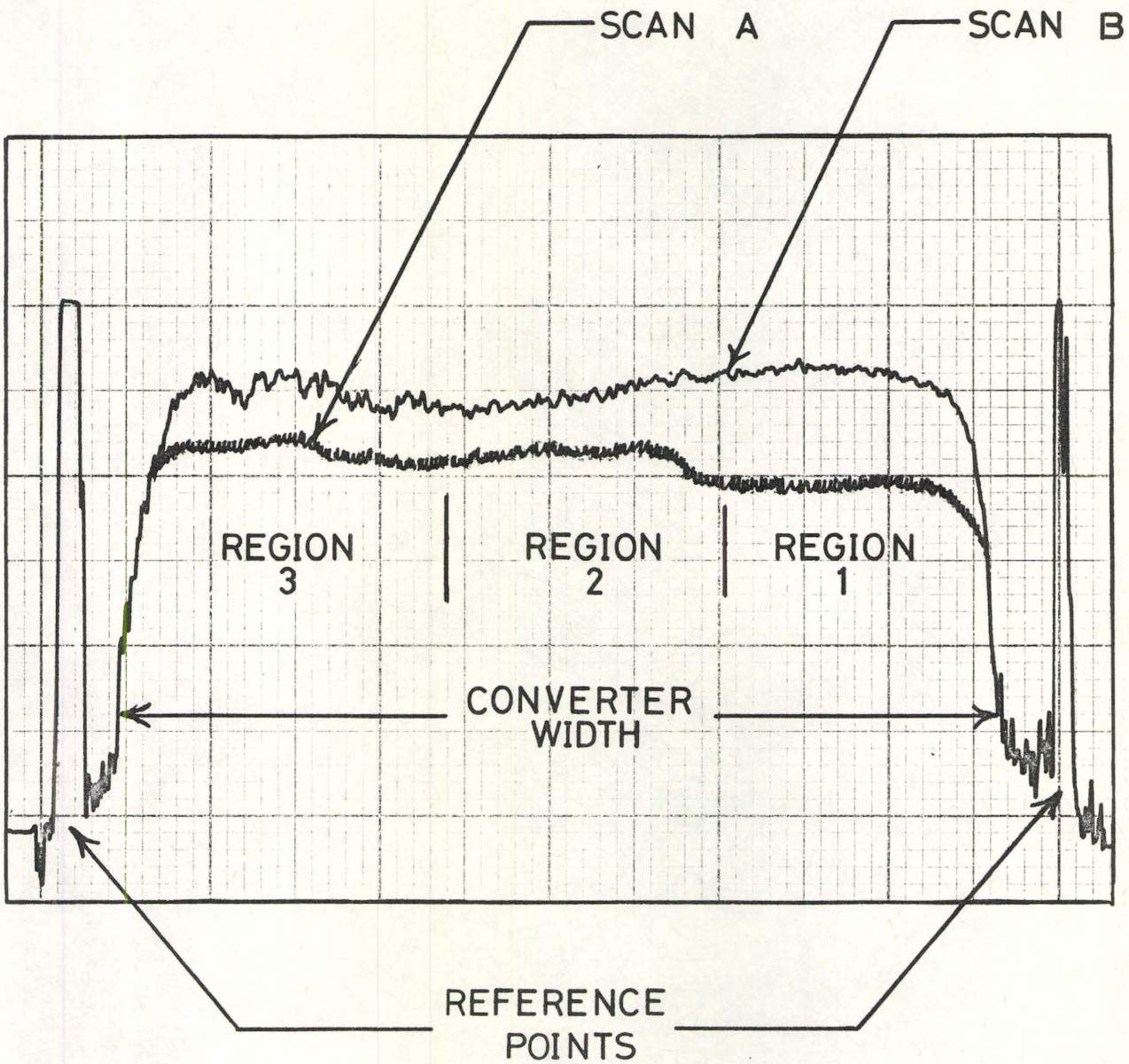

FIG. 22. Illustration of Scan Comparison technique.

3.4. Results

3.4.1. Magnesium Oxide Coated Converters

The gadolinium magnesium oxide converter was investigated with reference to thickness of MgO coating and applied electric field. The MgO coating had three areas of different thicknesses similar to the converter illustrated in Fig. 20. The exact thickness of each layer was not known but the ratio of layer thickness was approximately 1 : 2 : 3. A comparison of this coating with subsequent MgO converters indicated an approximate thickness of the layers to be 5 : 10 : 15 μm.

3.4.1.(a) Positive Applied Potentials

A series of exposures were taken with a positive potential applied to the field plate containing the Gd MgO converter as indicated in Fig. 19. A plot of the optical density for the MgO layers as measured with the portable densitometer versus the applied potential is found in Fig. 23. The density recorded for region one corresponds to an area of the converter where the MgO layer had fallen off and the Gd substrate was exposed. Region two was an area in the band containing three thicknesses of MgO and region three was in the band containing one thickness of MgO.

All curves of density versus positive applied potential produced negative sloping results. The

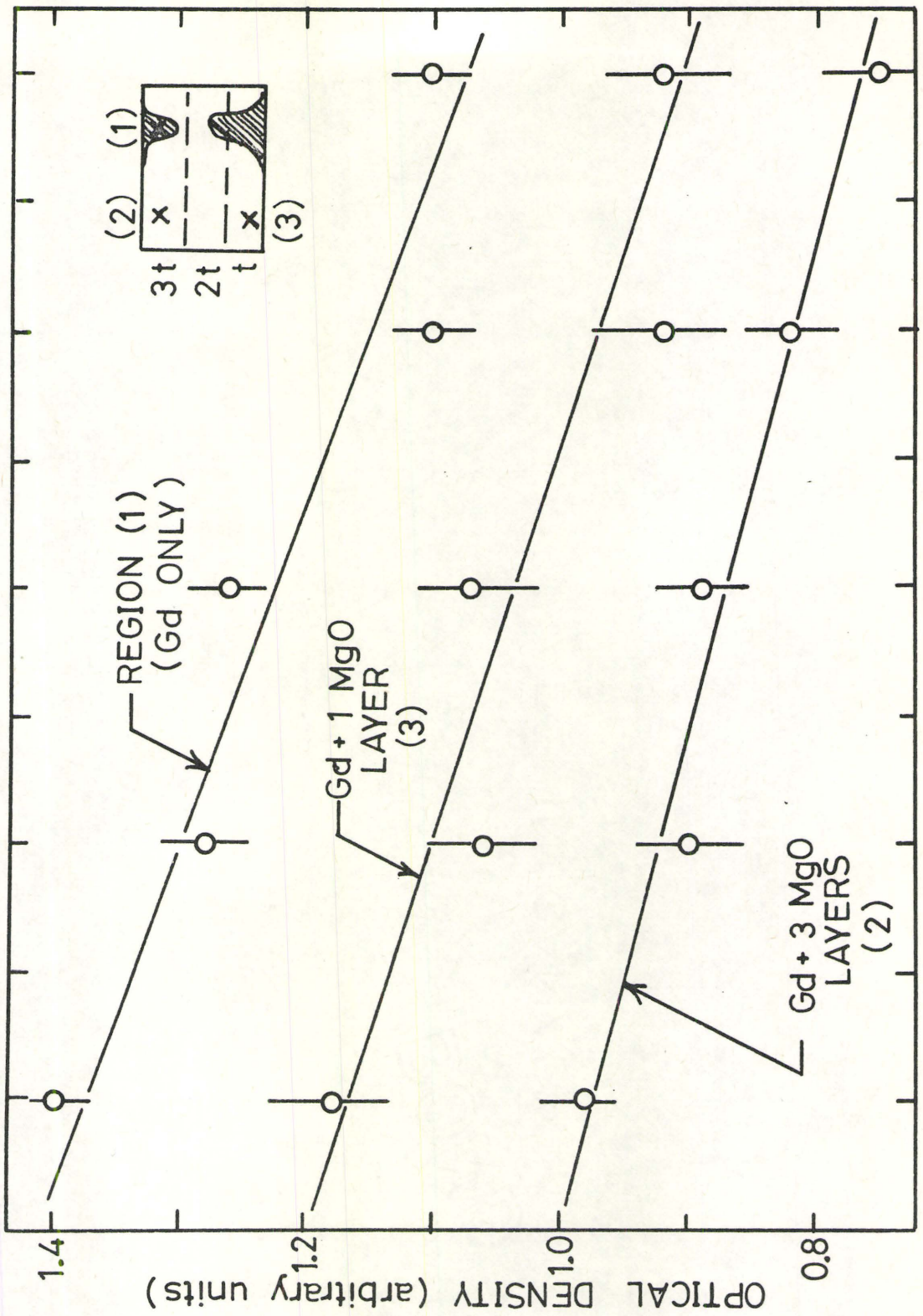

FIG. 23. Radiograph optical density (as measured with Portable Densitometer) for different thicknesses of MgO layers on a Gd substrate.

density as a function of MgO thickness also produced a negative sloped curve. However, the density using the portable densitometer contains background contributions as well. If this contribution is not uniform over the entire converter, then a comparison of the density associated with the various MgO thicknesses can be misleading.

Density values were obtained using the reference point technique for the same series of radiographs. The results are shown in Fig. 24 for the range of applied potential of interest. The density is recorded in arbitrary units. In this case region one, two and three correspond to one, two and three thicknesses of MgO. The optical density depreciates with increasing converter thickness in these results as well. In the range 0 to 400 volts applied potential a small enhancement of the density is observed. However, for applied potentials greater than 600 volts a negative slope is again observed.

The same scans used in evaluating the radiographs using the reference point technique were subjected to the scan comparison technique. The results are shown in Fig. 25. Negative effects on the density are again observed when either the converter thickness or the applied potential is increased.

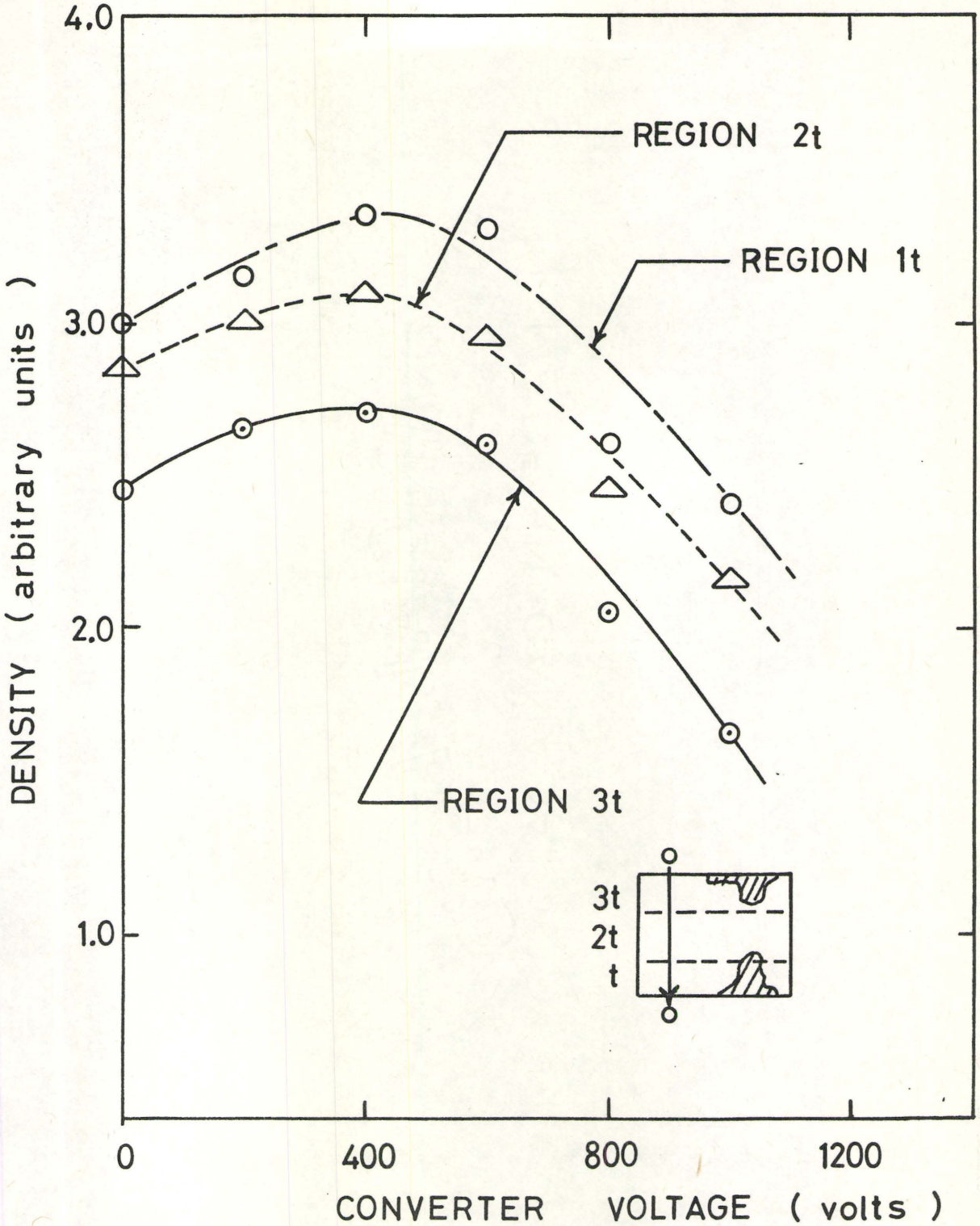

FIG. 24. Density values obtained for Gd-MgO converter using Reference Point technique and a positive potential applied to the Gd field plate.

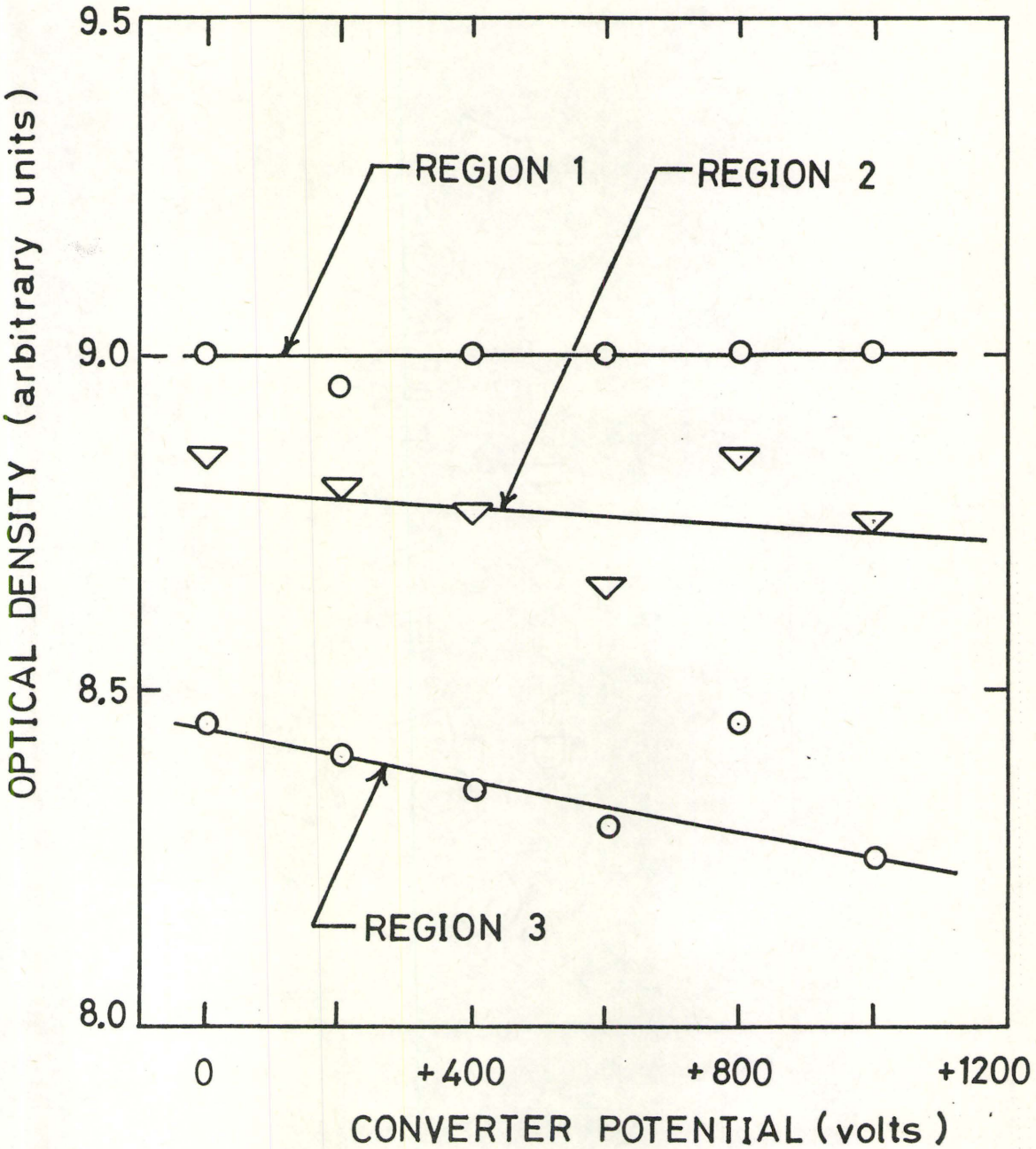

FIG. 25. Optical density values obtained for Gd-MgO converter using the Scan Comparison technique.

3.4.1.(b) Negative Applied Potential

The potential applied to the field plates was reserved and a second series of exposures were taken using the same Gd MgO converter. A plot of optical density as measured with the portable densitometer versus applied negative potential for the results is found in Fig. 26. Negative effects on the density with increasing MgO thickness and applied potential were observed.

The radiographs were also subjected to the reference point and scan comparison techniques. Results for the reference point approach (Fig. 27) indicates a peak in the optical density for all three MgO thicknesses in the 800 to 900 volt region of the applied potential. There is also a decrease in density with increasing converter thickness for these results.

Results for the scan comparison technique (Fig. 28) indicates a positive contribution to the effective optical density by the applied potential. The effective density at a potential of 1400 volts is nearly 10% better than for the zero voltage case. Better optical density is still obtained, however, with the thinner MgO coatings.

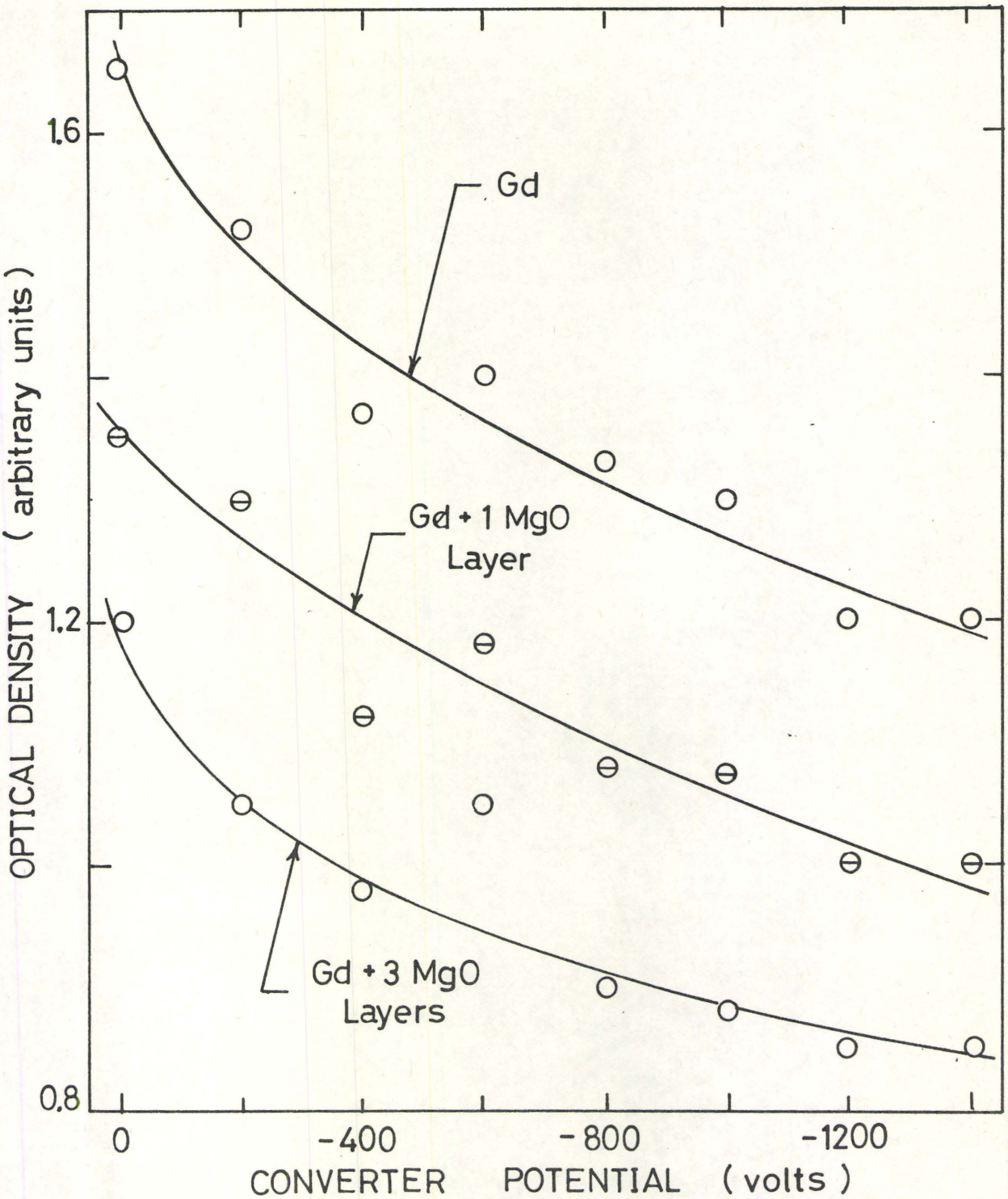

FIG. 26. Optical density as measured with portable densitometer for different thicknesses of MgO layers and a negative potential applied to the gadolinium substrate.

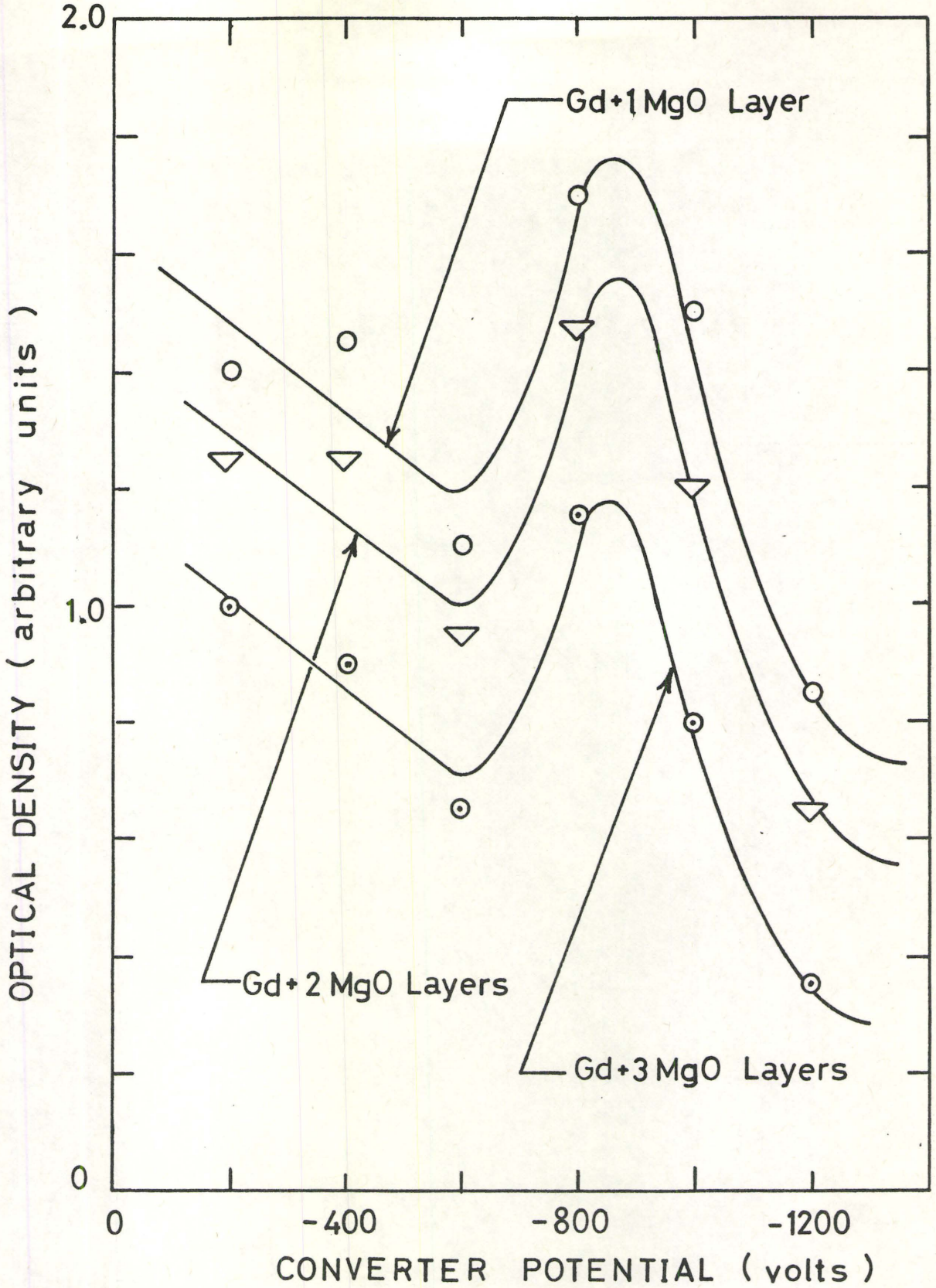

FIG. 27. Density values obtained for Gd-MgO converter using reference point technique and a negative potential applied to the Gd field plate.

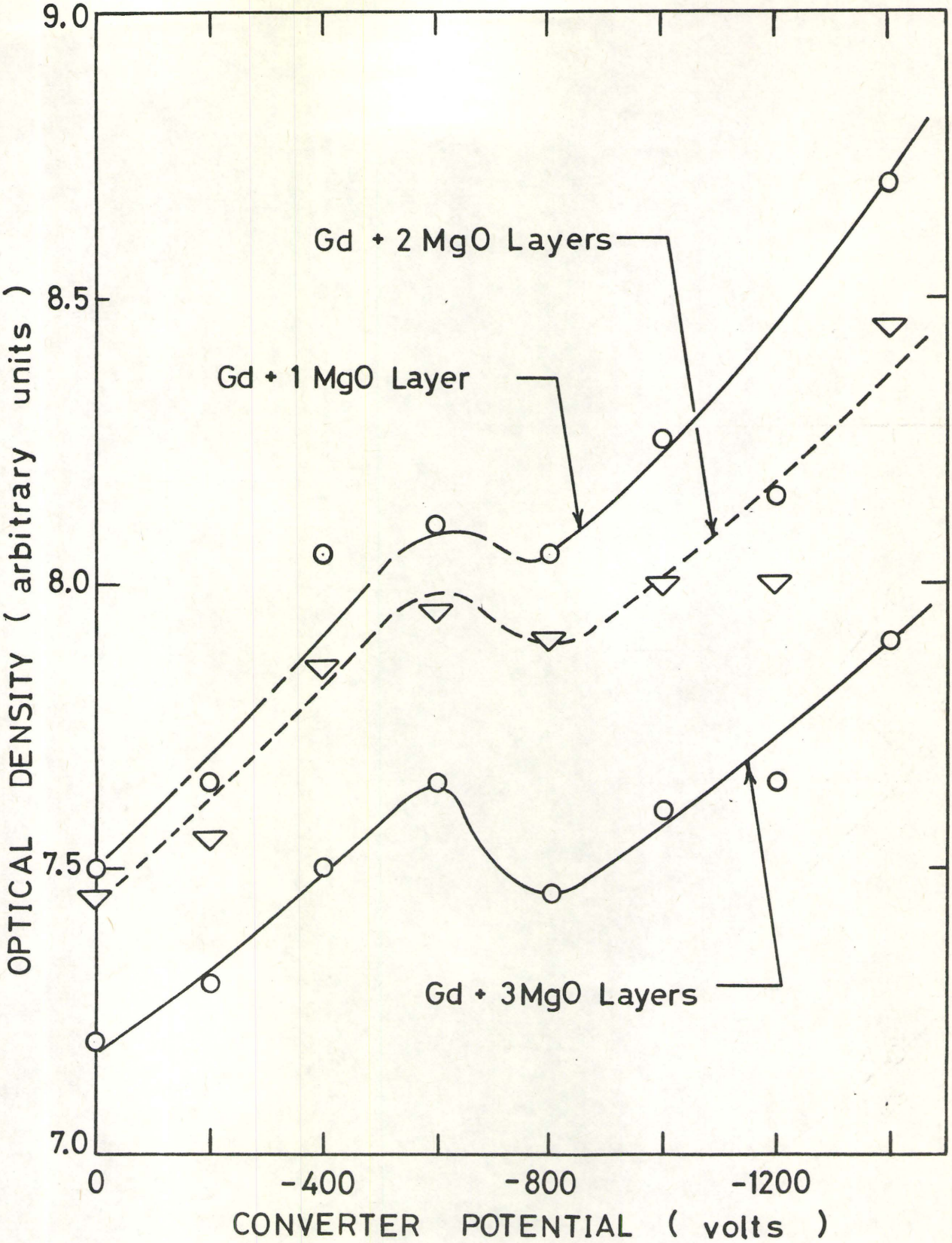

FIG. 28. Optical density values obtained for Gd-MgO converter using Scan Comparison technique and a negative potential applied to the Gd field plate.

3.4.2. Potassium Chloride Coated Converter

A piece of gadolinium about one square inch in area and an approximate thickness of 25 microns was used as the substrate for the KCl converter. Layers of KCl were deposited onto the gadolinium surface with a 0.1 - 0.25% of nominal density to produce a composite converter as shown in Fig. 29. Part of the converter was covered with a thin (0.5 to 2 μm) layer of aluminum to protect the KCl layer and retard the hygroscopic process that the salt coating is subject to.

The converter was installed in the vacuum cassette and neutron radiographs were taken for a series of applied field potentials. Both positive and negative voltages were applied to the field plate on which the Gd-KCl converter was mounted.

Readings of the density were obtained for four areas of the exposed radiographs using the portable densitometer. These areas are indicated in Fig. 29 and the results are shown in Fig. 30 for areas (1) and (2). The results indicate that there is no apparent consistency between applied voltage and radiographic density. However, when these results are plotted as a function of the number of exposures to the neutron beam (Fig. 31) a trend is observed. The density decreases linearly with exposure to the neutron beam. A possible reason for this effect is radiation damage in the KCl but only

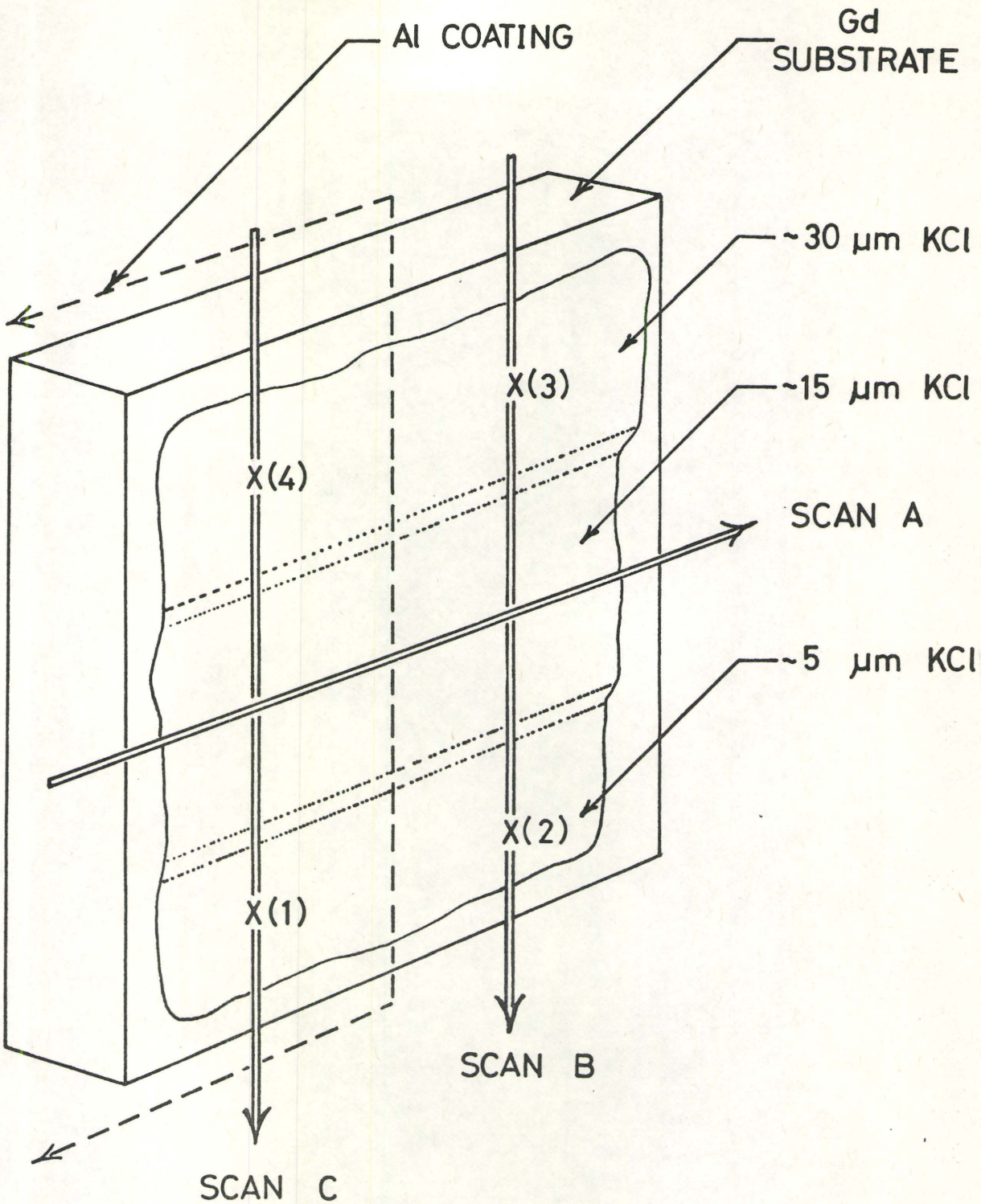

FIG. 29. Illustration of the Gd-KCl converter and the areas that were optically scanned.

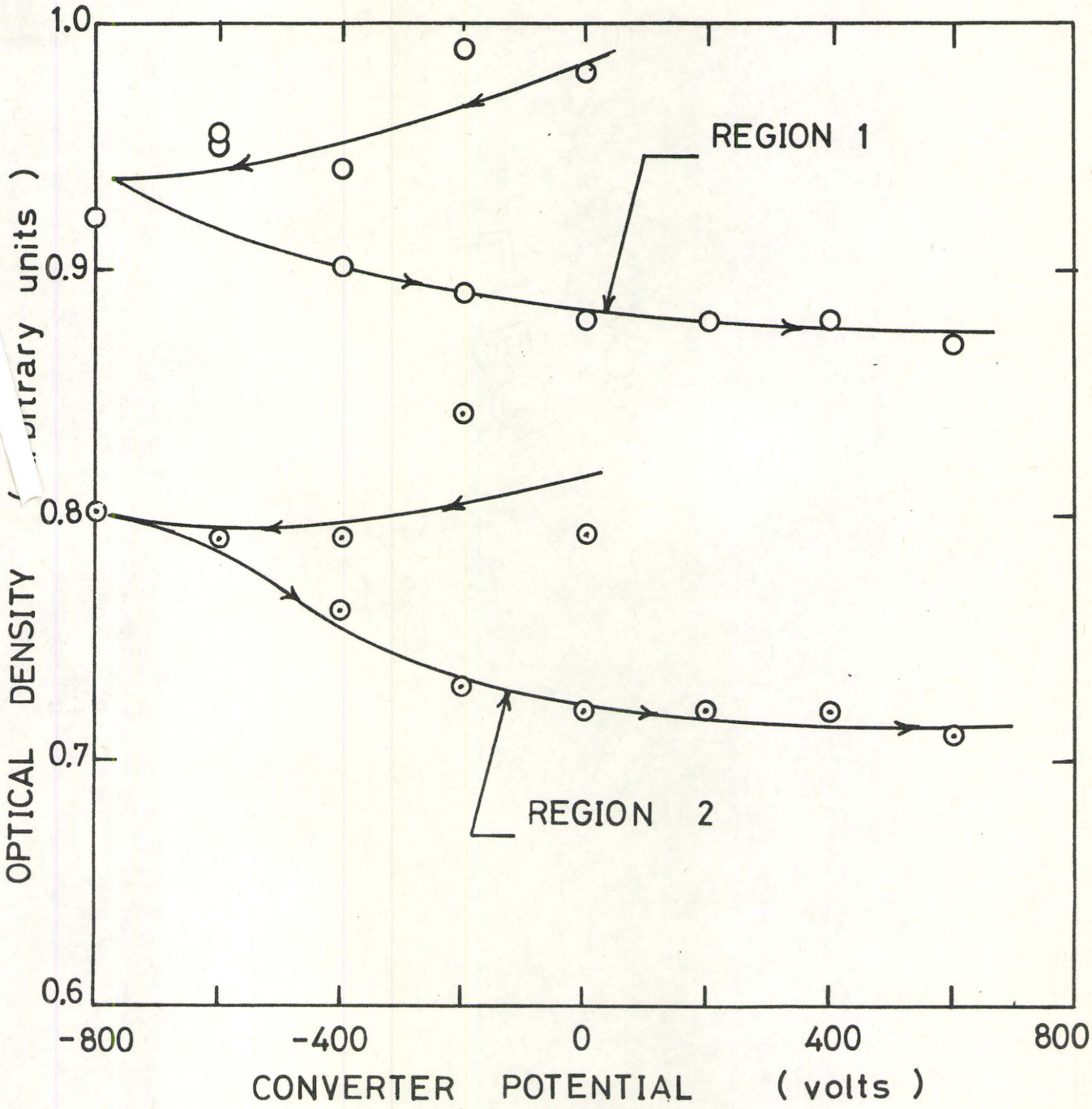

FIG. 30. Optical density for Gd-KCl converters as measured with the portable densitometer for range of applied potential relative to the Gd field plate.

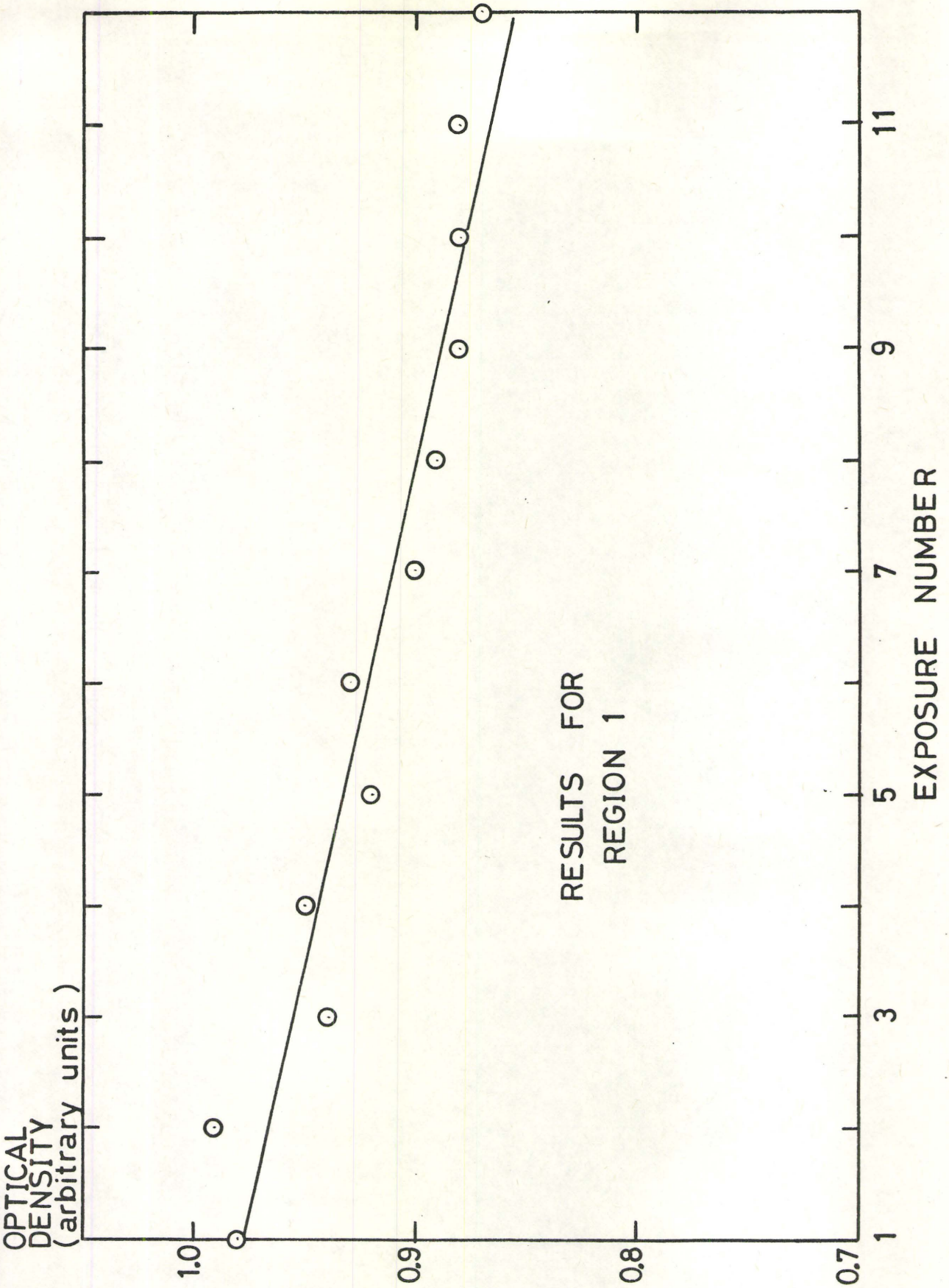

FIG. 31. Optical density for the Gd-KCl converter as a function of the neutron exposure number.

experimentation outside the scope of this paper can confirm this assumption.

Further evaluations were considered with this radiation effect noted. The scan comparison technique was used to evaluate the effect of the aluminum protective coating on the density. Results for a scan across the middle region of each radiograph that corresponds to "scan A" indicated in Fig. 29 are shown in Fig. 32. The ratio of densities for no coating/coating was used to compensate for the effect of neutron exposure. There is a peak in the density ratio for an applied voltage near 600 volts. The ratio is greater than unity indicating that the extra aluminum coating has a detramental effect on the optical density.

Further scans on the radiographs were done to investigate the effect of KCl thickness on the optical density. A scan across the three KCl thicknesses in the region of the converter with no protective aluminum coating (scan B in Fig. 29) revealed a positive contribution to optical density with increasing KCl thickness. As indicated by the results (Fig. 33) there is also a positive contribution to the optical density due to the applied potential. A peak in the density ratio was observed with a negative applied potential of 600 volts.

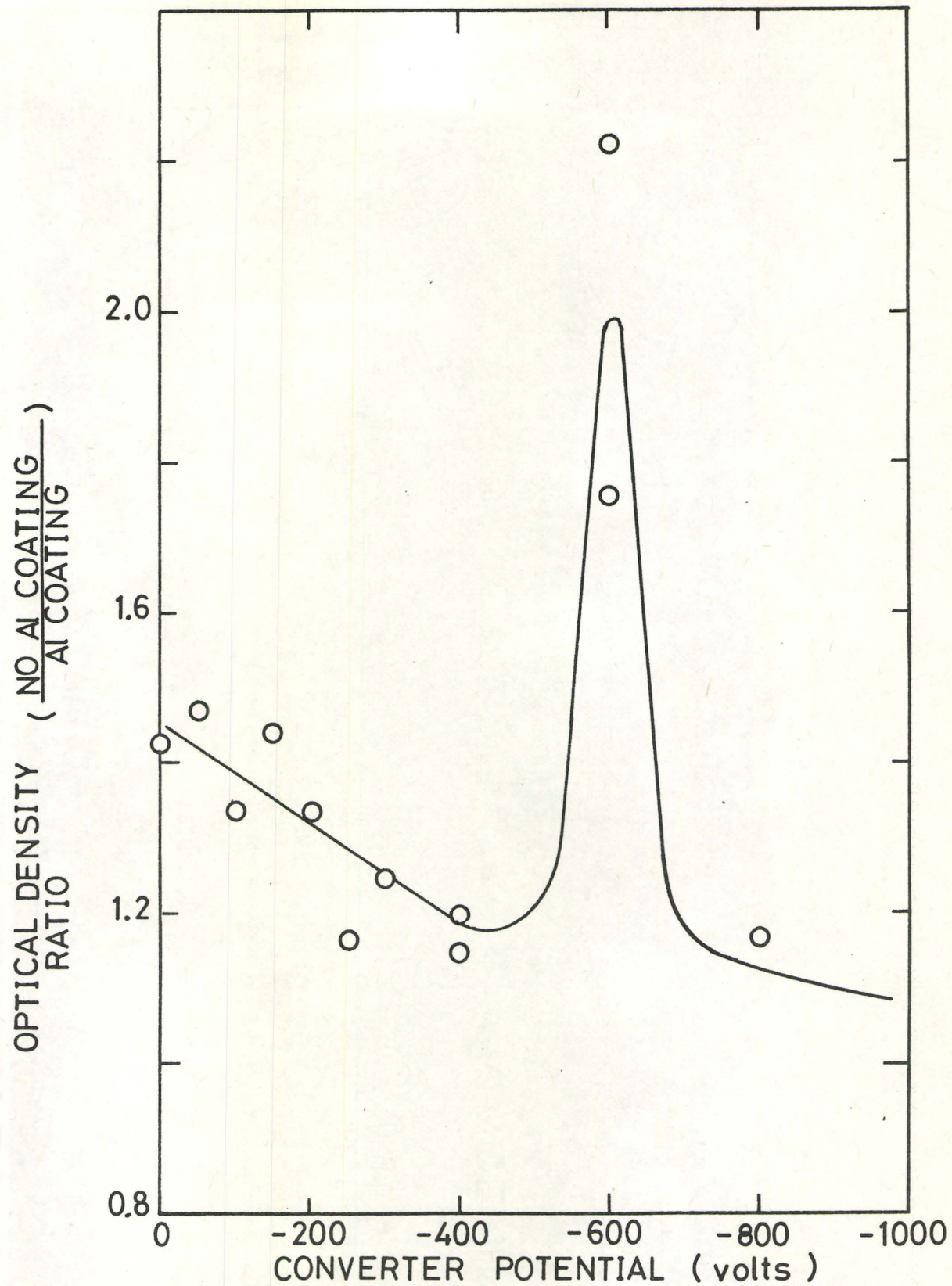

FIG. 32. Effect of Al protective coating on Gd-KCl converter.

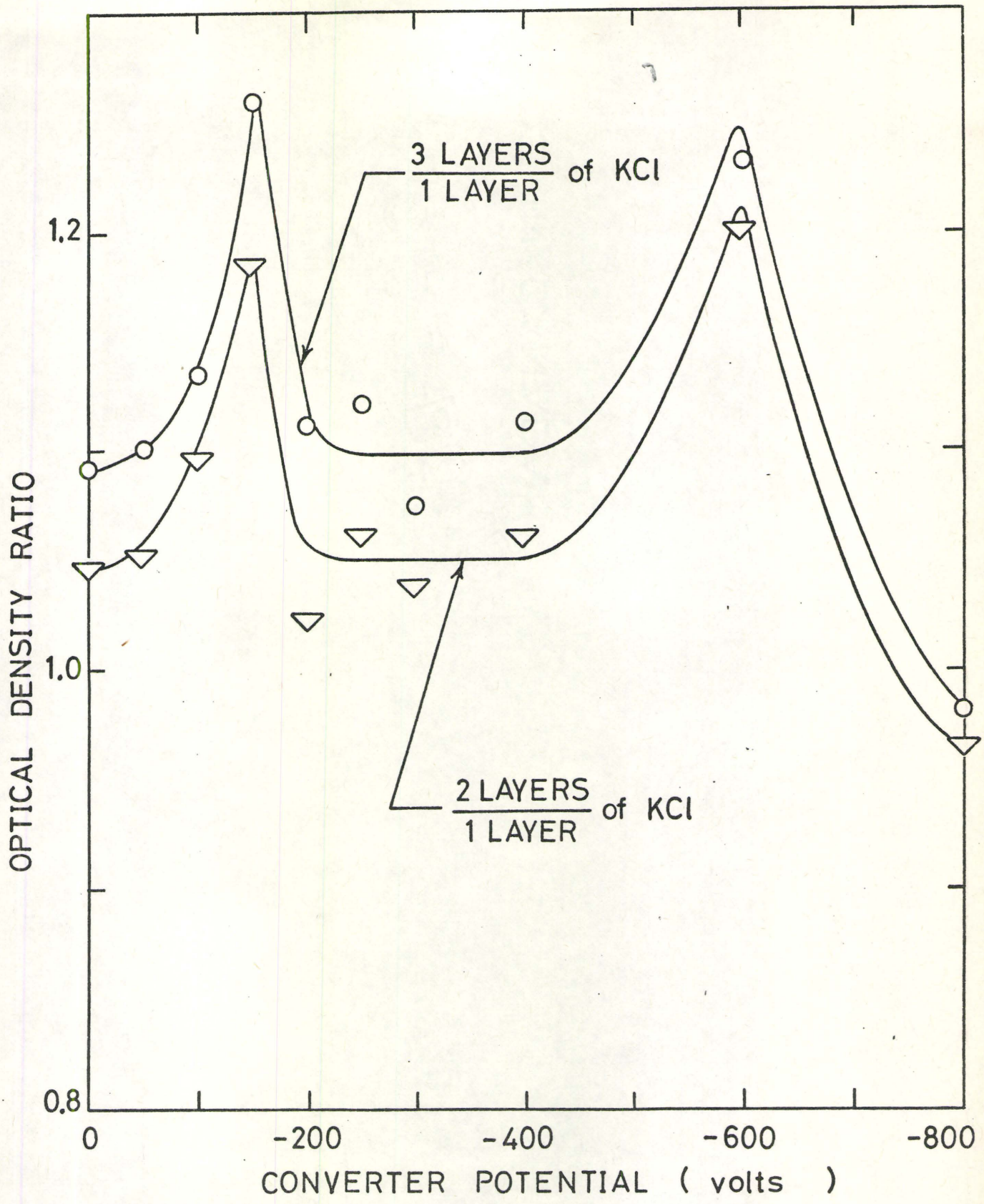

FIG. 33. Effect of KCl thickness on Optical Density for a Gd-KCl converter with no protective Al coating.

Similar calculations were done for a scan across the three KCl thicknesses in the region of the converter with the protective aluminum coating. These results also indicate a positive contribution to the optical density with increasing KCl thickness. However, results for the effect of the applied potential on the optical density (Fig. 34) are scattered to the point where any correlation between applied potential and optical density is minimal. This can be eliminated in future experimentation by omitting the protective aluminum coating on the KCl layers.

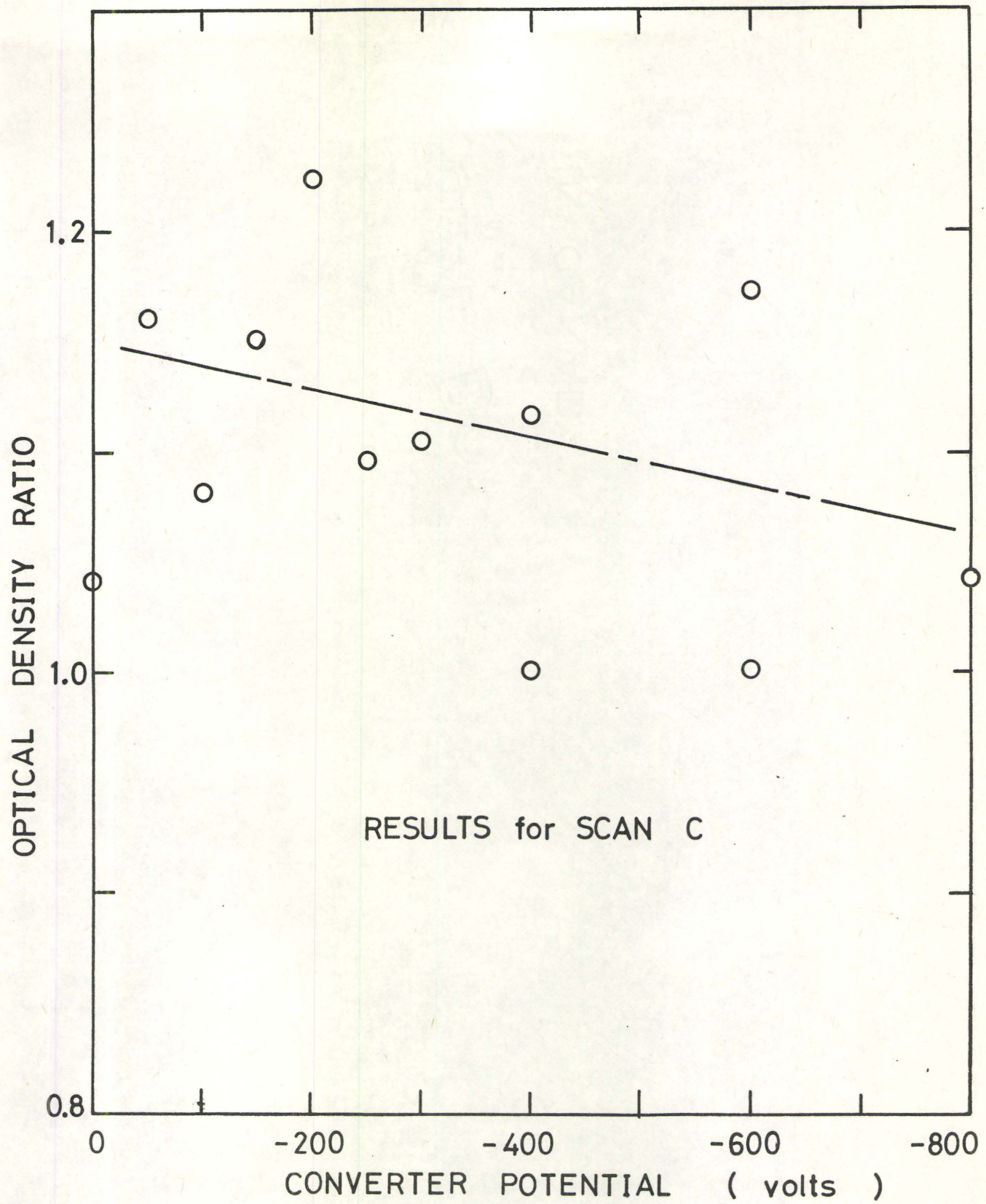

FIG. 34. Optical density of region with 3 layers of KCl relative to the density in the one layer region for a range of converter potentials and Al protective coating.

4. SUMMARY AND CONCLUSIONS

The possibility of enhancement in radiation conversion has been investigated for two approaches. One approach deals with a theoretical evaluation of enhancement for a converter with isotopic and density variations.

A model for the radiation conversion was generated and the model was used to evaluate the enhancement for linear variations in electron linear attenuation coefficients and neutron cross-sections with respect to position in the converter. The results for several different converter configurations revealed that enhancements in excess of 100 per cent were theoretically possible. The largest enhancements were predicted for converters with high neutron cross-sections and low electron attenuation coefficients. A positive contribution to enhancement was also observed when the converter thickness was increased from 6 to 25 μm for all configurations except the converter with increasing neutron cross-section and decreasing electron linear attenuation coefficient with penetration into the converter (Case 3). Enhancement for this configuration had a maximum value of 1.19 for a converter 5 μm thick.

The remaining configurations reach their asymptotic (maximum) enhancement for converters near 15 μm in thickness. The model predicts that converters of 15 μm thickness should have the same enhancement as thicker converters.

These results can be used to optimize a converter for enhancement. The converter should have as large a neutron cross-section as possible on the incident edge of the converter. The converter should have a minimum electron attenuation and a thickness of 15 to 20 μm. Then , depending on the space dependence of the various parameters, the converter should be capable of enhancements from 60 to 100 per cent over the present state-of-the-art converter.

A second approach to enhancement in radiation conversion has been based on the field-enhanced secondary emission mechanisms. Low density MgO and KCl layers on a natural gadolinium substrate were evaluated experimentally for enhancement. The degree of enhancement was based on the amount of optical density observed in the exposed neutron radiographs. The MgO-Gd converters were found to have a positive optical

density enhancement for increasing field values. However, a negative effect on enhancement was observed for increasing MgO thicknesses in the range 5 μm to 15 μm. The KCl-Gd converters showed a positive enhancement for increasing values of KCl thickness. Optical enhancements of 0.5% per μm were observed for KCl thicknesses in the 5 μm to 30 μm range. The effect of an applied electric field on the KCl-Gd converter was to produce enhancement at two potentials. A peak in the optical density was observed at 150 volts and another was observed at 600 volts. An increase in optical density of 18% was observed for the peaks. The effect of placing a thin protective layer of aluminum on the KCl coating proved to be disastrous for optical density enhancement. The ratio of optical densities for no coating to coating of aluminum was 2.2 for the 600 volt peak in the density curves. This effect indicates that the secondary electrons emitted from the KCl coating could be of very low energy, possibly in the electron volt range.

REFERENCES

5. References

1. H. Berger, "The Present State of Neutron Radiography and Its Potential", The President's Honour Lecture, Non-destructive Testing Society of Great Britain, Sept. 9, 1971.

2. L. W. Dalke, "Neutron Radiography - Its Capabilities, Limitations and Applications", N.E. 599, December 6, 1967.

3. H. Berger, "Now N-Rays Show What X-Rays Can't", Popular Science, June 1971.

4. M. Mullner and H. jex, "Converter Thickness for Optimum Intensity in Neutron Radiography", Nucl. Inst. Meth., 103, 229 (1972).

5. A.A. Harms and G.R. Norman, "The Role of Internal Conversion Electrons in Gadolinium-Exposure Neutron Imaging", J. Appl. Phys., 43, 3209 (1972).

6. B.K. Garside and A.A. Harms, "Detection Process in Neutron Radiography", J. Appl. Phys., 42, 5161, (1971).

7. J.R. Lamarsh, Introduction to Nuclear Reactor Theory. New York: Addison-Whesley, 1966.

8. A.A. Harms,B.K. Garside and P.S.W. Chan, "Edge-Spread Function in Neutron Radiography", J. Appl. Phys., 43, 3863 (1972).

9. H. Jacobs, J. Freely and F. Brand, "The Mechanism of Field Dependent Secondary Emission", Phys. Rev., 88, 492 (1952).

10. D. Dobischek, H. Jacobs and J. Freely, "The Mechanism of Self-Sustained Electron Emission from Magnesium Oxide", Phys. Rev., 91, 804 (1953).

11. J. Johnson and K. McKay, "Secondary Electron Emission of Crystalline MgO", Phys. Rev., 91 582 (1953).

12. E. Garwin and J. Llacer, "Mechanism of Secondary Emission and Single-Particle Statistics from Low-Density Films of Alkali-Halides", J. Appl. Phys., 41, 1489 (1970).

References (continued)

13. Hideo Ito and Shigetomo Yoshida, "Energy Distribution of Transmitted Secondary Electrons from Porous KCl Films", Japanese J.Appl. Phys., 11, 1454 (1972).

APPENDIX A

FORTRAN STATEMENTS
for
CONVERSION ENHANCEMENT PROGRAM

```
      PROGRAM TST (INPUT,OUTPUT,TAPE5=INPUT,TAPE6=OUTPUT)
      COMMON SIG0, SIG1, ALPHA1,ALPHA0
      EXTERNAL FJN
C
C-----------------  VARIABLE COMPOSITION CONVERTER  -----------------
C
      SIG0=1.
      ALPHA0=0.3
802   CONTINUE
      WRITE(6,100)
100   FORMAT(1H1,15X *  NEUTRON RADIOGRAPHY      DALTON MOLSON  *)
102   FORMAT(1H0,///  )
C
C-----------------  ALL LINEAR UNITS ARE IN MICRONS  -----------------
C
C ------------    ZR IS THE REFERENCE CONVERTER LENGHT -----------------
      ZR=25.4
      SIGC=0.14
      ALPHAC=0.20
      Z=6.35
      SIGMAX=1.
      ALMAX=0.30
800   CONTINUE
C
C
      WRITE(6,301)
      WRITE(6,302) ALPHAC, SIGC, ALPHA0, SIG0 ,Z
      WRITE(6,500)
500   FORMAT(1H0,6X≠ALPHA1≠3X≠SIG1≠6X≠FIFTH≠9X≠RUM≠7X≠NO≠4X≠Y≠4X
     1  ≠ALPHAT≠3X≠SIGT≠ 5X≠PSI≠  //  )
      SIGMIN=-SIG0/Z
      ALMIN=-ALPHA0/Z
      DALPHA=ALMAX/( 5.*Z)
      DSIGMA=SIGMAX/(20.*Z)
      A=0.
      BIG=Z
      ERROR=0.1E-06
      ALPHA1=(ALMAX-ALPHA0)/Z
3     CONTINUE
      ALPHAT=ALPHA0+ ALPHA1*Z
      SIG1=(SIGMAX-SIG0)/Z
C
C ----------------  CALCULATE CONSTANT C1 AND C2  -------------------
C
      C1A=SIGC+ALPHAC
      C1B=(1.-EXP(-C1A*ZR))*SIGC
      C2=C1A/C1B
 1    CONTINUE
      IF((SIG1+ALPHA1).EQ.0.) GO TO 400
C
C ----------------- CALL INTEGRATION FUNCTION  ----------------------
C
      Y=SQUANK(A,BIG,ERROR,FIFTH, RUM,NO,FUN)
C
C ----------------  CALCULATE THE VALUE FOR PSI  --------------------
C
      PSI=C2*Y
```


```
      SIGT=SIG0+SIG1*Z
      WRITE(6,200) ALPHA1,SIG1,FIFTH,RUM,NO,Y,ALPHAT,SIGT,PSI
200   FORMAT(1H0,F12.5,F8.5,2E13.4,I5,3F8.5,F9.5  )
400   SIG1=SIG1-DSIGMA
      IF(SIG1.LT.SIGMIN) GO TO 2
      GO TO 1
2     WRITE(6,300)
300   FORMAT(1H1)
      WRITE(6,102)
      WRITE(6,301)
301   FORMAT(1H0,  //,6X≠ALPHAC≠10X≠SIGC≠11X≠ALPHA0≠10X≠SIG0≠10X
     1  ≠LENGTH≠)
      WRITE(6,302) ALPHAC, SIGC, ALPHA0, SIG0 ,Z
302   FORMAT(1H0,F10.2, F15.2,  F16.3, F15.3,F15.2//  )
      WRITE(6,500)
      ALPHA1=ALPHA1-DALPHA
      IF(ALPHA1.LT.ALMIN) GO TO 4
      GO TO 3
4     CONTINUE
      WRITE(6,300)
      Z=Z/2.
      IF(Z.LT.0.9) STOP
      GO TO 800
      END
```

APPENDIX B.1

CASE ONE RESULTS : $\alpha_0 = \Sigma_0 = 0$

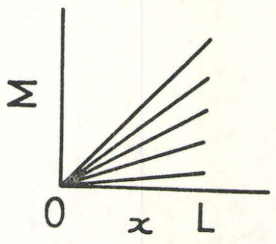

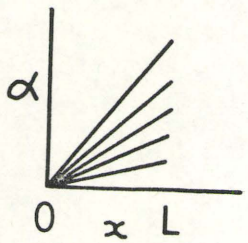

NEUTRON RADIOGRAPHY DALTON MOLSON

ALPHAC	SIGC	ALPHA0	SIG0	LENGTH
.20	.14	0.000	0.000	25.40

ALPHA1	SIG1	FIFTH	RUM	NO	Y	ALPHAT	SIGT	PSI
.01181	.03937	-.1744E-07	.1000E-06	161	.76923	.30000	1.00000	1.86846
.01181	.03740	-.1970E-07	.1000E-06	161	.76000	.30000	.95000	1.84604
.01181	.03543	-.2044E-07	.1000E-06	157	.75000	.30000	.90000	1.82175
.01181	.03346	-.1621E-07	.1000E-06	153	.73913	.30000	.85000	1.79535
.01181	.03150	-.3664E-08	.1000E-06	157	.72727	.30000	.80000	1.76655
.01181	.02953	-.7191E-08	.1000E-06	157	.71428	.30000	.75000	1.73500
.01181	.02756	-.5207E-08	.1000E-06	153	.70000	.30000	.70000	1.70030
.01181	.02559	-.4507E-08	.1000E-06	141	.68421	.30000	.65000	1.66194
.01181	.02362	-.3019E-08	.1000E-06	133	.66666	.30000	.60000	1.61932
.01181	.02165	-.1239E-09	.1000E-06	133	.64705	.30000	.55000	1.57168
.01181	.01969	-.1037E-07	.1000E-06	133	.62498	.30000	.50000	1.51807
.01181	.01772	-.1916E-07	.1000E-06	121	.59996	.30000	.45000	1.45730
.01181	.01575	-.2654E-07	.1000E-06	105	.57135	.30000	.40000	1.38781
.01181	.01378	-.1374E-07	.1000E-06	101	.53832	.30000	.35000	1.30758
.01181	.01181	-.1738E-07	.1000E-06	105	.49975	.30000	.30000	1.21391
.01181	.00984	-.1410E-07	.1000E-06	105	.45412	.30000	.25000	1.10307
.01181	.00787	-.1399E-07	.1000E-06	97	.39930	.30000	.20000	.96990
.01181	.00591	.1196E-08	.1000E-06	89	.33223	.30000	.15000	.80700
.01181	.00394	-.1079E-08	.1000E-06	77	.24845	.30000	.10000	.60347
.01181	.00197	-.1793E-07	.1000E-06	57	.14118	.30000	.05000	.34293
.01181	0.00000	0.	.1000E-06	9	0.00000	.30000	0.00000	0.00000

APPENDIX B.2

CASE TWO RESULTS : $\Sigma_0 = 1.0 \quad \alpha_0 = 0$

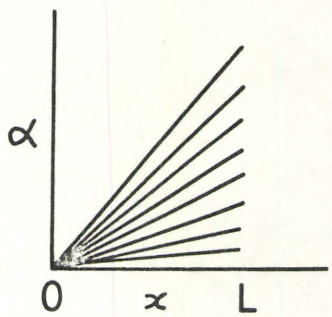

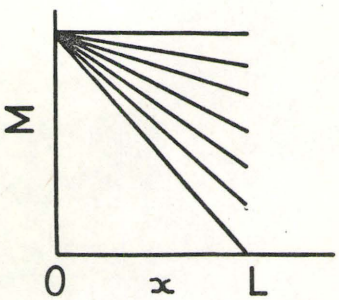

ALPHAC	SIGC	ALPHAO	SIGO	LENGTH
.20	.14	0.000	1.000	25.40

ALPHAI	SIGI	FIFTH	RUM	NO	Y	ALPHAT	SIGT	PSI
.01181	0.00000	-.3957E-07	.1000E-06	197	.98858	.30000	1.00000	2.40127
.01181	-.00197	-.4207E-07	.1000E-06	197	.98852	.30000	.95000	2.40112
.01181	-.00394	-.2259E-07	.1000E-06	201	.98846	.30000	.90000	2.40097
.01181	-.00591	-.1714E-07	.1000E-06	205	.98839	.30000	.85000	2.40081
.01181	-.00787	-.1753E-07	.1000E-06	205	.98833	.30000	.80000	2.40065
.01181	-.00984	-.1795E-07	.1000E-06	205	.98826	.30000	.75000	2.40048
.01181	-.01181	-.1839E-07	.1000E-06	205	.98819	.30000	.70000	2.40031
.01181	-.01378	-.1885E-07	.1000E-06	205	.98812	.30000	.65000	2.40014
.01181	-.01575	-.1933E-07	.1000E-06	205	.98805	.30000	.60000	2.39997
.01181	-.01772	-.1984E-07	.1000E-06	205	.98797	.30000	.55000	2.39979
.01181	-.01969	-.2037E-07	.1000E-06	205	.98790	.30000	.50000	2.39961
.01181	-.02165	-.2093E-07	.1000E-06	205	.98782	.30000	.45000	2.39942
.01181	-.02362	-.2151E-07	.1000E-06	205	.98774	.30000	.40000	2.39923
.01181	-.02559	-.2212E-07	.1000E-06	205	.98766	.30000	.35000	2.39904
.01181	-.02756	-.2276E-07	.1000E-06	205	.98758	.30000	.30000	2.39884
.01181	-.02953	-.2342E-07	.1000E-06	205	.98750	.30000	.25000	2.39863
.01181	-.03150	-.2412E-07	.1000E-06	205	.98741	.30000	.20000	2.39842
.01181	-.03346	-.2484E-07	.1000E-06	205	.98732	.30000	.15000	2.39821
.01181	-.03543	-.2560E-07	.1000E-06	205	.98723	.30000	.10000	2.39799
.01181	-.03740	-.2638E-07	.1000E-06	205	.98714	.30000	.05000	2.39776
.01181	-.03937	-.2720E-07	.1000E-06	205	.98704	.30000	0.00000	2.39753

APPENDIX B.3

CASE THREE RESULTS: $\Sigma_o = 0$, $\alpha_o = 0.3$

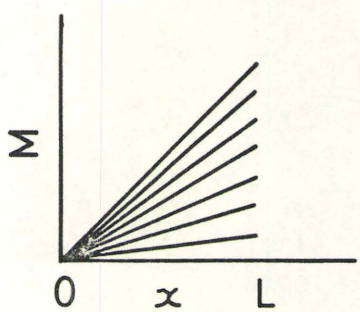

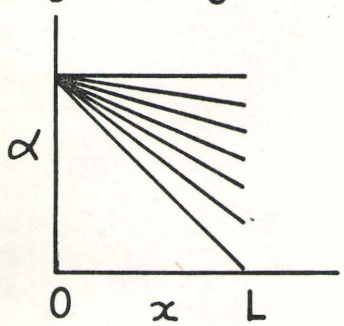

ALPHAC	SIGC	ALPHAO	SIGO	LENGTH
.20	.14	.300	0.000	25.40

ALPHA1	SIG1	FIFTH	RUM	NO	Y	ALPHAT	SIGT	PSI
0.00000	.03937	-.4325E-08	.1000E-06	125	.22418	.30000	1.00000	.54454
0.00000	.03740	-.1019E-07	.1000E-06	125	.21748	.30000	.95000	.52826
0.00000	.03543	-.9475E-08	.1000E-06	125	.21053	.30000	.90000	.51139
0.00000	.03346	-.6286E-08	.1000E-06	121	.20332	.30000	.85000	.49387
0.00000	.03150	-.1178E-07	.1000E-06	117	.19583	.30000	.80000	.47567
0.00000	.02953	-.1026E-07	.1000E-06	117	.18803	.30000	.75000	.45672
0.00000	.02756	-.1214E-07	.1000E-06	121	.17990	.30000	.70000	.43697
0.00000	.02559	-.1496E-07	.1000E-06	113	.17140	.30000	.65000	.41634
0.00000	.02362	-.1949E-07	.1000E-06	109	.16252	.30000	.60000	.39475
0.00000	.02165	-.1542E-07	.1000E-06	105	.15320	.30000	.55000	.37212
0.00000	.01969	-.1473E-07	.1000E-06	105	.14341	.30000	.50000	.34833
0.00000	.01772	-.2170E-07	.1000E-06	97	.13309	.30000	.45000	.32327
0.00000	.01575	-.4222E-08	.1000E-06	97	.12218	.30000	.40000	.29677
0.00000	.01378	-.7835E-08	.1000E-06	97	.11061	.30000	.35000	.26868
0.00000	.01181	-.4697E-08	.1000E-06	93	.09830	.30000	.30000	.23877
0.00000	.00984	-.1521E-08	.1000E-06	89	.08513	.30000	.25000	.20679
0.00000	.00787	.3808E-08	.1000E-06	85	.07097	.30000	.20000	.17240
0.00000	.00591	-.1371E-07	.1000E-06	69	.05565	.30000	.15000	.13518
0.00000	.00394	-.9029E-09	.1000E-06	65	.03894	.30000	.10000	.09459
0.00000	.00197	.1436E-07	.1000E-06	57	.02053	.30000	.05000	.04988

APPENDIX B.4

CASE FOUR RESULTS : $\Sigma_o = 1.0$, $\alpha_o = 0.3$

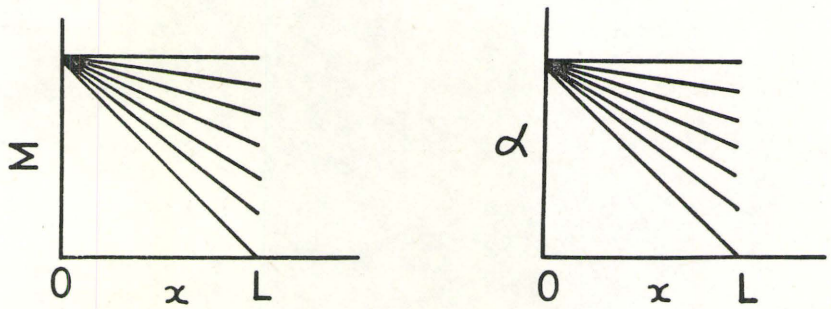

ALPHAC	SIGC	ALPHA0	SIG0	LENGTH
.20	.14	.300	1.000	25.40

ALPHA1	SIG1	FIFTH	RUM	NO	Y	ALPHAT	SIGT	PSI
0.00000	-.00197	-.1924E-07	.1000E-06	201	.76896	.30000	.95000	1.86781
0.00000	-.00394	-.2001E-07	.1000E-06	201	.76869	.30000	.90000	1.86715
0.00000	-.00591	-.2050E-07	.1000E-06	205	.76842	.30000	.85000	1.86648
0.00000	-.00787	-.2144E-07	.1000E-06	205	.76814	.30000	.80000	1.86581
0.00000	-.00984	-.2248E-07	.1000E-06	205	.76786	.30000	.75000	1.86514
0.00000	-.01181	-.2364E-07	.1000E-06	205	.76758	.30000	.70000	1.86446
0.00000	-.01378	-.2499E-07	.1000E-06	209	.76730	.30000	.65000	1.86378
0.00000	-.01575	-.2340E-07	.1000E-06	209	.76702	.30000	.60000	1.86309
0.00000	-.01772	-.2496E-07	.1000E-06	209	.76673	.30000	.55000	1.86239
0.00000	-.01969	-.2667E-07	.1000E-06	209	.76644	.30000	.50000	1.86169
0.00000	-.02165	-.2856E-07	.1000E-06	209	.76615	.30000	.45000	1.86099
0.00000	-.02362	-.3069E-07	.1000E-06	205	.76586	.30000	.40000	1.86027
0.00000	-.02559	-.3305E-07	.1000E-06	205	.76555	.30000	.35000	1.85955
0.00000	-.02756	-.3681E-07	.1000E-06	205	.76527	.30000	.30000	1.85883
0.00000	-.02953	-.3949E-07	.1000E-06	205	.76497	.30000	.25000	1.85811
0.00000	-.03150	-.4240E-07	.1000E-06	205	.76466	.30000	.20000	1.85737
0.00000	-.03346	-.4554E-07	.1000E-06	205	.76436	.30000	.15000	1.85663
0.00000	-.03543	-.4856E-07	.1000E-06	209	.76405	.30000	.10000	1.85588
0.00000	-.03740	-.5219E-07	.1000E-06	209	.76374	.30000	.05000	1.85513
0.00000	-.03937	-.5607E-07	.1000E-06	209	.76343	.30000	0.00000	1.85436